THE UNIVERSITY
of EDINBURGH

Investigating the effects of preclinical prion disease on blood protein composition and infectivity

Ciara Farren

Thesis presented for the degree of Doctor of Philosophy

College of Medicine and Veterinary Medicine

The University of Edinburgh

2020

Declaration

I certify:

(a) that the thesis has been composed by me, and

(b) either that the work is my own, or, where I have been a member of a research group, that I have made a substantial contribution to the work, such contribution being clearly indicated, and

(c) that the work has not been submitted for any other degree or professional qualification except as specified.

Ciara Farren

01/03/2020

Acknowledgments

I would like to express my sincere gratitude to the following people who have helped me in pursuing my interest in prion diseases. My supervisors, Dr Fiona Houston and Dr Andy Gill, I appreciate their constructive feedback and for affording me the opportunity to gain invaluable experience. My lab group, Dr Khalid Salamat and Boon Chin Tan, for their unwavering support and unselfish assistance in my times of need, always going above and beyond to help me. Dr Dominic Kurian and Sam Eaton, for their input with the proteomics work - especially when things did not go to plan and I needed advice in overcoming numerous obstacles. Without their help I would not have been able to complete this project.

I am especially grateful for the kindness and compassion of the incredible friends I have made at the Roslin Institute and in Edinburgh. In particular, Ale, Omar, Lukas, Selene, Charity, Deepti, Imogen, Jess and James. My time spent with them has been uplifting, memorable and inspiring. I will miss them all immensely. I would also like to take this opportunity to thank my wonderful and caring friends from London, especially Sanj, Monika and Jaymini. I am thankful for their many Skype chats, phone calls and visits but most of all for our enduring friendship.

I would like to thank my Godparents Charles and Mala Davison, as well as my parents Patrick and Suraya Farren, for their unconditional love and support. Above all, they motivated me to focus and persevere.

Additionally, I would like to mention my appreciation for the honourable efforts of Mr Babak Arvin, the amazingly kind and empathetic neurosurgeon who got me back on my feet. Also, Dr Lakshumy Sivasegaran and Ms Roopa Nair (as well as their proficient medical teams) for the professional skills and care.

Finally, I would like to dedicate this thesis to my late friend Arun Viswambaran. I am grateful for the precious times we spent together and miss him for the exceptionally talented, creative, fun and generous person he was.

Abstract

Since 1996 there have been 226 cases of variant Creutzfeldt-Jakob disease (vCJD) in the UK following dietary exposure to bovine spongiform encephalopathy (BSE) in the late 80s to early 90s. A recent study on archived appendix tissue has suggested that up to 1/2000 of the UK population may be silent carriers of infection. This is a significant portion of the UK population who may be incubating the disease and thus potentially passing it on to others via blood transfusion. As there is currently no effective screening method to test donated blood this is a major public health concern. The aim of this project was to utilize archived blood samples from transfusion experiments performed with BSE infected sheep, identify protein expression differences between uninfected and infected blood and discover potential diagnostic markers besides the abnormal prion protein (PrP^{Sc}).

Infected samples were taken from sheep 10 months after oral inoculation with BSE, when their blood was proven to be infectious but the sheep lacked clinical signs. Uninfected samples were taken from the same sheep prior to BSE exposure. Samples from 9 sheep were pooled to control for genetic and metabolic differences. The plasma was processed using ProteoMiner columns to deplete highly abundant proteins while simultaneously enriching for low abundant proteins. Subsequently, isotopic labelling was used to distinguish between the two samples and levels of protein expression were compared by mass spectrometry. Initially 153 proteins were identified based on one unique peptide match. The extent of differential expression was assessed by filtering the median H/L (heavy/light isotopes) and proteins between >1.5 and <0.666 were retained, leaving a dataset of 44 proteins. Elimination of the most common proteins reduced this to 37 proteins and after considering the current literature a candidate shortlist of 8 proteins were chosen to validate by western blotting and LI-COR imaging. The buffy coat fraction of blood from the same 9 sheep were similarly processed. The original dataset of 1148 proteins was cut down to 124 and Ingenuity Pathway Analysis (IPA) employed. This highlighted 191 biological processes of potential interest, including LXR/RXR activation, acute phase response signalling, leukocyte extraversion signalling and mitochondrial dysfunction. A shortlist of 8 candidate proteins were then determined for validation. These findings are the basis for a proposed biomarker panel for an effective preclinical diagnostic blood test.

Additionally, in order to investigate how cells pass infection by the human blood transfusion route, blood components from the natural scrapie flock were utilised to infect the Rov9 cell line. The aim of this work was to develop a system to study the processes by which live

white blood cells (WBCs) transfer infection to other cells. A cell culture model to study infectivity from scrapie infected WBCs of the Roslin Scrapie Flock was achieved. Further work is needed to examine whether membrane based cellular interactions are essential for efficient propagation of infection and thus spread of disease.

Lay summary

Compared to other neurodegenerative diseases, prion diseases are unique in that some forms are infectious. Following exposure of the UK population to bovine spongiform encephalopathy (BSE) there have been 226 cases of variant Creutzfeldt-Jakob disease (vCJD), the human form of BSE. It has been suggested that 1 in 2000 people in the age relevant population may be silent carries of vCJD. This figure has been estimated from detection of abnormal prion protein (PrP^{Sc}) in appendix tissue samples. It means that a substantial portion of the UK population may be incubating the disease and thus potentially passing it on to others via blood transfusion. This is a major health concern as there is currently no effective screening method to test for these individuals and thus it is a possibility that infected blood will be unknowingly given to a naïve recipient.

The aim of this project was to utilize archived blood samples from transfusion experiments performed with BSE infected sheep and screen for differences in protein expression between uninfected and infected blood to identify diagnostic markers besides PrP^{Sc}. Donor sheep were orally infected with BSE, their blood collected and transfused to recipient sheep. Since it is established which of the recipients developed BSE, donors with infectious blood can be identified. Infected samples were taken when blood was proven to be infectious but the sheep lacked clinical signs (mimicking the human silent carrier status). Uninfected samples were taken from the same sheep at a time point prior to their exposure to BSE. Samples from 9 sheep were pooled to control for genetic and metabolic differences. A signature of protein expression in the blood of animals that transmitted disease may be of potential significance for diagnostics. This can be determined by use of mass spectrometry and isotopic labelling to distinguish the two groups.

Before mass spectrometry samples were treated. Blood is a highly complex and may be separated into distinct fractions by centrifugation. Within plasma around twenty proteins (including albumin, transferrin and fibrinogen) constitute more than 98% of protein. Their presence can obscure detection of low abundant proteins. ProteoMiner technology utilizes a highly diverse library of hexapeptide ligands bound to beads within a small column. Each bead has an affinity for a specific protein. When samples are applied to the column high abundant proteins are concentrated on their beads while simultaneously, low abundant proteins are concentrated on theirs. This creates a final output that is more homogeneous. Following mass spectrometry, 35 proteins were identified as differentially expressed in

plasma. From this list candidate proteins were chosen to validate (confirm up or down expression in infected blood) based on previous literature on proteomics of prion diseases.

The buffy coat layer of blood contains most of the white blood cells. Pooled buffy coat samples from the same 9 sheep were processed in the same manner, and 122 proteins were identified by mass spectrometry. This larger dataset was then placed into Ingenuity Pathway Analysis (IPA) to investigate the biological context of changes in protein expression. From the suggested disease pathways of IPA and current literature, a shortlist of candidate biomarkers were chosen to follow up on. In total 4 biomarkers for plasma and buff coat samples were validated. Results from pooled samples show confirmation of the mass spectrometry predictions, thus providing preliminary data on determining a protein biomarker panel associated with prion infection in blood.

Table of Contents

Table of images

Table of tables

List of abbreviations

A1BG	Alpha-1-B glycoprotein
AD	Alzheimer's disease
APOD	Apolipoprotein D
ATP	Adenosine triphosphate
BSE	Bovine spongiform encephalopathy
C1QB	Complement C1q B chain
CSF	Cerebrospinal fluid
CJD	Creutzfeldt Jakob disease
fCJD	Familial Creutzfeldt Jakob Disease
sCJD	Sporodic Creutzfeldt Jakob disease
vCJD	Variant Creutzfeldt Jakob disease
CNS	Central Nervous System
CVO	Circumventricular organs
CWD	Chronic wasting disease
DC	Dendritic cells
DCN	Decorin
DDA	Direct Detection Assay
ELISA	Enzyme-linked immunosorbent assay
ER	Endoplasmic reticulum
ECM	Extracellular matrix
FBLN1	Fibulin 1
FDC	Follicular dendritic cells
FFI	Fatal familial insomnia
FBLN1	Fibulin1
GALT	Gut associated lymphoid tissue
GPI	Glycosyl phosphoinosityl
GABAA	Gamma-aminobutyric acid type A
GSS	Gerstmann-Sträussler-Scheinker syndrome
HABP2	Hyaluronan binding protein 2
hGH	Human growth hormone

hnRNP K	Heterogeneous nuclear ribonucleoprotein K
HPX	Hemopexin
IC	Intracerebral
ID	Infectious Dose
IHC	Immunohistochemistry
ITIH2	Inter-alpha-trypsin inhibitor heavy chain H2
IV	Intravenous
IHC	Immunohistochemistry
IPA	Ingenuity pathway analysis
LTP	Long-term potentiation
miRNA	MicroRNA
MRI	Magnetic resonance imaging
MS	Mass spectrometry
MSN	Moesin
NCJDRSU	National CJD Research & Surveillance Unit
OP	octarepeat region
PARK7	Parkinson disease protein 7
PBMCs	Peripheral blood mononuclear cells
PBS	Phosphate-buffered saline
PET	Position emission tomography
PHE	Public Health England
PFA	Paraformaldehyde
PMCA	Protein misfolding cyclic amplification
PrP^{C}	Cellular prion protein
PrP^{Sc}	Disease-associated prion protein
PRNP	Prion protein gene
RAMALTs	Rectoanal mucosa-associated lymphoid tissues
RBCs	Red blood cells
RER	Rough endoplasmic reticulum
Rt-QuIC	Real-time quaking-induced conversion
s100A8	S100 calcium binding
SLO	Secondary lymphoid organs

SMS	Spermine synthase
Tht	Thioflavin T
TTR	Transthyretin
TSE	Transmissible spongiform encephalopathy
VDBP	Vitamin D Binding Protein
WBCs	White blood cells
UK	United Kingdom
US	United States

Chapter 1: Introduction

1.1 Prion diseases and prion biology

1.1.1 Prion diseases

Prion diseases are rare, fatal, neurodegenerative conditions that have arisen in a large range of mammalian species (see Table 1.1). They are characterised by long incubation periods but are typically progressive once clinical symptoms commence. Prion diseases are also referred to as 'transmissible spongiform encephalopathies' (TSEs) due to the typical sponge like appearance taken on by the brain from neuronal loss during the course of disease. All prion diseases are characterised by the accumulation of misfolded prion protein (PrP^{Sc}). Although the topology or folded composition of each prion is unique, the principles governing aggregation and propagation are considerably distinctive (Hu and Huang 2013).

Table 1.1: Prion diseases. There are over 20 different types of prion disease, this table lists some examples (Mabbott 2017).

Prion disease	Affected species	Cause
Iatrogenic Creutzfeldt–Jakob disease	Human	Accidental medical exposure to CJD-contaminated tissues or tissue products
Sporadic Creutzfeldt–Jakob disease	Human	Unknown. Theories include somatic mutation or spontaneous conversion of PrP^{C} to PrP^{Sc}
Variant Creutzfeldt–Jakob disease	Human	Ingestion of BSE-contaminated food or transfusion of blood or blood products from CJD-infected blood donor
Familial Creutzfeldt–Jakob disease	Human	Germline mutations of the *PRNP* gene
Gerstmann–Sträussler–Scheinker syndrome	Human	Germline mutations of the *PRNP* gene
Kuru	Human	Ritualistic cannibalism
Fatal familial insomnia	Human	Germline mutations of the *PRNP* gene
Bovine spongiform encephalopathy	Cattle	Ingestion of contaminated food
Scrapie	Sheep, goats, mouflon	Acquired. Ingestion, horizontal transmission, vertical transmission unclear

Human prion diseases can occur sporadically, be hereditary or be acquired. Thus far, there are seven subtypes that constitute human prion diseases: Kuru, Gerstmann-Sträussler-Scheinker syndrome (GSS), fatal insomnia (FI), sporadic Creutzfeldt-Jakob disease (sCJD), familial (fCJD) and variant CJD (vCJD). The subtypes are distinguished by defined differences in cause, clinical phenotype, brain histopathology, and critically, in the structure of pathogenic PrP^{Sc}. GSS is a slow but progressive hereditary autosomal dominant disease. It was the first human prion disease in which a mutation in *PRNP* was discovered as the cause. The rarest is fatal and sporadic familial insomnia (Sikorska and Liberski 2012).

The most common form is sporadic (sCJD) which occurs in Europe with a frequency of 1 case per million of the general population per year (Sikorska and Liberski 2012). Acquired forms of disease account for only 5 % of cases of human prion disease and include kuru, iatrogenic CJD and vCJD (Imran and Mahmood 2011). Kuru is a unique geographical isolate, found exclusively in the Fore linguistic group of Papua New Guinea Eastern Highlands. It arose from the ritualistic practice of consuming the dead bodies of relatives as a mark of respect. It has seen a decline since a ban on ritualistic cannibalism was introduced in the mid-1950s (Manuelidis et al. 2009). Iatrogenic CJD was initially observed in 1974 in a patient who received cadaveric corneal transplant from a donor with sporadic CJD (Duffy et al. 1974). Since then there have been several cases of human prion disease associated with iatrogenic transmission by the use of neurosurgical instruments, cadaveric dura mater grafts and intramuscular injections of cadaveric pituitary-derived human growth hormone (hGH) and gonadotrophin hormone. Most cases of treatment with hGH have occurred in France and those linked to treatment with dura mater grafts have mainly occurred in Japan (Nozaki et al. 2010). vCJD was first reported 1996 in 10 United Kingdom (UK) patients (Will et al. 1996). Caused by transmission from cattle infected with bovine spongiform encephalopathy (BSE), it is a major problem faced by Europe for the last 30 years.

BSE was first diagnosed in southern England in 1986 (Wells et al. 1987). The initial clinical signs include changes in temperament, aggressive behaviour, the development of a head tremor and exaggerated startle reflexes. Late clinical signs include ataxia, stumbling and recumbency and can typically extend over several weeks (Wilesmith et al. 1992). As the incubation period is about 5 years, presumably the start of the epidemic in the national herd was exposure to food borne infection in the early 1980s. During this time changes occurred with the industrial rendering processes, where livestock carcass waste was converted to tallow and meat and bone meal. This is a likely cause for increasing survivability of prion infectivity in meat and bone meal where previously sufficient inactivation was applied to prevent recycling of infection (Wilesmith, Ryan, and Atkinson 1991). It has been shown that

experimental oral infection of cattle can be achieved with as little as 1 mg of BSE infected bovine brain (Wells et al. 2007). Another example of where a similar process of infection has taken place is in the appearance of prion disease in big cats and exotic ungulates (antelope, nyala and kudu) in zoo collections (Cunningham et al. 2004); (Lezmi et al. 2003); (Jeffrey and Wells 1988); (Kirkwood and Cunningham 1994). Strikingly, there have been no cases in domestic dogs (Kirkwood and Cunningham 2007). As well as the classical form of BSE, atypical BSE are potentially sporadic or genetic forms of prion diseases in cattle. Two forms of atypical BSE were identified mostly in older animals and were named according to the electrophoretic migration of their PrP^{Sc} on Western blots (Casalone et al. 2004); (Biacabe et al. 2004). High or H type BSE PrP^{Sc} is larger thus migrates at a slower rate and is detected in a higher position than classical BSE. Low or L type BSE PrP^{Sc} is smaller and migrates at a faster rate than classical BSE so is detected in a lower position during electrophoresis (Langeveld et al. 2011). Along with the differences in size, there are also different biochemical properties, transmission characteristics and PrP^{Sc} distribution (Priemer et al. 2013).

In the case of other animal prion diseases, classical scrapie is considered the archetypal prion disease as it has been known to fatally affect adult sheep (aged 2-4 years) in Britain since the early 18th century. Sources of infection include the placenta (Schneider et al. 2015) and milk (Konold et al. 2013) as well as environmental contamination such as bedding, pasture, fencing and housing. Studies have shown shedding of infection in urine, faeces and saliva, hence facilitating spread and maintenance within flocks (Terry et al. 2011); (Gough and Maddison 2010). Due to the stability of abnormal prion proteins, attempt to cleanse and disinfect housing have limited effect (Konold et al. 2008). Furthermore, prions may persist in the soil for at least 18 months, they can also retain their infectious properties even when bound to plants (Maddison et al. 2010); (Pritzkow et al. 2015). This is a big issue for disease control within the farm environment. In contrast with BSE, where no apparent changes in the biological phenotype of BSE isolates have been identified through the epidemic (Green et al. 2005), several agent strains are recognised with classical scrapie (Bruce et al. 2002). A major distinction between the classical scrapie strains that are readily spread within susceptible sheep population and the atypical form of scrapie, is that atypical scrapie has unique molecular and phenotypic characteristics and is thought to perhaps occur spontaneously in older sheep (Greenlee 2018). Furthermore it transmits very poorly under natural conditions (Fediaevsky et al. 2010). Asymptomatic scrapie has worldwide distribution with similar incident rates which support a separate aetiology from classical scrapie (Cook et al. 2016); (Mitchell et al. 2010); (Dagleish et al. 2008).

Chronic wasting disease (CWD) is a prominent prion disease affecting various cervid species. Originally described in captive mule deer in 1967 (Williams and Young 1980), CWD

has since been reported in both farmed and wild cervids, including white-tailed deer, mule deer, elk and moose. Surveillance has established presence in many central and eastern states of the US, as well as in 5 provinces of Canada (Gilch et al. 2011). The prevalence in cervids in Scandinavia is very low with 1 in 2,500 cervids (0.04%) in Finland and 23 in 41,125 cervids (0.05%) in Norway. However these numbers may increase with further testing detecting more cases (Gale 2018). Characterisation of European isolates is currently being pursued, however preliminary data suggest that CWD strains identified in Europe and North America are different and that there is strain diversity in the European cervid population (EFSA et al. 2019). CWD has been described as the sole prion disease truly endemic in wild animal populations (Windl and Dawson 2012). Clearly contagious, CWD infectivity has been found in the lymphoreticular systems as well as in blood and urine (Mathiason et al. 2010). It cannot be said for sure if CWD is a danger to public health. However, there are some interim results from a study where CWD was transmitted to macaques that were fed infected meat (muscle tissue) or brain tissue from both clinical and asymptomatic CWD infected deer and elk (CDC 2018). Various schemes have been employed for control and limiting geographical range. In an attempt to eradicate CWD in Norway and prevent its spread to the rest of Europe, culling of herds has taken place in 2018 (GSSO 2018). In the United States (US), there has been limited success achieved with attempts to manage CWD. Control measures include surveillance, carcass regulations (banning importation of brain or spinal tissues), bans on baiting stations, as well as non-selective hunting and culling of deer (Conner et al. 2008). Within endemic areas, such as the state of Colorado, management programmes focus on containing CWD prevalence in localised areas, thus reducing risk of spread along putative movement corridors (Blanchong 2010).

1.1.2 Prion protein chemistry, function and misfolding

The gene *PRNP* encodes prion protein (PrP), it is illustrated in Figure 1.1. It is a glycosylated membrane protein of about 230 amino acid residues, depending on species. Ubiquitously expressed across tissues in all mammalian species, it is predominantly associated with neurons, non-neuronal cells in the nervous system (glia and Schwann cells) and the lympho-reticular system. PrP is able to adopt two confirmations, either a native α-helix rich structure (PrP^{C}) or a misfolded, disease associated β-sheet abundant complex (PrP^{Sc}). The latter is self-propagating. It is able to recruit and convert PrP^{C}, aiding assembly of PrP^{Sc} oligomers and amyloid plaques in the brains. PrP^{Sc} is less soluble than PrP^{C} but more resistant to protease digestion (Choi et al. 2009). In the infectious or acquired forms of prion disease the refolding of PrP^{C} to PrP^{Sc} is initiated by the uptake of misfolded PrP^{Sc}. In the genetic forms of the disease, *PRNP* polymorphisms predispose individuals to the formation of a misfolded prion protein which in turn promote further misfolding (Bagyinszky et al. 2018). The process whereby PrP^{Sc} is the only disease-causing agent, is described as the ‘protein-only

hypothesis' (Prusiner 1998). It is puzzling that a protein underlying such fatal neurodegenerative disorders is highly conserved. This suggests that the existence of PrP^C has some important beneficial, physiological activities. The function of PrP^C however, is as yet unresolved.

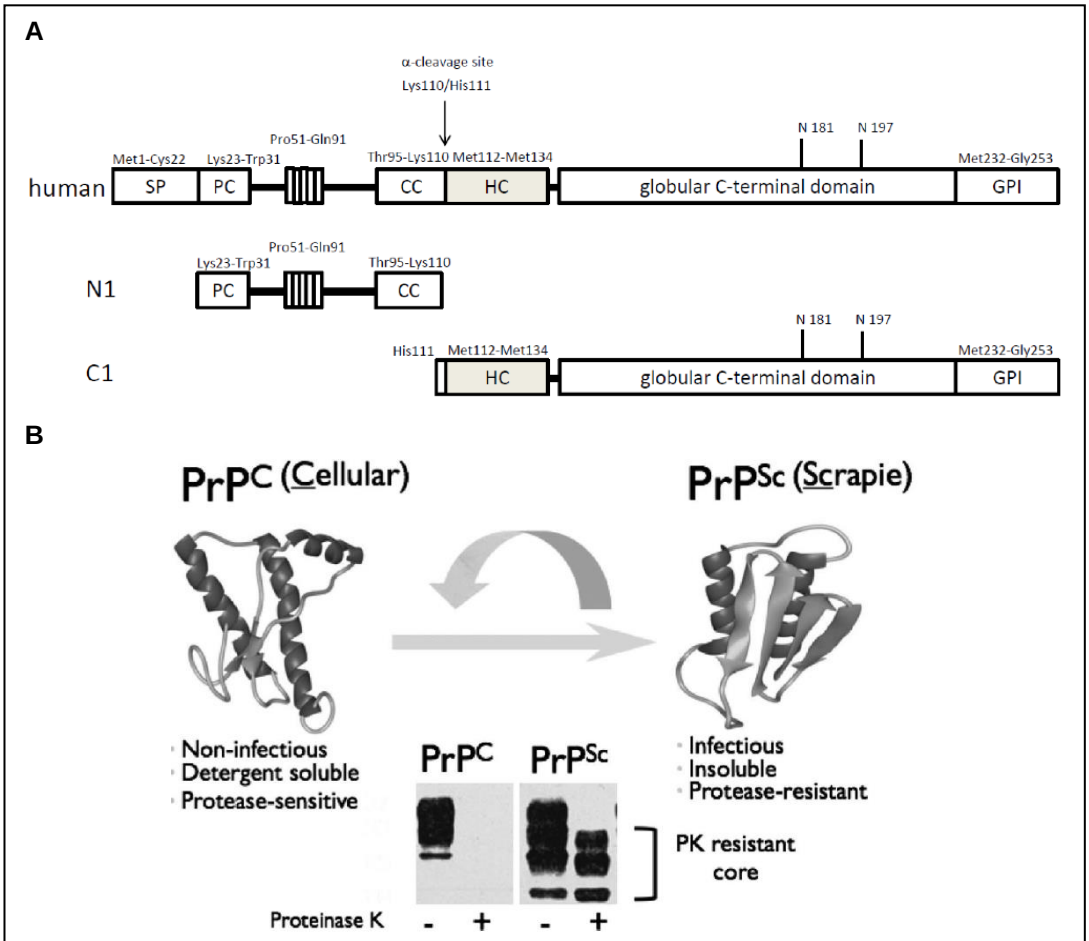

Figure 1.1: (A) Organisation of human PrP. Unprocessed PrP is 253 amino acid residues in length and consists of an octarepeat region (OR), a hydrophobic region, one disulphide bond, two N-linked glycosylation sites at positions 181 and 197 and a glycosyl phosphoinositol (GPI) anchor at position 230 attached to the C-terminus. N-terminal (N1) is 23 to 110. C-terminal (C1) is 111 to 253 SP = signal peptide, PC = positively charged region, CC = charged cluster region, HC =hydrophobic core region (Yusa et al. 2012). **(B) Normal and pathogenic prion protein.** As represented in the diagram PrP^C is composed of predominantly α helixes, while PrP^{Sc} is mainly made up of β sheets. The western blot shows expected band pattern before after treatment with proteinase K (PK) (Brown and Mastrianni 2010).

PrP^C is synthesised in the rough endoplasmic reticulum (RER) and transits the Golgi apparatus as it moves to the cell surface (Riesner 2003a). Following translation and extrusion into the lumen of the endoplasmic reticulum, PrP^C undergoes several posttranslational modifications to adopt the distinctive structure of a C-terminal globular domain and a N-terminal flexible tail (Riek et al. 1997). Two charged clusters (CC1 and

CC2), an octarepeat region (OR) and a hydrophobic domain make up the N-terminal tail. Additionally, there are two N-glycosylated sites at positions 181 and 197 and a glycosyl phosphoinosityl (GPI) anchor at position 230 of the C-terminus. Both N-glycosylation sequons can be variably glycosylated, resulting in unglycosylated, mono-glycosylated and di-glycosylated species (Rudd et al. 1999); (Stimson et al. 1999). After transportation to the cell membrane, the GPI anchor allows PrP^C to reside extracellularly in lipid rafts (Naslavsky et al. 1997). Here it is a potential candidate for ligand uptake, cell adhesion or membrane signalling. It undergoes rapid constitutive endocytosis and subsequent recycling or degradation (Morris, Parkyn, and Jen 2006).

PrP^C is actively expressed in both neurons and glial cells of the central nervous system (CNS). Immunocytochemical studies by light and electron microscopy in both primate and rodent brains indicate its location in the pre- and post-synaptic compartments of nerve terminals in neurons (Sales et al. 1998). Due to this, one possible function of PrP^C is in preserving normal synaptic structure and function through regulation of synaptic transmission and plasticity (the ability of synapses to change their strength based on previous activity) (Jeffrey et al. 2000). Studies of PrP^C deficient mice show that they display weakened inhibitory GABAA (gamma-aminobutyric acid type A) receptor-mediated synaptic transmission and impaired long-term potentiation (LTP) (Collinge et al. 1994). This can be rescued by a human *PRNP* transgene (Whittington et al. 1995). LTP in the hippocampus underlies learning and memory formation, thus any defects in LTP may result in cognitive defects. This is exemplified in the reduction in spatial learning and memory in PrP^C deficient mice (Criado et al. 2005). PrP^C has also been suggested to play a key role in sleep homeostasis. With prolonged sleep deprivation *PRNP* knockout mice were found to have reduced slow wave activity and altered hormonal reactivity to stress (Sanchez-Alavez et al. 2007). Coincidently, deterioration of slow wave activity was also found to contribute to sleep deficits in Alzheimer's disease (AD) was reversed by enhancing GABAAergic inhibition (Busche et al. 2015)

As PrP^C is expressed a few days after embryonic implantation and thus has been proposed to play a role in development (Manson et al. 1992). It has been found that PrP^C deficient mice exhibit reduced proliferation rates of neuronal progenitor cells in the embryonic, new born and adult CNS (Bribian et al. 2012). Another suggested function of PrP^C is in neuroprotection. PrP^C is also able to bind metal copper ions and thus it has been proposed to participate in resistance to oxidative stress by preventing reactive oxygen species (ROS) generation via free copper mediated redox reactions (Xu and Zhu 2012); (Brown et al. 1997). Copper binding may also inhibit prion disease propagation. Neuroblastoma cells cultured in the presence of copper have reduced accumulation of PrP^{Sc} and a significant delay in PrP^C

conversion was observed when scrapie infected hamsters were treated with copper (Hijazi et al. 2003).

A number of hypotheses have been proposed for the sequential events involved in conversion of healthy PrP^{C} to abnormal PrP^{Sc}. Such processes are depicted in Figure 1.2. Early ideas for the underlying molecular mechanism formulated in the 'prion hypothesis' proposed that PrP^{Sc} acted as a template for PrP^{C} to misfold (Prusiner 1998). Studies in the mid-90s demonstrated that the mixing of immune-isolated PrP^{C} with PrP^{Sc} in a suitable buffer system caused the PrP^{C} to take on PrP^{Sc} characteristics (Kocisko et al. 1994). The formation of aggregates or new 'seeds' are also thought to be critical to the misfolding cascade.

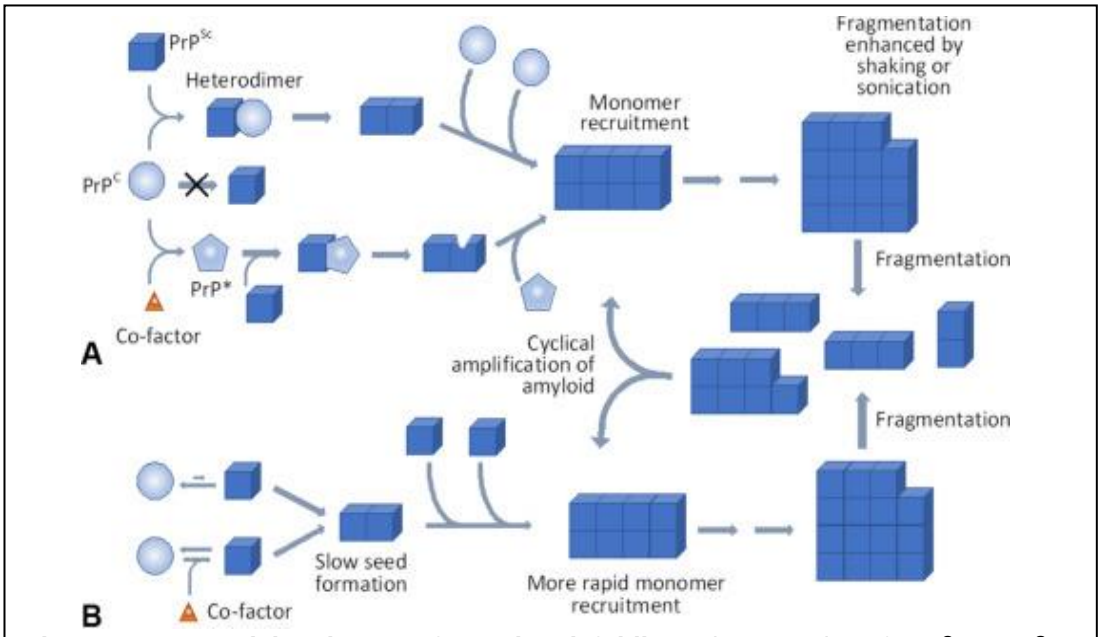

Figure 1.2: Potential pathways of protein misfolding. A) conversion of PrP^{C} to PrP^{Sc} does not occur spontaneously but instead requires interaction of both molecules. The formation of this heterodimer then catalyses the conversion of PrP^{C} to PrP^{Sc} and subsequent addition of PrP^{C} to create fibrils. Alternatively, a cofactor may unfold PrP^{C} to an intermediate PrP* which facilitates heterodimer formation. B) another possibility is that PrP^{C} to PrP^{Sc} exist in equilibrium but a cofactor may shift this in favour of PrP^{Sc}. For both pathways amyloids may fragment resulting in additional seeds further driving the process of conversion (Gill and Castle 2018)

1.1.3 Genetic susceptibility to prion diseases

The single nucleotide polymorphism (SNP) at codon 129 of *PRNP* is a known genetic risk factor for the development of human prion diseases. It either encodes methionine (M) or valine (V) and has a profound effect on susceptibility. For vCJD in the UK, all pathological

positive cases that had undergone genetic testing were homozygous M/M at codon 129 (Saba and Booth 2013). The exception was one heterozygous (M/V) individual identified in 2016 (Mok et al. 2017). Thus it is unknown whether codon 129 heterozygosity confers resistance to prion disease or whether it results in elongating the incubation period. Sporadic CJD also predominantly affects methionine (M/M) homozygous individuals, with MV heterozygosity reported to confer resistance (Palmer et al. 1991). For iatrogenic CJD following administration of cadaver-sourced pituitary derived growth hormone, an excess of valine (V/V) homozygotes were first reported in early UK cases as a marker of susceptibility. The V/V genotype has now greatly decreased while M/M genotype increased, suggesting contrasting conferred incubation times (up to 40 years after treatment). These discrepancies may potentially be explained by the compatibility of host genotype and the strain of the infecting prion, whereby different prion strains are preferentially propagated by prion proteins of different primary sequence (Collinge and Clarke 2007).

A clear relationship between sheep host genetics and susceptibility to scrapie is well established. Susceptibility is strongly modulated by polymorphisms in PRNP. In sheep PRNP encodes alanine (A), arginine (R) and glutamine (Q) at codons 136, 154 and 171. Polymorphisms at these codons are mainly responsible for changes in resistance or susceptibility of a sheep to scrapie, as measured by attack rate or incubation period (Goldmann 2008). Having a valine (V) at codon 136 is associated with increased susceptibility, while R at codon 171 is associated with increased resistance. Hence, VRQ/VRQ sheep are the most susceptible and ARR/ARR sheep the most resistant (Hunter et al. 1996). Additionally, substitution of methionine (M) by threonine (T) or of leucine (L) by phenylalanine (F) at codons 112 and 141 respectively have been shown to result in longer scrapie incubation periods (González et al. 2014); (Laegreid et al. 2008). This relationship between PRNP and scrapie susceptibility has served as the basis for implementation of a scrapie control programme to breed sheep based on genetic selection. The National Scrapie Plan (NSP) was launched in 2001, with cost of blood sampling, laboratory genotyping and scheme administration met by the government. It required negative selection of the VRQ allele (rams with VRQ allele were killed or castrated) and became well established throughout the pure breeding sector of the sheep industry, with membership of over 12,000 flocks by 2006. A comparison of ram lambs born in 2002 with those of 2006 depict distinct changes in PrP genotype (Dawson, Moore, and Bishop 2008).

1.1.4 Peripheral pathogenesis

In relation to prion diseases, peripheral pathogenesis refers to the accumulation and replication of prions within secondary lymphoid organs (SLO) before their spread to the brain where they ultimately cause neurodegeneration and death. Peripheral pathogenesis is

dependent on prion strain, affected host animal species, age, genetics and route of infection (oral, peritoneal, subcutaneous or intravenous [IV]). In many prion diseases, such as scrapie, CWD and vCJD, infection is acquired by the oral route.

Following initial tissue entry, prion agents replicate in follicular dendritic cells (FDCs) of the small intestine Peyer's patches and there is subsequent dissemination to peripheral lymphoid tissues (spleen, tonsils and peripheral lymph nodes) (Manuelidis et al. 2000). Studies have shown that prion accumulation within SLO is important for efficient transmission of the disease to the CNS subsequent to peripheral exposure. Survival times were extended in mice that lacked spleens after the intraperitoneal injection of scrapie prions (Fraser and Dickinson 1970). Additionally, the absence of Peyer's patches also prevented neuroinvasion of scrapie prions from the gut lumen (Glaysher and Mabbott 2007); (Donaldson, Else, and Mabbott 2015). Prions exploit key cells of the SLO in order to efficiently infect the host. Mice that lack mature B and T cells (severe combined immunodeficient or SCID mice) are protected from peripheral infection with prions (McFarlin et al. 1971); (Klein et al. 1997). However, T cells appear to lack the cellular requirements to sustain prion infection alone as their deficiency does not affect prion disease pathogenesis (Raeber 1999). Although in the absence of B cells, the accumulation of prions in the spleen and subsequent neuroinvasion are significantly impeded, B cells alone are unable to support prion replication. Prion replication does not occur in transgenic mice which express high levels of PrP^C only on B cells (Montrasio et al. 2001). This highlights that the role of B cells in prion pathogenesis is likely to be indirect, perhaps in the homeostatic support of other cellular subpopulations within the lymphoreticular organs or because they play a critical role in the normal development of FDC. Moreover, Mok et al. (2012) have shown that deficiency in recirculating B cells prevented the spread of prion infection between SLO. Their data suggests that the actions of B cells, interacting with and acquiring surface proteins from FDCs, recirculating between SLO via the blood and lymph, mediate initial propagation of prions from the draining lymphoid tissue to peripheral tissues. Hence, B cells are required for prion propagation as in their absence FDC function is impaired.

FDCs are non-haematopoietic cells that are present within the B cell follicles of SLO. Tumour necrosis factor-α (TNF-α) and lymphotoxins (LT) are cytokines produced by B cells. TNF-α and LT maintain FDCs in their differentiated state, in their absence FDCs rapidly de-differentiate (Mackay and Browning 1998). It has been shown that prion accumulation in SLO and neuroinvasion are significantly impeded in mice deficient in TNF-α and LT stimulation thus hinting at the significant role played by FDC in establishing prion infections (Mabbott, Williams, et al. 2000); (Glaysher and Mabbott 2007). To determine that FDCs were the essential sites of prion replication within SLO, experiments have been performed with

transgenic mice. When expression of PrP^C was switched off on FDCs, prion replication in the spleen was blocked. In contrast, when PrP^C expression was switched on only on FDCs, this was enough to sustain high levels of replication in the spleen (McCulloch et al. 2011).

Although PrP^{Sc} has been detected in the small intestine Peyer's patches of cattle infected with BSE (Hoffmann et al. 2011), BSE prions are thought to have little involvement with SLO during the preclinical phase of infection (Kaatz et al. 2012). However, the transmission of BSE prions to other species (humans, sheep and mice) is distinctively characterised by their accumulation in lymphoid tissues (Hill et al. 1997); (Foster et al. 2001). Following oral exposure, prions must cross the gut epithelium before establishing infection upon the FDC within the gut-associated lymphoid tissues (GALT). This is done by exploiting specialist phagocytic epithelial M cells as depicted in Figure 1.3. M cells line gut associated lymphoid tissues and are important for efficient mucosal immune responses against certain pathogenic bacteria (Hase et al. 2009). A number of studies show that prions make use of M cells in order to establish infection within the host (Miyazawa et al. 2007); (Takakura et al. 2011); (Donaldson et al. 2016). Antigens that have been transported across the gut epithelium by M cells are released into the basolateral pocket beneath where they are sampled by mononuclear phagocytes. After antigen uptake these cells undergo maturation and migrate to local SLO to initiate an immune response. Conventional DCs also transport antigens within Peyer's patches and towards the mesenteric lymph nodes (Cerovic et al. 2014); (Mabbott et al. 2011). FDCs do not travel in blood or lymph fluid, thus, circulation of infectivity in the body is thought to involve other key cells (such as dendritic cells, B lymphocytes and platelets) (Mabbott, Mackay, et al. 2000). As B cells recirculate between SLO for several weeks they often acquire antigens from FDCs within the germinal centres (Schmidt et al. 2013); (Suzuki et al. 2009). It has been shown that when the migration of B cells between SLO was blocked, the dissemination of prions from these tissues were also blocked (Mok et al. 2012). Hence, recirculating B cells appear to mediate the initial spread of prions via blood and lymph.

The distribution of PrP^{Sc} in the brains of BSE infected sheep with signs of disease have proven to be similar irrespective of the route of inoculation being IC, IV or oral (Gonzalez et al. 2005). This suggests a common pattern of neuroinvasion and CNS spread. The presence of vascular amyloid PrP^{Sc} deposition in the basement membrane of endothelial cells of the hypothalamus, give an indication that infectivity may reach the brain from the blood (van Keulen et al. 2000). However, these plaques are rare in prion diseases, thus they do not justify haematogenous neuroinvasion being a frequent event or even having an important role (Gonzalez et al. 2002).

Following amplification in lymphoid tissue, prions travel via the sympathetic and parasympathetic pathways to ultimately infect the brain. From abdominal lymphoid organs, nerve fibres spread along splanchnic nerves to the spinal cord as part of the sympathetic nervous system. The enteric nerve plexus of the gut wall connects to the vagus nerve, which is part of the parasympathetic arm of the nervous system (Jeffrey and Gonzalez 2007). Alternatively, some cells may carry prion agents from the bloodstream to the CNS by crossing the blood-brain barrier (a specialised layer of endothelial cells joined by tight junctions). DCs and T cells are capable of breaching this barrier during the pre-clinical stages of prion disease (Mabbott and MacPherson 2006). Once the infectivity enters the CNS, it spreads to particular brain areas. The exact localisation is dependent on the

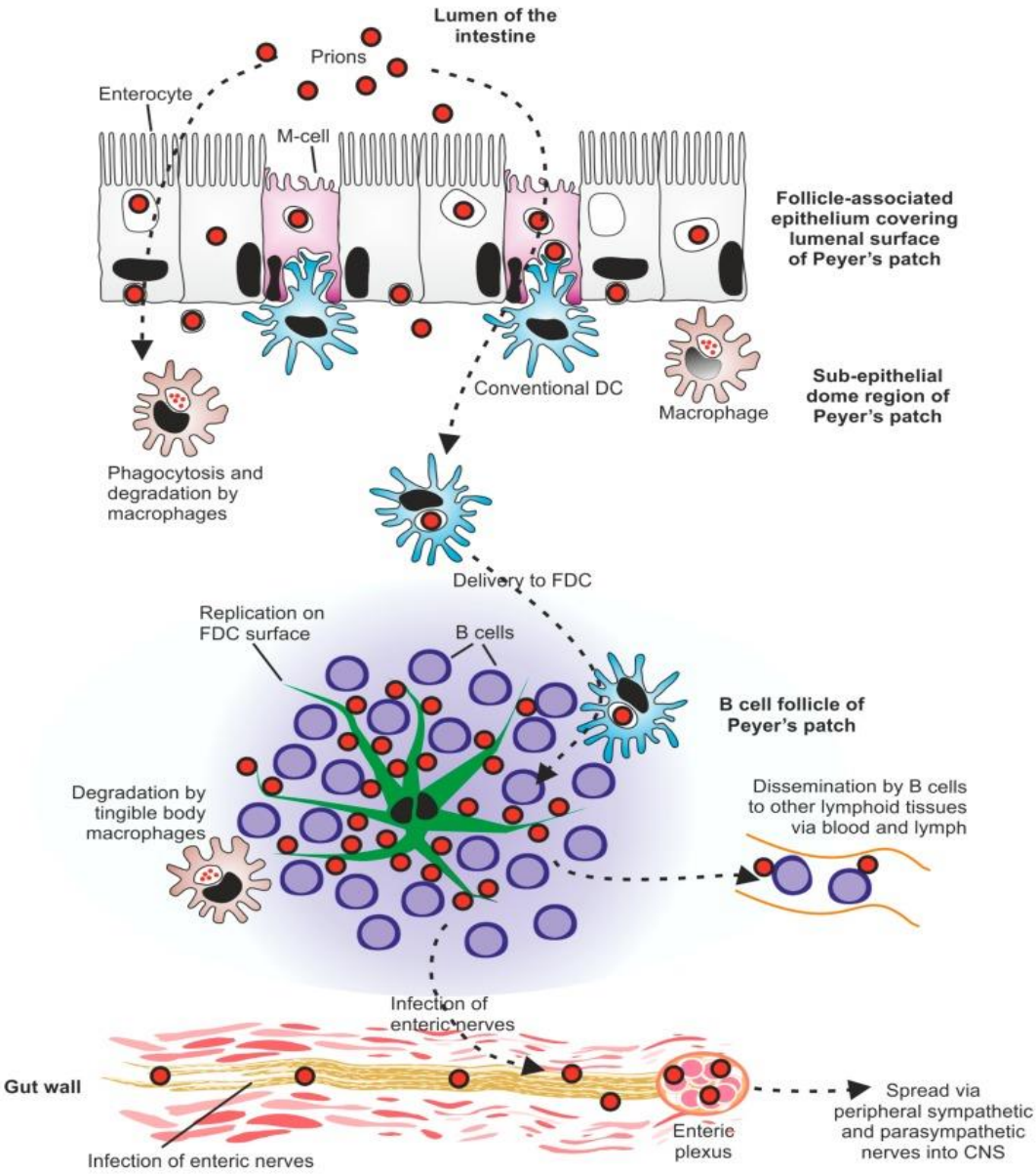

Figure 1.3: The movement of prions (PrP^{Sc}). Diagram depicting the spread of prions from the intestine to the CNS (Mabbott 2017).

particular prion strain. The circumventricular organs (CVO) are specific organs in the brain which have fenestrated capillaries and are more permissive than other areas of the brain to the passage of large molecules. They provide a two way communication between the CNS and the rest of the body (Siso, Gonzalez, and Jeffrey 2010). It has been shown that PrP^{Sc} accumulation in CVOs of sheep is an early, consistent event that is not affected by route of challenge or disease strain. This suggests that CNS entry of infectivity can occur through these structures (Siso, Jeffrey, and Gonzalez 2009). There is no evidence that the arrival of PrP^{Sc} in the CVOs is cell mediated, as WBCs are not observed in these organs at preclinical or clinical stage of disease. PrP^{Sc} is thus likely to be present in plasma, as cell free soluble molecules. Once infection is established in the CVOs, there is potential for further spread to neighbouring neural structures through efferent connections. Neuroinvasion may occur via the vagus nerve from the blood. If blood enters the area postrema or through CVOs, the neurons here would start to accumulate PrP^{Sc} immediately. It is also possible that the neurons of neighbouring structures, such as the dorsal motor nucleus of the vagus (DMNV) or the hypothalamus, to which CVOs are connected, amplify infectivity or accumulate PrP^{Sc} more rapidly hence, leading to their detection in these structures first.

Accumulation of PrP^{Sc} can be demonstrated in placenta (Andreoletti et al. 2002), mammary gland (Ligios et al. 2005), salivary gland (Vascellari et al. 2007) and kidney (Siso et al. 2006) of prion disease affected sheep. In both scrapie and BSE, PrP^{Sc} can be detected in the mesenchymal cells between collecting ducts and loops of Henle in the renal pelvis in the absence of inflammation. This indicates that the mesenchymal cells become infected from blood after filtration in the glomeruli or by extravasation from the vasa recta (Siso et al. 2008). Furthermore, PrP^{Sc} in the mammary gland and infectivity in milk is likely to derive from blood (Lacroux et al. 2008); (Konold et al. 2008). In the case of sheep with classical scrapie, prion protein may be detected in biopsies of accessible lymphoid tissue (third eyelid, tonsil, rectal mucosa) (O'Rourke et al. 2002). Infectivity and deposition of prion protein is widely found throughout lymphoreticular tissues in the preclinical phases of disease before neuroinvasion takes place (Jeffrey, Martin, et al. 2001); (Gonzalez et al. 2008); (Foster et al. 1996). In the case of sheep experimentally infected with BSE, it was possible to detect PrP^{Sc} in the spleen and Peyer's patches of ileum at 16 months post inoculation. PrP of the lymphoreticular, alimentary tract tissues and CNS could be detected at 20 months, coinciding with clinical onset (Jeffrey, Martin, et al. 2001). In cattle evidence of infection is restricted to the CNS and not shown to include lymphoid tissue (Wells et al. 1998). The pattern of neuropathological lesions remained consistent throughout the BSE epidemic (Simmons et al. 1996).

1.2 vCJD and blood borne infectivity

1.2.1 BSE epidemic and zoonotic transmission

While sCJD has been prevalent and recognised for over 100 years, vCJD was first reported in 1996 as a result of food-borne transmission of BSE. BSE or 'mad cow disease' was a direct result of continued exposure of farmed animals to feedstuffs containing infected meat and bone meal (MBM) derived from rendered carcases. The evidence for a connection between vCJD and BSE was first suggested based on epidemiology, later studies indicated that the responsible agents were identical (Bruce et al. 1997). This was shown by experimental work with mice. BSE produces a characteristic pattern of disease in mice that is retained after experimental passage though intermediate species (Fraser et al. 1992); (Bruce et al. 1994); (Foster et al. 1996). Bruce et al. (1997) was able to show this distinct pattern was exhibited by both mice with vCJD and mice with BSE, they displayed similar neuropathology, incubation periods and lesion profiles. The link between vCJD and BSE was also demonstrated by similarities in the histopathological pattern of the disease transmitted to macaques (Lasmezas et al. 1996). This demonstrated that vCJD is a unique prion disease since is it an acquired infection across a species barrier. The most likely primary source of vCJD is by the oral route with BSE contaminated meat products. A number of laws were introduced as safety precautions, including bans on specified bovine offal (SBO) in 1989. Legislation ended UK production of mechanically recovered meat (MRM), in December 1995 and of head meat in March 1996 (Cooper and Bird 2003).

There have been 230 vCJD cases reported in 12 countries, with the majority in the UK (178) and France (27) (Seed et al. 2018); (NCJDRSU 2017). In the UK, the median age at the onset of the disease was 26.5 years and the median age at death 28 years (compared to 67 years and 68 years respectively for sCJD). The youngest case was aged 12 years at onset while the oldest case was aged 74 years. From year to year the numbers of new cases of vCJD fluctuate. Data from the National CJD Surveillance Unit suggest that since 2001 incidences of vCJD in the UK are declining (with no cases reported in 2014 and 2015), thus indicating that the epidemic may be limited. Until 2015, all cases were methionine homozygous (MM) at codon 129 (Mok et al. 2017). The exception and new incidence in a heterozygous (MV) individual raises concerns about a new wave of incidence in a population of people previously thought to be resistant. It raises the question of whether vCJD infection of heterozygous individuals can establish a permanent subclinical carrier state. Although this may be not be a problem for infected individuals it could be potentially disastrous epidemiologically, leading to an unrecognized yet self-sustaining epidemic (Aguzzi and Glatzel 2006).

To date, there have been 4 instances of vCJD as a result of transmission of prion infection by blood transfusion. These were identified through follow-up of the 66 traceable recipients of blood components from 18 UK blood donors who went on to develop vCJD (Hewitt et al. 2006). All 4 cases resulted in transmission following transfusion of non-leucodepleted red cells. The first recipient (Case 1) developed symptoms of vCJD 6 years after receiving a transfusion of blood donated 3 years before the donor (Donor 1) developed symptoms of vCJD (Llewelyn et al. 2004). The second recipient (Case 2) died from a nonrelated cause 5 years after receiving blood from a donor (Donor 2) who subsequently developed vCJD. This was the first recorded case of autopsy detected subclinical infection in the UK (Peden et al. 2004). The third recipient (Case 3) developed vCJD symptoms 7 years after receiving a transfusion of blood donated around 21 months before the donor (Donor 3) developed symptoms of vCJD (Wroe et al. 2006). The fourth recipient (Case 4) developed vCJD symptoms 8 years after receiving blood donated about 17 months before the donor (Donor 3) developed symptoms of vCJD (NCJDRSU 2013). Another case, identified by testing the spleen post mortem, was a haemophiliac patient who received plasma derivatives from a donor who developed vCJD 6 months after donating blood. The patient had the 129 MV genotype and died from an unrelated cause (Calizzani et al. 2014).

1.2.2 Subclinical prevalence of vCJD

It may be the case that a vast number of asymptomatic vCJD carriers exist in the UK population. The existence of a chronic, asymptomatic carrier state is an unavoidable consequence of the typically long incubation periods of prion diseases, which vary from months to decades. Anyone who contracted the infection but failed to exhibit clinical signs and symptoms may be considered as a ‘silent carrier.’ It is conceivable that they will develop the disease in due course (perhaps being triggered by a specific event) or that the carrier state would persist for an indefinite period of time in which case they may be regarded as ‘permanent subclinical carriers.’ Thus, ‘subclinical’ implies that a patient will never develop clinical disease. Contrastingly, the term ‘preclinical’ refers to a person (or animal) before they start to show signs of disease.

Studies in rodents, where immune deficient mice are exposed to prions, indicate that the permanent subclinical carrier state may be a common phenomenon (Frigg et al. 1999). However, mice do not have to be immunodeficient to exhibit this subclinical carrier state (Hill and Collinge 2003). Zlotnik and Rennie (1963) have shown that transmission of scrapie to mice via the intragastric route resulted in no clinical signs (as observed after 13 months). Passaging of brain and spleen pools from these subclinical cases into further mice, resulted

in their development of clinical disease at 6 months. The existence of human hosts incubating the infectious agent for months to decades without exhibiting any symptoms is a significant challenge for diagnosis and surveillance. The possibility that such patients may be unknowingly passing the infection on to others is a major public health concern. Attempts to accurately judge the magnitude of this issue are hindered by it being impossible to quantify the number of subclinical individuals without a durable preclinical test and thus, the level of risk to recipients of blood transfusion. This also impacts on implementation of effective hazard management strategies. Consequently, the vCJD epidemic may be prolonged, or in a much worse scenario, vCJD may become endemic and self-sustained (Aguzzi and Glatzel 2006).

The prevalence and geographical distribution of subclinical vCJD is still unknown. The age of disease onset has not changed across the last 2 decades. This suggests that there has been a cohort of individuals exposed to infection over a specific time frame. This suggests an existence of age related susceptibility or exposure between the ages of 10-20 years, individuals who would now be between 30 and 55 years (Cooper and Bird 2003). Studies on archived, paraffin embedded appendix tissue samples (looking for abnormal prion protein) give an indication of the carrier status of the UK population. This was deemed a suitable test based on the knowledge that extensive lymphoreticular involvement is a characteristic of symptomatic vCJD (Hill et al. 1999); (Ironside et al. 2002). PrP^{Sc} was also detected in appendectomy samples removed from two patients prior to the onset of vCJD symptoms (Hilton et al. 1998; Hilton et al. 2002). The first retrospective study reported an estimated prevalence in 1 in 4000 individuals with abnormal PrP in their appendixes (with 3 positive specimens identified) (Hilton et al. 2004). Another study was implemented between 2007 and 2011 to analyse tonsils by two independent immunoassays, immunohistochemistry and Western blot. Here 150,000 tonsils were tested and none were positive (de Marco et al. 2010). The appendix study was repeated between 2000 and 2012, with samples being screened by immunohistochemistry. Out of 32, 441 samples from patients born between 1941 and 1985, 16 were positive. Patients in this time period were tested as they would be the generation potentially exposed to BSE in the food chain. (Gill et al. 2013a). A weakness of this study however, is that the period of human exposure to BSE may be more extended than previously thought. Additionally, although vCJD occurs more commonly in the younger age groups, reactive appendix samples were found across all age groups. From this it may be hypothesised that many healthy people could exhibit peripheral PrP^{Sc} accumulation in their appendix. Thus a third appendix tissue study was initiated to look at samples outside of the presumed BSE exposure period (before 1980 and after 1996) (PHE 2016), (Gill et al. 2020). As positive samples were found in both groups examined it does not clearly answer the question of whether abnormal prions detected by immunohistochemistry in the British population is limited to those exposed to the BSE epidemic. It may actually be that there is a

low background of PrP^{Sc} in appendices unrelated to intensity of exposure to BSE or that human exposure began in the late 1970s and continued until the mid-90s (Seed et al. 2018).

1.2.3 Prevention of infection

In the UK about 2.1 million units of blood components are transfused each year. This includes red cell concentrates for patients with haemorrhage or anaemia and platelet concentrates for patients with acute or chronic thrombocytopenia at risk of bleeding. To implement risk minimization for spread of vCJD, as of 1998 all blood donations are filtered to remove white blood cells (WBCs), leaving < $1x10^6$ leucocytes per pack. This was based on the detection of leucocyte associated infectivity in prion disease rodent models (Brown et al. 1998). It has been demonstrated that leucodepletion of red blood cells (RBCs) provides a major reduction in disease transmission. Lacroux, Bougard, et al. (2012) demonstrated that with the PG127 sheep infection model transfusion of standard RBCs (prepared from 400 mL of blood) transmitted the disease with 100% efficiency. In comparison, only one out of the five recipients of the leucodepleted RBCs had any evidence of infection when culled. However these results are in contrast to the findings by McCutcheon et al. (2011). In this study sheep were orally infected bovine BSE infected brain homogenate. Blood and blood components were then prepared with commercially available leucodepletion filters to the same specifications as required for routine transfusion medicine. It was demonstrated that all blood components could support prion disease transmission by blood transfusion. Strikingly, following leucodepletion, infectivity titres were still sufficient to transmit BSE. Little difference was seen in the incubation period in recipients of paired non-leucodepleted plasma and red cells with their leucodepleted equivalents.

Further studies have demonstrated that positive transmission can be achieved in non-human primates from blood products from both symptomatic and non-symptomatic infected donors. Nineteen macaques were transfused with leucodepleted blood products (RBCs and plasma) from primate donors with high levels of peripheral PrP^{Sc} after being exposed to vCJD. Five of the macaques developed typical vCJD phenotype and had detectible PrP^{Sc} in lymphoid organs as confirmed by Western blot detection. The results confirmed the transmissibility of vCJD by transfusion in primates (Comoy et al. 2017).

As well as implementing leucodepletion of all blood used for transfusion, a number of other precautionary measures were taken to limit the risk of potential vCJD transmission and protect the UK blood supply. In 1997, blood components or tissues obtained from any individual who later developed clinical vCJD were withdrawn from use. In 1999 it was ensured that all plasma derivatives used in the UK were manufactured using only donations from countries with a low risk of vCJD. In 2004, following the first case of vCJD by blood

transfusion, individuals who had themselves received a transfusion since 1980 were excluded from donated blood (SaBTO 2015).

Novel diagnostic strategies, including the use of surrogate markers of prion infection alongside use of prion reduction strategies, may help to control the risk of iatrogenic prion spread through blood transfusions. A sensitive and specific, high through-put screening test would inevitably lead to disease mitigation by identifying subclinical carriers. Substantial efforts are required to make this happen. Although the initial outbreak of vCJD appears to be over, subsequent epidemic waves among those already infected are a considerable concern. Furthermore, not clearly knowing the size or extent of the subclinical population leaves a continued risk to blood safety. Thus, precautionary measures remain in place for transfusion of blood components and on going surveillance is necessary (Seed et al. 2018).

1.2.4 Transfusion study experiments

Following confirmation of CJD transmission from human blood to laboratory animals, it was suggested that extreme caution would be appropriate when blood is used for transfusion purposes. The infectivity of blood components that had been spiked with scrapie infected hamster brain cells as well as blood from mice infected with a mouse adapted GSS strain were investigated by Brown et al. (1998). Both the exogenous spike and the endogenous infectivity experiments determined that infectivity was present in plasma as well as white blood cells. Furthermore, Brown (1999) showed that in mice infected with a mouse adapted stain of GSS infectivity in the buffy coat fraction of blood was present during the preclinical phase of disease. However, 5 x more buffy coat (and 7 x more plasma) was required to transmit disease by the IV route than by the IC route.

From the human vCJD cases acquired following blood transfusion it is known with certainty that a single unit of vCJD prion infected red cell concentrate is sufficient to cause transmission of disease. This indicates that the concentration of ID_{50} units in blood is substantially high. ID_{50} is measured by end point dilution titration in mice by the IC route, it is the dilution at which 50% of mice become infected. The infectious titre of vCJD isolates in transgenic mice expressing bovine prion protein is $10^{6.33}$ (Douet et al. 2014). It is unknown whether the virulence of BSE prions are enhanced when passaged from human to human, compared to the original bovine to human situation (Aguzzi and Glatzel 2006). Passaging experiments of scrapie infectivity between mice and hamsters indicate that this is possible. Shi, Xiao, et al. (2015) determined that the passage of mouse adapted scrapie strains (ME7-ha and 139A-ha) into hamsters resulted in markedly shortened incubation times compared to

their parent mouse strains. Alternatively, Bishop et al. (2008) found no difference in transmission efficiency when inoculating HuTg mice with BSE and vCJD.

One of the first indications that prion diseases might be transmissible by blood transfusion arose from experiments performed with sheep experimentally infected with BSE or with natural scrapie (Houston et al. 2008); (Houston et al. 2000); (Hunter 2002). Sheep are a good model for this process due to the similar pathogenesis of sheep BSE and human vCJD. As is the case with vCJD infection, BSE infected sheep also harbour infection in peripheral tissues, PrP^{Sc} deposition is extensively found in the lymphoreticular system (Foster et al. 1996); (Hill et al. 1997). Another limiting factor for successful transmission of prion diseases by blood in rodent models is the small volumes of blood that can be injected. However, with sheep the volumes of blood that can be transfused are comparable to those used in human transfusion practice. Houston et al. (2008) collected blood and/or buffy coat (450-500 mL which is equivalent to 1 unit in transfusion medicine) from donors (orally infected with BSE or naturally infected with scrapie) at different time points during infection. Overall efficiency of transmission was high, 36% of recipients of blood from BSE donors and 43% of recipients of blood from scrapie infected donors became infected. The incubation period of those that received blood from preclinical or clinical donors were similar. This highlighted the possibility that disease could be transmitted from symptom free vCJD infected humans, risking the spread among the UK population.

1.2.5 Blood infectivity: Distribution of infectivity in blood components

The animal bioassay of infectivity is the only method available to directly measure the presence of the infectious agent (Ingrosso et al. 2002). Cervenakova et al. (2003) IC inoculated mice with mouse adapted strains of vCJD or GSS, blood was collected fractionated and blood components inoculated into groups of healthy mice. Brains and spleens of these mice were harvested and tested for PrP^{Sc} presence by Western blot. They found that levels of 20-30 infectious doses per mL were present in buffy coat and plasma during both the incubation and symptomatic stages of disease. Platelet pellet infectivity was lower (10 ID/mL) and RBCs were not infectious.

Transmission by infected blood and WBCs in sheep was confirmed by Andreoletti et al (2012). Andreoletti et al. (2012) determined the minimum infectious dose (ID_{50}) able to transmit prion infection in sheep by transfusion using VRQ/VRQ recipient sheep that were transfused with whole blood which had been spiked with successive 1/10 dilutions of brain homogenate prepared from sheep orally inoculated with the classical scrapie strain PG127 (Andreoletti et al. 2012). Previously brain homogenate had been titrated by end point dilution in tg338 mice, and had a titer of $10^{6.6}$ ID_{50} IC/g (Andreoletti et al. 2011). The lowest dose

resulting in transmission was observed in sheep (1 infection out of 2 challenged individuals) that were transfused with blood containing 10^3 ID_{50} IC in tg338 mice (Andreoletti et al. 2012).

This high efficiency of transmission by blood transfusion contrasts with the very low infectious titer measured by IC inoculation of blood into transgenic mice expressing ovine PrP. Infectious titre of whole blood ranged between 3 -16 ID/mL as estimated from IC inoculated into tg338 mice. Plasma and RBCs, expressed as the equivalent volume of whole blood, were estimated to have 8.6 and 2.7 ID IC in tg338 per mL of blood respectively. The infectivity in WBC was measured by end point dilution titration by IC inoculation of ten folds serial dilutions in tg338 mice and the titre determined as between 4.5 - 13.4 ID per mL (Andreoletti et al. 2012). In another experiment performed at the same time by Andreoletti et al. (2012), VRQ/VRQ sheep were orally challenged with $10^{6.7}$ ID_{50} IC in tg338 of the same PG127 brain homogenate stock. Whole blood samples were collected at the last stage of the incubation period, between 2-5 weeks before clinical onset. IV administration of 0.2ml of blood from these asymptomatic infected donor sheep was sufficient to infect the transfusion recipient with 100% efficacy. Since 0.2ml produced 100% transmission, Douet et al. (2016) performed further experiments to extend this study and further titrate scrapie infected whole blood by IV transfusion in sheep. It was then established that 0.1 mL of whole blood (but not 0.01 mL) from an asymptomatic scrapie infected donor sheep can transmit the disease (Douet et al. 2016).

Furthermore, Andreoletti et al. (2012) were able to show that freshly prepared WBCs from the same sheep have a comparable capacity to whole blood to infect prion disease free, VRQ/VRQ transfusion recipient sheep. Incubation periods of recipient sheep receiving whole blood or WBC preparations were similar, thus hinting at comparable infectious dose in both products. While all recipients of fresh WBCs succumbed to clinical disease, the IV administration of PFA fixed WBCs only resulted in infection of two out of four recipient sheep. Contrastingly, IV administration of crude plasma (100 mL) resulted in infection of only three out of four of the recipient sheep and the incubation periods were longer than those sheep who received whole blood. None of the sheep that received plasma prepared from 20 mL of whole blood were infected. The incubation periods of sheep administered PFA fixed WBCs exceeded those observed for plasma recipients. Hence, this outcome suggests that the PFA fixation partially inactivates WBC infectivity. However, when IC inoculated into tg338 mice, the same fresh and PFA WBC homogenates produced 100% attack rates with similar incubation periods.

The level of prions in blood vary in different species as well as with different prion strains (Weissmann et al. 2002). Identifying the cell phenotype or cell free protein fractions that harbour prion infectivity may contribute to greater understanding. PrP^C has been identified

on human lymphocytes, monocytes, granulocytes, platelets and red cells by flow cytometry and Western blotting (Holada and Vostal 2000). The normal cellular prion protein is strongly expressed by myeloid dendritic cells (Burthem et al. 2001). In humans, it has been shown that the majority of blood PrP^{C} is present in the plasma and platelet fraction (MacGregor et al. 1999). In terms of infectivity, Douet et al. (2014) have reported infectivity in erythrocytes, leukocytes, and plasma of an individual with vCJD. This was confirmed by IC inoculation of tgBov mice.

Infectivity of WBC subpopulations were further investigated in subsequent studies. Douet et al. (2016) showed that the IV administration of 10^5 WBCs from scrapie infected donor sheep is sufficient to cause disease in recipient sheep. Cell sorted $CD45R^+$ (predominantly B lymphocytes), $CD4^+/CD8^+$ (T lymphocytes), and $CD14^+$ (monocytes/macrophages) blood cell subpopulations were shown to contain prion infectivity as determined by bioassays in ovine PrP transgenic mice. However, although the IV administration of 10^6 $CD45^+$ or $CD4^+/8^+$ living cells was able to transmit the disease, similar numbers of $CD14^+$ cells failed to infect the recipients. Hence, mononucleated blood cell populations display different abilities to transmit prion disease by the transfusion route. Furthermore, Dassanayake et al. (2016) were able to show that scrapie prions are associated with monocytes and T lymphocytes circulating in the peripheral blood of sheep naturally infected with classical scrapie through immunohistochemistry and PMCA.

Bioassays of white tailed deer have demonstrated that all body fluids (saliva, urine, faeces and blood) contain infectious prions. Both clinical and preclinical CWD infected deer were able to cause CWD in naïve white tailed deer following transfusion of whole blood (Mathiason et al. 2009). In deer with CWD, cellular (mononuclear leukocytes and platelets) but not cell free plasma fractions of blood were shown to transmit infection. B cells from blood or retropharyngeal lymph nodes and platelets (but not CD14+ monocytes or plasma) contained PrP^{Sc} capable of transmitting CWD. This suggests a significant role for B cells and platelets in trafficking CWD infectivity (Mathiason et al. 2010). In contrast, no infectivity has been detected in blood of cattle with natural BSE or of cattle with experimental BSE (Bradley 1999).

1.3 Diagnosis of prion diseases

1.3.1 Current diagnostic methods

The clinical and pathological manifestations of genetic prion diseases can be broadly segregated into distinct phenotypes fCJD, GSS, FFI. The recognition of phenotypes is

essential for diagnosis and care. Diagnosis of genetic prion diseases require a combination of clinical feature observations (dementia, motoric incoordination, myoclonus, visual disturbances, weakness, seizures). Neuropathological findings are distinct between the three diseases. Spongiform degeneration and astrogliosis distributed throughout the cortex and deep nuclei of the brain is found in the case of fCJD. There will be multiple amyloid plaques bound by antiprion protein antibodies in GSS. While in FSS there is a lack of spongiform degeneration and presence of neuronal dropout and gliosis primarily within the thalamus and inferior olivary nucleus of the brain stem (Gambetti et al. 2003). For the genetic forms of prion disease, a family history consistent with autosomal dominant inheritance would also be indicative. Hence molecular genetic testing for a *PRNP* disease causing mutation is used.

In the case of nongenetic prion disease (sCJD) other options include use of electroencephalogram (EEG), brain imaging (magnetic resonance imaging [MRI] or position emission tomography [PET] scans) (Demaerel et al. 1999). While these tests can support diagnosis, definitive confirmation is only made by post-mortem histological and biochemical analysis of brain tissue (Galeno et al. 2017). Increases in the levels of 14-3-3 protein, neuronal specific enolase and total tau (nonphosphorylated) proteins which accompany progressive neuronal death are considered markers for nongenetic prion disease, hence, examination of cerebrospinal fluid (CSF) is considered useful (Satoh et al. 1999); (Huang et al. 2003). Clinical features of vCJD are strikingly different to that of sCJD. Most commonly, persistent and early psychiatric signs and symptoms are expressed including anxiety, withdrawal, depression or emotional lability. Sensory disturbances such as paraesthesia and painful limbs are also typical. Neurological signs appear around 6 months after the psychiatric symptoms, they include dysarthria, dysphasia, severe ataxia with falls and involuntary movements. vCJD also lasts longer than sCJD at 6-39 months and median death at 14 months (Will et al. 2000). Microscopic examination and immunohistochemistry for PrP of the brain reveals and abundance of ‘florid plaques’ in the cerebral and cerebellar cortices (Ironside and Head 2004). Unlike sCJD, PrP^{Sc} is also distributed in lymphoid tissues all over the body, from lymph nodes, tonsils and the spleen (Liberski and Ironside 2004). Tonsil biopsy using immunohistochemistry for detection of PrP^{Sc}, is additionally considered for individuals in whom vCJD is suspected (Zeidler et al. 1999).

In the case of detection for animals with prion diseases, there are a number of commercially available kits for post mortem testing. In Europe, the most widely used BSE tests typically performed on brain samples are the Prionics-Check Western test (Western blot for PK resistant prion protein) and the BioRad Platelia test (ELISA detection). In total, about 8 million BSE tests are performed per year, however the requirement to test healthy slaughtered cattle for BSE in the UK ended in 2013 (FSA 2017).

One difference between sheep scrapie PrP^{Sc} and bovine BSE PrP^{Sc} is in the proteinase K cleavage sites and thus the size of PrP27–30 (with scrapie PrP^{Sc} having a slightly larger fragment). Detection of this has been established by development of an antibody against the sequence lying between the two proteinase K cleavage sites. The presence of a signal, using this antibody on Western blot suggests sheep scrapie PrP^{Sc} while the absence suggests the presence of BSE PrP^{Sc} (Stack, Chaplin, and Clark 2002). Furthermore, scrapie PrP^{Sc} is deposited in the rectoanal mucosa-associated lymphoid tissues (RAMALTs) of infected sheep relatively early in the course of infection (Espenes et al. 2006). Hence, samples from this site can be used to diagnose preclinical scrapie in sheep (Gonzalez et al. 2008). The examination of RAMALT biopsy specimens for the diagnosis of prion disease has been described in elk, and small numbers of mule and white tailed deer too (Keane et al. 2009). Ante-mortem evaluation of tonsil biopsy specimens have also been used to determine preclinical CWD in deer (Schuler et al. 2005).

1.3.2 Blood screening methods

A validated screening test for preclinical vCJD carriers is much sought after for the significant protection it would offer. However, there are major challenges that exist. For instance, there is a lack of samples from subclinical vCJD individuals to validate assays. Animal models are the only means by which preclinical samples may be generated (Sawyer et al. 2015). Additionally, there is a need to detect the very low concentration of PrP^{Sc} likely to be present at the preclinical stage of disease. For methods based on PrP^{Sc} detection, PrP^{Sc} needs to be detected against a high background of PrP^{C}. However, most antibodies do not discriminate between them. Some example initiatives include use of a 15B3 prion specific antibody developed by Prionics and a Seprion resin manufactured by Microsence. Both methods concentrate PrP^{Sc} so it can be detectable by ELISA and flow cytometry (Korth, Streit, and Oesch 1999). Grosset et al. (2005) also designed fluorescent labelled palindromic peptides to discriminate between PrP^{C} and PrP^{Sc}, when binding occurs the shift in confirmation modified the fluorescent properties of the label.

As well as the low concentration of PrP^{Sc} in blood, a possible reason for poor detection is aggregate size, solubility, and protease resistance. In comparison to blood, the brain is a solid organ that permits aggregate accumulation on and within infected nerve cells. It has been proposed that the large amyloid fibrils that characterize prion diseases are protective, rather than pathological, by sequestering more hazardous subfibrillar oligomers into comparatively innocuous deposits (Treusch, Cyr, and Lindquist 2009). Hence, the small subfibrillar oligomers are actually the principal causes of disease, probably by providing an increased number of multiplication seeds. Silveira et al. (2005) assessed PrP^{Sc} containing

aggregates by their size, infectivity and converting activity. To do this they disaggregated PrP^{Sc} from scrapie-infected hamster brain, sonicated and separated by size through filtering and asymmetric flow field fractionation. The samples were then analysed by light scattering and non-denaturing gel electrophoresis. Their results suggested that the most efficient initiators of prion diseases are non-fibrillar particles, 14-28 PrP molecules in mass. If this is the case and smaller aggregates are the predominant form of PrP^{Sc} found in the blood, it would indicate that PrP^{Sc} of the blood is more infectious than brain derived PrP^{Sc}.

Thus, while blood is highly infectious the amount of PrP^{Sc} in the blood is very low and additional amplification steps are required for efficient detection (Saa, Castilla, and Soto 2006). Such procedures include protein misfolding cyclic amplification (PMCA) and real time quaking induced conversion (RT-QuIC). PMCA relies on a small amount of abnormal PrP^{Sc} (the seed) to convert excess normal PrP^{C} (the substrate) following incubation. Repeated rounds of sonication break down the growing chains giving rise to a rapidly increasing amount of abnormal protein available to trigger conversions. PMCA has been reported to have great sensitivity and specificity. Following one round of 96 PMCA cycles (2 days) PrP^{Sc} at up to 100 million-fold (10^{8}) dilution of vCJD brain tissue was detectable. After two rounds, 10 billion-fold (10^{10}) dilution could be reached (Moda et al. 2014). PMCA is a highly efficient technique, which has been used to identify PrP^{Sc} in the blood of early preclinical to terminally ill stages of disease in scrapie and BSE infected sheep (Halliez et al. 2014; Lacroux et al. 2014). Furthermore, Concha-Marambio et al. (2016a) used PMCA to analyse blood from 12 cases of vCJD and 153 controls (including healthy control as well as patients with sCJD and other neurodegenerative conditions). There results show PrP^{Sc} could be detected with 100% sensitivity and specificity in blood samples from vCJD patients. Bougard, Brandel, Belondrade, et al. (2016) were able to identify 18 patients with clinical vCJD among 256 French and British plasma samples with 100% sensitivity and specify. Importantly, this method was also accurate for blood samples from two individuals 1.3 and 2.6 years before development of clinical symptoms.

RT-QuIC employs multiwall plates and a thioflavin T (ThT) based fluorescence detection of the prion-seeded amyloid. The assay involves cycles of vigorous shaking and incubation, during incubation PrP^{Sc} acts as a seed inducing conformational changes in *E.coli* expressed recombinant PrP (recPrP) substrates integrating them into a growing amyloid fibril. These aggregates may then be detected with fluorescent plate readers using the amyloid sensitive ThT dye. One advantage of RT-QuIC over PMCA is that the agitation can be performed more easily and consistently than sonication, which has varied delivery of the vibrational energy to samples (Atarashi et al. 2011). A major difference between the two techniques is that PMCA amplifies prion infectivity, while RT-QuIC products do not appear to be infectious (Groveman, Raymond, et al. 2017). RT-QuIC has been used to analyse whole blood

collected from deer and hamsters inoculated with CWD brain material, throughout disease incubation in time course studies. PrP^{Sc} could be detected in the blood of animals, within minutes following exposure to the inoculum. Detection dropped at the middle stage of infection but rose again during the late stage, coinciding with neuroinvasion (Elder et al. 2015). Orrú et al. (2011) is another study of RT-QuIC on blood, here an additional antibody based immunoprecipitation step was used to enhance detection. This method allowed for detection in 10^{14} fold serial dilutions of brain material spiked into plasma.

The Direct Detection Assay (DDA) is an alternative to both PMCA and RT-QuIC, with the potential to be sufficient for clinical sensitivity at the early stages of preclinical prion disease. It works with the use of a solid state, steel binding matrix to capture and concentrate PrP^{Sc} which is then detected immunologically using ELISA. Through rodent studies, Sawyer et al. (2015) have shown that DDA has an analytical sensitivity equivalent to a 109-fold dilution of prion infected brain material. Edgeworth et al. (2011) was able to detect PrP^{Sc} in blood from 15 symptomatic patients with 70% sensitivity and 100% specificity, which is almost as effective as diagnosing sCJD using CSF samples (Atarashi et al. 2011). Jackson et al. (2014) detected PrP^{Sc} in a study of blood samples from national blood collection and prion disease centres of the US and UK. This is coupled with direct immunodetection giving specificity of 99% for vCJD infected blood samples.

1.3.3 Detection of preclinical infectivity in blood

In terms of identifying preclinical prion disease, PMCA is the most widely accepted technique for research purposes, although it is not currently being used as a diagnostic test. The method is highly specific for the detection of PrP^{Sc} with a several million fold increase in sensitivity compared to that of standard Western blot assays (Castilla, Saa, and Soto 2005). After amplification, PrP^{Sc} was detectable in the blood of hamsters experimentally infected with scrapie at the early preclinical phase of the disease (Saá, Castilla, and Soto 2006); (Soto et al. 2005). Sawyer et al. (2015) were able to use DDA to consistently detect preclinical infection using wild type CD1 mice experimentally infected with the Rocky Mountain Laboratory (RML) scrapie strain. In both studies, the methods showed higher detection sensitivity early in the preclinical stage of the incubation period when blood was less infectious. Thus, it is important to note that PrP^{Sc} levels do not always reflect the titre of infectivity in blood.

Lacroux et al. (2014) tested the sensitivity of PMCA with the vCJD/BSE model of disease. In both sheep and primates, the assay enabled identification of infected individuals in a very early stage of the asymptomatic incubation phase. Bougard, Brandel, Belondrade, et al. (2016) further proved the sensitivity of PMCA by using the technique to detect silent carriage

of prion 1.3 and 2.6 years before clinical onset in two donors who later developed CJD. This was performed on archived plasma. It has also been suggested that WBCs are the most appropriate targets for preclinical detection by PMCA. Lacroux et al. (2014) were able to use buffy coat samples from macaques IV challenged with vCJD brain homogenate or blood from a clinically affected vCJD macaque to seed PMCA reactions. When using WBCs as a template, the method enabled identification of vCJD/BSE in asymptomatic experimental animals in the early phase of the incubation period. Concha-Marambio, Chacon, and Soto (2020) also used PMCA to detect prions in blood during the preclinical stage of infection in vCJD infected macaques, as early as 2 months postinoculation, without false positives from noninfected animals. Additionally, Halliez et al. (2014) investigated blood components as PMCA seeds, the seeding ability of platelets was weaker than that associated with WBCs, hence WBCs are potentially more infectious.

The detection of PrP^{Sc} varies at different times throughout the incubation period. Peripheral administration of prions results in initial replication in lymphoid tissues and the spleen (Kimberlin and Walker 1979); (Glatzel and Aguzzi 2000). Thus, the rise of PrP^{Sc} in blood during the early preclinical phase is considered to coincide with the time of its replication in lymphoid organs. The reduction of PrP^{Sc} in blood occurs when infectivity in peripheral tissues has reached a plateau and starts to migrate to the brain. It is possible that the proportion of PrP^{Sc} carrying lymphocytes in circulation is much higher during the exponential phase of peripheral replication than during the stationary phase. Studies on the pathogenesis of mouse scrapie show that high quantities of PrP^{Sc} appear in the brain only a few weeks before onset of clinical signs (Kimberlin and Walker 1979). In comparison, Jeffrey, Ryder, et al. (2001) orally infected sheep with brain tissue from BSE infected cattle. The results suggested that in some BSE infected sheep, neuroinvasion occurred in the absence of detectable PrP accumulation in visceral tissue or peripheral nervous system. The detection of PrP^{Sc} in blood at the symptomatic phase of the disease may also be due to disruption of the blood-brain barrier resulting in leakage of cerebral proteins into the blood (Banks 1999). Prion disease causes extensive brain degeneration by neuronal death, synaptic alterations and changes to the brain (Castilla, Hetz, and Soto 2004). All of which may impact on the blood-brain barrier, allowing movement of PrP^{Sc}, which at this time would be highly abundant in the brain (Saá, Castilla, and Soto 2006).

As the incubation period may last several decades, it is unknown how many people may be in an asymptomatic phase of vCJD. Additionally, it is possible that some infected patients may never develop clinical symptoms but will remain in a carrier status with potential to transmit to other individuals. The ideal blood based diagnostic test for prion diseases would be specific, efficient and reliable. It would need to be able to detect individuals premortem, throughout the incubation period and have the ability to be vastly scaled up to screen the

large numbers of blood donations. Within the UK approximately 2.5 million units of blood are transfused each year (NICE 2015); (NHS 2018). Screening with PMCA is not feasible. It a technically challenging technique, with a long incubation time, which limits its routine use. The absence of screening tests and effective therapies to treat this disease are barriers in preventing further infections. A possible alternative to detection of prions in blood is looking at alternative biomarkers for infection.

1.3.4 The search for alternative biomarkers of prion infection

The European Medicines Agency (2001) defines 'biomarkers' as measurable characteristics that reflect physiological, pharmacological or disease processes. There are genomic, transcriptomic, proteomic and metabolomic models for biomarker discovery. Omic investigations lend themselves to biomarker discovery as they investigate multiple molecules simultaneously. Surrogate markers that are currently in use for patients with clinical signs of CJD, include 14-3-3, tau, apolipoprotein E and cystatin C (Van Everbroeck, Boons, and Cras 2005); (Otto et al. 2002); (Burkhard et al. 2001). High levels of 14-3-3 proteins present in patient CSF is a criteria for suspected sCJD to be upgraded to probable sCJD (Herbst et al. 2009). Additionally, neurofilament light polypeptide (Nfl) has been shown to be elevated in serum of patients with sCJD but further work is required for its potential role in monitoring disease progression (Thompson et al. 2018); (Mok and Mead 2020).

1.3.4.1 Transcriptomic studies

Transcriptomics is the study of the transcriptome or total messenger RNA (mRNA) within a cell or organism. The transcriptome reflects those genes that are actively expressed at a given time point as the mRNA (with the noncoding introns spliced out) is the template for protein synthesis during translation. Transcriptional profiling has enabled the more precise characterization of cell lineage and cell state genetic profiles (Lowe et al. 2017). In regards to prion disease biomarker research, many studies focus on gene expression in brain tissue using DNA microarrays and subtraction hybridization, but it likely that any subtle transcription alterations that occur in neurons at the onset of disease are masked. For example, Almeida et al. (2011) identified 966 differentially expressed genes in the medulla following oral infection of cattle with bovine spongiform encephalopathy. Analysis of 14 genes revealed that prion infection may cause dysfunction of several different networks. These networks include extracellular matrix, cell adhesion, complement and coagulation cascades, MAPK signalling and the transforming growth factor (TGF) beta signalling pathways.

Riemer et al. (2004) identified 114 genes with altered expression patterns in the diseased brains of scrapie infected mice. The data demonstrated the presence of a strong inflammatory reaction and stress response, which also relate to gene expression patterns found in brains of individuals affected by AD and aging (Zhang et al. 1999). Xiang et al. (2004) analysed the gene expression profiles from brains of mice IC inoculated with scrapie strains ME7 and RML. They discovered 121 genes with a twofold increase in expression in both ME7 and RML infected mouse brains. These genes encode proteins involved in proteolysis, protease inhibition, cell growth and maintenance, the immune response, signal transduction, cell adhesion as well as molecular metabolism. A further study by Xiang et al. (2007) revealed altered cholesterol metabolism during the neurodegeneration in mouse scrapie (ME7) model. Functional analysis showed that the most affected biological process was cholesterol metabolism and that this was indicated to be inhibited in diseased brains. Brown et al. (2005) identified 78 genes that were differentially expressed greater than 1.5-fold within the preclinical ME7 infected hippocampus prior to the late stage glial cell activation. Further analysis revealed oxidative and endoplasmic reticulum (ER) stress, activated ER and mitochondrial apoptosis pathways, and activated cholesterol biosynthesis were involved at this stage of the disease.

Sawiris et al. (2007) identified 296 differentially expressed genes in brain tissue from mice with late stage BSE. The genes were found to be associated with ubiquitin function, lysosomal function, molecular chaperoning of protein folding, apoptosis, calcium ion binding, zinc ion binding or regulation of transcription. Skinner et al. (2006a) investigated cDNA microarray to profile gene expression changes in the brains of mice infected with two strains of scrapie (ME7 and RML). They highlighted a core group of 349 prion related genes that consistently showed altered expression in mouse models. Functional analysis revealed protein synthesis, inflammation, cell proliferation and lipid metabolism pathways. They found that the key interaction partner for these prion related genes was the regulatory cytokine TGFB1. They also discovered that the majority of genes expressed in neurons were down regulated and involved in regulatory pathways such as synapse function, calcium signalling, long term potentiation and ERK/MAPK signalling. Hwang et al. (2009) determined gene expression throughout disease progression in the brains of eight distinct mouse prion strain combinations. They identified 333 differentially expressed genes and mapped them into functional pathways and networks in an attempt to reflect the definitive neuropathological events taking place. The novel functions shared by the differentially regulated genes include leukocyte extravasation, androgen metabolism, phospholipid metabolism, microglial activation, calcium signalling pathways and haematopoiesis.

Barbisin et al. (2014) conducted large-scale transcriptional profiling of brains from BSE infected cynomolgus macaques. They found 300 transcripts with expression changes greater

than twofold. Out of the 86 genes with known functions, bioinformatics analysis showed most were involved in cellular development, cell death and survival, lipid homeostasis, and acute phase response signalling. The microarray analysis of brain tissue from patients with sCJD by Xiang et al. (2005) resulted in identification of 79 upregulated and 275 downregulated genes, which showed at least 1.5- and 2-fold changes, respectively. Major alterations included prominent upregulation of the genes encoding immune and stress response factors and significant downregulation of genes encoding synaptic proteins. However, further characterization of these genes are crucial in understanding the basis of prion disease pathological processes. The common feature of these prion disease transcriptomic studies on brain tissue is the identification of changes occurring in pathways to go with immune response, acute phase response and metabolism.

In place of studying brain tissue for potential genetic changes relating to prion disease, some studies have focused on other tissues. This is because studying changes in lymphoid tissues or blood is also more likely to be useful for identifying potential biomarkers related to preclinical infection, while identifying changes in the brain may result in detecting changes due to neurodegenerative processes that are not specific to prion disease. Kim et al. (2008) identified 14 genes with altered expression prior to the onset of clinical symptoms in spleens of mice infected with ME7, 22L and RML-Chandler scrapie strains. The function of these genes included cellular process of immunity, the endosome/lysosome system, hormone activity, and the cytoskeleton. Following oral inoculation of lambs with scrapie, cDNA from the ileal Peyer's patch were used to study gene expression profiles by Skretting et al. (2004). They were able show differential expression of 23 genes, the genes shared homologies with genes encoding proteins involved in the mitochondrial ATP production. Filali et al. (2014) performed gene expression profiling of mesenteric lymph nodes from sheep with natural scrapie. They found a total of 105 genes that were differentially expressed with a twofold change in expression. Of these, 43 were upregulated and 62 downregulated. The genes were largely associated with focal adhesion, PPAR signalling and ECM-receptor interaction.

There is a highly diverse cell population circulating within blood, a potential route to overcome the hurdles of biomarker discovery when examining blood is to isolate specific cell populations and use these as a basis for gene or protein profiling studies. Brown et al. (2007) analysed blood by qPCR from sheep experimentally infected with scrapie to investigate the extent of differential expression of *ERAF* (erythroid-associated factor) in order to explore the role of erythrocytes in prion disease. However, the results revealed that the extent of differential expression of erythroid genes within peripheral blood is not sufficient to provide a discriminatory diagnostic test. After exploring the gene expression profiles of WBCs from cattle orally infected with atypical BSE, Panelli et al. (2011) discovered that there was significant modification of genes linked to T and B cell development and activation.

Identifying other biomarkers associated with prion infectivity in blood may help in understanding the molecular mechanisms underlying prion disease pathogenesis and the pathways critical for disease progression. This would allow for a more rigorous and specific blood test to be developed and may reveal potential targets for intervention. Xerxa et al. (2016) performed microarray analysis in whole blood of atypical BSE infected cattle and revealed 32 differentially expressed genes to be in common between clinical and preclinical stages of disease. The study highlighted that immune response and metabolism pathways may play an important role in peripheral prion pathogenesis.

Additionally, microglial transcriptional changes and upregulation of interferon sensitive genes have been detected at the very early stages of CJD infection, well before the PrP^{Sc} and clinical signs (Baker, Lu, and Manuelidis 2004). In another study, (Huzarewich et al. 2011) found that a total of 1753 transcripts exhibited fold changes greater than three in FDCs, dendritic cells, and macrophages isolated from the spleens of prion infected versus uninfected mice. The gene for leucine-rich proteoglycan decorin (DCN) was found to be one of the genes most overexpressed in infected mice, furthermore the levels were mirrored in mice infected with scrapie as well as BSE and vCJD. Genes related to iron metabolism and homeostasis were significantly decreased in infected spleens, these pathways have been previously implicated in prion pathogenesis of the brain (Singh et al. 2009); (Greenough, Camakaris, and Bush 2013); (Andersen, Johnsen, and Moos 2014). The common pathways identified as important in prion disease of these transcriptomic studies on non-brain tissue are the immune response and metabolism.

1.3.4.2 Proteomic studies

Proteomics is the large-scale study of all the proteins expressed in a cell, tissue or organism with the aim to understand their functional relevance by studying biological pathways and networks (Cho 2007). Proteomic studies for prion disease often focus on brain tissues, the biomarkers found highlight neuropathogenesis mechanisms. Moore et al. (2014) identified 1,567 proteins from RML mice infected and uninfected brain homogenates. Ingenuity pathway analysis (IPA) of the top 100 ranked proteins show the molecular and cellular functions affected in disease state. This includes elevated lipid transport and metabolism, fatty acid metabolism, molecular transport and cell-to-cell signalling but disruption in vesicle transport and metal binding. Choi et al. (2016) identified152 differentially expressed proteins in ME7 scrapie-infected mouse brains. Biological analysis of upregulated proteins reveal major functions that relate to neuronal processes (cell-to-cell signalling, synaptic transmission) as well as metabolic pathways (acyl-CoA synthetase, glycolysis, oxidative reduction processes). The hippocampal proteome of ME7 mice was investigated by Asuni et

al. (2014), out over 200 proteins individual proteins 8 were identified based on a 2-fold change cut off, 4 were components of astrocytes. In human prion disease the brain proteome was analysed by Shi, Chen, et al. (2015) who identified 379 commonly differentially regulated proteins in cerebellum tissues of CJD, FFI and genetic CJD patients. The significant biological categories affected include oxidative phosphorylation and metabolism.

Chen et al. (2014) assessed the differential protein expression in CSF of sCJD patients. They found 437 proteins, 49 proteins within the 95% confidence interval. Of these 12 were upregulated and 13 were downregulated significantly. The most affected pathways of the differentially expressed proteins in CSF of the sCJD patients were complement and the coagulation cascade, followed by metabolism (glycolysis and gluconeogenesis). Proteomic studies have also been performed on easily accessible body fluid. Simon et al. (2008) identified disease-induced biomarkers in the urine of BSE infected cattle (from a range of time points during disease progression). Five unique proteins were identified including clusterin and cathelicidin1. Plasma samples from asymptomatic RML infected mice were investigated by Wei et al. (2011a) in a quantitative proteomic approach. Overall 708 proteins were identified, 53 with a 2-fold increase and 58 exhibiting 2-fold decrease. Proteins that were significantly upregulated included those to do with the immune system and metabolism. Metabolism is a reoccurring theme of these proteomic studies on prion disease.

1.3.4.3 Metabolomic studies

Metabolomics is the study of metabolites (low molecular weight compounds that participate in metabolic reactions) present in a cell or organism under a given set of conditions (Liu 2019). Bourgognon et al. (2018) analysed the brains of mice infected with RML scrapie revealing disease related alterations in neuronal metabolism, 141 biochemicals (out of 498) were significantly altered by prion infection. Those functions affected included glucose tolerance, glycolysis, sphingolipid signalling and inflammation signalling. Although there have not been many published metabolomic studies performed on prion disease biomarker discovery there has been a considerable amount of research done on the influence of the microbiome in pathogenesis of neurological disorders (Sampson et al. 2016); (Minter et al. 2016); (Donaldson and Mabbott 2016). The gut microbiome has proven crucial for several metabolic and immunological functions, as well as involvement in brain development and specific interactions with the enteric and central nervous systems (Ogbonnaya et al. 2015); (Fung, Olson, and Hsiao 2017). In one study, Xu and Wang (2016) showed a positive correlation between around 50 microbial metabolites and AD early age of onset and cognitive decline. They identified a total of 27 genetic pathways associated with AD

biomarkers, including pathways related to axon guidance, immune systems, neurone signalling and lipid metabolism.

1.3.4.4 Challenges of Omic studies

The key aspect of genomic, transcriptomic, proteomic and metabolomic studies is that a complex system can be understood better if considered as a whole. They differ from traditional hypothesis driven studies, by instead using holistic approaches where no hypothesis is applied but all data acquired is analysed to generate and define hypothesis that may be further tested (Kell and Oliver 2004). Although advances have been made in omic fields, this non-targeted and non-biased manner results in datasets on expression levels of thousands of genes, proteins or metabolites. Clearly this is a huge challenge for commonly used statistic methods, in subtraction of background noise and normalisation of data (as well as reproducibility) to allow comparison between different experiments. However technology and software are still evolving, holding promise for progression.

One great challenge of genomic research is to enable mechanistic dissection of biological processes on a high through-put scale. Transcriptomics by microarray or RNAseq (RNA sequencing) is now in frequent use. Analysis of mRNA provides direct insight into cell specific gene expression features by recognising the presence or absence of a transcript and quantifying it, but also by identifying single nucleotide polymorphisms (SNPs), allele specific expression and gene fusions. Such information is fundamental for understanding the cellular dynamics and how changes in the transcriptome profiles affect health and disease (Manzoni et al. 2016). However, the process is not without limitations. Specifically gene expression microarrays measure the changes seen in mRNA abundance and not the corresponding protein, thus there are restrictions over the interpretation of such data.

The proteome is a dynamic reflection of both genes and the environment. Proteins are ubiquitously affected in disease and disease response, hence it is thought that the proteome holds particular promise to the discovery of biomarkers. This is reflected in the protein disease biomarkers already in use. An important consideration when comparing proteomic studies to those of the genome or transcriptome is the vast increase in potential complexity. The 4-nucleotide code of DNA and mRNA are translated into a complex code of 20 amino acids. To form a final functional protein the primary sequence of peptides (of varying lengths) may be folded into a large number of possible confirmations with chemical modifications (such as phosphorylation, glycosylation and lipidation). Additionally, multiple isoforms of the same protein can be derived from alternative splicing (Manzoni et al. 2016). These degrees of variation contribute to the heterogeneity of the proteome (at any given time) and while a

great deal of information may be obtained through proteomic investigations analysis is challenging. Furthermore there are technical issues, such as the inability to accurately detect low abundant proteins, mass spectrometry bias towards identification of peptides with high concentrations, the lack of uniformity across research groups can lead to differences in protein fragmentation or differences in algorithms used to run analysis and integration with genomics data (Bell et al, 2009).

The advantage of studying the global metabolite profiles in a cell tissue or organism in metabolomics is that the metabolome is the final downstream product of gene transcription. Therefore, changes in the metabolome are amplified relative to changes in the transcriptome and the proteome. While the metabolome contains the smallest domain (~5000 metabolites), it is more diverse with many different molecules making it physically and chemically complex (Wilson's 2008). Since metabolic pathways are largely conserved between species, is a key tool for translating results from cellular and animal models to human (Bourgognon and Steinert 2019). However, there are some critical limitations to this field such as the need to improve analytical techniques to detect and process results, the on going production of population specific reference metabolomes and the incomplete understanding of the biological role of all detectable metabolites (Manzoni et al. 2016).

In the case or prion diseases, they are unique in that they may arise in a few different ways. Spontaneous or genetic forms of the disease arise and progress within the brain, with minimal replication in non-central nervous system tissues. However, the opposite is found of diseases associated with ingestion of the infectious agent or owing to blood transfusion. There are a number of drawbacks from studies on biomarkers of different prion infected tissues. For example, samples are highly diverse in regards to cellular complexity and stage of disease. It is difficult to find diagnostic biomarkers, especially for preclinical stages of disease, that will encompass all forms of prion diseases (Rubenstein 2012).

1.4 Conclusion

Following the exposure of the UK population to BSE there are an estimated 1/2000 of the age relevant population that may be subclinical carriers of vCJD. This means that they may be unknowingly incubating the disease and potentially passing it on to others via blood transfusion or even through use of contaminated surgical or dental instruments. It is important to identify such individuals as they pose a public health concern. Furthermore, there are currently limited diagnostic tools for preclinical disease available on easily

accessible samples. The hypothesis is that preclinical prion infection results in altered expression of blood proteins. The blood proteome will be investigated for detectable changes in protein composition during disease progression. Identifying and validating a signature of differentially expressed proteins in infected blood may reveal valuable biomarkers for potential use in diagnostics. It may be possible to utilise these proteins as an alternative to detecting PrP^{Sc} for diagnosing prion disease. This may provide the bases for development of a preclinical, ante-mortem screening test for suspected individuals.

There are many unresolved queries in prion science regarding blood infectivity. It is unknown why blood is so infectious (as little as 100 µL can transmit the disease) despite the presence of such a low level of PrP^{Sc}. It is possible that blood PrP^{Sc} has different characteristics to brain derived PrP^{Sc}, or that co-factors in the blood are equally important in passing infection. Within blood, live WBCs seem to be important for transmission of disease via the IV route. The hypothesis is that the nature of prion infectivity in blood differs fundamentally from brain derived infectivity, and relies on interactions between living cells for efficient transfer of infection to a new host. The differential treatment of WBCs may hint at the features necessary for optimal infection to occur or show that there are factors involved that simply cannot be replicated ex vivo. For instance, freeze-thawing cells disrupts the integrity of the cellular membrane and paraformaldehyde (PFA) fixation chemically bonds surface proteins thus restricting cell to cell interactions (Andreoletti et al, 2012). Investigating these scenarios, in comparison to fresh or untreated WBCs, may shed light on the mechanisms involved in the spread of infection.

1.4.1 Objectives:

1. To determine differential protein expression in plasma and WBC enriched-buffy coat blood fractions from BSE-infected sheep.
2. To validate candidate protein biomarkers for prion infection on blood samples collected from BSE-sheep.
3. To use an *in vitro* cell culture model to study the molecular and cellular interactions involved in transfer of infection from scrapie-infected leucocytes.

Chapter 2: Materials and Methods

2.1 Identification of protein biomarkers that distinguish prion-infected blood from uninfected blood

2.1.1 Preparation of samples of sheep blood components

Blood samples were taken from BSE infected sheep used in previous blood transfusion experiments (McCutcheon et al. 2011). Prion disease free donor sheep were sourced from the DEFRA scrapie free flock. All sheep were of the susceptible ARQ/ARQ *PRNP* genotype. This genotype confers disease susceptibility and also has the shortest incubation time following experimental infection with BSE. Sheep were orally infected with 5 g of bovine BSE infected brain homogenate (TSE archive, APHA Weybridge), their blood (2 units, 1 unit = 450 mL in blood packs containing 63 mL anti-coagulant CPDD.A1) was collected 10 months after infection and blood components (whole blood, red blood cells, buffy coat, plasma and platelets) were prepared for transfusion to recipient sheep. Mock-infected donors were inoculated with 5 g normal bovine brain homogenate at similar time as the infected cohort. At regular intervals (and prior to both inoculation and transfusion), 10 -20 mL of each blood component were sampled for analysis and archive storage. The sheep were monitored for clinical signs of prion disease. Brain and lymphoid tissues (spleen, tonsil, distal ileal Peyer's patch, prescapular and mesenteric lymph nodes) were collected from each animal (whether or not clinically positive) for detection of PrP^{Sc} by IHC and Western blot to confirm or rule out the presence of infection.

From nine donor sheep (ID numbers: N257, N236, N233, N251, N261, N189, N231, N232, N157) 1 mL aliquots of uninfected plasma (time point 0, pre-challenge) were thawed at room temperature, then combined and vortex mixed to create a pooled sample. These sheep were chosen because they all transmitted infection (the sheep that received their blood came down with disease). The pooled plasma was stored in 1 mL aliquots at -80 ^{o}C for later use. The procedure was repeated for infected plasma (time point 12 months, after blood collection for transfusion to recipient sheep) from the same sheep. Similar uninfected and infected pools were prepared using buffy coat samples (250 μL aliquots) from the same nine sheep. Individual plasma and buffy coat samples taken at different time points from the same nine sheep, and three negative control donors (N239, N170, N217) were also used in Western blot validation experiments. Figure 2.1 illustrates pooled plasma and individual plasma sample preparation.

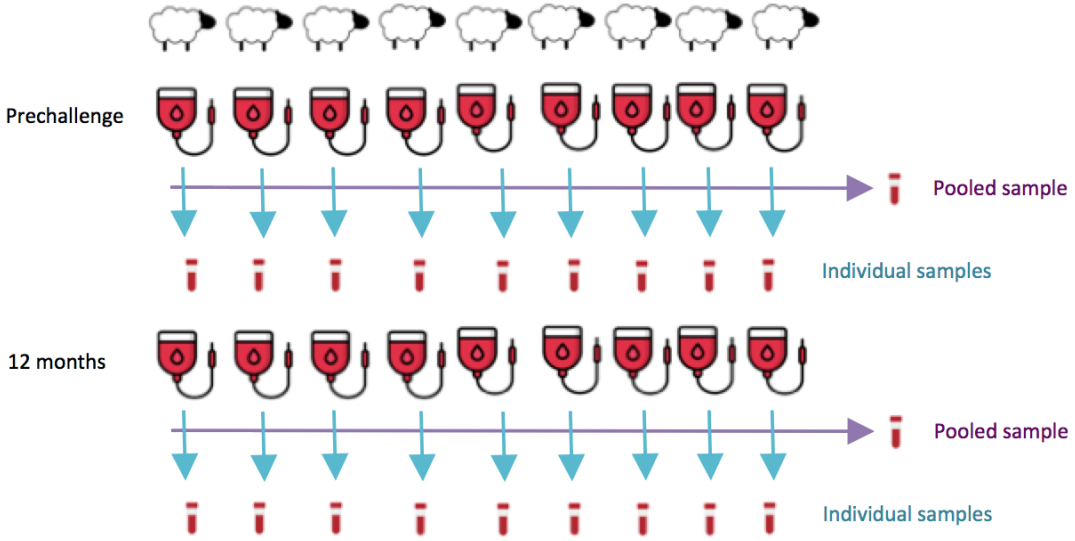

Figure 2.1: Pooled and Individual plasma samples from nine sheep. From nine sheep plasma samples were taken at both an uninfectious, prechallenge time point (before exposure to BSE) and infectious, 12 month time point (where their donated blood caused infection when transfused to recipient sheep). A pooled plasma sample which was used in initial experiments was created by mixing all nine sheep samples, individual sheep plasma samples from the same two time points were used in follow up experiments. The same procedure was repeated for buffy coat samples of the same nine sheep at these two time points. Similarly, plasma and buffy coat samples from three age-matched sheep (not exposed to BSE) with blood collected at the same time points were also prepared as negative controls.

For Western blot validation of mass spectrometry data, 1 mL of previously prepared uninfected or infected plasma/buffy coat pools or individual plasma/buffy coat samples were taken from -80 ^{o}C storage and thawed at room temperature. 200 µL of plasma was diluted in 250 µL of Extraction buffer (RIPA Lysis and Extraction Buffer, ThermoFisher Scientific 89900 and 1 % Halt™ Protease Inhibitor, ThermoFisher Scientific 1858566), vortex mixed and stored at -80 ^{o}C in aliquots of 100 µL for later use.

2.1.2 Measurement of total protein by Micro bicinchoninic acid assay (BCA)

The Pierce™ Biotechnology Microplate BCA Protein Assay Kit –Reducing Agent Compatible (ThermoFisher Scientific, 23252) is stored at room temperature. Reagents, protein standards and controls were prepared following kit instructions. BSA standards were prepared in Milli-Q water (2000 µg/mL, 1500 µg/mL, 1000 µg/mL, 750 µg/mL, 500 µg/mL, 250 µg/mL, 125 µg/mL) and 9 µL of each concentration dispensed into a 96 well plate in triplicate. Plasma and buffy coat samples were diluted to fit within the BCA assay linear range of 125-2000 µg/mL. A 1/20 stock solution was prepared followed by two-fold serial dilutions (1:2, 1:4, 1:8,

1:16, 1:32 and 1:64). 9 µL of sample at each dilution was pipetted directly to the centre of the microplate well followed by 9 µL of Reconstitution Buffer and 4 µL of Compatibility Reagent. The Standard Control is the working constitution buffer without reducing agent (it does not contain protein). The Sample Control is the working constitution buffer with reducing agent (also does not contain protein). To evaluate and avoid random error by using the average value, triplicates of each standard and test sample were used. The plate was incubated at 37 ^{o}C for 15 mins. 260 µL of Working Reagent was added to all wells and the plate further incubated at 37 ^{o}C for 30 minutes. After cooling at room temperature, absorbance at 570 nm was determined by Spectrophotometer Pharmacia LKB.Ultraspec3 and absorbency readings saved to Excel. In Excel the mean value for the absorbance reading of the Sample Control replicates was subtracted from all sample replicates. Using the Standard Control as the blank, a standard curve was prepared by plotting the average blank-corrected absorbance value for each BSA standard versus its concentration. This was used to determine the protein concentration of the unknown sample by rearranging the equation of the line.

2.1.3 ProteoMiner Enrichment Kit for enriching low abundant proteins

The BioRad ProteoMiner Kit (Small-Capacity kit 1633006, Large-Capacity kit 1633007) contains a vast library of hexapeptide ligands bound to beads pre-packaged in mini-spin columns. The columns were prepared as per the manufacturer's guidelines. The column storage material (nondisclosed solution) was collected and discarded following centrifugation at 1000 x g for 60 seconds. 600 µL of wash buffer was used to wash the column through centrifugation. The pooled plasma and pooled buffy coat samples were diluted to give a total protein load of 45 mg, so as not to exceed the column total protein capacity of the Large Capacity kit (50 mg). Binding to beads was facilitated by addition of 900 µL of sample to the column and continuous stirring by a rotary platform for 2 hours at room temperature. The column was centrifuged at 1000 x g for 60 seconds to remove unbound high-abundant protein. The column was washed by centrifugation four times with 600 µL of wash buffer to remove any remaining material (sample washes), and washed once with 600 µL of Milli-Q water to remove any traces of wash buffer (water wash). The enriched elution samples were obtained by sequential addition of urea buffer (8 M Urea in 50 MM HEPES) as opposed to the kit provided elution buffer so as to be compatible with mass spectrometry. 100 µL of urea buffer was added to the column and the column incubated at room temperature for 15 minutes with intermittent vortex mixing. The first eluate (Elution 1 or E1) was collected after centrifuging at 1000 x g for 60 seconds. This was repeated to generate enriched elutions 2 and 3 (E2 and E3). Samples were stored at -20 ^{o}C overnight.

2.1.4 Sodium Dodecyl Sulfate PolyAcrylamide Gel Electrophoresis (SDS PAGE) to separate proteins by molecular weight

Samples were retrieved from the freezer and thawed at room temperature. A second BCA assay was performed following protein enrichment with ProteoMiner. Two dilutions (1:3 and 1:6) of the Enriched Elutions E1, E2 and E3 were prepared. E1, E2 and E3 were pooled to generate E4 and the same dilutions (1:3 and 1:6) were prepared. For the column Flow Through a 1:20 stock solution was made followed by a series of two fold dilutions (1:2, 1:4, 1:8, 1:16, 1:32 and 1:64). Two-fold serial dilutions were prepared for the Sample Wash and Water Wash. Samples were loaded onto a 96 well plate in duplicates and the procedure repeated as previously described.

Prior to protein identification by mass spectrometry, SDS-PAGE was used to visualise depletion of high abundant proteins in the eluted samples. Using the results of the second BCA assay, the volume of each sample containing 10 µg of protein was calculated for comparison. Samples were diluted with 10 X Reducing agent (500 mM dithiothreitol, or DTT; ThermoFisher Scientific) and 4 X NuPAGE® Lithium dodecyl sulfate (LDS) Sample Buffer then heated at 100 ^{o}C for 10 minutes and centrifuged at 1000 x g for 1 minute. Samples were loaded on a 12 % Bis-Tris (BioRad) gel, along with a molecular weight marker (BioRad Precision Plus Protein Kaleidoscope™ Standards 1610374), and electrophoresis performed at 180 V for 50 minutes (or until the dye front reached close to the bottom of the gel), using 1 X SDS Running Buffer and NuPAGE® Antioxidant (according to the manufacturer's instructions). The gel was removed from its cassette and left to stain on a shaking platform with 3 mL of undiluted BioRad Coomassie Blue Stain (161-0436) for at least 1 hour. The gel was rinsed in Milli-Q water and images were captured with the LI-COR C-DiGit scanner.

2.1.5 Reduction, Alkylation and Tryptic Digestion to prepare samples for mass spectrometry

The pooled Enriched Elution samples (E4) for both infected and uninfected plasma and buffy coat were removed from the -20 ^{o}C freezer and thawed at room temperature. Volumes of each sample corresponding to 200 µg of protein were pipetted into proteomic grade aliquot tubes (Sigma-Aldrich). 5.8 µL of freshly prepared 250 mM DTT (in 50 mM HEPES, 1 M NaOH, pH 8) was added and the aliquots were placed on a shaking platform in an incubator set at 37 ^{o}C for 1 hour. After cooling at room temperature, 6.6 µL of 375 mM iodoacetamide (in 50 mM HEPES, 1 M NaOH, pH 8) was added. The aliquots were covered with aluminium foil and incubated in darkness at room temperature for 40 minutes with intermittent vortexing. Following this, 5.6 µL of 250 mM DTT (in 50 mM HEPES, 1 M NaOH, pH 8) was added and samples incubated at room temperature for a further 20 minutes with intermittent vortexing. Samples were diluted

with addition of 950 µL of 50 mM HEPES (1 M NaOH, pH 8). Trypsin (Promega Sequencing Grade Modified V5111) was added to give a ratio of 1 µg of trypsin to 20 µg of protein. After overnight incubation at 37 ^{o}C the samples were stored at -20 ^{o}C.

Samples were then forwarded for isotopic labelling and mass spectrometry analysis performed by Dominic Kurian. The procedure was repeated for buffy coat samples.

2.1.6 Mass spectrometry

To distinguish between infected and uninfected sample peptides were labelled using stable isotopic reductive dimethylation (ReDi) on OASIS HLB columns. Raw spectra data was processed by DataAnalysis (Bruker) software and the resulting peaklists were searched using Mascot 2.4 server (Matrix Science) against UniProt Bovine sequence database.

Methods performed by Dominic Kurian:

Protein digestion, dimethyl-labelling and liquid chromatography-tandem mass spectrometry

The ProteoMiner depleted samples were resuspended in a buffer containing 8 M Urea, 0.1% SDS, 50 mM ammonium bicarbonate (pH 8.0). Aliquots containing 100µg of proteins each of infected and uninfected samples were digested with trypsin following standard methods of in-solution digestion. The resulting peptides were cleaned up and labelled by reductive di methylation on Solid Phase Extraction cartridges.

Stable isotopic reductive dimethylation of the resulting peptides was performed on OASIS HLB columns (Waters) following standard methods (Boersema et al. 2009). The peptides were acidified by addition of trifluoroacetic acid to 0.1 % (v/v) before loading onto conditioned OASIS HLB columns. Peptides from uninfected and infected samples were labelled with ‘light’ and ‘heavy’ labelling reagents, respectively. The ‘light’ buffer consisted of 0.8 % (w/v) formaldehyde and 0.12 M sodium cyanoborohydride carrying hydrogens in their natural isotopic distributions in triethyl ammonium bicarbonate (TEAB) buffer. ‘Heavy’ buffer consists of 0.8 % (w/v) deuterated formaldehyde and 0.12 M sodium cyanoborohydride in TEAB buffer. The bound peptides were washed and eluted with 0.1 % (v/v) trifluoroacetic acid in 70 % (v/v) acetonitrile. The eluted peptides were concentrated using a speed vacuum concentrator. The labelled ‘light’ and ‘heavy’ peptides were mixed together before fractionation by strong cation exchange chromatography on a Polysulphoethyl A column (PolyLC Inc USA). Fractions were desalted on Stage-Tip columns (Rappsilber, Mann, and Ishihama 2007). Each fraction of peptides was loaded on to a Acclaim PepMap100, C_{18}, 3

μm, 100 Å, 75 μm (internal diameter) × 50 cm column using an UltiMate RSLCnano LC System (Dionex).

The peptides eluted by reversed-phase chromatography were analysed by a micrOTOF-Q II mass spectrometer (Bruker) which was operated in data-dependent mode, automatically switching between MS and MS2 mode. The m/z values of tryptic peptides were measured using a MS scan (300-2000 m/z), followed by MS/MS scans of the six most intense peaks. Rolling collision energy for fragmentation was selected based on the precursor ion mass and a dynamic exclusion was applied for 60 seconds

Raw spectral data were processed by DataAnalysis (Bruker) software and the resulting peaklists were searched using Mascot 2.4 server (Matrix Science) against UniProt Bovine sequence database containing 24,480 entries. Mass tolerance on peptide precursor ions was fixed at 25 ppm and on fragment ions at 0.1 Da. The peptide charge states were set as 2+ and 3+. Carbamidomethylation of cysteine was used as a fixed modification and oxidation of methionine and light and heavy dimethylation of N-terminus and lysine were chosen as variable modifications. False discovery rate was limited to < 1% for peptide IDs after searching decoy databases. Dimethyl quantification was performed by using WARPLC plugin on Proteinscape 3.1 software (Bruker) to integrate extracted ion chromatogram of every precursor. Peptide ratios were normalized based on setting overall peptide median ratio at one, which corrects for unequal protein sampling and a coefficient of variability of peptide ratios were also determined for each of the quantified proteins.

2.1.7 Validation of biomarkers by Western blot and LI-COR imaging

For quantitative, Western blotting infected and uninfected samples (diluted in Extraction buffer) were thawed from -80 ^{o}C in the derogated cat 3 lab. Following addition of 2 X Sample Buffer (4 % SDS, 34 % glycerol, 0.1% Bromophenol blue, 0.1 M DTT, 1 X Glycine), the samples were denatured at 100 ^{o}C for 5 mins and resolved by electrophoresis on commercial 12 % Bis-Tris (BioRad) gels in 1 X SDS Running Buffer at 180 V for 50 minutes. Two duplicate gels were resolved by electrophoresis in parallel in the same electrophoresis tank at the same time. One gel was incubated in InstantBlue™ (Expedeon) protein stain at room temperature for 1 hour on a rotating platform. Visualisation and quantification of the whole protein signal per lane was carried out using the LI-COR Odyssey scanner and software (Infrared Imaging System Scan, 700 channel). The other gel was used to transfer protein on to 0.2 μm Nitrocellulose membrane (BioRad 162-0112) at 18 V, 0.06 A for 1 hour.

This was performed using the BioRad transfer block (170-3940). Following this, the membrane was washed in Phosphate-buffered Saline (PBS)- 0.1 % Tween (0.1 % PBS-T) three times for 5 mins at room temperature on a rotating platform, blocked (in 10% Roche commercial blocking solution) for one hour and then incubated overnight in primary antibody diluted in 0.1 % PBS-T (see Table 2.1 for individual working dilutions). The primary antibodies used were: Fibulin1 (Abcam 192417), Vitamin D Binding Protein (Invitrogen PA5-29082), Hemopexin (Invitrogen PA5-29521), Moesin (Novus NB1 1-90372), working dilutions listed in Table 2.1.

The following day the membrane is washed thrice in 0.1 % PBS-T and then incubated in secondary antibody (Donkey anti-rabbit IgG ThermoFisher Scientific 31238, diluted 1/5,000 in 0.1 % PBS-T). After three more washes in 0.1 % PBS-T the membrane was submerged in BM Chemiluminiscence Western Blotting substrate (Roche). Detection and quantification of protein by measuring the western blot band signal was subsequently performed using a second LI-COR imaging machine, the C-Digit LI-COR Blot Scanner and Image Studio Lite software (12 minute exposure). In order to calculate a normalised western blot signal, the western blot band signal is divided by the ratio. The ratio for the pooled samples was the average whole LI-COR total protein signal per InstantBlue™ stained gel for either uninfected or infected time point. The ratio for the individual samples was calculated by dividing a sample's whole protein signal by that of the highest whole protein signal of all the samples run on the same gel.

Table 2.1: Working dilutions for primary antibodies.

Antibody	Manufacturer	Reference	Species raised in	Species reactivity	Working dilution
Polyclonal Anti-Fibulin 1 antibody	Abcam	EPR10913	Rabbit	Human, mouse, rat	1:750
Polyclonal antibody, Vitamin D binding protein	Fisher Scientific UK Ltd	13413207	Rabbit	Human, mouse	1:750
Polyclonal antibody, Hemopexin	Fisher Scientific UK Ltd	13403677	Rabbit	Human	1:2500
Polyclonal Moesin Antibody	Novusbio	NBP1-90372	Rabbit	Human, mouse, rat	1:2500

All antibodies were optimised for use with either sheep plasma or buffy coat samples.

2.1.8 Statistical analysis

Two sample T tests were performed to test the statistical significance of the normalised western blot results (described in Figure 2.2). This was done to analyse if the average difference between groups is significant of due to random chance. The diagram illustrates the comparison tests performed. Graphs were plotted and T-tests calculated using GraphPad Prism 7.

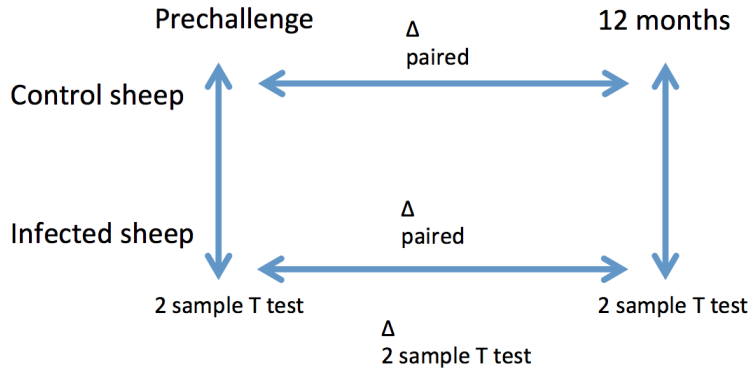

Figure 2.2: Diagram of comparison T tests performed. To analyse the significance of the normalised western blot data of each potential biomarker protein T tests were performed comparing each group at each time point and the difference between time points (prechallenge subtracted from 12 months).

2.2 Rov9 cell line infection experiment

Rov9 cells are rabbit kidney epithelium cells modified to overexpress VRQ sheep PrP. They were developed as a quantitative assay to assess prion infectivity by (Arellano-Anaya et al. 2011). The stocks used here were provided by Didier Vilette and stored at -80 ^{o}C.

2.2.1 Passage of Rov9 cells

In order to keep cells alive and growing under cultured conditions confluent cells were passaged every 7 days. To initially establish the cultures from frozen stock, medium was warmed to 37 ^{o}C in a water bath. 10% Opti-MEM medium (Reduced Serum Medium, ThermoFisher Scientific 31985062) was prepared with 10 % Foetal bovine serum (Gibco, 15392402), and Penicillin-Streptomycin (PS) antibiotics (100 X ThermoFisher Scientific 15140122). The vial was thawed and cells were added directly into the T25 flask containing Opti-MEM medium. The next day, medium was changed and cells left in incubator until confluence. For passage cells were washed twice with pre-warmed sterile PBS, trypsinated with 400 µL of 1 X Trypsin-EDTA (Sigma) to each T25 flask and flasks were incubated at 37 ^{o}C for 5 mins. Cells were then disrupted by forceful tapping of flasks. 3.6 mL of fresh medium

(1/4 split) was added to the flask. Dissociation of the cellular clumps was achieved by up and down movements with the stripette. 1 mL of cell suspension was added to new flasks containing 3.6 mL of fresh medium which were placed into incubator at 37 ^{o}C. Doxycycline was added once the medium is prewarmed at 37 ^{o}C. Since Rov9 cells have an inducible promoter and they express ovine PrP^{C} in a doxycycline-dependent manner, doxycycline (Sigma-Aldrich, D3447) was prepared in a stock of 5 mg/mL (5000 X) in absolute ethanol and added to Opti-MEM medium at a concentration of 1µg/µL only when the PrP^{C} expression was required for infection with infected brain homogenate.

2.2.2 Peripheral Blood Mononuclear Cell (PBMC) isolation

PBMCs were isolated from blood collected from sheep in the Roslin Scrapie Flock. Two genotypes denote susceptibility or resistance to disease. VRQ/VRQ sheep are highly susceptible to scrapie and were the source for infected blood, while ARR/ARR sheep are resistant, and were used as negative controls (Hunter 1997). 100 mL of blood in EDTA anticoagulant were collected by jugular venepuncture from the sheep. Sterile scissors were used to cut blood bags and divide the blood between 50 mL falcon tubes. To separate blood, the falcon tubes were balanced and centrifuged at 3000 x g with brake off for 15 mins at room temperature. Once this initial spin was completed, buffy coats (containing leucocytes) were removed from the interface between red cells and plasma by use of stripette, placed in 50 mL falcon tubes and diluted up to 50 mL in PBS and carefully layered over 20 mL of Lymphoprep (STEMCELL Technologies). Buffy coats and Lymphoprep were centrifuged for 30 mins at 3000 x g with brake off. PBMC were harvested from the interface of the density gradient and supernatant, diluted in PBS and spun at 1500 x g for 15 mins at room temperature with brake on to remove residual Lymphoprep. Supernatant was then discarded ensuring not to disturb the pellet. This was followed by three consecutive PBS washes of the PBMCs at 1500 x g for 15 mins at room temperature. Cells were suspended in 10 mL of Opti-MEM medium and a 1 mL 1/10 dilution of cells in 0.2 % Trypan blue (ThermoFisher Scientific) was used to count cells in the haemocytometer.

2.2.3 Infection of Rov9 cell line with PBMC

To compare the infection of Rov9 cells with differentially treated PBMC, aliquots of 1 x 10^{7} infected PBMC pellets and aliquots of 1 x 10^{7} uninfected PBMC pellets were used. Rov9 cells were first grown to confluency in a 12 well plate. To inoculate the Rov9 cells with fresh PBMCs, cells were resuspended in warm media and added to individual plate wells directly after isolation from whole blood. Next, both infected and uninfected pellets were freeze/thawed three times to lyse cells before Rov9 cell inoculation (10 mins on ice, 10 mins at room temperature thrice). Additionally, paraformaldehyde (PFA) fixation was performed by

treating infected and uninfected cell pellets with 2% filtered PFA. Aliquots of cell pellets in PFA were placed on ice for 10 mins, washed twice with PBS. The differentially treated PBMC pellets were added to Rov9 cells in the 12 well plate and left for 4 days before addition of fresh medium and weekly passaging (Salamat et al. 2011). Rov9 cells with no PBMC inoculation was used as a negative control, while inoculation of Rov9 cells with 1% brain homogenate of SSBP1 infected sheep or 1% brain homogenate from natural scrapie sheep provided a positive control. At each passage, cells were split 1/4 for storage, 1/4 for passaging, 1/4 for processing by western blot and 1/4 discarded. More detail is provided within Chapter 5.

2.2.4 Processing of cell lysate for western blot

The cell lysate was collected using TL1 Lysis buffer (0.5% Sodium Deoxycholate, 0.5% Triton X-100, 50 mM Tris-HCL). Following removal of medium, and after two washes in cold PBS, 1.5 mL of TL1 buffer was added to each T25 flask. Flasks were then placed at 4 ^{o}C for 10 mins. Cell lysate was extracted by collection of T25 flask content in 15 mL falcon tubes and centrifugation at 2000 x g, 4 ^{o}C for 2 mins. The pellet (cell debris) was discarded and the supernatant (containing the cell membrane protein) was stored at -20^{o}C or digested using proteinase K (PK) for detection of PrP^{Sc} by western blot. Total protein of the cell lysate was measured using microBCA as per suppliers guidelines and the cell lysate was diluted to 1 mg/mL. For PK digestion, 2 µg of Proteinase K Solution (ThermoFisher Scientific AM2546) was added per 500 µL of cell lysate (for a final concentration of 4 µg PK/mg protein) and the samples placed at 37 ^{o}C for 2 hours. PK was then inactivated by addition of 4 µL of 4 mM Pefabloc protease inhibitor, and pellet obtained by centrifugation at 13000 x g for 30 mins. Pellets were resuspended in 20 µL 2 X Sample Buffer (Sodium Dodecyl Sulfate 4 %, Glycerol 34 %, Bromophenol Blue 0.1 %, Dithiothreitol 0.1 M, Tris-Glycine 1 X) and after denaturing at 100 ^{o}C for 5 mins resolved by electrophoresis and western blot (Salamat et al. 2011) performed to visualise presence of PrP^{Sc}. After migration, the protein gels were transferred to nitrocellulose membrane and blocked with blocking reagent. The membranes were revealed with ROS-BC6 primary antibody (McCutcheon et al. 2014) at 0.25 µg/mL concentration in PBS-Tween (0.1%) overnight. After three washings with PBS-T, they were incubated with goat-antimouse secondary antibody (1 ng/mL) before immunodetection using BM Chemiluminiscence Blotting Substrate (Roche).

2.2.5 Preparation of brain homogenate

Scrapie/Uninfected brain homogenate was prepared into 10 % as required for Western blot by first thawing frozen brain samples on ice. 1-2 mL of sterile PBS was pipetted into a universal tubes. 1 g of brain tissue (frontal cerebral cortex, cerebellum and thalamus) was

cut into small pieces with sterile scalpels and placed into the tube of PBS. Using an Omni electronic homogenizer (Camlab) the tissue was homogenised until no clumping was observed (any fibrous tissues were removed). The brain tissue was diluted into a total of 10 mL of PBS and thoroughly mixed. Aliquots of 500 µL brain homogenate were stored at -80 ^{o}C in 1.5 mL screw topped Eppendorf tubes.

Brain homogenate was removed from storage and thawed before use. Brain homogenate was PK digested (for a final concentration of 4 µg PK/mg protein at 37 ^{o}C for 2 hours), processed in 2 X Sample Buffer and resolved by western blot in the same manner as described for Rov9 cells (2.2.4).

2.2.6 recPrP Protein Purification: Full length Mouse PrP (flMoPrP) production

RecPrP was purified to a high level following methodology previously described by Makarava and Baskakov (2008) and (Barron et al. 2016). Glycerol stocks (GATC-FML-Sam.000000.2 Mo rPrP Wt S7 23-230 E.coli Rosetta 08/10/10) were used to grow large numbers of bacterial cell. These were induced to produce recPrP by addition of 1 M Isopropyl β-D-1-thiogalactopyranoside (IPTG). Inclusion bodies were then harvested, resolubilised and protein purification performed by Ni-NTA Immobilized Metal Affinity Chromatography (IMAC) on the AKTA FPLC machine. IMAC fractions containing the most protein were combined and loaded on to a super loop using a syringe. Desalting (using a HiPrep 26/10 Desalting column on the AKTA FPLC) was conducted for buffer exchange and removal of low molecular weight substances.

To achieve a level of high recPrP purity, Reverse Phase High Performance Liquid Chromatography (RP-HPLC) on the Dionex Ultimate 3000 was completed on the desalting fractions. The peak was collected as one fraction (shown in Figure 2.3 A and western blot in Figure 2.3 B), protein concentration was estimated using NanoDrop, 1 mL aliquots lyophilised using a SpeedVac (45 ^{o}C, HPr 5.4 vac for 3 hours) and stored at -80 ^{o}C. .

To use the recPrP, aliquots were removed from storage and samples resuspended in PBS. Following NanoDrop confirmation of protein concentration, the recPrP was diluted in PBS, processed in 2 X Sample Buffer and resolved by western blot as previously described (2.2.4).

A.

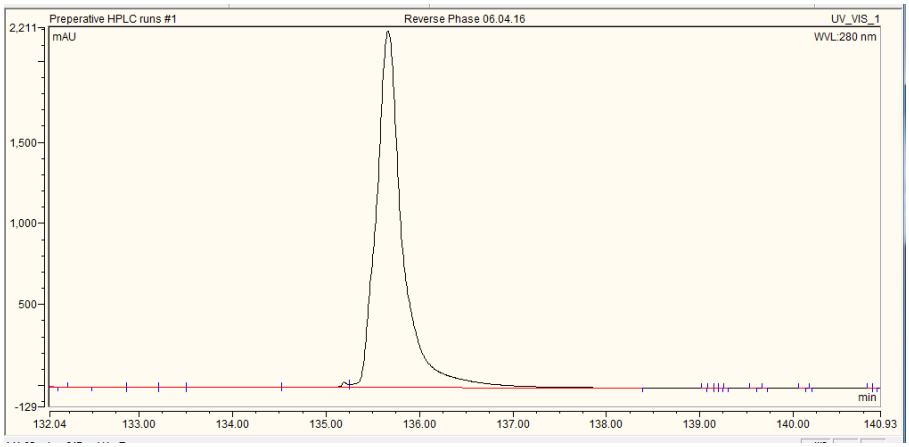

B.

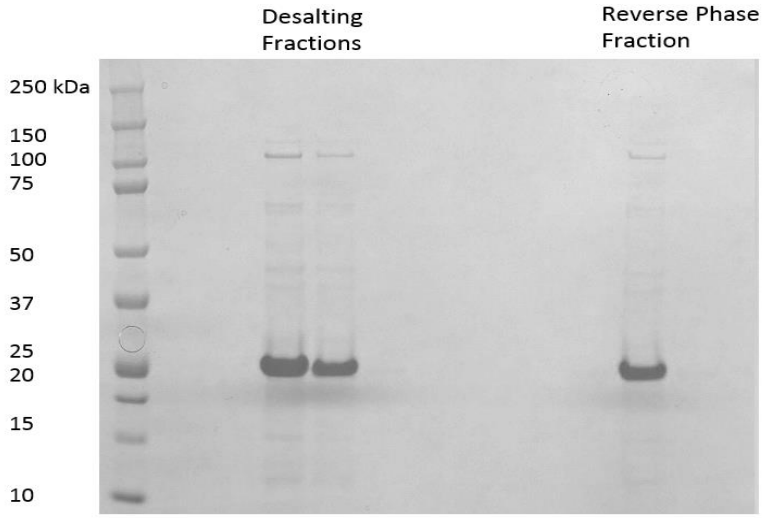

Figure 2.3: Examples of RecPrP purification. A high level of protein purification was achieved through Immobilized Metal Affinity Chromatography (IMAC), Desalting and Reverse-phase chromatography. (A) is a snapshot of the reverse-phase chromatogram, the UV peak indicates protein eluted from the column. (B) is a SDS-PAGE gel of Desalting and Reverse Phase fractions. The intense band at ~25kDa indicates a large amount of flMoPrP; there are fewer impurities (non-specific bands) in the Reverse Phase fraction.

Chapter 3: Proteomic markers that distinguish prion infected and uninfected plasma

3.1 Introduction

The blood borne transmission of vCJD is a major concern for blood transfusion banks, plasma derived product manufacturers and public health authorities. A significant challenge for diagnosis and surveillance is that hosts may incubate the infectious agent for months to decades without exhibiting any symptoms. Hence, a method for identifying donors or blood donations that pose a risk is highly desirable (Lacroux et al. 2014). An ideal preclinical test would have the ability to identify an individual throughout the incubation period. The test would have high levels of sensitivity and specificity, be able to be performed on easily accessible samples and have the ability to scale up for high throughput. Sensitivity is the ability of a test to correctly classify an individual as 'diseased,' it is also called the true positive rate or probability of detection. While specificity refers to the ability of a test to correctly classify an individual as 'disease free,' also known as the true negative rate (Parikh et al. 2008).

Immunohistochemistry of the obex brain region exploiting anti-prion protein antibodies has long been seen as the 'gold standard' for prion diagnostics for animal prion diseases (Schaller et al. 1999). Other antibody specific diagnostics (such as Prionics or BioRad tests) utilise western blot or ELISA techniques. However, detection of PrP^{Sc} has to be performed against the background of PrP^{C}. This is an issue as most antibodies bind both PrP^{Sc} and PrP^{C}. Furthermore, since the current detection method of PrP^{Sc} is dependent on its resistance to PK digestion, it is not suitable for detection of PK sensitive PrP^{Sc} (Rubenstein 2012). The major issue with most of these tests is that they can only be applied to post mortem samples, not live animals or individuals.

A key reason for the difficulties faced in constructing a reliable premortem diagnostic test is the low level of PrP^{Sc} present in body fluids. Protein misfolding cyclic amplification (PMCA) is an exception to other diagnostic methods. It is a technique whereby detection sensitivity is increased through amplification of PrP^{Sc}. It works by utilising the ability of the misfolded protein to convert a pool of normal PrP^{C} to a PK-resistant form thus 'amplifying' the original entity. The detection of PrP^{Sc} from blood of vCJD patients is 100% sensitive and specific using this technique (Concha-Marambio et al. 2016b). Additionally, Bougard, Brandel,

Bélondrade, et al. (2016) identified preclinical blood from two individuals 1.3 and 2.6 years before they developed and displayed vCJD symptoms. The assay was also able to detect vCJD infection in the early preclinical stage in primates (Lacroux et al. 2014). Real-time quaking induced conversion (RT-QuIC) also exploits the ability of PrP^{Sc} to induce PrP^{C} to misfold. The formation of PrP^{C} aggregates is monitored in real time by their ability to bind to a fluorescent dye (thioflavin T) (Wilham et al. 2010); (Atarashi et al. 2011). The use of RT-QuIC on the cerebrospinal fluid (CSF) of suspected patients with sCJD is commonly used to confirm diagnoses. The reported sensitivity is between 69% -89% for neuropathologically confirmed sCJD and specificity between 99%-100% (McGuire et al. 2012); (Park et al. 2016); (Bongianni et al. 2017); (Groveman, Orrú, et al. 2017).

Alternative, 'surrogate' protein biomarkers to complement PrP^{Sc} in detection would be invaluable and perhaps overcome the hurdles in preclinical diagnostics (Rubenstein 2012). The modern day trend in clinical research for biomarkers is not to find a single factor but instead a panel of biomarkers in which the total diagnostic performance tends towards 100% sensitivity coupled with 100% specificity (Piubelli et al. 2006). Clinical analysis of blood is a widespread diagnostic procedure in medicine. The integral role blood plays in human physiology implies that it should be a universal reflection of a patient's state. The cellular components are erythrocytes, thrombocytes, lymphocytes, monocytes and granulocytes and the liquid portion is called plasma (Geyer 2017). In regards to proteinaceous biomarker discovery, the most challenging feature of the plasma proteome is the exceptionally wide concentration range of proteins. In fact, more than 10,000 proteins have been identified in human plasma (www.plasmaproteomedatabase.org accessed on November 2018) making the plasma proteome the most heterogeneous and complex sub-proteome of the human body (Hortin, Sviridov, and Anderson 2008). Hence many studies on plasma proteomics involve a step in minimising sample complexity whilst reducing protein dynamic range.

Once a biomarker candidate has been discovered it requires confirmation and validation. This is an issue in addressing preclinical human prion diseases due to the availability of samples and disease being confirmed either at a late stage or after death. To overcome this issue and address the unmet need for blood based prion disease biomarkers, samples used here are from an archive collected during previous transfusion experiments in BSE infected sheep. This reflects the real life scenario where three individuals developed vCJD following transfusion of infected blood from donors who later succumbed to vCJD themselves. Sheep are a good model for what occurs in humans as they share similarities in disease pathogenesis. BSE infected sheep harbour infection in peripheral tissues, PrP^{Sc} deposition is extensively found in the lymphoreticular system (Jeffrey, Martin, et al. 2001). This is similar

to humans infected with vCJD (Hill et al. 1999). In contrast, BSE infectivity in cattle does not have widespread tissue distribution (Buschmann and Groschup 2005); (Espinosa et al. 2007). Additionally, the relative size of sheep and humans allow for volumes of blood comparable to those used in human transfusion practice to also be transfused in sheep studies.

3.1.1 Aims of work

The aim of this chapter is to identify differences in protein expression between uninfected and infected plasma samples from BSE infected and uninfected sheep. Through mass spectrometry comparison it may be possible to identify changes in protein expression that indicate disease status. Predicted proteomic differences must be tested to ensure correct identification and reproducibility of results. Up or down regulation of particular proteins in the original plasma samples will be verified to confirm the mass spectrometry data. This will provide preliminary data on determining a protein biomarker panel associated with prion infection in blood of asymptomatic patients. To elaborate on the viability of a particular protein as a potential diagnostic marker, comparison of its detection in human samples is ideal.

3.2 Results

3.2.1 Use of ProteoMiner to deplete highly abundant proteins in plasma

The samples used in this study are from a previous transfusion study of BSE infected sheep. Since it is established which of the recipients developed BSE, donors with infectious blood can be identified. Infected samples were taken when blood was proven to be infectious but the sheep lacked clinical signs (mimicking the human silent carrier status). Uninfected samples were taken from the same sheep at a time point prior to their exposure to BSE brain material. Hence, the two time points investigated were prechallenge (uninfected) and 12 months after (infected). The plasma from nine sheep were pooled to control for genetic or metabolic differences between sheep. This was done for samples at both time points. Before performing mass spectrometry the plasma went through an initial processing step.

Around twenty proteins (including albumin, transferrin and fibrinogen) constitute more than 98% of protein mass in plasma (Geyer et al. 2016). Their presence can obscure detection of less abundant proteins. In order to enrich the plasma samples for less abundant proteins the ProteoMiner enrichment kit was employed. Due to conventional antibody mediated depletion methods being specific to human or mouse proteins thus potentially not recognising sheep antigens, ProteoMiner was chosen as the method for these samples. To decrease highly abundant proteins and enrich less abundant proteins in complex biological samples ProteoMiner technology utilises a vastly diverse library of hexapeptides bound to beads held within the column. There are a total of 64 million unique beads. Each bead features a distinctive hexapeptide ligand with affinity for a specific protein. When the sample is applied to the beads, hexapeptide ligand bind to their particular protein by interacting with exposed amino acid sequences. Simultaneously, highly abundant proteins saturate their high affinity ligands (excess proteins is washed away) and less abundant proteins are concentrated on their high affinity ligands as illustrated in Figure 3.1. Proteins bound to the beads (representatives of all original components) are eventually eluted. Thus the dynamic range of protein concentrations in the samples is greatly reduced. Table 3.1 indicates the source of samples collected from completion of ProteoMiner.

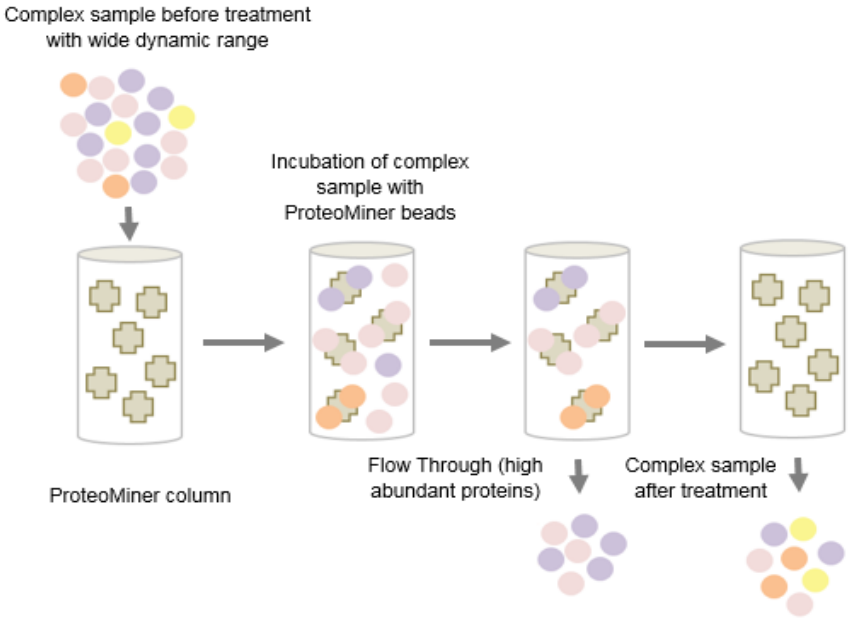

Figure 3.1: Flowchart explaining the process of the ProteoMiner technology. The ProteoMiner columns contain vast libraries of hexapeptide ligand beads. Each bead is unique to an individual protein. Once a complex sample is applied to the column, proteins within that sample bind to their specific beads of the column. Less abundant proteins are retained while highly abundant proteins saturate their high affinity ligands. With subsequent washing of the column excess protein is removed (in Flow Through). Finally a more homologous sample is recovered by addition of an elution buffer. The result is depletion of a significant portion of the high abundant proteins within the sample and this enables the detection of less abundant proteins.

Table 3.1: Description of the origin of samples obtained from the ProteoMiner column.

Flow Through	Sample with excess levels of high abundant proteins.
Sample Wash	Wash Buffer used to remove excess unbound protein.
Water Wash	MilliQ water used to remove surplus Wash Buffer from column.
Enriched Elution	Elution Buffer used to elute protein from column.

The table highlights names and describes the source of the samples that were collected from the column and run on a SDS-PAGE gel to monitor efficiency of technique following repeat experiments.

A.

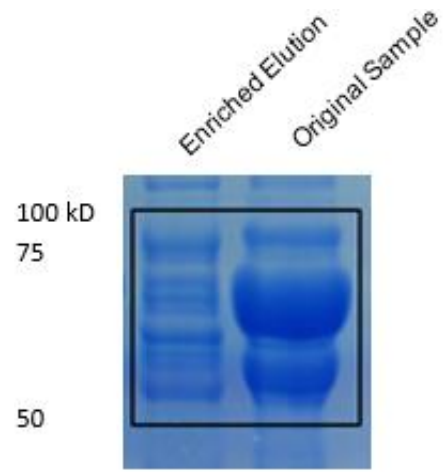

B.

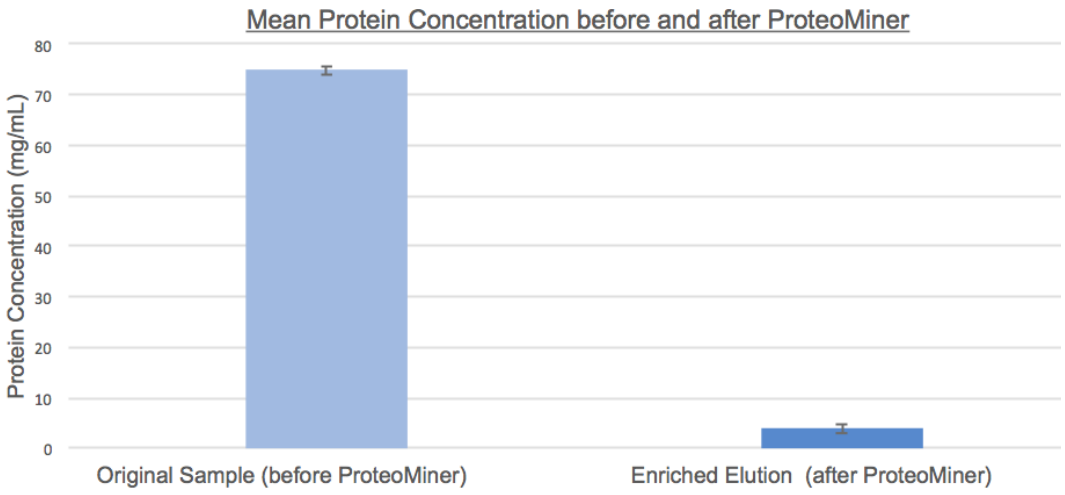

Figure 3.2: Results following use of ProteoMiner on pooled plasma. A portion of Coomassie Instant Blue™ stained gel is shown in (A). The Enriched Elution is obtained from eluting the final sample off of the ProteoMiner column; the Original Sample is before ProteoMiner is performed. The image illustrates that bands on the gel become visible (in Enriched Elution lane); representing low abundant proteins that are no longer obscured and are now detectable (compared to Original Sample lane). The bar chart (B) shows protein concentration of the plasma before and after ProteoMiner, it is an average from four repeat experiments. As determined by microBCA the Original Sample concentration fluctuated between 80 – 68 mg/mL while the concentration Enriched Elution ranged from 2.5 - 4 mg/mL. Thus a 95 % reduction in plasma protein concentration was achieved (Standard Deviation 0.7 for data after ProteoMiner).

The results from ProteoMiner on the pooled plasma samples from sheep before and 12 months after infection with BSE indicate that a large proportion of highly abundant proteins have been removed, facilitating an enhanced detection of less abundant proteins. Figure 3.2 A depicts the substantial reduction in amounts of 60 kDa albumin protein (from the Original sample, before ProteoMiner) on the SDS-PAGE gel for uninfected pooled plasma and is representative of results for infected pooled plasma too. At the same time there is an appearance of a multitude of fine bands (in the Enriched Elution, after ProteoMiner) representing the presence and detectability of less abundant proteins. In order to determine the protein content of the samples before and after ProteoMiner, microBCA assays were performed. There is a 95 % reduction in protein concentration (bar chart in Figure 3.2 B).

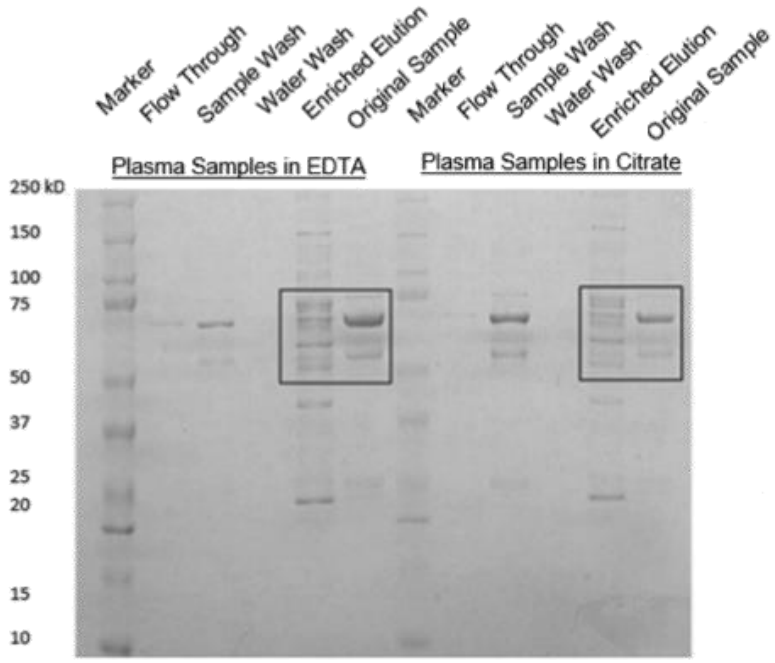

Figure 3.3: SDS-PAGE comparison of ProteoMiner samples from plasma in two different anti-coagulants (EDTA and Sodium Citrate). The archived samples used in this study had been stored in either EDTA or Sodium Citrate anti-coagulant. In order to evaluate if this had an affect on ProteoMiner performance, comparison experiments were performed. This figure shows samples where a total of 10 µg of protein was loaded per gel lane. Following this, the gel was stained with Coomassie Instant Blue™. The results are fairly similar for samples in both anticoagulants. Bands within the boxes indicate enhanced detectability of Enriched elution low abundant proteins. Thus it was decided that moving forward only samples collected in EDTA (the current anticoagulant used in blood collection) would be used.

The results from using the ProteoMiner enrichment kit highlight the importance of ProteoMiner in expanding the visibility of less abundant protein in complex solutions. Uninfected pooled plasma was initially used to optimise the technique in the category 2 lab.

These tests included analysing plasma collected in two different anticoagulants, EDTA and Sodium Citrate. Figure 3.3 shows that there is depletion of abundant samples prepared in both anticoagulants. The boxes highlight the areas of the gel which illustrate this most clearly. The Original Sample has been run next to the Enriched Elution and for both plasma in EDTA and plasma in Citrate, the strong band for albumin (60 kDa) has been replaced with many bands for less abundant proteins. Since the ProteoMiner is viable with both types of anticoagulant, it was decided that moving forward only plasma collected in EDTA would be used (as there were more samples collected in EDTA available from infected sheep and it is the current anticoagulant used for blood collection). Furthermore, the best denaturing temperature and protein loading concentrations for resolving proteins by SDS-PAGE were determined. It was concluded that denaturing of proteins at 100 ^{o}C and loading 10 µg of protein per sample gave the best results for comparison.

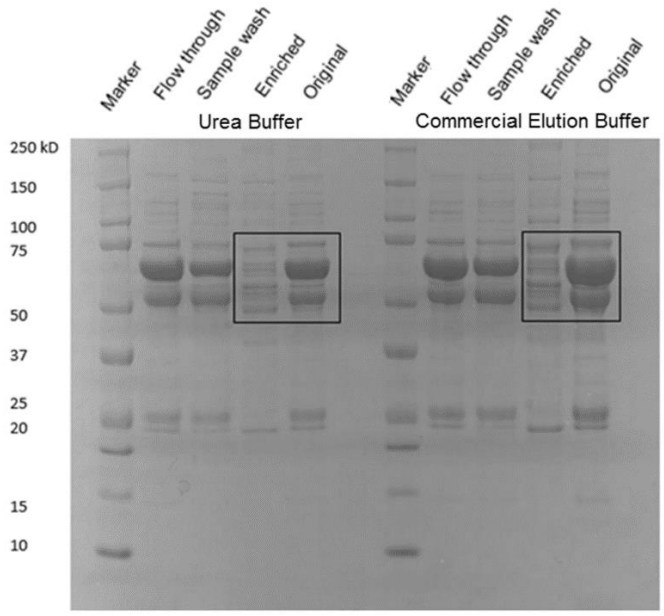

Figure 3.4: Use of two different elution buffers (Urea buffer and Commercial elution buffer) with ProteoMiner on uninfected plasma. The ProteoMiner kit provides a Commercial elution buffer that contains CHAPS. CHAPS is not compatible with mass spectrometry. For this reason, a substitute Urea based buffer was tested and the results compared to the Commercial buffer. Plasma was added to two ProteoMiner columns simultaneously and 10 µg of protein from each collected sample resolved on the same gel. The figure shows that low abundant protein bands become evident in the enriched fraction with use of the Urea buffer. Hence, the Urea buffer was suitable for continued use.

Proteins are eluted from the ProteoMiner column using a Commercial elution buffer containing 8 M Urea and 2 % CHAPS. Urea is a strong denaturant. As binding affinity required proper three dimensional folding of a protein, reagents that weaken interactions

between protein and ligand can be used for elution. CHAPS is a detergent used for solubilizing proteins. Detergents are not compatible with mass spectrometry. Whilst surfactants are commonly used in protein preparation, their presence can affect enzymatic digestion and the subsequent analysis of the resulting peptides by mass spectrometry. Since the ProteoMiner kit provided elution buffer includes CHAPS, the enriched elution eluted in this buffer may not be compatible with mass spectrometry and this would thus interfere with analysis. To avoid this issue other buffers were trialled. The change from the commercial elution buffer to a Urea based buffer (8M Urea in 50MM HEPES without CHAPS) achieved the same level of highly abundant protein reduction and enhanced detection of less abundant protein. This is depicted in Figure 3.4. The boxes on the gel highlight a comparison between the Enriched Elution and Original Sample. Many bands appear in the Enriched Elution following the use of ProteoMiner thus highlighting the detection of less abundant proteins that were previously masked for both samples eluted in Urea buffer and the Commercial elution buffer.

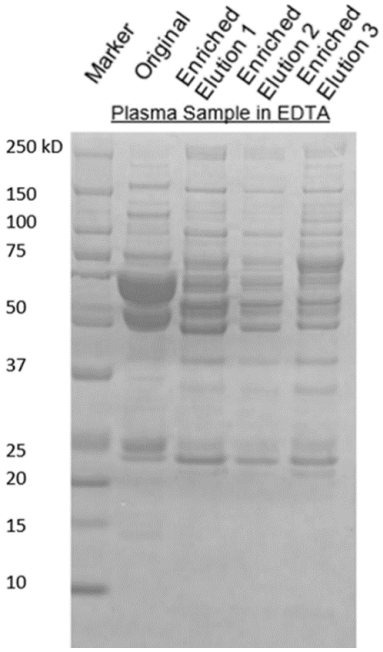

Figure 3.5: Testing the ProteoMiner large capacity kit with pooled uninfected plasma. Following optimisation of the technique using the small capacity ProteoMiner kit, work was scaled up to the large capacity kit. The small capacity ProteoMiner kit is able to simultaneously concentrate low abundant proteins and deplete the concentration of high abundant proteins in samples with a total protein load of ≥ 10 mg, while the large capacity kit has a protein loading capacity of ≥ 50 mg. Plasma has a protein concentration of 50 – 80 mg/mL, thus 1 mL of undiluted plasma can be used with the large capacity ProteoMiner kit. The gel in this image shows a practice run with the large capacity kit. Unlike with the small capacity kit, the final sample is eluted three times. The signal of low abundant protein species have been amplified in the three enriched elutions.

After testing the reproducibility of the results, work was scaled up to use the large capacity kit (Figure 3.5). The large capacity ProteoMiner columns works best with samples of a protein content greater than 50 mg/mL, hence 1 mL of undiluted sample could be applied to the column. Three rounds of sample elution are required (Elution 1, Elution 2, Elution 3). Following experimental trials in the containment level 2 lab (and containment 3 lab training), the large capacity ProteoMiner kit was used on pooled infected and uninfected samples in the category 3 lab.. Table 3.2 provides the protein concentration of samples before and after ProteoMiner as obtained by microBCA assay. Figure 3.6 are the final gels where the depletion of highly abundant protein in the samples may be observed. Figure 3.7 depicts the workflow involved. The three elutions were combined to give Elution 4. After reduction and alkylation (to break protein disulphide bonds and prevent disulphide bonds reforming, improving peptide yield and sequence coverage) and tryptic digestion (to digest proteins into peptides), Elution 4 was forwarded for isotopic labelling and mass spectrometry analysis.

Table 3.2: Total protein amount of samples before and after ProteoMiner.

Total protein (µg)		
Uninfected Plasma pool	Original	82373
	Enriched Elution 4	5874
Infected Plasma pool	Original	78039
	Enriched Elution 4	4575

1 mL of undiluted pooled plasma is added to the ProteoMiner large capacity kit column. (separate columns for uninfected and infected plasma). The procedure results in three rounds of 100 µL eluted sample from the column (Enriched Elution 1, 2 and 3), these are combined to obtain Enriched Elution 4. The table indicates the protein concentration of the original plasma sample (before ProteoMiner) and Enriched Elution 4 (after ProteoMiner). There has been a 94-93% reduction in protein concentration for the uninfected and infected pooled plasma samples.

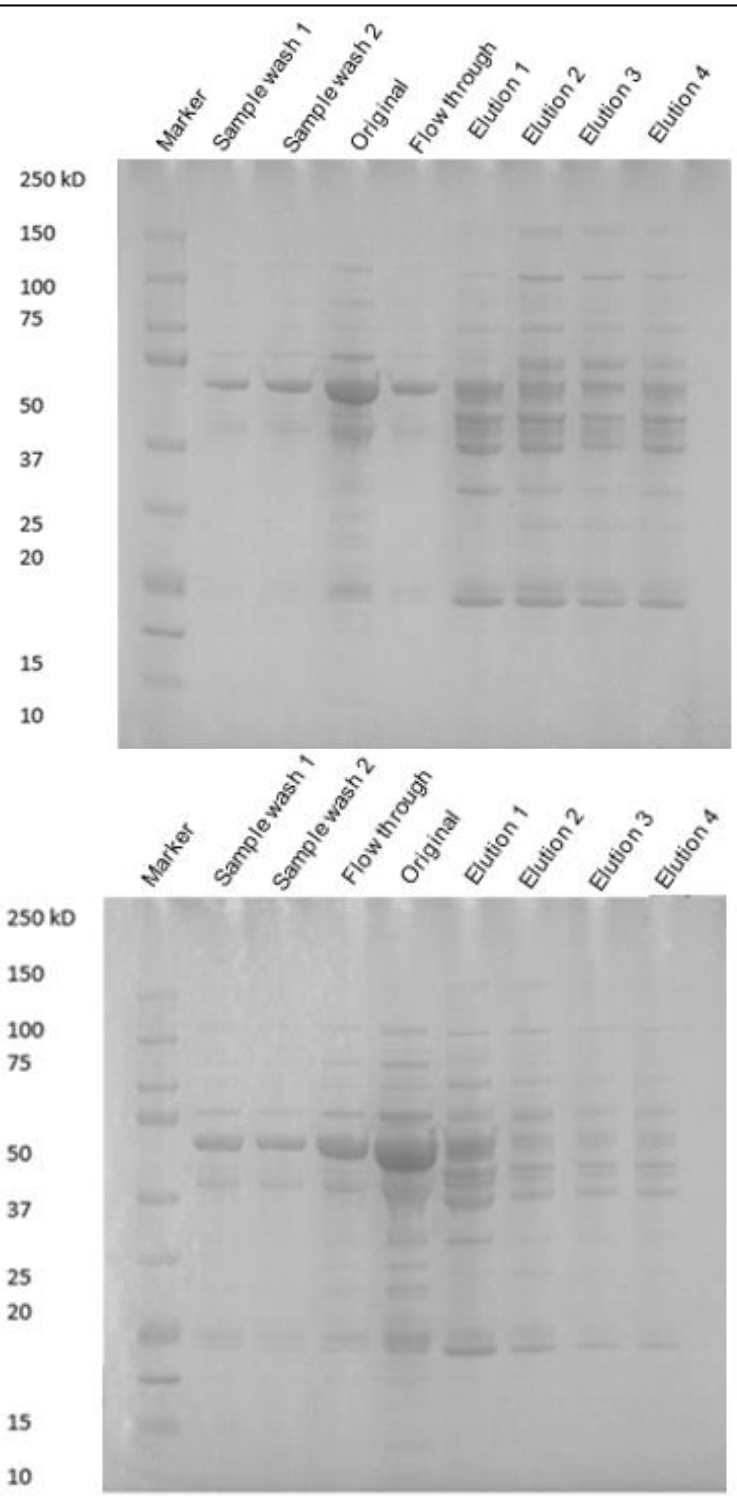

Figure 3.6: Samples from pooled uninfected and infected plasma that were depleted on separate ProteoMiner columns were resolved on separate gels. After fully optimising the use of ProteoMiner and performing a practice run using the large capacity kit, samples for mass spectrometry were prepared in the derogated containment level 3 lab. 1 mL of uninfected plasma and 1 mL of infected plasma were applied to individual ProteoMiner columns simultaneously. Samples of the three elutions were taken before they were combined to create Elution 4 (to determine protein concentration by microBCA assay and to resolve on gel). Following reduction, alkylation and tryptic digestion Elution 4 was forwarded for mass spectrometry analysis.

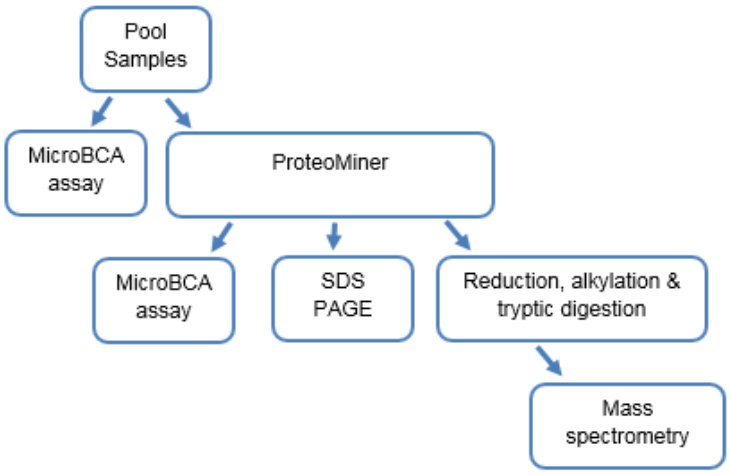

Figure 3.7: Flowchart depicting sample preparation. This is an overall summary of the steps involved to prepare samples prior to mass spectrometry. First, 1 mL aliquots of uninfected plasma from nine sheep were pooled to control for differences between sheep. A sample of the original pool was taken for microBCA analysis to determine protein concentration. 1mL of pooled sample was applied to a large capacity ProteoMiner column. Samples from the ProteoMiner column were microBCA assayed to calculate 10 µg of protein to resolve on comparison gels with the original sample. Following a check of SDS-PAGE results (to ensure a reduction in the most abundant proteins), the enriched elution was taken through reduction, alkylation and tryptic digestion steps. The exact same procedure was performed simultaneously with pooled infected plasma (taken from the same nine sheep but at a different time point during the transfusion study experiment, when their blood was proven to be infectious). Finally, both uninfected and infected samples were forwarded for isotopic labelling and mass spectrometry analysis.

3.2.2 Mass spectrometry of plasma and identification of potential biomarkers

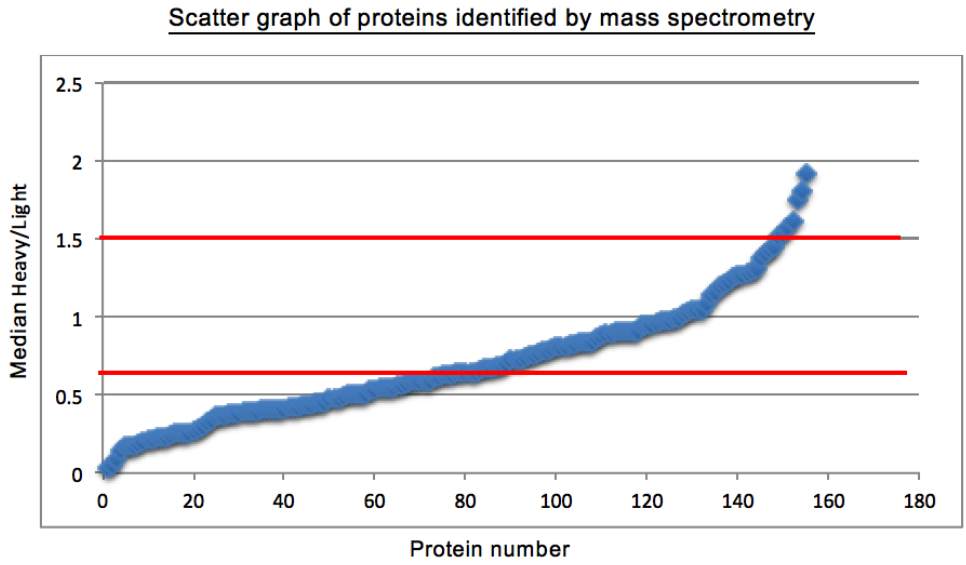

Figure 3.8: Scatter plot of proteomics data showing protein expression obtained from mass spectrometry of pooled uninfected and infected plasma. Light and heavy isotopes were used to distinguish between the uninfected and infected samples respectively. The red lines indicate cut off points for the H/L ratio. The differentially expressed proteins are the outliers. The original dataset of 153 proteins was thus reduced to 44 proteins.

Liquid chromatography-tandem mass spectrometry (LC-MS) is a powerful and robust analytical technique. Liquid chromatography separates multiple components of complex mixtures while mass spectrometry delivers structural identify with high molecular specificity and detection sensitivity (Pitt 2009). The individual abilities of liquid chromatography and mass spectrometry are enhanced by their tandem combination, experimental error is reduced.

The use of plasma in this study, a complex biological sample with a high protein dynamic range, meant that liquid chromatography fractionation was an essential step in the isolation and identification of target proteins. Liquid chromatography uses a column packed with porous, solid material known (the stationary phase), where the sample is injected and a solvent (the mobile phase) passes to transport the sample. Separation is achieved through exploiting the different affinities of chemical compounds in the sample for the stationary phase versus the mobile phase. After a sample is injected on to the column, it is adsorbed on the stationary phase and the solvent passes through the column separating compounds one by one. The component with the most affinity to the stationary phase is the last to

separate as the high affinity corresponds to more time taken to travel to the end of the column. The most commonly used liquid chromatography is reverse-phase chromatography (RP-LC). This is because it allows for precise control of variables such as organic solvent type, concentration and pH. In RP-LC the mobile phase is polar and the stationary phase is non-polar or hydrophobic. This means that polar molecules pass through the column at a faster rate than non-polar molecules. The separated compounds may then be determined by mass spectrometry.

Mass spectrometers operate by three main processes: ionisation, separation and detection. First the sample is introduced to the ionisation chamber and analyte molecules are converted into an ionised or charged state. Subsequently, ions are separated according to their mass to charge ratio (m/z) by a mass analyser. A detector records the m/z and ion counts. The last step involves a post processing software that determines the species and quantity of each ion (within the resolution limit of the instrument).

Proteins that are differentially expressed in infected plasma compared with uninfected plasma can be evaluated by isotopic labelling and quantitative LC-MS. Protein samples were first reduced and alkylated and subsequently digested into peptides using trypsin. The resulting peptides were labelled with stable isotopic reductive dimethylation strategy (Boersema et al. 2009). Reductive dimethylation labelling is performed using regular (light) or deuterated (heavy) forms of formaldehyde and sodium cyanoborohydride to add two methyl groups to each free amine. Peptides from uninfected and infected samples were labelled by reductive dimethylation (with light (L) and heavy (H) isotopic labels respectively). Upon LC-MS, extracted ion chromatograms of the light and heavy counterparts of each peptides, were calculated to derive relative peptides abundance and protein ratios were derived from the individual peptides ratios that belongs to each proteins.

Spectral data was searched against the ENSEMBL sheep database. Originally 153 proteins were identified in the plasma samples based on one or more unique peptide match. The data was then filtered by setting the coefficient variation (%CV) to less than 100%. The %CV is calculated by dividing the standard deviation of peptide profiles by the mean, proteins with %CVs greater than 100 have expression ratios that are considered unreliable. The extent of differential expression was assessed by filtering the median heavy/light (H/L chain) isotopes and retaining proteins between >1.5 and <0.666, leaving a dataset of 44 proteins (Figure 3.8). These stringent cut offs are applied to minimise the inclusion of false positives resulting from the lack of biological replication, removing proteins with potentially unreliable

expression ratios that would otherwise be classified as differentially expressed. The normalised fold change refers to the H/L ratio, hence proteins with a value <1 are down regulated in the infected sample. There is no change in expression for proteins with a value of 1, while upregulated proteins the number is >1. The most common plasma proteins already manipulated by ProteoMiner (such as albumin, transferrin and fibrinogen) were eliminated leaving 35 proteins (Table 3.3). A shortlist of 8 candidate proteins (Table 3.4) was established by comparison of the dataset with current literature. Validation of these proteins would reflect on the validation of the full list of proteins.

Table 3.3: List of 35 differentially expressed proteins identified by mass spectrometry in uninfected and infected pooled plasma.

Normalised fold change	Gene	Protein
0.22	SERPINA3	serpin peptidase inhibitor
0.27	HPX	hemopexin
0.27	IPSP	serpin peptidase inhibitor
0.36	SERPINA1	serpin family A member 1
0.39	SAA1	serum amyloid A-2 protein
0.39	TTR	transthyretin
0.39	IPSP	serpin peptidase inhibitor
0.47	IGLC6	immunoglobulin Lambda-6 Chain C Region
0.53	A1BG	alpha-1-B glycoprotein
0.56	C1QB	complement C1q B chain
0.5	ATP6V1A	ATPase H+ transporting V1 subunit A
0.59	IGL	immunoglobulin Lambda
0.59	ATP5H	ATP synthase, H+ transporting, mitochondrial Fo complex subunit D
0.59	C5	complement component 5
0.61	ITIH4	inter-alpha-trypsin inhibitor heavy chain family member 4
0.63	GC	GC, vitamin D binding protein
0.63	MT-ND1	NADH-ubiquinone oxidoreductase chain 1
0.64	CDH5	cadherin 5
0.66	C3	complement C3
1.55	GSN	gelsolin
1.55	SERPINF1	serpin family F member 1
1.58	BPIA2	BPI fold-containing family A member
1.61	APOD	apolipoprotein D
1.69	SHBG	sex hormone binding globulin
1.78	C1S	complement component 1, s subcomponent
1.80	F2	prothrombin precursor
1.89	CONG	conglutinin precursor
1.91	HABP2	hyaluronan binding protein 2
1.95	ITIH1	inter-alpha-trypsin inhibitor heavy chain 1
2	FBLN1	fibulin 1
2.02	ITIH2	inter-alpha-trypsin inhibitor heavy chain 2
2.16	C4BPA	complement component 4 binding protein alpha
2.27	CD5L	CD5 molecule like
2.36	SERPINA5	serpin family A member 5
2.73	PON1	paraoxonase 1

To identify proteins, data was searched against the ENSEMBL Sheep database. Clear-cut offs were applied to bring the original list of 153 proteins down to 35 proteins (full list in Appendix Table 1). Uninfected plasma was labelled with a light (L) isotopic label, and uninfected plasma with a heavy (H) isotopic label. The normalised fold change is a ratio, thus <1 signifies a decrease in protein expression in the infected sample while >1 relates to an increase.

Table 3.4: The 8 potential plasma biomarkers that were selected for validation.

Normalised fold change	Gene	Protein	Protein function	Examples of relevant studies showing relation to neurodegenerative diseases
0.27	HPX	hemopexin	Binds heme and transports it to the liver for iron detoxification and recycling.	Yu et al. (2003); Sui et al. (2004); Castano et al. (2006); Moore et al. (2014).
0.39	TTR	transthyretin	Transports thyroxin and retinol.	Yu et al. (2003); Riemer et al. (2004); Castano et al. (2006); Piubelli et al. (2006); Brechlin et al. (2008); Perrin et al. (2011); Rubenstein (2012); Barbisin et al. (2014); Song et al. (2014); Sui et al. (2014).
0.53	A1BG	alpha-1-B glycoprotein	Unknown function.	Sui et al. (2014); Muenchhoff et al. (2016).
0.56	C1QB	complement C1qB chain	Component of the C1q complex, involved in the complement system and innate immunity.	Afagh et al. (1996); Botto et al. (1998); Dandoy-Dron et al. (1998); Klein et al. (2001); Riemer et al. (2004); Xiang et al. (2004); Gehlenborg et al. (2009); Flores-Langarica et al. (2009); Erlich et al. (2010).
0.63	VDBP	vitamin D binding protein	Transports vitamin D metabolites.	Bishnoi, Palmer, and Royall (2015).
1.61	APOD	apolipoprotein D	Involved in lipid metabolism.	Dandoy-Dron et al. (1998); Riemer et al. (2004); Xiang et al. (2004); Skinner et al. (2006); Moore et al. (2014); Muffat and Walker (2010); Dassati, Waldner, and Schweigreiter (2014).
1.91	HABP2	hyaluronan binding protein 2	Binds hyaluronic acid and may play a role in coagulation.	Nagga et al. (2014).
2.00	FBLN1	fibulin 1	Binds to fibrinogen and other extracellular matrix structures.	Ahn et al. (2010).

A light (L) isotope was used to label uninfected plasma, while a heavy (H) isotope was used to label infected plasma. The selection of potential plasma biomarkers was based on the current literature and previous association with prion diseases or other neurodegenerative conditions. Five show decreased expression in infected samples, while three are increased. This is highlighted by the normalised fold change (<1 decrease, >1 increase). The function of each protein was obtained from UniProt.

The infected plasma sample is a pool from samples collected from 9 sheep 12 months post oral challenge with BSE brain material. Previous studies on sheep similarly inoculated, indicate that at this preclinical stage the level of PrP^{Sc} is undetectable in lymphoreticular organs or the CNS (Jeffrey, Ryder, et al. 2001); (Bellworthy et al. 2005). Hence, investigating the changes occurring with other proteins circulating within the body at the preclinical stage of infection is important. These blood-based proteins may give an indication of what is taking place during on going TSE infection. The full list of differentially expressed proteins suggests the changes occurring are involved in the immune system (particularly triggering and regulation of the compliment cascade), hemostasis (formation of fibrin and platelet activation), metabolism of lipids and signal transduction. The candidate biomarkers (Table 3.4) were selected by looking at publications where studies have suggested a connection between the protein (or corresponding gene) to either prion diseases or other neurodegenerative diseases.

Hemopexin is closely involved in the maintenance of iron/redox homeostasis in mammalian tissues. Hemopexin has previously been determined as a potentially relevant marker for prion diseases. It is one of the molecular transport proteins shown to be increased in the brains of scrapie infected mice (Moore et al. 2014). In regards to other neurodegenerative disorders, hemopexin has been reported to display a six and a half-fold upregulation in sera from patients with Alzheimer's disease (AD) (Yu et al. 2003). Significant upregulation was seen in serum of triple transgenic (PS1M146V/AβPPSwe/TauP301L) mice with AD (Sui et al. 2014). Additionally, hemopexin has been identified by mass spectrometry as increased in the CSF of AD patients (Castano et al. 2006).

Transthyretin is one of three prealbumins. Its main role is in the transport of thyroid hormones in the plasma and CSF. Transthyretin has been identified at high levels in CSF from patients with CJD (Brechlin et al. 2008). It is associated with increased expression during disease and has previously been suggested as a relevant CJD marker (Piubelli et al. 2006). It has been shown to be upregulated in the plasma of AD patients (Song et al. 2014) and early stage AD patients (Perrin et al. 2011). Gene expression profiling of BSE infected macaque brains show upregulation of transthyretin (Barbisin et al. 2014). Upregulation of the transthyretin gene has also been observed in scrapie infected brain tissue as determined by RT-PCR analysis of terminally ill scrapie infected and mock infected mouse brains (Riemer et al. 2004). Transthyretin is commonly found in proteomic analysis of prion disease and AD samples, it is also one of proteins identified in the previously mentioned studies for hemopexin (Rubenstein 2012); (Sui et al. 2014); (Yu et al. 2003); (Castano et al. 2006).

Alpha-1-B glycoprotein is of unknown function, however it has been linked to AD. In tracking plasma biomarkers using samples from AD patients, Song et al. (2014) suggested a upregulation of alpha-1-B glycoprotein in three replicate experiments. A significant increase in A1BG expression was observed by Muenchhoff et al. (2016) in plasma of AD patients when investigating protein changes at the asymptomatic and symptomatic stages of disease. Additionally, when screening the serum of

AD mice to identify potential novel protein biomarkers for early AD alpha-1-B glycoprotein was shown to be significantly upregulated (Sui et al. 2014). This upregulation is in contrast to our dataset where these proteins were downregulated

Among the proteins detected by mass spectrometry analysis were components of the complement system. C1q is the first component of the classical complement pathway. The C1q complement consists of 18 protein chains: six A, six B and six C. C1q binds to fibrillar β-amyloid (Aβ) found as extracellular deposits in tissues leads to activation of the classical complement pathway as well as pro-inflammatory events. An increase of C1qB-chain immunoreactivity was reported in neurons of AD patients (Afagh et al. 1996). Hence, the presence of C1q with amyloid deposits in the brain has lead to it association with AD pathology. C1q B chain has been shown to be upregulated (Riemer et al. 2004) or at least altered (Xiang et al. 2004) in scrapie infected brain tissue. Additionally, a 4-5 fold increase was observed in the level of C1qB mRNA in scrapie infected mice brains at the terminal stage of disease (Dandoy-Dron et al. 1998). In a transcriptomic study of 8 mouse prion diseases, three genes coding for C1q were shown to be among the top 10 upregulated genes in the brain (Gehlenborg et al. 2009). Mice deficient in C1q or complement receptors have been shown to be partially or fully protected against spongiform encephalopathy upon exposure to prions. The reduction in splenic accumulation of prion infectivity and PrP^{Sc} indicates that activation of specific complement components is involved in the initial trapping of prions in lymphoreticular organs at the early stage of infection (Botto et al. 1998). FDCs are a major extracerebral prion reservoir. It has been speculated that signalling mediated by binding of complement triggers a specific state of differentiation or activation of FDCs that allow accumulation of prions (Klein et al. 2001); (Flores-Langarica et al. 2009). C1q may also play a role in the PrP aggregation process. The interaction between C1q and PrP could represent an early step in the disease where elimination of the prion seed is prevented subsequently leading to further aggregation (Erlich et al. 2010).

Vitamin D binding protein is encoded by a gene that belongs to the albumin gene family. Although multifunctional, its main role is in binding vitamin D and its plasma metabolites and transporting them to target tissues. Vitamin D binding protein has been found to be elevated in the CSF of neurodegenerative disorder cases such as AD and PD. Raised serum vitamin D binding protein has been suggested to be useful indicator of future AD, hence it has been implicated in the pathogenesis of AD (Bishnoi, Palmer, and Royall 2015).

Apolipoprotein D is a high density lipoprotein, which unlike other lipoproteins (that are mainly produced in the liver) is mainly produced in the brain and testes. Its involvement in stress responses suggest it may have a neuro-protective role during ageing and neurodegeneration (Muffat and Walker 2010). Apolipoprotein D has previously been identified as a gene with upregulation in prion diseases from looking at scrapie infected brain tissue (Riemer et al. 2004). It has also been shown to be a differentially expressed gene in scrapie infected mouse brain, with >1.5 fold enhanced

expression (Xiang et al. 2004). Apolipoprotein D was elevated, compared to uninfected age matched controls, in brains of mice infected with the RML mouse strain of scrapie (Moore et al. 2014). It was first reported to exhibit increased expression in the brains of scrapie infected animals only at the terminal stage of disease by Dandoy-Dron et al. (1998). Dandoy-Dron et al. (1998) found a 3-8 fold increase in the level of mRNA in brains of scrapie infected mice. Similarly, an average twofold change increase was observed in scrapie infected mice using cDNA microarray (Skinner et al. 2006b). Apolipoprotein D has been found to be elevated in a variety of neurological disorders, including AD, schizophrenia and stroke (Dassati, Waldner, and Schweigreiter 2014).

Hyaluronan binding protein 2 is part of the S1 family of serine proteases. Secreted by the liver it binds hyaluronic acid and may play a role in coagulation. Hyaluronic acid impairs the integrity of the blood brain barrier (Al-Ahmad et al. 2019) and has been suggested as a potential biomarker for patients with vascular dementia, due to the detection of elevated levels in their CSF (Nägga et al. 2014). Both Hyaluronan binding protein 2 and Fibulin 1 were among the top upregulated proteins detected by the mass spectrometry. Fibulin 1 is found in association with the extracellular matrix and is involved in cell adhesion and motility. Fibulin 1 binds to fibrinogen and incorporates it into blood clots (Tran et al. 1995). Blood clots formed in the presence of Aβ peptide have an abnormal structure and are resistant to degradation. As its binding causes fibrinogen to oligomerize, it has been suggested that the interaction of Aβ with fibrinogen may contribute to the vascular abnormalities found in AD (Ahn et al. 2010). The vascular abnormalities that patients with AD may exhibit include altered cerebral blood flow, damaged cerebral vasculature and hemostasis impediments (de la Torre 2004). Vascular diseases such as atherosclerosis correlate in severity with dementia and AD (Bell and Zlokovic 2009). Functional decreases in blood flow and/or metabolic rate have been detected prior to the development of abnormalities seen on structural imaging, EEG or level of 14-3-3 in CSF in prion disease patients (Taber et al. 2002); (Mathews and Unwin 2001); (Matsuda et al. 2001); (Staffen et al. 1997).

The appearance of these proteins (or their genes) in other prion or neurodegenerative disease datasets in disease profiling studies give a strong indication of their usefulness as prospective biomarker candidates.

3.2.3 Biomarker validation in pooled samples

3.2.3.1 Testing and optimization of antibodies on sheep plasma

The ability to confirm the extent of differential expression of the chosen protein biomarkers between uninfected and infected plasma is of critical importance if any are to be deemed suitable for potential

clinical use. To validate the mass spectrometry predictions and quantify specific proteins the western blot technique was used. This approach involves separating proteins by molecular weight through gel electrophoresis, their transfer ('blotting') to a membrane, which is then antibody probed, and their subsequent detection by chemiluminescent, fluorescent or colorimetric tools. The result is a specific protein band that may be visualised. The benefit of western blot over other immunoassay methods is that if the target protein is altered (downregulated or overexpressed) the pixel density of the band changes. This change can be measured by LI-COR technology.

Following microBCA assay to calculate protein concentration, initial tests were performed on pooled samples of uninfected plasma. The plasma was diluted in RIPA buffer and aliquoted out for storage. This was done in an attempt to alleviate protease degradation, a potential problem for protein freeze thawed multiple times or stored at -20 ^{o}C. The samples differ from that used for mass spectrometry in that they had not been ProteoMiner treated. Antibodies for each potential biomarker were tested under various conditions (Table 3.5 and 3.6), however many showed cross reactivity (they were unable to recognise the intended target or resulted in non-specific binding and alternative protein bands). This was despite high percentage human and sheep amino acid similarity (protein identity) as established from comparing human and ovine peptide sequence identity on UniProt. This was done because the mass spectrometry data was searched against the ENSEMBL sheep database, while most antibodies are produced to react with human samples. Only three antibodies (fibulin 1, vitamin D binding protein and hemopexin) showed specific binding and were taken forward for further testing. The molecular weights for each biomarker are 26 kD (fibulin 1), 58 kD (vitamin D binding protein) and 56 kD (hemopexin). The molecular weights determined for vitamin D binding protein and hemopexin are as expected from predictions based on human or mouse data. Fibulin 1 is predicted to have a molecular weight of 95 kD which is cleaved into 70 kD and 26 kD fragments (Sasaki et al. 1996). The antibody used here detects the 26 kD form (Aviva Systems Biology FBLN1 Ab OACD03419). A large band with high fluorescent intensity may obscure any small changes between samples. Optimisation by testing different protein loading (while keeping western blotting conditions stringent) was performed for efficient quantification by LI-COR scanning (Figure 3.9). After further optimisation experiments, it was decided that both hemopexin and vitamin D binding protein antibodies worked best with 8 µg of protein, while the clearest bands seen for fibulin 1 was with 5 µg.

Table 3.5: Table of antibodies tested for the chosen protein biomarkers in order to validate the mass spectrometry data.

Protein	Western blot compatible Antibody Name	Company	Reference	Human and sheep amino acid similarity (protein identity %)	Species Reactivity
Hemopexin	Polyclonal antibody, hemopexin	Fisher Scientific UK Ltd	13403677	73%	Human
Transthyretin	Polyclonal antibody, anti-Transthyretin	Fisher Scientific UK Ltd	12848892	72%	Human, mouse, rat
Alpha 1 B glycoprotein	A1BG Polyclonal Antibody	Thermo Fisher Scientific	PA5-14207	68%	Human
Complement C1q B chain	C1Q B Antibody Polyclonal	Thermo Fisher Scientific/Life Technologies	PA5-42554	74%	Human, canine, equine
Vitamin D binding protein	Polyclonal antibody, vitamin D binding protein	Fisher Scientific UK Ltd	13413207	79%	Human, mouse
Apolipoprotein D	Polyclonal antibody, apolipoprotein D	Fisher Scientific UK Ltd	13481377	73%	Human, mouse
Hyaluronan binding protein 2	Anti-HABP2 Antibody Polyclonal	Cambridge Biosciences/Atlas Antibodies	HPA019518	82%	Human
Fibulin 1	Anti-Fibulin 1 antibody	Abcam	EPR10913	93%	Human, mouse, rat

All antibodies were rabbit polyclonal. The human and sheep amino acid similarity (protein identity %) is a comparison of the human and ovine target peptide sequence, it is included as a probable indicator of antibody performance. Many antibodies are produced to react with human proteins, however the samples tested in this experiment are from sheep.

Table 3.6: Optimization of antibodies to select proteins for Western blot.

Protein	Manufacturers recommended dilution for primary Antibody	Primary Antibody dilutions tested	Secondary Antibody dilutions tested	Protein Load tested (µg)	Western blot result
Hemopexin	1:1000 – 1:5000	1:5000 1:3000 1:2500 1:2000 1:1000	1:10 000 1:50 000 1:100 000 1:200 000	2, 4, 6, 8, 10 7, 8, 9, 10	Quantifiable band signal at 56 kD achieved with 8 µg of protein,1:2500 primary antibody dilution and 1:5000 secondary antibody dilution.
Transthyretin	1:1000	1:2000 1:1500 1:1000 1:500	1:10 000 1:50 000 1:100 000 1:200 000	2, 4, 6, 8, 10	Cross reactivity (multiple nonspecific bands).
Alpha 1 B glycoprotein	1:1000	1:2000 1:1500 1:1000 1:500	1:10 000 1:50 000 1:100 000 1:200 000	2, 4, 6, 8, 10	Cross reactivity.
Complement C1q B chain	1:2000	1:3000 1:2500 1:2000 1:1000	1:10 000 1:50 000 1:100 000 1:200 000	2, 4, 6, 8, 10	Non-target band identified.

Vitamin D binding protein	1:1000 – 1:5000	1:5000 1:3000 1:1000 1:750 1:500	1: 5 000 1:10 000 1:50 000 1:100 000 1:200 000	2, 4, 6, 8, 10 7, 8, 9, 10	Quantifiable band signal at 58 kD achieved with 8 µg of protein Works with 1:750 primary antibody dilution and 1:5000 secondary antibody dilution.
Apolipoprotein D	1:1000	1:2000 1:1500 1:1000 1:500	1:10 000 1:50 000 1:100 000 1:200 000	2, 4, 6, 8, 10	Cross reactivity.
Hyaluronan binding protein 2	1:1000	1:2000 1:1500 1:1000 1:500	1:10 000 1:50 000 1:100 000 1:200 000	2, 4, 6, 8, 10	Cross reactivity.
Fibulin 1	1:1000 – 1:5000	1:5000 1:3000 1:1000 1:750 1:500	1: 5 000 1:10 000 1:50 000 1:100 000 1:200 000	2, 4, 6, 8, 10 4, 5, 6, 7	Quantifiable band signal at 26 kD achieved with 5 µg of protein. Works with 1:750 primary antibody dilution and 1:5000 secondary antibody dilution.

The antibodies for the potential biomarkers were tested at a range of concentrations, combined with dilutions of secondary antibody (Donkey anti-Rabbit IgG ThermoFisher Scientific 31238, manufacturer's guide dilution 1:10 000 - 1:200 000) across multiple uninfected plasma protein concentrations. Only three antibodies (Hemopexin, Vitamin d binding protein and Fibulin 1) yielded specific bands.

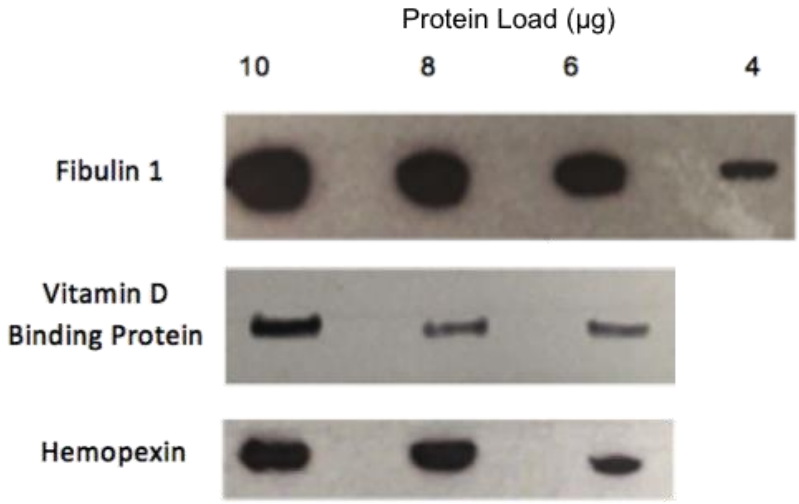

Figure 3.9: Optimisation of protein loaded before quantification for each biomarker antibody. A range of protein loads were tested (with the manufacturer's suggested dilution of antibody) to obtain an appropriate western blot band signal required for quantification. As a large band signal may obscure any slight differences between the two samples (uninfected and infected plasma), a thinner band is more favourable for comparison and detection of minute changes. Shown here are example western blots for a range of protein concentrations loaded for each working antibody.

3.2.3.2 Quantification of proteins in pooled uninfected and infected plasma

In order to determine specific protein expression of these potential biomarkers, western blot and LI-COR imaging was employed. Samples used here were equivalent to the plasma pools depleted by ProteoMiner prior and analysed by mass spectrometry. The difference in protein expression was measured in the infected sample compared to the uninfected sample (the uninfected sample was set as the norm).Two gels were run in parallel to resolve loading differences between lanes (where the same concentration of protein is loaded, as calculated through microBCA assay). One gel was stained with Coomassie Instant Blue™ and used to measure the whole protein content of each lane giving a 'whole protein signal'. Thus small differences between loading of individual samples may be established (and accounted for) when calculating differences in specific protein expression (Eaton et al. 2013).

A 'ratio' value is calculated for a particular sample by dividing that sample's whole protein signal by the average whole protein signal for all samples (on the same gel) of the same protein concentration. A 'normalised western blot signal' can then be calculated by dividing the western blot band signal (detected from LI-COR scanning the antibody probed, chemiluminescence stained nitrocellulose membrane) by the ratio. These steps are depicted in Figure 3.10 A. Figure 3.11 gives example gels for each biomarker chosen for validation. To plot the graph in Figure 3.12 A a 'comparison' value is calculated from the normalised western blot signal by dividing the normalised western blot for the infected pooled plasma by that for the uninfected plasma.

The results of the pooled plasma corroborate the mass spectrometry data, despite the mass spectrometry being performed on ProteoMiner manipulated pooled plasma samples (while pooled plasma used in the western blots for verification were not ProteoMiner treated). For fibulin 1 mass spectrometry suggested there would be an increase in expression in the infected plasma sample. From running 6 experiments comparing expression in uninfected and infected pooled plasma an upward trend in fibulin 1 expression may be observed (Figure 3.12 A). There is not much variation from experiment to experiment, as illustrated by the table in Figure 3.12 B. The paired T test for the Comparison data (Normalised western blot signal for uninfected and infected pooled plasma) gives a P value of 0.0028. This means the result is significant. Both vitamin D binding protein and hemopexin were predicted by the mass spectrometry to decrease in expression from the uninfected to the infected pooled plasma. For vitamin D binding protein there is a clear decrease in expression. The P value for the Comparison data across 6 experiments is 0.007. This is highly significant. Similarly, in

the case of hemopexin there is also a downward trend in expression exhibited by the western blot results. The P value for the paired T test of the hemopexin Comparison results is 0.06. This is at the margin of statistical significance.

A.

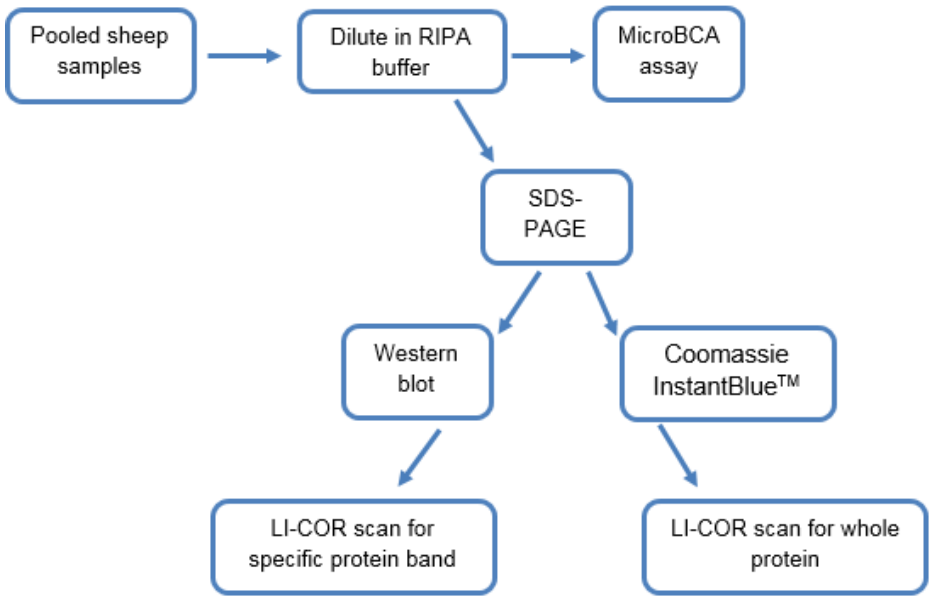

B.

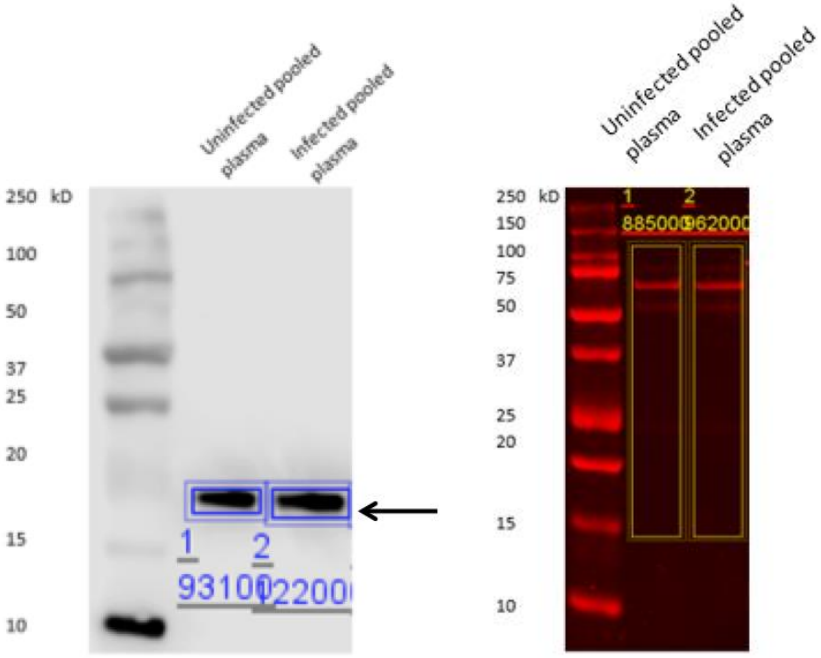

Figure 3.10: Steps involved in the LI-COR Western blot determination of protein expression. (A) is a flow diagram summarising the procedure performed with pooled plasma sheep samples. Volumes equivalent to the same protein concentration of pooled uninfected and pooled infected plasma were simultaneously loaded on to two gels. One gel (B) is taken through the full western blot procedure (arrow pointing to band of interest). The second gel (C) is stained with Coomassie Instant Blue™ to determine whole protein content of the lanes. Protein is transferred to a nitrocellulose membrane by blotting. Following blocking, application of primary antibody (here anti-Fibulin1), secondary antibody and chemiluminescence solution the membrane is scanned by LI-COR and band signal is detected by measuring pixel density.

A.

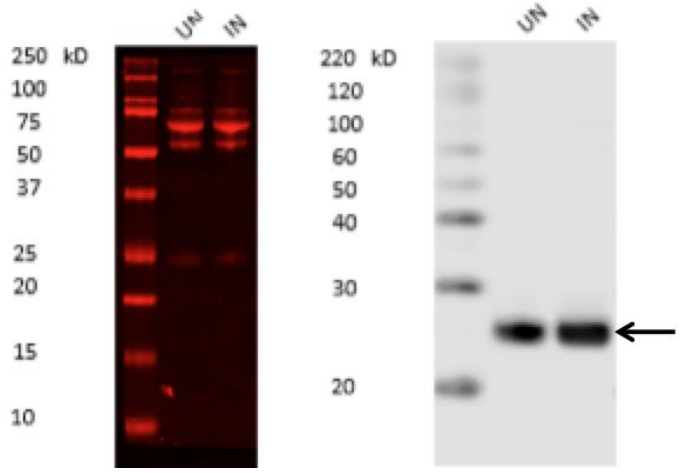

B.

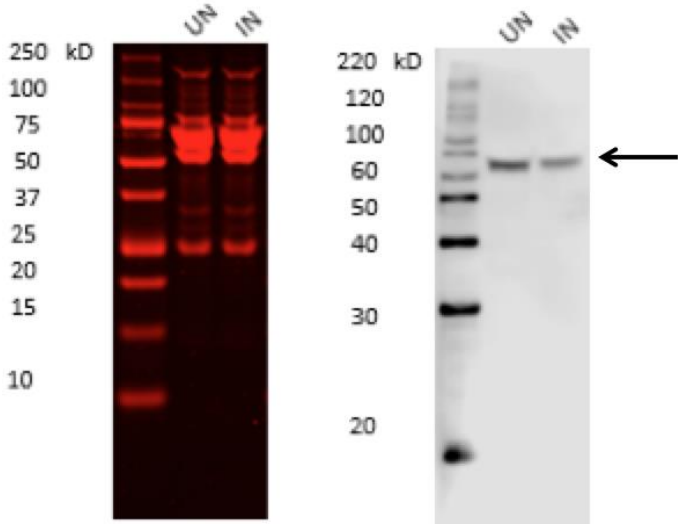

C.

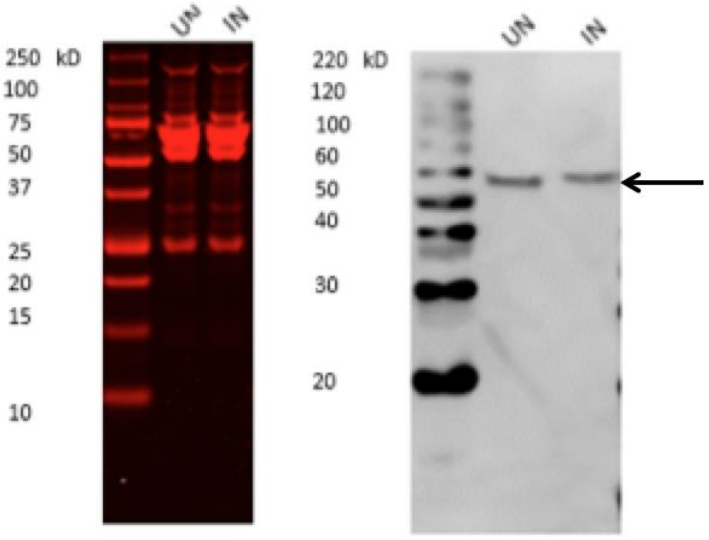

Figure 3.11: Example blots for the three biomarkers with uninfected (UN) and infected (IN) pooled plasma. Duplicate gels are run in parallel, one gel is stained with Coomassie Instant Blue™ to detect the whole protein content of the lane. The second gel passes through the full western blot procedure and a specific individual band is determined. The arrows indicate bands of interest (A) Fibulin 1 is at 26 kD, (B) Vitamin D Binding Protein at 58 kD and (C) Hemopexin at 56 kD.

A.

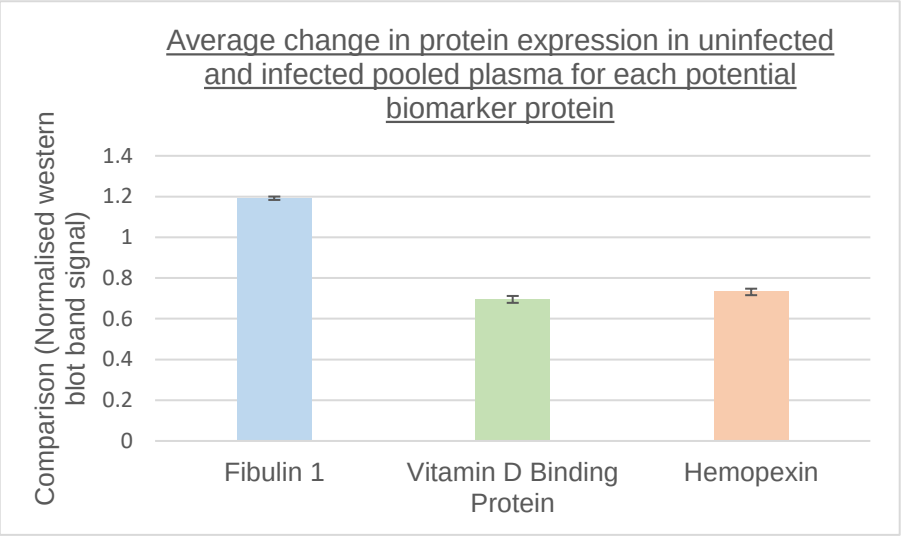

B.

Sample	Comparison (Normalised western blot band signal)						Mean	Std Dev	SEM
	Experiment no. 1	Experiment no. 2	Experiment no. 3	Experiment no. 4	Experiment no. 5	Experiment no. 6			
Fibulin 1	1.18	1.14	1.13	1.23	1.22	1.25	1.19	0.048	0.020
Vitamin D Binding Protein	0.66	0.72	0.77	0.83	0.65	0.54	0.70	0.102	0.042
Hemopexin	0.63	0.74	0.73	0.70	0.68	0.91	0.73	0.096	0.039

Figure 3.12: Results for biomarker expression in pooled uninfected plasma compared to pooled infected plasma. Graph A illustrates the average difference in protein expression for the three biomarkers. The table (B) shows this data from 6 repeat experiments. Experiments are numbered in order of date performed. The standard deviation (Std Dev) across the six experiments is low, indicating the accuracy of results.

3.2.4 Biomarker validation in individual samples

After confirming that the results for the change in expression between pooled uninfected plasma and pooled infected plasma for the potential biomarkers were reproducible by western blot it was decided to expand the work to look at results in individual sheep samples. The results for the potential biomarkers with the pooled plasma should be somewhat reflected by the results from individual sheep. It will also highlight if there is any single sheep that has skewed the data in a certain direction. These sheep were the same nine sheep that were used to make the pooled samples. To use as controls, three age matched negative control sheep from the same study, which had been orally dosed with uninfected cattle brain homogenate, were chosen. This was to ensure that any changes observed were not just age dependent. Furthermore, an aliquot of pooled plasma was used as a positive control, the results of which should be the same across all analyses. Unfortunately due to issues with sample storage, although this sample was run on each gel the data was not quantifiable across all time points. Seven time points that cover the transfusion study were selected for analysis, these time points represent different stages during the incubation period of infection (Prechallenge, 4 months, 8 months, 10 months, 12 months, 18 months post-infection and Clinical). Fewer samples were available at the 4 months and 18 months time points. For 18 months, where only one negative control sheep had blood taken, control sheep from the closest time points (12 months) were used as substitutes and run on the same gel. Not all sheep had blood collected at these time points during the course of the transfusion study. Additionally, no samples for sheep N233 were collected at 10 months post-infection (summarised in Table 3.7).

Table 3.7: List of individual sheep and time points that plasma samples were collected at during the transfusion study.

Sheep ID	Sheep No.	Time point						
		Pre-challenge	4 months	8 months	10 months	12 months	18 months	Clinical
N257	1							
N236	2							
N233	3							
N251	4							
N261	5							
N189	6							
N231	7							
N232	8							
N157	9							
N239	10*							
N170	11*							
N217	12*							

* Control sheep

The shading signifies the presence of samples available for data analysis. Not all sheep has samples taken at every time point. The control sheep are age-matched with the infected sheep but were not exposed to BSE.

Samples from the twelve sheep at the seven time points were removed from -80 ^{o}C storage (Sheep IDs listed in Table 3.6), diluted in RIPA buffer and microBCA assays were performed to determine protein concentration. Following this, the protein load was further optimised to achieve to ensure the appropriate amount per lane needed in efficient quantification. Similar to the procedure used in determining differences in protein expression in the pooled uninfected and infected samples, the individual sheep samples for each specific time point were run on duplicate gels. One gel was stained with Coomassie Instant Blue™ for analysing whole protein content of the lanes. The second gel was taken through the western blot procedure and individual protein bands captured by LI-COR scanning. In order to calculate a normalised western blot signal, the western blot band signal is divided by the ratio (as done for the pooled samples). However, here the ratio is determined by dividing that sample's whole protein signal by the highest whole protein signal (out of those from the twelve sheep run on the same gel). The procedure is depicted in Figure 3.13.

Two gels were produced for each of the seven time point, with samples from control sheep interspersed between experiment sheep to avoid bias (one Coomassie Instant Blue™

stained for the whole protein signal, and one taken through the full western blot procedure to obtain a western blot band signal). This was done for the three different biomarkers (at least forty-two gels). Figure 3.14 shows example gels for the initial individual sheep blots. For technical reasons yielding poor results, the data could not be interpreted. Analysis of gels were inconsistent due to large discrepancies in whole protein band signal from Coomassie Instant Blue™ stained gels (when there should have been equal loading between lanes, across samples). This was possibly a consequence of inaccuracy in sample preparation, pipetting errors or resolving gels in different gel tanks. Western blot band signals were also implausibly variable. After performing these experiments, a fault was discovered with one of the transfer units this resulted in poor and inconsistent transfer of protein to membrane depending on equipment being used affecting certain time points more than others. In Figure 3.14 much fainter signals can be seen on the second half of the gel (samples following the second marker for sheep 12, 7, 8, 9 and the uninfected pool). The transfer tank was then taken out of use. In an attempt to overcome the variation between running experiments on different days and using different equipment the experiment was altered. Further gels were processed for the specific biomarkers. This time, two gels were resolved for an individual sheep but with samples from multiple time points. Similar inconsistences were also observed when analysing the data.

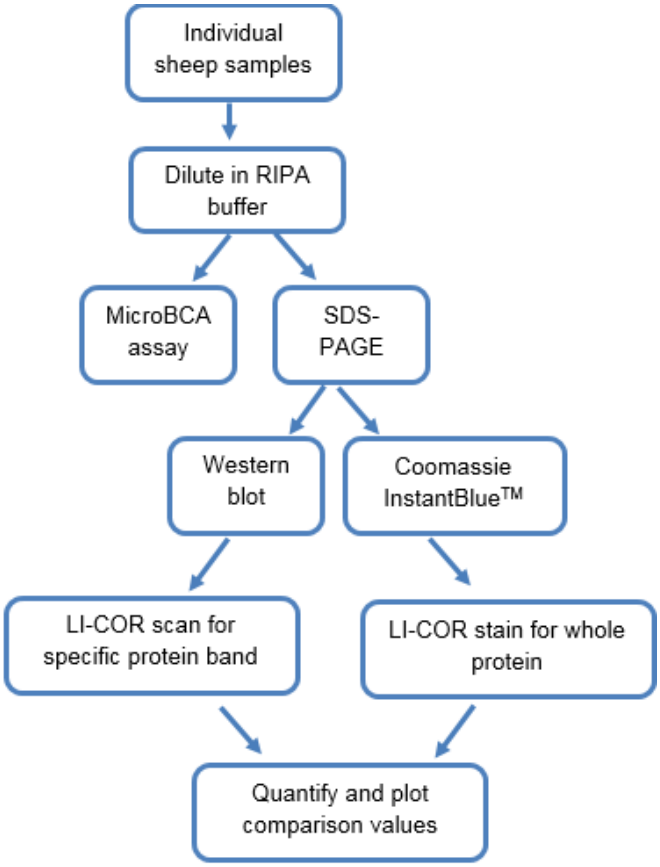

Figure 3.13: Overview of individual plasma analysis. In order to determine the level of protein expression for each candidate biomarker in the individual sheep plasma, samples were resolved on gels and analysed by LI-COR. The flow chart shows the steps involved to run each gel. Plasma from nine sheep were individually diluted in RIPA buffer (to prevent protein precipitation). Samples were taken for microBCA assay to establish protein concentration. Following this 1 mg/mL stock solutions were prepared and appropriate quantities of protein (as optimised for use with each particular biomarker antibody) resolved in duplicate gels by SDS-PAGE electrophoresis. One gel is forwarded for the whole western blot procedure and membranes antibody probed to obtain specific bands that allowed for quantification. The second gel is stained over night in Coomassie Instant Blue™ and a signal for the whole protein content per lane (per sample) quantified. A ratio value is obtained by dividing the whole protein signal by the highest whole protein signal across the gel (as the same protein concentration for each of the nine sheep samples should have been loaded, thus taking into account loading discrepancies). The western blot signal is then divided by the ratio and this value plotted on graphs. Initially this was performed on samples that covered several time points across the transfusion study. Due to inconsistencies between experiments this was scaled back to compare the two time points used initially for uninfected and infected samples in the mass spectrometry analysis (Figures 3.18,3.20, 3.22).

A.

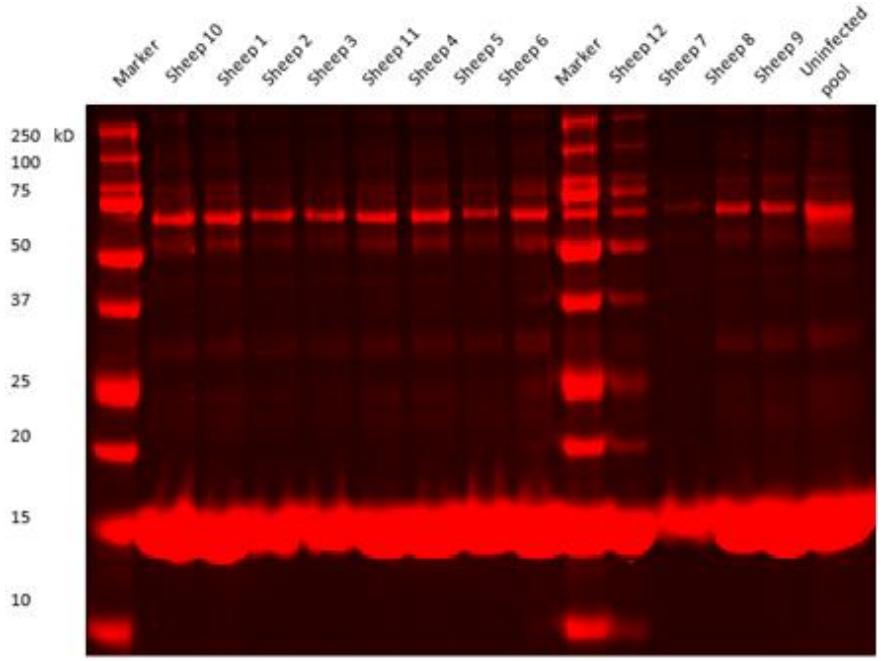

B.

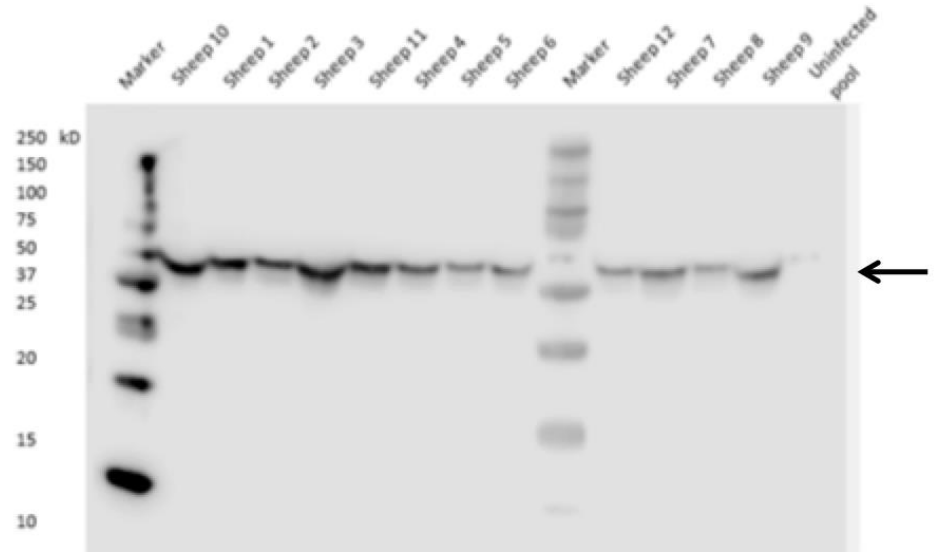

Figure 3.14: Representative Coomassie Instant Blue™ stained gel and western blot for individual sheep plasma samples at 8 months, probed for hemopexin (8 µg of protein loaded). The initial experiments on individual sheep plasma show uneven protein load across lanes (A). The uninfected pooled plasma (last lane of B) does not show up on the western blot and this may be a result of poor sample storage or handling. Additionally there is spill over from the marker lane into the neighbouring lane of the Coomassie Instant Blue™ stained gel.

Following on from the successful validation of the mass spectrometry data with the pooled samples, it was predicted that the changes seen in the pooled samples would also be reflected in the individual samples that made up these pools at their particular time points (prechallenge and 12 months post infection). As the results from running the individual samples for different time points on different gels were not consistent with the mass spectrometry data or from validation with the pooled samples, it was decided to start again as well as redesign the experiment. First, microBCA assays of the original samples in RIPA buffer were performed again. Extra care was taken with calculations (ensuring not to include predicted values above or below the standard curve). Figure 3.15 shows a test run following this. There is improved loading and a more consistent whole protein signal. The validation of mass spectrometry data using individual sheep samples was then simplified.

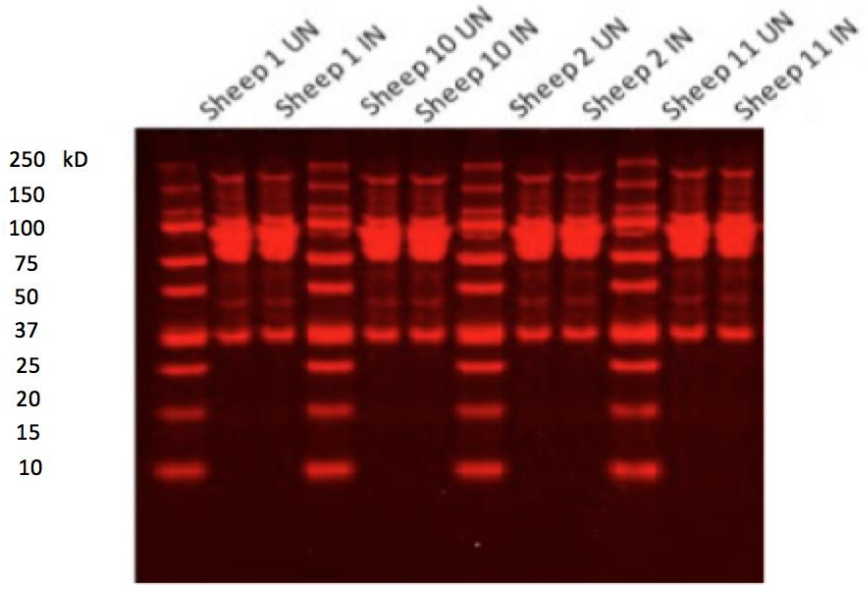

Figure 3.15: Preliminary test for even protein loading following repeat microBCA of individual sheep plasma samples at two time points (8 µg of protein loaded). The total protein loading is less variable after redoing microBCA assay for original samples and preparing stock dilutions and samples in loading buffer again. Uninfected and infected plasma (prechallenge and 12 months post infection) from the same sheep are resolved side by side, both control and infected sheep are shown here.

Only two time points were compared, the same two time points compared with pooled plasma (uninfected or prechallenge and infected or 12 months). Multiple sheep (including the same control sheep) were run on each gel. Ideally, using this method would overcome some of the obstacles encountered in the first experiment. A total of six gels were run for each biomarker (including 3 for whole protein staining).

Figure 3.16 A shows fibulin 1 expression for individual sheep plasma samples at two time points, example gels are given in Figure 3.17.There is no change hence no statistically significant difference in fibulin 1 expression for control sheep at the two time points. The difference in fibulin 1 levels in BSE infected sheep between prechallenge and 12 months is highly statistically significant (paired T test P value = 0.0055). Figure 3.16 B shows the difference in fibulin 1 expression between the two time points (the normalised western blot values at prechallenge subtracted from the normalised western blot values at 12 months). Comparing difference between the control and infected sheep is significant (T test P value = 0.0165). If there was no change in fibulin 1 expression between the two time points for both infected and control groups of sheep, then it would be expected that the difference (12 month expression – prechallenge expression) would be the same when comparing one group to the other. As this is not the case (indicated by Figure 3.16 B and the significant P value), it can established that the expression of fibulin 1 in infected sheep varies to that of control sheep.

Vitamin D binding protein expression for control and test individual sheep are depicted in Figure 3.18 A, with representative gels shown in Figure 3.19. The paired T test result for comparing protein expression of infected sheep at prechallenge and infected sheep at 12 months is significant (P value =0.0113). Comparing expression of vitamin d binding protein in control sheep and infected sheep at 12 months also gives a significant result (T test P value = 0.0222). The difference between normalised western blot signals (prechallenge subtracted from 12 months) for the two groups (control and infected sheep) can be seen in the second graph (Figure 3.18 B). It is almost significantly different (T test P value = 0.0763).

In the case of hemopexin (Figure 3.20 A and Figure 3.21) although the average hemopexin levels at 12 months for infected sheep were lower compared to prechallenge levels, it is not a statistically significant difference. The reason for this is likely to down to the great variability seen in hemopexin levels across all sheep. The difference between 12 months and prechallenge normalised western blot results is shown in Figure 3.20 B. Comparing control and infected sheep, this difference is bordering on the significance (T test P value = 0.0655).

A.

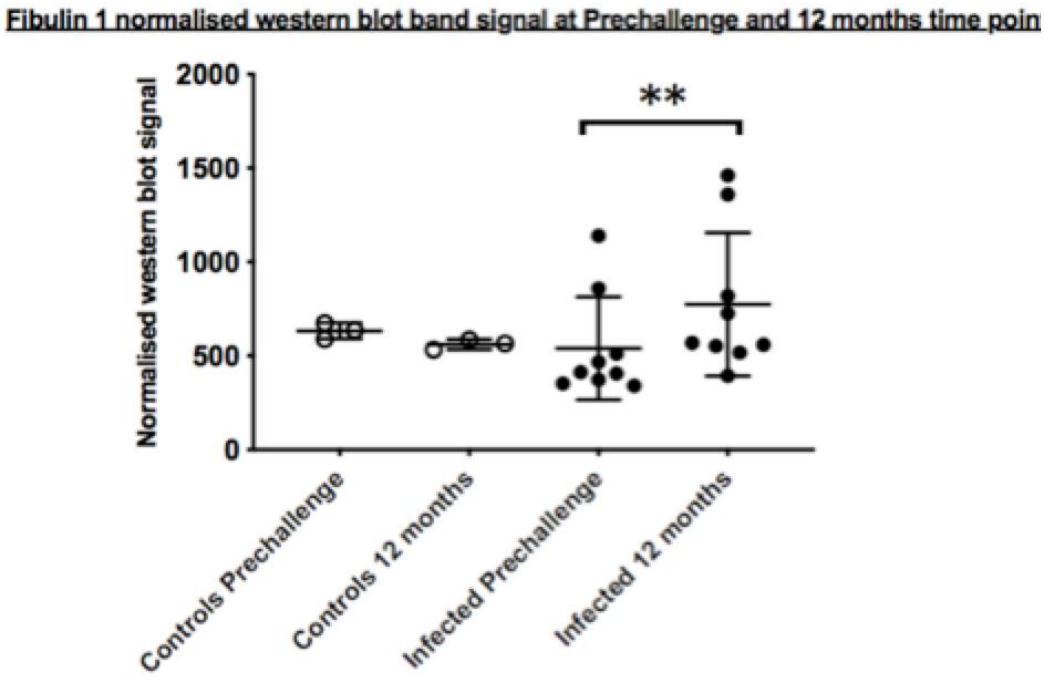

B.

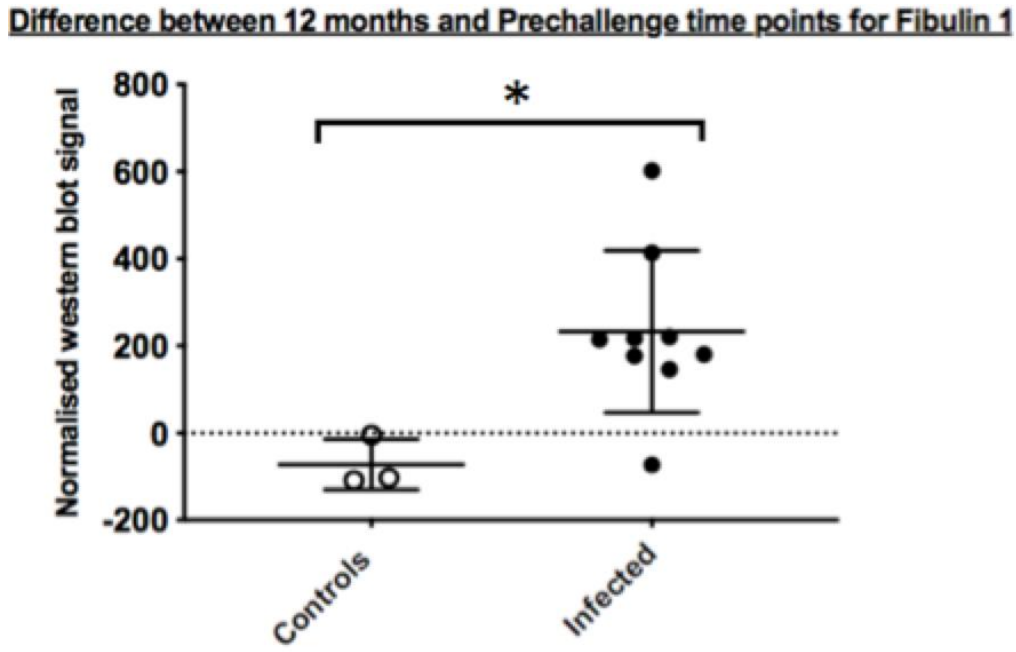

Figure 3.16: Fibulin 1 expression in individual sheep plasma at Prechallenge compared to 12 months post infection. Graph (A) shows a clear increase in fibulin 1 expression in infected sheep at the 12 months time point compared to at Prechallenge. The asterisk indicates a paired T test with a significant result (P=0.0055). The level of fibulin 1 expression for control sheep is consistent at both time points (there has been no change over time in control sheep). Graph (B) is the difference between 12 months and Prechallenge (the normalised western blot band signal at prechallenge subtracted from the normalised western blot band signal at 12 months) plotted for control sheep and infected sheep.The asterisk shows a significant value was calculated in the T test perfomed (P = 0.0165) when comparing the two sheep groups.

A.

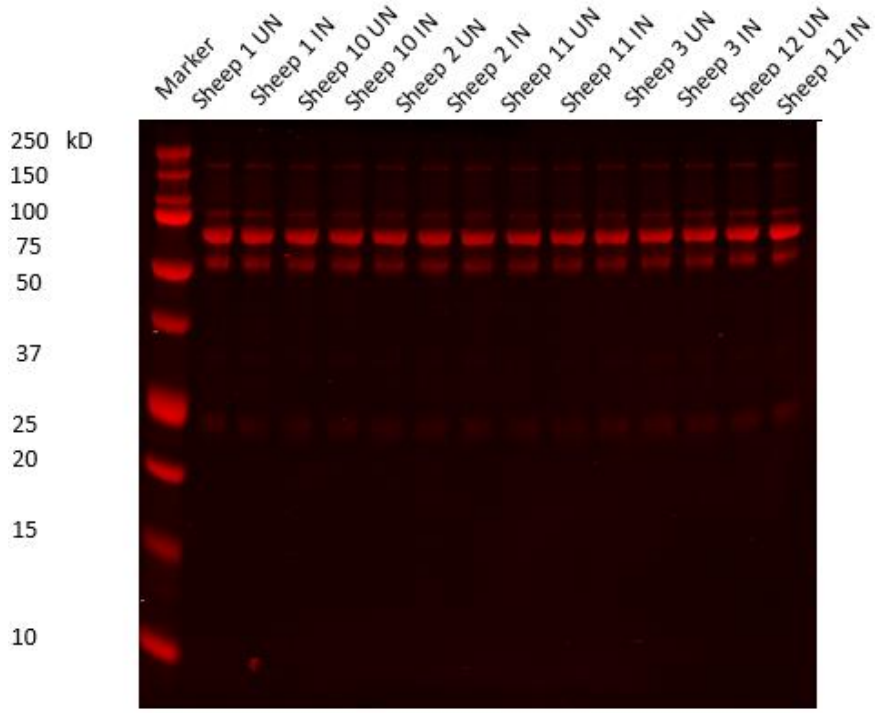

B.

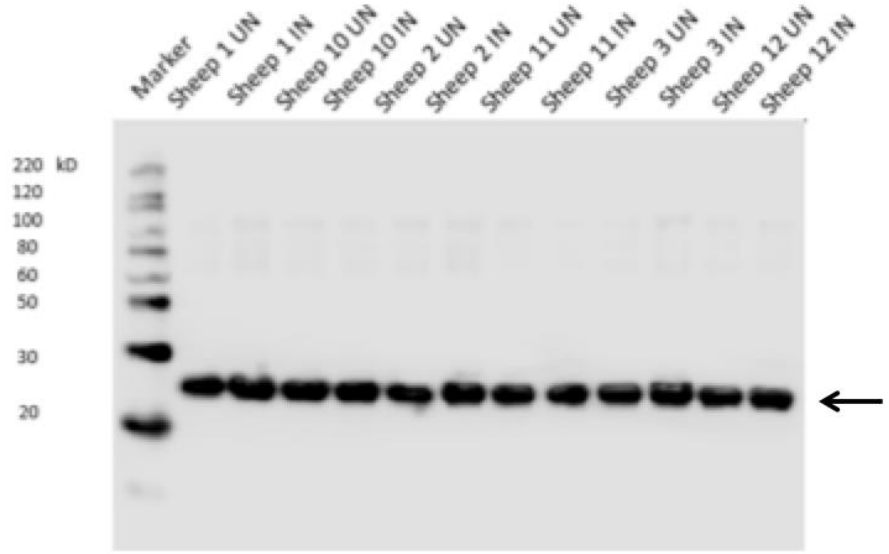

Figure 3.17: Representative gels are shown for individual plasma sheep samples at prechallenge and 12 months post infection probed for fibulin 1 (5 µg of protein loaded). Gel (A) is a Coomassie Instant Blue™, LI-COR scanned gel for quantification of whole protein signal. This discussion should be in the text. The second image (B) is of the membrane post-western blot and LI-COR scanned (arrow points to band of interest). UN/uninfected (Prechallenge) and IN/infected (12 months) samples for each sheep were loaded next to one another for easy comparison. Control sheep were interspersed between the test sheep to avoid bias.

A.

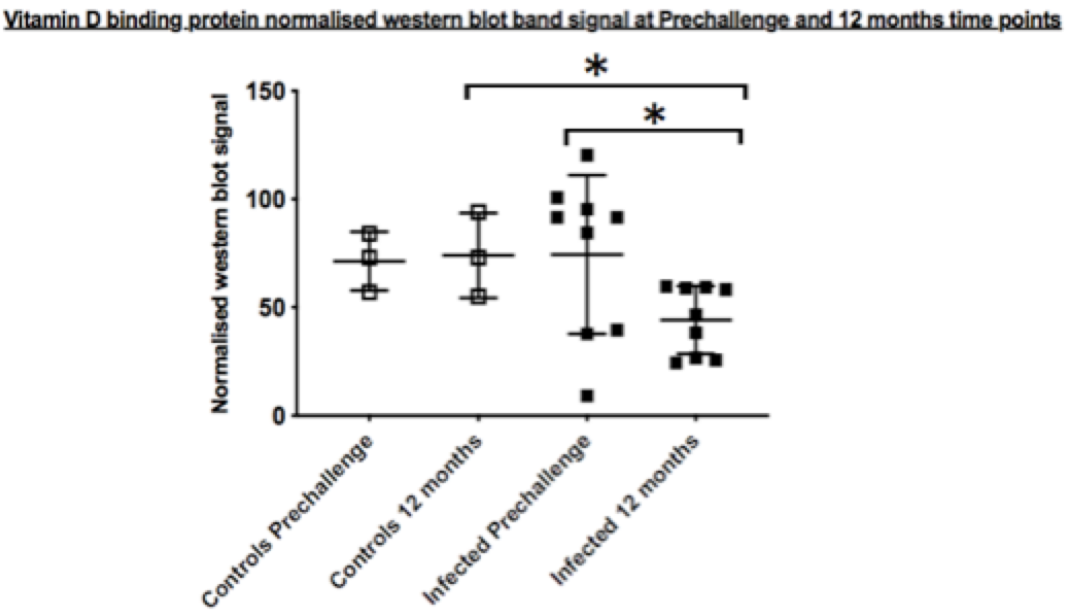

B.

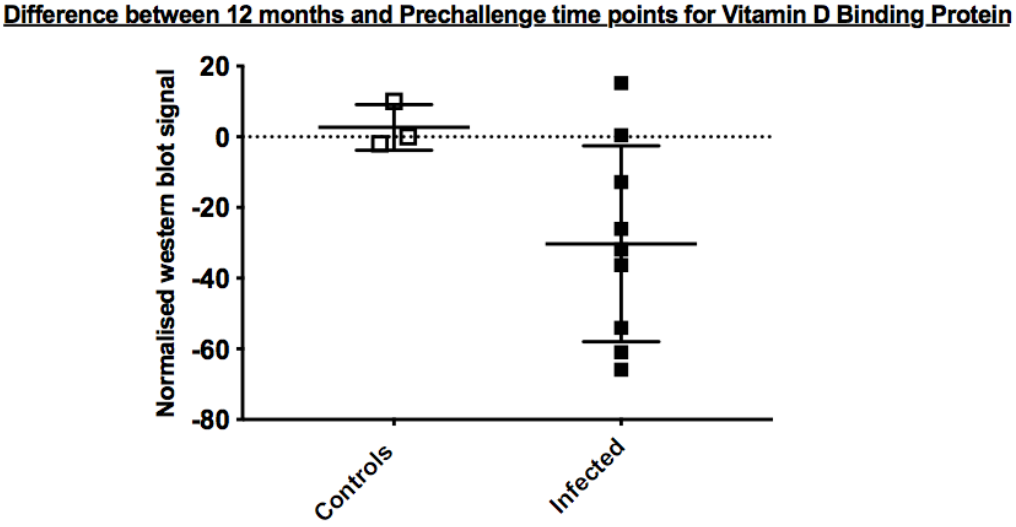

Figure 3.18: Vitamin D binding protein expression in individual sheep at Prechallenge compared to 12 months. The graph (A) shows the level of vitamin D binding protein expression has decreased from prechallenge to 12 months in infected sheep. This is in contrast to the control sheep where there is no change vitamin D binding protein expression from prechallenge to 12 months. There is a significant difference (Paired T test P=0.0113). A significant difference was also observed when comparing control sheep at 12 months to infected sheep at 12 months (T test P=0.0222). Graph (B) shows the difference between 12 months and Prechallenge normalised western band signal for control and infected sheep (the normalised western blot band signal at prechallenge subtracted from the normalised western blot band signal at 12 months). Comparing control and infected sheep shows an almost significant change in vitamin D binding expression between the two groups (T test P=0.0763).

A.

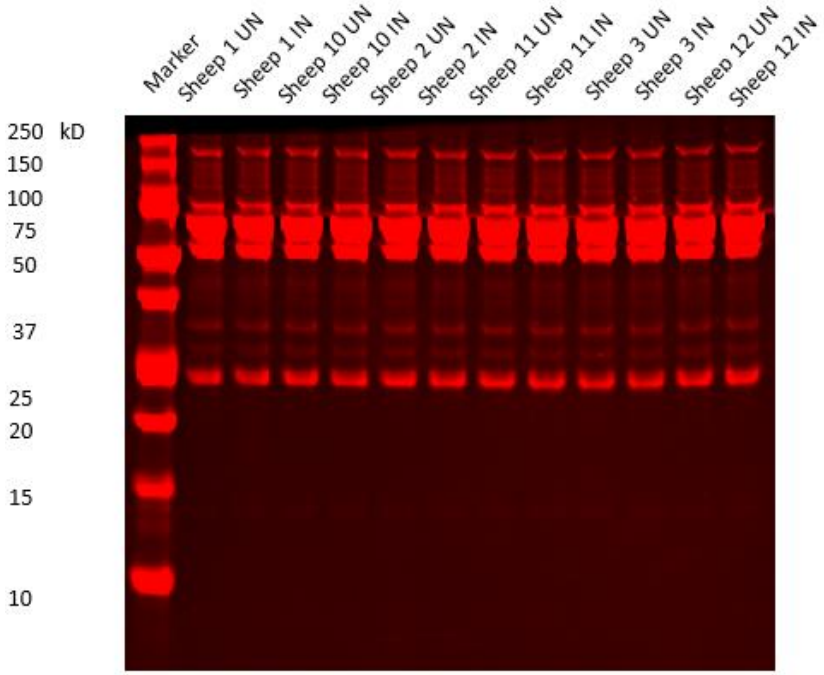

B.

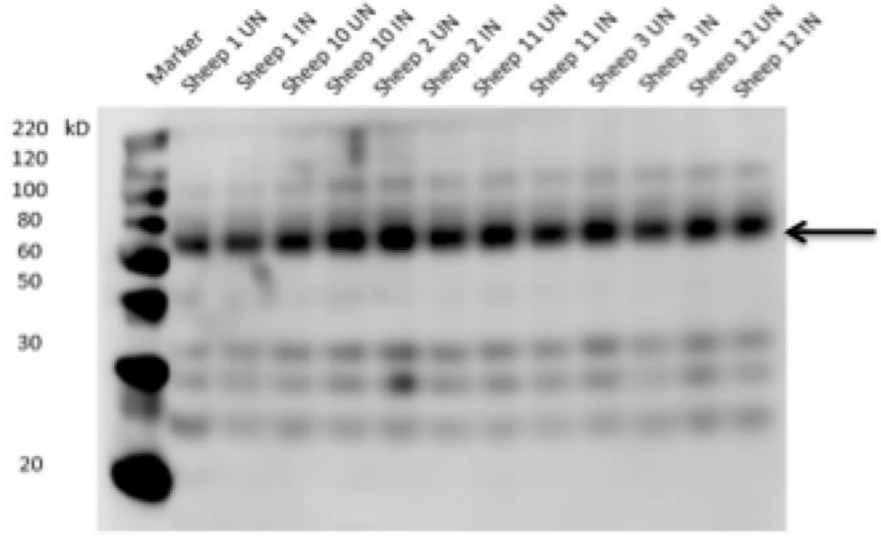

Figure 3.19: Representative gels are shown for individual plasma sheep samples at prechallenge and 12 months post infection probed for vitamin D binding protein (8 µg of protein loaded). Two gels of the same samples were resolved at the same time, with UN or uninfected (Prechallenge) and IN or infected (12 month) placed side by side for easy comparison. The first (A) is Coomassie InstantBlue™ stained to obtain the whole protein signal. Protein on the second gel is transferred to a membrane that is antibody probed and LI-COR scanned (B). The arrow highlights the band of interest. Although, like the antibodies for the other biomarkers, the vitamin D binding protein antibody had been optimised for use, a new batch from the same manufacturer were used in these experiments. Hence, this antibody stock seems to be more sensitive than that used previously on the pooled samples (Figure 3.12) and the blot also shows non-specific bands.

A.

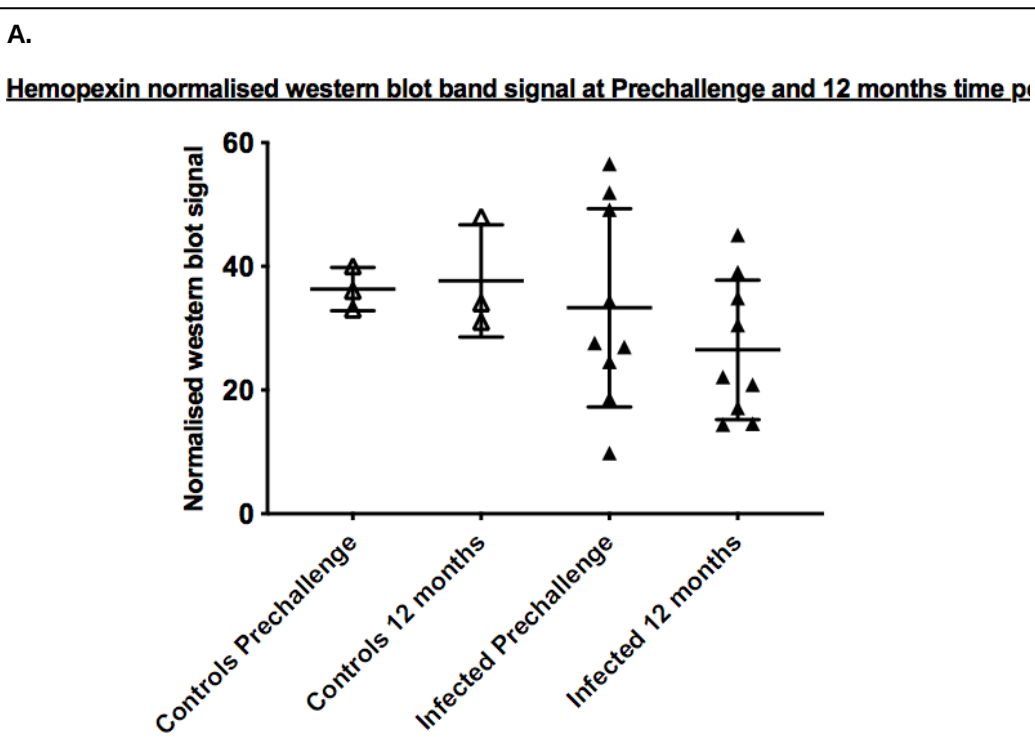

B.

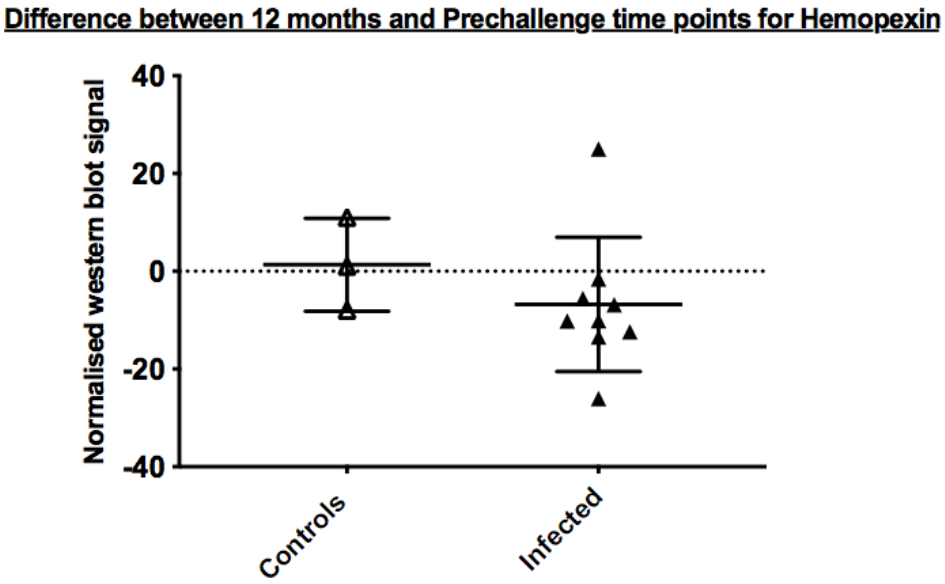

Figure 3.20: Hemopexin expression in individual sheep at Prechallenge compared to 12 months. Graph (A) shows data for expression of hemopexin in control and infected sheep at two time points. Although the level of hemopexin is unchanged between Prechallenge and 12 months for control sheep, there is a decrease in expression for infected sheep at the same time. The last graph (B) plots the difference between western blot signals at 12 months and Prechallenge (normalised western blot signal at prechallenge is subtracted from the normalised western blot signal at 12 months) for control and infected sheep. The difference is bordering on significant (P=0.0655).

A.

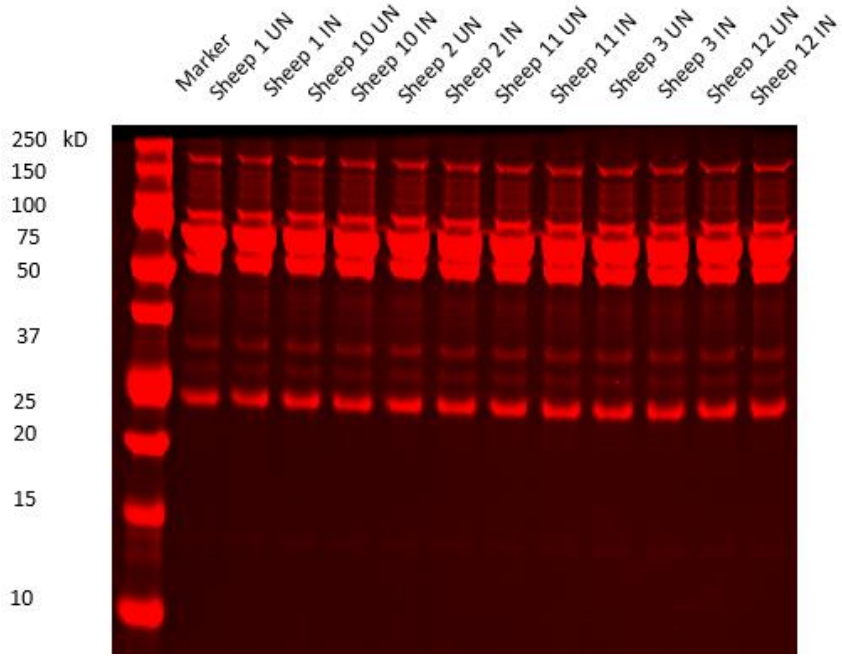

B.

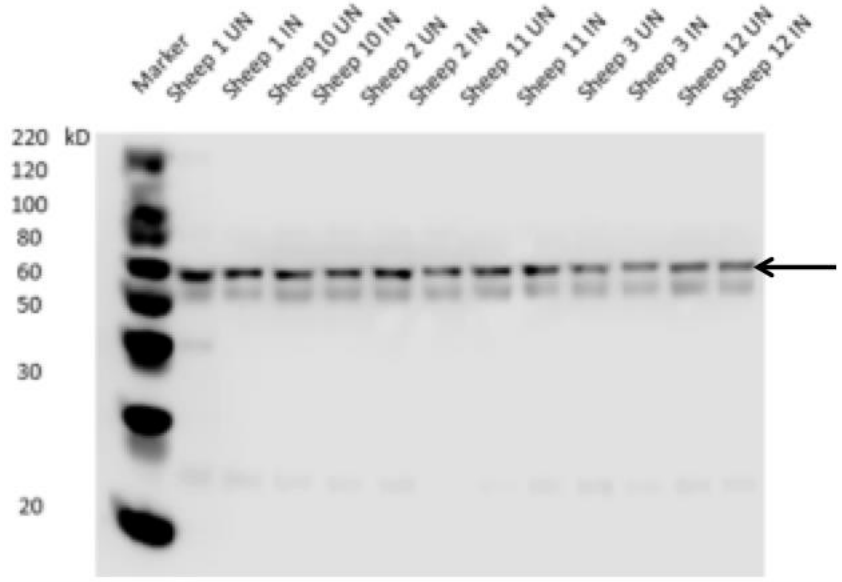

Figure 3.21: Representative gels are shown for individual plasma sheep samples at prechallenge and 12 months post infection probed for hemopexin (8 µg of protein loaded). Both (A) and (B) illustrate the method used to quantify the level of hemopexin in individual plasma samples. Samples are resolved on two gels simultaneously. One (A) is Coomassie Blue stained to obtain a whole protein signal per lane. Protein on the second gel is transferred to a membrane and antibody probed to acquire specific western blot band signals (B). The data is analysed to get a comparison in expression at different time points. The arrow on (B) identifies the protein of interest. Although optimisation of the antibody was performed and used on pooled sheep plasma samples, a new batch of antibody was used in experiments on individual sheep plasma. Thus, some non-specific bands are visible here.

3.3 Discussion

The aim of this work was to investigate the effects of preclinical prion disease on blood protein composition. This was done through use of archived plasma samples from transfusion studies performed on BSE infected sheep. It is of particular importance to identify any relevant changes in protein expression profiles between uninfected and infected time points to pick out information potentially relevant for use in diagnostics. It would be more efficient to implement a biomarker panel, alongside testing for PrP^{Sc}. As previously highlighted, there is a need for a test to clearly detect preclinical disease, distinguish these patients and prevent inadvertent cross-transmission.

Samples from nine sheep were pooled to normalise protein expression differences caused by genetic or metabolic variation between outbred animals. A challenge in the proteomic analysis of plasma samples is that a small number of highly abundant proteins obscure less abundant proteins. To address this issue as part of the preparation of samples for mass spectrometry analysis ProteoMiner was utilised. This results in a partial depletion of highly abundant proteins in samples and concentration of less abundant proteins, thus a more equalised sample. Mass spectrometry highlighted a difference in the expression of 153 proteins between uninfected and infected plasma pools, this list was refined to 35 proteins after filtering and removing the top common plasma proteins. From here 8 proteins were selected to validate mass spectrometry quantification and further explore their suitability for use as candidate biomarkers. Validation of these candidate biomarkers would reflect on the validation of the full list of 35 proteins. Out of these 8, only antibodies for 3 proteins cross-reacted with a protein of the predicted molecular weight and showed low levels of non-specific reactivity in Western blot and LI-COR analysis. After testing on pooled uninfected and infected samples, samples for the individual 9 sheep (as well as 3 negative controls) were investigated for differences in protein expression from 7 time points that covered the breadth of the transfusion study. Due to technical issues, this did not yield reliable results, and the analysis was not continued because of time constraints. Instead, to confirm the results of the pooled plasma samples, individual sheep samples from two time points (prechallenge and 12 months) were analysed.

The trends predicted by mass spectrometry may be observed in the results of western blotting of the pooled infected and uninfected samples. The mass spectrometry analysis indicated twice as much fibulin 1 expression was found in infected compared to uninfected samples. This was the highest out of the 8 candidate proteins (Table 3.4) and the sixth

highest in the list of 35 proteins with differential expression between uninfected and infected samples (Table 3.3). For the six repeat experiments carried out on uninfected and infected plasma pools, there is a similar increase in fibulin 1 expression from uninfected to infected samples (average 1.19 for the comparison value based on normalised western blot signals which is not as much as the mass spectrometry predicted). For vitamin D binding protein there is a consistent decrease in expression, matching the mass spectrometry prediction. The comparison value is 0.70. The comparison value for hemopexin is very close to this at 0.73. This is surprising as although the mass spectrometry predicted both proteins to decrease in expression the normalised fold change for each protein are not close. The normalised fold change predicted by mass spectrometry for vitamin D binding protein is 0.63 while for hemopexin it is 0.27. The statistics for the pooled plasma western blots show there are significant changes in protein expression. The paired T test for comparison values (normalised western blot signal for uninfected and infected pooled plasma) gives a P value of 0.0028 for fibulin 1. This is highly significant. For vitamin D binding protein it is 0.007 (very significant) and for hemopexin it is 0.06 (borderline significant).

A possible reason for the discrepancy witnessed between the mass spectrometry data and the individual plasma blots (uninfected vs infected time points) is the sensitivity of techniques. Accuracy of validation, and reproducibility of results, may have been affected by the use of different aliquots of plasma used in validation. Although the same sheep were used between the pooled and individual samples experiments, different aliquots taken from the sheep archive were used. Perhaps there are differences in protein content between stored aliquots from the same sheep. This can be determined and accounted for by the microBCA assays performed before resolving proteins by SDS-PAGE. It is also possible that multiple freeze thawing of these aliquots would have affected protein content, allowing for degradation of proteins to occur with ease. In an attempt to prevent this from occurring and alleviate the issue, pooled and individual sheep plasma aliquots were diluted in RIPA buffer (with protease inhibitor) prior to western blotting. Another possible reason for the magnitude of difference between the mass spectrometry data and the western blot results is the use of ProteoMiner. ProteoMiner was only applied to pooled samples sent for mass spectrometry analysis and not on pooled samples or individual samples used in western blot validation. ProteoMiner may have altered the proteins of interest. Thus the magnitude of differential expression seen in the untreated samples would not completely reflect the mass spectrometry samples. Furthermore, differences between the mass spectrometry data and the individual sheep blots may be explained by the natural complexity of blood, the thousands of proteins present contribute to its dynamic composition. This would be unique from sheep to sheep. The individual sheep have been taken as biological replicates, however it is possible that protein expression would vary widely from sheep to sheep. This

would be affected by genetics, hormone levels, concurrent infections, stress responses or even the time of day when blood was taken.

Technical reasons may also account for the differences seen in the predicted protein expression by mass spectrometry and the results obtained from western blotting. A major issue with the experiments performed using the individual sheep samples is the LI-COR analysis of the Coomasie Instant Blue™ stained gels. Although there is supposed to be equal loading between lanes (with the same concentration of loaded for each sample), there is some variability between samples (as can be seen by comparing lanes from gels in Figure 3.16). Hence, consistant signals in the total protein gels were not achieved, allowing differential exposure to be normalised. Although two gels are run in parallel to measure protein content of samples and account for any slight differences between them, the accuracy of reading the whole protein signal per lane is affected by over spillage from neighbouring lanes. Overloaded lanes could be underestimated (due to signal outside of the boxes), and neighbouring lanes being overestimated this overspill. It may be a result of how well the samples were resolved by SDS-PAGE or discrepencies in sample loading. In addition, the whole protein concentrations from the LI-COR anlaysis of the Coomasie Instant Blue™ stained gels are heavily skewed by albumin. This is because albumin makes up about 80% of total protein in plasma. If there are individual expression variations in albumin betweem sheep it would heavily affect the quantification of specifiic proteins. A closer attention to the protein concentration calculations measured by microBCA assay is required to resolve this issue. Additionally, analysis of the whole protein gel could have been performed useing averages of sections for each lane (avoiding the strong albumin band).

In an attempt to account for the shortcomings in the technical procedure of the individual sample blots further experiments were performed. The pooled plasma was prepared from prechallenge (uninfected) and 12 months (infected) time point samples. Thus the best comparison with the pooled plasma western blots are individual values at prechallenge and 12 months for the nine infected sheep. Having samples from the same sheep at different time points on the same gel is a better comparison. This seems to have rectified the previous issues seen with the large scale experiment of individual sheep samples analysed across seven time points, as the results here align with those from the pooled plasma western blots and the mass spectrometry predictions. The results for fibulin 1 clearly show a statistically significant increase in protein expression when comparing the same sheep at prechallenge and 12 months post infection time points (paired T test P value = 0.0055). Likewise, for vitamin D biding protein there was a statistically significant decrease in protein expression in the same sample sets (paired T test P value = 0.0113). In the case of hemopexin, although

there was a decrease in mean protein levels in 12 months compared to prechallenge samples, there was a greater spread in the data points for the individual samples at both time points, and the difference was not statistically significant (p = 0.1767). In addition to these comparisons, the difference between 12 months and prechallenge was calculated (normalised western blot signal of prechallenge was subtracted from 12 moths). This difference between protein expression at the two time points was then compared for control and infected sheep. The T test P value for fibulin 1 was significant at 0.0165, while those for vitamin D binding protein and hemopexin were almost significant (P = 0.0763 and P = 0.0655 respectively). This highlights that there was a clear change (either increased or decreased protein expression) between the control and infected sheep for each biomarker.

In a similar study, where ARQ/ARQ sheep were orally infected with 5 g brain tissue from BSE infected cattle, there was no detectable presence of PrP^{Sc} in the CNS 10 months after inoculation. It is only at 16 months that disease specific PrP accumulation was detectable in the lymphoreticular tissue and CNS (Jeffrey, Ryder, et al. 2001); (Bellworthy et al. 2005). The infected samples used to provide the plasma pool prepared for mass spectrometry were collected from nine sheep at 12 months post inoculation. Although at this point it may not be possible to identify PrP^{Sc} by immunohistochemistry, this may be due to the sensitivity of the technique. There may be exceptionally low levels beginning to build up, or other changes and pathological processes occurring that do not produce lesions that can be measured by immunohistochemistry. Furthermore, Bellworthy et al. (2005) show that despite the lack of detectable PrP^{Sc} at 10 months following infection the spleen was positive by mouse bioassay. This highlights that there is the presence of infectivity at 10 months and suggests that infectivity precedes the presence of PrP^{Sc}. It can be expected that this is also the case for spleen tissue at 12 months (for the transfusion study sheep). The spleen is the largest lymphatic organ, one of its key roles is in filtering blood, removing old red blood cells and storing platelets and white blood cells (Tarantino, Scalera, and Finelli 2013). The experiments performed here specifically look at the proteins in the plasma fraction of blood. The full list of differentially regulated proteins during disease as predicted by mass spectrometry is outlined in table 3.3. The proteins can be categorised into the following processes: regulation of the immune system, cell signalling, protein transport, cell structure and cell movement.

A number of the proteins chosen as potential biomarkers showed differential regulation that opposed findings from previous studies on prion or neurodegenerative diseases. This may be due to experimental design (how analysis was performed), the type of sample investigated (genes, mRNA, brain tissue, CSF, blood serum or plasma), the study

participants (rodent, macaque or human) or even the type of disease and clinical stage. Patient preparation, sample collection, sample preparation and sample storage can all play a role in proteomic variations (Apweiler et al. 2009). There are limitations to the information derived from DNA/RNA analysis and although genomics provides a vast amount of information linking gene activity to disease it is incapable of showing a complete and accurate profile of protein abundance or final state of activity. Multiple proteins may be generated from each gene through post-translational modification and mRNA splicing (Cho 2007). mRNA levels also do not always reflect protein expression (Gygi et al. 1999). Additionally, there will be disparity in sample complexity when comparing different protein sources. Plasma or serum has the advantage of being easily accessible but has a high dynamic range, the presence of abundant proteins mask more conservatively expressed molecules (Moxon et al. 2009). Withdrawing CSF is a more invasive procedure, less volume may be obtained at a time and there may also be contamination by blood-derived proteins. However, CSF has the advantage of proximity to region of disease, it is less complex with easier identification of proteins low in abundance and also identification of peptides that are biologically active (Caudle et al. 2008). Despite this, the overlap between the brain proteome and the CSF proteome is quite low, about 34% (Macron et al. 2018). Further challenges are involved in extrapolating findings from animal studies to human cases, there will be species differences that have not been taken into account (Bracken 2009). Since there is an overlap in pathophysiological mechanisms between dementia, AD, PD and prion diseases there may also be an overlap in protein expression in early disease stages (Castellani, Perry, and Smith 2004).

C1QB, C5, C3, C1S, C4BPA, CD5L are all involved in the complement and coagulation cascades. Their up or down regulation in the dataset is varied and may be a result of the complexes they form and consequential pathways they are involved in. It is has been established that innate immunity is key for prion disease progression. Abnormal prions replicate in follicular dendritic cells of the small intestine and B cells play a vital role in dissemination through circulation of infectivity in the body (Bradford and Mabbott 2012). The blood of the sheep used in this study was able to cause infection when transfused into recipient sheep at 10 months post inoculation. This means that at 12 months post inoculation the blood was definitely infectious. The immune proteins with differential expression as highlighted by mass spectrometry may be involved in initial coordination of the immune system allowing the build up and spread of prions to take place. For example, C1Q and C3 opsonize prions via the classical complement activation pathway, which may aid in their targeting of the agent to lymphoid follicles. Mice lacking complement components C1Qa, C2 or C3 were deficient in peripheral prion pathogeneses under specific conditions (Klein et al. 2001; Mabbott et al. 2001). C1Q also regulates dendritic cell development from monocytes

via DC-SIGN (Hosszu et al. 2010) and enhances receptor mediated uptake of PrP^{Sc} by dendritic cells (Flores-Langarica et al. 2009).

A number of the mass spectrometry determined dataset proteins are primarily expressed in the liver (e.g. paraoxonase 1, hemopexin). Perhaps this is a clue to the organs involved in preclinical prion infection or an indication that acute phase reactants are also involved in preclinical prion disease. Acute phase proteins (APPs) include complement proteins, antiproteases and clotting factors with the function to isolate and neutralize pathogens and proteases, opsonize and clear debris, as well as to attenuate the local inflammatory response in order to minimize damage to healthy tissue and mediate a return to homeostasis (Ramadori and Christ 1999). The association between APPs and prion diseases have been highlighted by their elevated presence in the sera of CJD patients (Fratini et al. 2012); (Volkel et al. 2001). APPs (including transthyretin) were also detectable in serum during the asymptomatic phase of scrapie in sheep (Batxelli-Molina et al. 2010). The synthesis of cytokines and APPs are proposed to be a systemic response to non-CNS aspects of prion disease pathology, such as PrP^{Sc} accumulation in the spleen or lymph organs. Increased protease activity may be a necessary response to the extracellular protein deposition seen during prion disease (Cunningham et al. 2005). Furthermore, analysis of the peripheral tissues of an asymptomatic vCJD-infected patient showed PMCA detectable seeding activity by the liver (and lungs) when none was seen by brain material of the same patient (Douet et al. 2017). Hence, PMCA amplification determined presence of vCJD prions in the liver early in the preclinical stage of disease before involvement of the brain and preceding neurological symptoms.

One of the most down regulated proteins on the list in Table 3.3 is SERPINA3, a member of the serine protease inhibitor family of APPs. Serpins are predominantly produced in the liver, however they are also synthesized in the brain and have been shown to be involved in neuroinflammation and neurodegeneration (Baker et al. 2007). Contrasting to my dataset, upregulation of SERPINA3 mRNA has been found in human prion disease brain samples (Vanni et al. 2017). Upregulation of SERPINA3 gene expression of BSE infected macaque brains has also been reported (Barbisin et al. 2014). This suggests SERPINA3 may be involved in the pathogenesis and progression of prion disease. Perhaps low levels are seen at the preclinical stage of disease and high levels during clinical disease.

Many of the differentially regulated proteins have links to protein transport or the movement of proteins from one location to another. Fibulin 1 is one of the top upregulated proteins in

the list. It binds to fibrinogen and is incorporated into fibronectin-containing matrix fibers. It has a role in cell adhesion and migration along protein fibers within the extracellular matrix (ECM). Hence it is important for developmental processes and also contributes to the supramolecular organization of ECM architecture (Tran et al. 1995). It has been suggested that ECM genes control susceptibility to prion infection as prion-susceptible cells have poorly developed ECM structure and more PrP^{C} deposition in that matrix (that can be converted to PrP^{Sc} thus facilitating future infection) (Linden et al. 2008); (Imberdis and Harris 2014). Another protein from the dataset which is important for protein and cell transport is vitamin D binding protein. A key function of vitamin D binding protein is in sequestering actin (Krishnan and Moens 2009). Actin is (usually in association with myosin) is responsible for cell movement (Dominguez and Holmes 2011). Decrease in expression in vitamin D binding protein, and thus decreased activity of the actin scavenger system would result in higher levels of actin and thus intensification of cell motility. The ability of cells to move freely may be key for preclinical infection. It has been shown that the actin-cytoskeleton dramatically changes during B cell activation and impaired actin cytoskeleton can devastate the normal activation of B cells (Keppler et al. 2018); (Li et al. 2018). Immune cells, specifically B cells, are important for peripheral prion pathogenesis (Aguzzi et al. 2003). Hence, the actions of vitamin D binding protein and its impact on actin may lay the foundation for resulting dissemination of prions around the body. Additionally, during cell motility the cell movement and shape changes require active restructuring of the actin (Chhabra and Higgs 2007). These are high energy demanding circumstances that directly rely on ATP availability (Balaban 1990); (van Horssen et al. 2009). Within the plasma dataset there is consistent upregulation of proteins such as MT-ND1, ATP6V1A and ATP5H. ATP6V1A is a component of vacuolar ATPase, ATP-driven proton pumps that function to acidify intracellular compartments and transport protons across the plasma membrane (Forgac 2007). ATP5H is a subunit of the enzyme mitochondrial ATP synthase which catalyses ATP synthesis by oxidative phosphorylation. Energy generated by hydrolysis of ATP is used for all cellular processes (Jonckheere, Smeitink, and Rodenburg 2012). MT-ND1 is part of NADH dehydrogenase, one of the complexes involved in the electron transport chain of oxidative phosphorylation (Yusnita, Norsiah, and Rahman 2010). The involvement of these proteins in energy pathways and their upregulation in infected plasma suggests enhanced cell energy levels, perhaps facilitating increased cell movement during the preclinical disease stage.

There are some similarities in the plasma dataset to findings of other studies that look at differential expression (gene or protein) in blood or other tissues during prion disease or other neurodegenerative diseases. Sui et al. (2014) found both transthyretin and hemopexin (as well as a number of apolipoproteins) to be down regulated in the serum of transgenic AD mice compared to wild type mice. Similarly, Castano et al. (2006) found transthyretin to be

reduced and hemopexin increased (alongside differential expression of a range of apolipoproteins) in CSF from AD patients. Brechlin et al. (2008) identified transthyretin as a potential marker of CJD through analysis of patient CSF and serum. Yu et al. (2003) analysed plasma from patients with AD and found enriched levels of hemopexin. These studies also show changes in blood proteins may reflect what is occurring in the brain or hint at activities leading to disturbances with normal brain function. Differences in up or down regulation of a particular protein may reflect a signature unique to blood borne proteins of preclinical prion infection in the BSE infected sheep of this study (Rubenstein, 2012). To expand on the current work and establish reasons for discrepancies with other studies, in the future it would be ideal to also have a list of differentially expressed proteins at the clinical stage of disease in these sheep. Expression of overlapping proteins would then give an indication of disease progression.

When comparing uninfected and infected plasma there were 153 proteins modulated. Given that not all of the chosen proteins for biomarker validation could be identified by antibody detection it would be difficult to assemble a panel of markers that would be necessary for unambiguous identification of preclinical disease. However, the western blot data for the three biomarkers that could be further investigated using pooled plasma samples validate the mass spectrometry data to a great extent. This provides evidence for the changes being true and not just a result of any possible biases introduced by use of ProteoMiner (as ProteoMiner was only used on samples prior to mass spectrometry analysis). Although there were some variable results from the individual sheep samples, this can be attributed to differences in experimental design and execution. When comparing the same two time points used for mass spectrometry, clear trends with significant difference can be seen. Thus, it can be said with some confidence that these proteins may be exploited for diagnostic purposes. A biomarker panel consisting of multiple proteins, used in conjunction with detection of PrP^{Sc} would greatly enhance sensitivity and specificity of a diagnostic test. The next step would be to design specific probes against the biomarkers and optimise bioassay conditions. A comparison of protein profiles with other forms of neurodegenerative disorders would depict the selectivity of the bioassay. A large scale validation using preclinical blood samples (combined with or confirmed by PMCA) would ensure the diagnostic value of the bioassay. Furthermore, this would establish that protein expression is not highly variable between individuals thus preventing their usefulness as accurate biomarkers (Huzarewich, Siemens, and Booth 2010).

This will provide preliminary data on determining a protein biomarker panel associated with prion infection in blood of asymptomatic patients. This may be of importance for future

diagnostics as there is currently no effective preclinical test available. A non-invasive test (on readily accessible body fluids) with the ability to detect the early stages of vCJD is critical in identifying people who are infected but appear completely healthy and to follow disease progression. The ultimate end-goal of developing preclinical, diagnostics and biomarkers is that they are able to facilitate detection of disease before possible contaminated blood products can enter circulation. Furthermore, the ability to detect and quantify progression over the course of the disease would allow for the evaluation of therapeutic strategies (Rubenstein, 2012). An important issue to consider is the ethical dilemma that a successful diagnostic test would create in identifying people at risk. While blood can be identified to prevent onward transmission through blood transfusion, there is no cure, no available treatment and no way of telling if and when the disease will manifest for preclinical patients. Additionally, a test with 99.9% specificity would still result in 0.1% of people with a positive result not actually being infected, so 1000 people out of 1 million who donated blood would incorrectly be told they potentially had vCJD. Such an outcome is unjustifiable when a positive test result would have such an enormous and devastating effect on patients, as well as their families (Tabrizi, Elliott, and Weissmann 2003); (Growdon 2011).

To expand on the work in this chapter, some of the problems described here in data analysis would need to be rectified. The initial large scale experiment looking at individual sheep samples across seven time points did not work. Looking at the data, substantial deviations can be seen between experiments. As some time point samples were analysed later than other it may be that slightly different conditions in experimental procedure from day to day have had an effect on the results., yielding variable blot development. It implies a batch bias in the outcome and highlights the difficulty in interpreting the results. Only after all experiments were performed a mechanical problem with the western blot transfer machine was discovered. It may account for this discrepancy. The uninfected pooled plasma sample was used as an additional control and positive indicator. Unfortunately, it did not work for many of the blots (bands were not quantifiable) thus was not a good comparison. Had time allowed and once technical issues were resolved, repeating the analysis of the longitudinal sample series would have been critical in providing provided details on changes in the protein biomarker expression across the course of disease from preclinical to the symptomatic stage (and show variation from sheep to sheep).

The small cohort of sheep investigated also warrants caution. In order to differentiate between normal or healthy, preclinical and pathological a larger number of study participants would be necessary. In an ideal scenario (without time or money limitations), this experiment would have involved performing mass spectrometry on plasma for each individual sheep at both uninfected/prechallenge and infected/12 month time points. Following this proteins that

consistently display the highest or lowest expression change, across the nine sheep, would be chosen for further validation. It may be a good idea to test more time points during the transfusion study (if archived samples are available and easily accessible). It would also be of interest to test plasma samples from humans or other more accessible samples, such as urine. One possible avenue to improve on our data would be to look at other fractions of blood. Protein expression changes in cells associated with efficient disease transmission may be of particular importance in the identification of preclinical biomarkers. White blood cells have been shown to be the most efficient blood cells in transmitting infection via the transfusion route (Andreoletti et al. 2012), therefore this approach was extended to reach the buffy coat samples of the same BSE infected sheep from the transfusion study.

Chapter 4: Proteomic markers that distinguish prion infected and uninfected buffy coat

4.1 Introduction

Blood is essential for transfusions and is the basis for various other life-saving products. There is currently no screening test to detect donors who may be incubating prion disease or in the early clinical stages. A reliable blood test for the early diagnosis is needed to both exclude infected blood and prevent onward transmission but also identify asymptomatic individuals. In Chapter 3 I investigated proteomic markers of preclinical infection. Testing, archived BSE infected sheep plasma, 44 differentially regulated proteins were identified by mass spectrometry and three were validated by western blotting. Here, the same procedure was repeated but on the buffy coat fraction of blood from the same sheep.

Although not seen in BSE or atypical scrapie cases, prion infection of the lymphoreticular system is necessary for neuroinvasion in many prion diseases (Sigurdson et al. 1999); (Andreoletti et al. 2000); (Bartz et al. 2005). PrP^{Sc} is initially present in lymphoreticular tissue prior to accumulation in the central nervous system and the development of clinical signs (Andreoletti et al. 2000); (Aguzzi, Nuvolone, and Zhu 2013). Hence, for the development of a preclinical test it may be advantageous to look for blood-based markers of infection rather than focussing on markers associated with neurodegeneration. Circulating immune cells have the ability to carry of PrP^{Sc} and thus traffic infectious prion agent around the body. Although prion infection still occurs in the absence of follicular dendritic cells (FDCs), it is severely delayed suggesting that FDCs are significant cellular sites of peripheral replication (Brown et al. 1999); (Mabbott, Mackay, et al. 2000). Targeting cells that may be involved in prion replication may increase the chance of picking up disease specific changes (Rhiannon et al. 2010). Furthermore, it has previously been established that WBCs are the most infectious component of blood. Intracerebral inoculation of rodent models has shown that 40% of the blood infectivity titre is associated with the buffy coat (Brown et al. 1998); (Gregori et al. 2006). The intravenous administration of just 10^5 WBCs is sufficient to cause scrapie in recipient sheep (Douet et al. 2016). Additionally, transmission of experimental BSE and natural scrapie has occurred following the transfusion of buffy coat from asymptomatic incubating sheep (Houston et al. 2000); (Hunter 2002). In this chapter I will look at the suitability of WBCs to determine alternative biomarkers associated with prion disease.

4.1.1 Aims of work

The aim of this work is to establish differences in protein expression between uninfected and infected buffy coat samples. In doing so, provide preliminary evidence for a blood based diagnostic test centred on a panel of biomarkers that could be used to identify individuals with prion disease.

4.2 Results

4.2.1 Use of ProteoMiner to deplete high abundant proteins in buffy coat

In order to identify potential biomarkers, uninfected and infected buffy coat samples were compared for differential protein expression by mass spectrometry. Western blotting of specific proteins was then performed to validate the mass spectrometry predicted results. If confirmed, any specific changes in protein expression may be exploited as a signature for the disease and be beneficial in a diagnostic setting (Xerxa et al. 2016). The buffy coat samples used in Chapter 4 were taken from the same nine BSE infected sheep from which plasma samples were taken in Chapter 3. These sheep are from the transfusion study (Houston et al. 2008), details of which can be found in Chapter 2 Materials and Methods (2.1.1).

The buffy coat portion of blood contains the highest concentration of WBCs (as well as platelets) and thus represents the cells with the most infectious capability. An initial SDS PAGE of uninfected buffy coat sample was resolved to determine whether protein depletion was a necessary step. The results depict the presence some large bands that represent highly abundant proteins (Figure 4.1). These include albumin (50 kD), transferrin (76kD) and haptoglobin (23 kD). Highly abundant proteins may be obscure the detection of less abundant proteins. Hence it was decided to proceed with ProteoMiner.

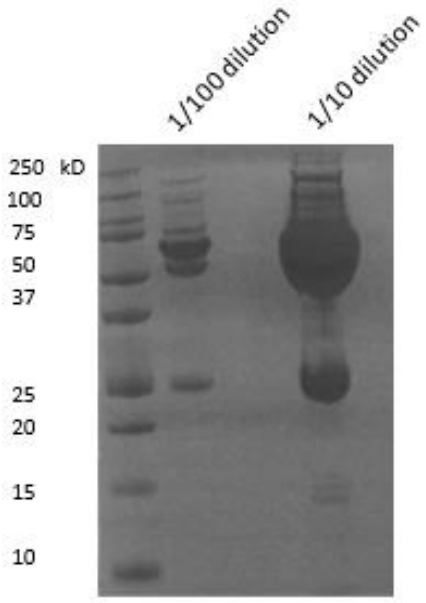

Figure 4.1: Initial gel of pooled uninfected buffy coat sample. In order to assess if it was necessary to use ProteoMiner on the buffy coat samples a test gel was performed. Here a 1/100 and 1/10 dilution of uninfected pooled buffy coat were resolved by SDS PAGE and stained with Coomassie InstantBlue™.

To simplify blood buffy coat samples, ProteoMiner technology was utilized (as previously described on plasma in Chapter 3). Highly abundant proteins were depleted while simultaneously enriching for less abundant proteins using columns containing high affinity ligands. Hence, the presence of highly abundant proteins would not obscure the detection of less abundant proteins that may be of interest as disease biomarkers. Initially the pooled uninfected buffy coat samples were put through the small capacity kit to ensure compatibility with the kit and optimise the procedure. The gel in Figure 4.2 shows a reduction in highly abundant proteins in the enriched elution lane compared to the original sample lane. Many fine bands now appear in the enriched elution sample lane. Hence, less abundant proteins are more readily detected. The pooled uninfected buffy coat and the pooled infected buffy coat were put through two separate ProteoMiner columns but the samples collected were resolved on the same gel.

The small ProteoMiner kit requires a total protein load of $\geq$10 mg, the large capacity kit processes samples at $\geq$50 mg. Having proven the buffy coat samples were compatible with the small capacity kit the experiment was scaled up to the large capacity kit. 1 mL of undiluted buffy coat sample is added the ProteoMiner large capacity kit column. Two separate columns are used for uninfected and infected samples. The large capacity kit requires three rounds of 100 µL of elution buffer to be added to the column to elute the final sample. This results in three 100 µL elutions (elution 1, 2 and 3). Following 30 µL removal for microBCA assay, these elutions are combined to give enriched elution 4. A microBCA was performed to calculate volumes of each sample required to load 10 µg of protein on the SDS-PAGE gel (along with microBCA determined 10 µg of the original sample for comparison). Table 4.1 shows the protein concentrations for the original sample (before use of ProteoMiner) and elution 4. There is a 99-97% reduction in protein concentration achieved from use of the ProteoMiner kit. This is similar to what was seen with the plasma samples. The results for uninfected pooled buffy coat and infected pooled buffy coat can be seen in Figure 4.3. In the enriched elutions the presence of less abundant proteins is depicted by the appearance of multiple fine bands. Reduction, alkylation and tryptic digestion was performed on pooled uninfected and pooled infected buffy coat samples before they were passed on for mass spectrometry analysis.

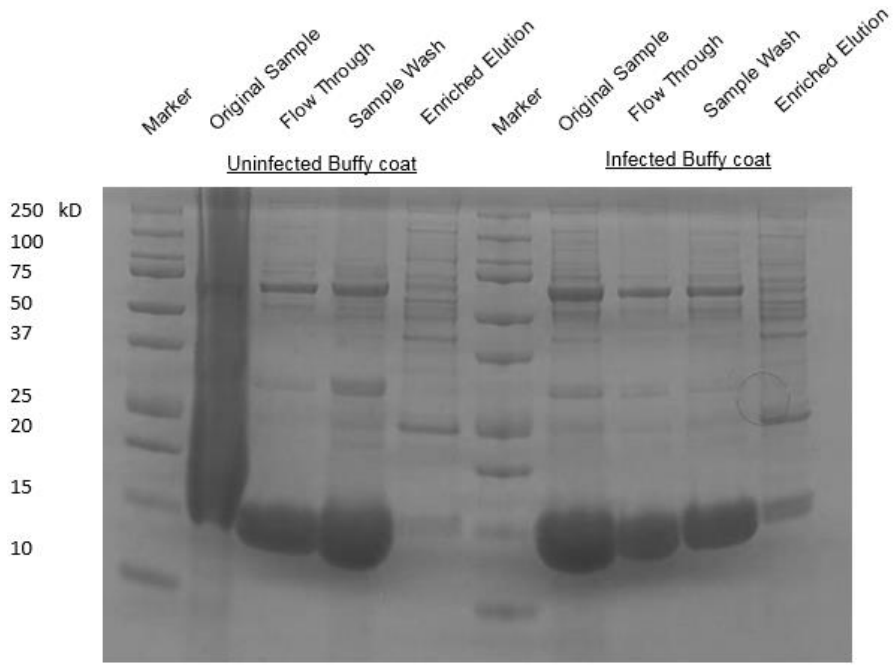

Figure 4.2: Small capacity ProteoMiner enrichment kit results. SDS-PAGE gel showing samples collected from use of the small capacity kit. Bands of low abundant proteins clearly become evident in the lane of the enriched fraction. The original uninfected sample in the first lane of the gel was diluted 1/10 (whereas the infected original sample was diluted 1/100).

Table 4.1: Protein concentrations of buffy coat samples.

Total Protein (µg)		
Uninfected Buffy coat	Original	82373
	Enriched Elution 4	3213
Infected Buffy coat	Original	78039
	Enriched Elution 4	6588

Total protein concentrations for the original sample (before ProteoMiner) and Enriched Elution 4 (after ProteoMiner) are presented in the table.

A.

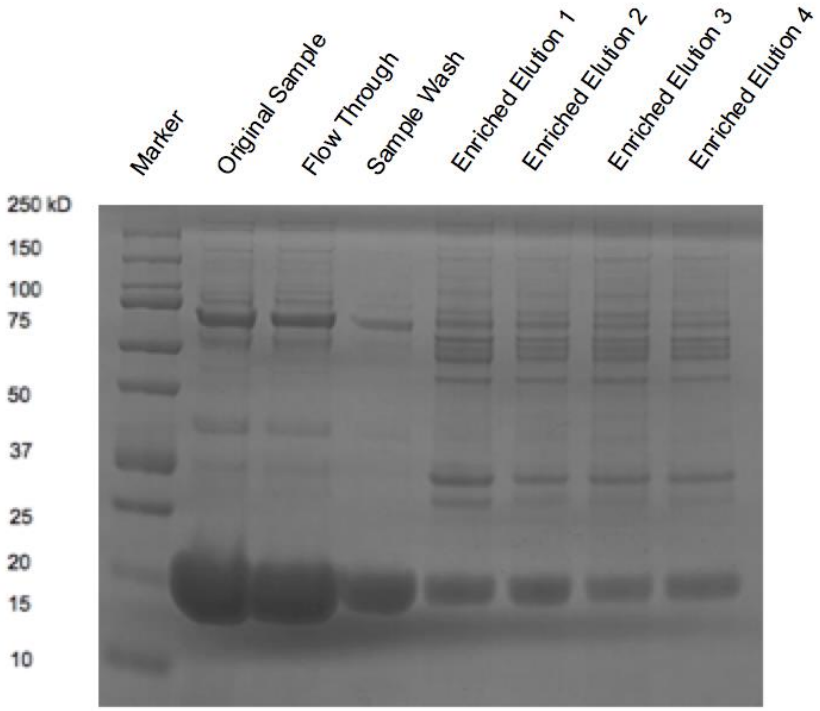

B.

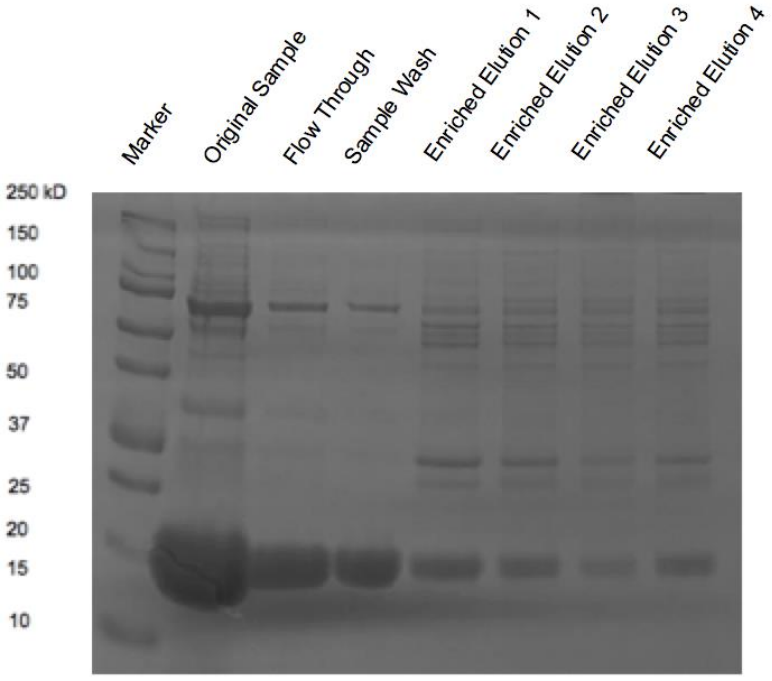

Figure 4.3: Pooled uninfected and infected buffy coat were run on separate ProteoMiner large capacity kit columns. Samples were collected at each stage when using the ProteoMiner kit, following a microBCA to determine protein concentration, 10 µg of each sample was then resolved by SDS-PAGE. Separate gels for uninfected (A) and infected (B) pooled buffy coat samples are shown. The three enriched elutions (enriched Elution 1, 2 and 3) obtained from the column were combined to create Elution 4. The gels show the appearance of multiple fine bands representing low abundant proteins that may now be detected following removal of some of the high abundant proteins.

4.2.2 Mass spectrometry of buffy coat

Buffy coat samples from the same BSE infected sheep as the plasma samples in Chapter 3, were analysed by liquid chromatography-tandem mass spectrometry (LC-MS) in the same manner as described previously. LC-MS is a highly sensitive and powerful tool for large scale identification of peptides. Uninfected (taken before BSE exposure) and infected samples (12 months later) were labelled with light (L) and heavy (H) isotopic labels respectively. Mass spectrometry data was filtered by ensuring the median H/L chain isotopes was set to >1.5 and <0.666, the coefficient variation was less than 100% and that identification was based on more than one peptide. The original dataset of 1148 proteins (Appendix 2) was reduced to 124 (Appendix 3).

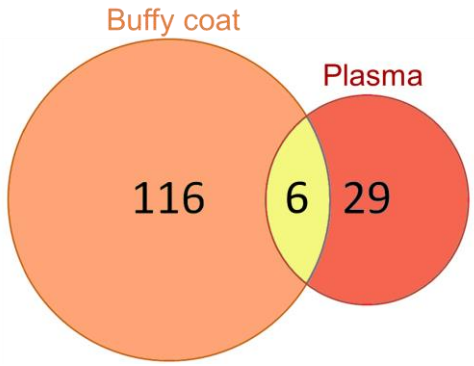

Figure 4.4: Venn diagram demonstrating the overlap between the buffy coat and plasma filtered datasets.

Comparing both the buffy coat and plasma datasets for differentially expressed proteins shows that there are six overlapping proteins (6/35 for plasma and 6/122 in buffy coat). Four of the six were up or down regulated in the same manner in both datasets (Table 4.2). The Venn diagram (Figure 4.4) visually depicts that 6 proteins are common between buffy coat and plasma, whereas 116 and 29 proteins are unique for buffy coat and plasma respectively. They differ substantially, with 87 buffy coat proteins not identified in the plasma samples. Out of the six proteins identified in both datasets, two (transthyretin and alpha-1B-glycoprotein) had already been picked out as candidate biomarkers for further validation. Their expression changes are essentially reversed in the two datasets (Table 4.2). Expression of transthyretin and alpha-1B-glycoprotein increased in the buffy coat dataset and decreased in the plasma dataset. This is consistent with redistribution of these proteins from the plasma to buffy coat cells. Unfortunately, the antibodies tested for these proteins were unable to produce clear signals by western blot and so further validation was not possible. The remaining four proteins (serum amyloid A protein, ATP synthase subunit D,

cadherin-5, inter-alpha-trypsin inhibitor heavy chain H1) have very similar fold change values thus there is an agreement in expression between the two datasets.

Table 4.2: Proteins identified in both buffy coat and plasma datasets.

Gene	Protein	Fold change in Buffy coat data	Fold change in Plasma data
SAA1	Serum amyloid A protein	0.56	0.25
TTR	Transthyretin (Prealbumin)*	2.87	0.25
A1BG	Alpha-1B-glycoprotein*	2.26	0.34
ATP5H	ATP synthase subunit D, mitochondrial	0.66	0.38
CDH5	Cadherin-5	0.43	0.41
ITIH1	Inter-alpha-trypsin inhibitor heavy chain H1	1.74	1.25

*Candidate proteins chosen for validation

Mass spectrometry indicated that these six proteins as being differentially expressed in both the buffy coat and plasma samples when comparing uninfected to infected. Both transthyretin and alpha-1B-glycoprotein were previously considered for further validation on the plasma samples, however results could not be quantified.

The list of 124 differentially regulated proteins and their functions (Appendix 3) suggest that metabolic processes take place during the preclinical prion disease. Many of the proteins are involved in metabolism or energy conversion pathways, such as T complex protein 1 subunit epsilon, proteasome subunit beta 10, mitochondrial ATP synthase subunit 5H, Isocitrate dehydrogenase [NADP]. Furthermore, a number of proteins are associated with cell structure

Table 4.3: Serpin peptidase inhibitor proteins identified in buffy coat or plasma datasets.

Buffy coat dataset			Plasma dataset		
Gene	**Protein**	**Normalised fold change**	**Gene**	**Protein**	**Normalised fold change**
SERPINF2	Serpin family F member 2	0.56	SERPINA3	Serpin family A member 3	0.14
SERPINC1	Serpin family C member 1	1.51	SERPINA1	Serpin family A member 1	0.23
SERPINA5	Serpin family A member 5	1.58	IPSP	Serpin family A	0.25
			SERPINF1	Serpin family F member 1	0.99
			SERPINA5	Serpin family A member 5	1.52

and motility including integrin beta chain-2, actin alpha 1 and myosin light chain 6. A number of serpin family proteins appear in the buffy coat and plasma datasets (Table 4.3). Serpins are the broadest and largest family of proteins with protease inhibitor activity, with over 1,500 members identified to date (Law et al. 2006). The Human Protein Atlas lists 43 different serpins in blood (https://www.proteinatlas.org/search/serpin). They make up 2.4 % of differentially expressed buffy coat proteins and 14.3 % of differentially expressed plasma proteins. Considering that more than 10.5 thousand blood-plasma proteins that have been detected (Ponomarenko et al, 2016), it is 0.4% likely (very unlikely) that this identification of serpin is due to chance. As mentioned in the previous chapter, differential overexpression of SERPINA3 has been identified in human prion disease (Vanni et al, 2017) and strongly upregulated in brains of scrapie infected mice (Barbisin et al. 2014). However SERPINA3 is down regulated in the plasma dataset. This may be due to the infected plasma in my study being from a preclinical time point, before PrP^{Sc} accumulation in the brain that may have contributed to the affects on SERPINA3 expression seen in these studies. However, the changes in protein expression seen in this study between uninfected and infected time points may induce greater disease susceptibility.

4.2.3 Bioinformatic analysis and selection of potential biomarkers

Two free online bioinformatic tools previously utilised for investigating the plasma dataset in Chapter 3 were also applied to the buffy coat dataset. Reactome is an open-source, peer-reviewed pathways database which provides basic visualisation and interpretation of pathway knowledge. The relevant pathways identified by analysis of the buffy coat protein expression data by Reactome are listed in Table 4.4. Five out of nine are related to metabolism, two to DNA repair and one to cell cycle. The P value gives the probability that the overlap between the query dataset and the pathway occurred by chance. DAVID Bioinformatics Resources provides functional analysis tools to understand the biological meaning behind lists of genes or proteins. Pathways interpreted by DAVID as important for the buffy coat data are listed in Table 4.5. Out of the fifteen that are highlighted, nine are to do with metabolism. Others include Parkinson's disease and leukocyte transendothelial migration. The P value is a measure of a given protein in a dataset belonging to a particular pathway due to chance. The smaller this score the more the dataset is specifically associated (enriched) with the pathway. A P value that is equal to or smaller than 0.05 is considered strongly enriched (DAVID 2007). As all the pathways score small P values it indicates that the result is non-random and potentially interesting or worth following up in closer detail. The information provided by Reactome and DAVID gives an indication for the

involvement of energy related pathways during preclinical infection. Proteins significant to other neurodegenerative diseases may also be affected during preclinical prion disease. To investigate the data further and determine potential biomarkers, additional analysis was required.

Table 4.4: Reactome predicted functional pathways for differentially expressed buffy coat proteins (https://reactome.org/). 'Entities P value' is a calculation of the proteins appearing in a particular pathway by chance.

Reactome pathways		
Description	**Origin**	**Entities P value**
Association of TriC/CCT with target proteins during biosynthesis	Metabolism of proteins	6.59E-6
Detoxification of reactive oxygen species	Cellular responses to stimuli	3.78E-5
DNA Damage Recognition in GG-NER	DNA repair	5.43E-4
Citric acid cycle (TCA cycle)	Metabolism	1.48E-4
Formation of TC-NER pre-incision complex	DNA repair	2.54E-4
mRNA splicing	Metabolism of RNA	2.82E-10
Deposition of new CENPA-containing nucleosomes are the centromere	Cell cycle	4.11E-5
Heme degradation	Metabolism	3.04E-5
Pentose phosphate pathway	Metabolism	2.67E-4

Table 4.5: The top functional pathways suggested by DAVID Bioinformatics Resources (https://david.ncifcrf.gov). 'Count' refers to the number of genes present in the dataset that are relevant to the suggested pathway, it must be greater than 1 and the default is 2. The 'P value' refers to the modified Fisher extract P-value, Enrichment score.

DAVID Pathways	
Pathway	**P value**
Carbon metabolism	7.1E-8
Biosynthesis of antibiotics	2.0E-7
Biosynthesis of amino acids	1.1E-5
Metabolism pathways	7.5E-4
Porphyrin and chlorophyll metabolism	2.2E-3
Spliceosome	2.4E-3
Glycolysis/Gluconeogenesis	1.1E-2
Pentose phosphate pathway	1.6E-2
Citrate cycle (TCA cycle)	2.0E-2
Tryptophan metabolism	4.4E-2
Ameobiasis	4.8E-2
Arginine and proline metabolism	5.1E-2
Leukocyte transendothelial migration	5.2E-2
Glutathione metabolism	5.9E-2
Parkinson's disease	9.9E-2

With a greater number of proteins available in the buffy coat dataset than the plasma dataset, network analysis could be employed. IPA is a functional analysis tool which is used to help

search for and discover targeted information on genes, proteins, chemicals and drugs using extensive biological knowledge. Complex searches are made for prediction of biomarkers and enable disease specific hypothesises to be generated. Canonical pathways are deemed significant to the input data set by testing two parameters. First, a ratio of the number of proteins from the data set that map to the pathway divided by the total number of proteins that map to the canonical pathway. Secondly, a P value is calculated using Fisher's exact test to determine the probability that the association between the proteins in the data set and the canonical pathway is due to chance alone. The smaller the P value the less likely that the association is random (Qiagen 2012). Protein expression direction is not taken into account for this calculation. A Z score is a statistical measure of the match between expected relationship direction and observed protein expression. It gives a prediction for the activation state of a particular pathway (as well as the magnitude of increase or decrease). A Z score >2 or <-2 is considered significant. Out of the 191 canonical pathways suggested by IPA, the top 3 based on P value and ratio of proteins are LXR/RXR Activation –log(p value) = 5. 28, Acute Phase Response Signalling –log(p value) = 4.33 and Mitochondrial Dysfunction –log(p value) = 4.31. Out of these, only a Z score for LXR/RXR Activation was achieved (Z score = -0.378). The lack of Z score for the other pathways may due to conflicting directions in which proteins are regulated. It may also be down to IPA not having enough information on the molecules involved in each pathway compared to those of the dataset to make a valid judgment. In comparison the Z score for Leukocyte Extravasation Signalling is 0.447, indicating upregulation.

From this it can seen that there is a suggestion here of the involvement of the immune system in the early stages of prion infection. LXR/RXR activity has been shown to regulate the immune response, for example in macrophages LXRs inhibit proinflammatory gene expression (Schulman 2017). The acute phase response is part of the innate immune system creating a systemic reaction (Gruys et al. 2005b). Mitochondrial dysfunction has also been linked to activation of innate immunity (Carney 2018). Leukocyte extravasion refers to the migration of leukocytes across the endothelium (Middleton et al. 2002). It is known that the immune system plays an important role in peripheral replication of infectious prion protein before its efficient spread toward the CNS and to the brain (Aguzzi et al. 2003); (Beekes and McBride 2007). Providing further evidence for this, the buffy coat dataset is indicating activity in immune cells during the preclinical time point.

The fifty-one canonical pathways presented by IPA as relevant for the buffy coat data set were narrowed down to key five canonical pathways. This was done by conducting an in depth literature search. Only pathways that have previously been identified as potentially

significant in prion or neurodegenerative diseases were selected. Table 4.6 displays these five canonical pathways and their proteins that map to the buffy coat data set. The ratio refers to the number of proteins in the dataset that map to the pathway. As the ratio for all pathways is ≤0.05, this signifies that the presence of these proteins in their associated pathways are not due to chance. Out of these proteins candidate biomarkers were chosen for Western blot based validation. To identify the relevant proteins from each pathway a search of published literature was performed to evaluate previous association with prion or neurodegenerative diseases.

Table 4.6: Shortlist of IPA canonical pathways. For each pathway chosen for the biomarker panel, the table lists proteins present in the dataset obtained from mass spectrometry of pooled uninfected and infected buffy coat samples.

		IPA pathways	
Ingenuity Canonical Pathways	**-log (p-value)**	**Ratio**	**Molecules**
Spermine Biosynthesis	1.95	0.5	SMS
Leukocyte Extravasation Signalling	2.18	0.02	ITGB2,CDH5,MYL6,ACTN1,MSN ERM, LFA-1
Mitochondrial Dysfunction	4.31	0.04	PRDX3,ATP5PD,PARK7,CAT CYB5A,UQCRC1,TXNRD2
Acute Phase Response Signalling	4.33	0.04	TTR,ITIH2,SAA1,LBP,SAA2, S100A8, SERPINF2,HNRNPK
LXR/RXR Activation	5.28	0.05	TTR,SAA1,S100A8,LBP,LDL, HPL,SAA2,A1BG,SERPINF2

An ideal non-invasive, easily applicable blood test for prion diseases would have practical applications in a clinical setting. A good biomarker panel is one that can discriminate between states and provide accurate information on subsequent clinical outcome. It would be able to differentiate between healthy patients and those with prion disease at both a preclinical and clinical stage. This can be addressed by assessing deregulation of several biological systems rather than focussing on just one. In doing so, better detection is facilitated as it takes into account the heterogeneous blood protein composition and individual variability between patients. The inclusion of several biological pathways or processes that may be involved in disease pathogenesis is a common feature of many blood based biomarker panel studies. Ray et al. 2007 proposed a panel of 18 plasma proteins involved in numerous pathways altered early in AD pathogenesis including inflammation, cell growth, angiogenesis, stress response, lipid metabolism, oxidative stress and antioxidant response. It was able to distinguish AD patients from healthy controls with 89% accuracy,

confirm the prospective power of multiple blood biomarkers incorporated into a panel for accurate diagnosis. However, including a smaller number of predictors will both reduce the efforts and costs for measurement as well as reduce the statistical problems associated with evaluation of the results.

Specific proteins from each pathway were chosen as potential biomarkers for their IPA confirmed relevance (as part of important biological pathways), previous association to prion or neurodegenerative diseases (from published literature), but also due to the availability of antibodies (antibodies are only available for a limited number of proteins). Reviewing the current literature ensures no prospective candidates are ignored. It also ensures that the chosen biomarkers can be measured in medical departments across diverse patient populations and are not reliant on the development of new technology or statistical methods.

Additionally a panel of biomarkers rather than a single protein are more likely to be implemented in diagnostic screening. This would be so as to balance time and cost concerns with high specificity and accuracy. Table 4.7 lists the potential biomarkers for validation of the mass spectrometry analysis; the proteins presented offer a wide coverage of potentially relevant biological pathways. This is a fundamental step in beginning to understand what differs between healthy and diseased individuals.

Table 4.7: Potential buffy coat biomarkers selected for validation.

Normalised fold change	Gene	Protein	Pathway	Examples of relevant studies showing relation to neurodegenerative diseases
0.33	SMS	spermine synthase	Spermine Biosynthesis	Antony et al. (2003); Bera and Nandi (2007); Speldewinde and Grant (2015); Phadwal et al. (2018).
0.64	hnRNP K	heterogeneous nuclear ribonucleoprotein K	Acute Phase Response Signalling	Villa et al. (2011); Berson et al. (2012); Hennig et al. (2015); Appocher et al. (2017).
1.56	ITIH2	inter-alpha-trypsin inhibitor heavy chain H2	Acute Phase Response Signalling	Okroj et al. (2012); Ashton et al. (2015); Dieks et al. (2013); Meier et al. (2015); ; Watanabe et al. (2019).
1.58	PARK7	Parkinson disease protein 7	Mitochondrial Dysfunction	Kiachopoulos et al. (2004); Winklhofer and Tatzelt (2006); Nguyen et al. (2014); Prusiner et al. (2015).
1.59	MSN	moesin	Leukocyte Extravasation Signalling	Riemer et al. (2004); Xiang et al. (2004); Chadwick et al. (2010); Jayasena et al. (2015).
2.84	s100A8 S100	s100A8 S100 calcium binding	Acute Phase Response Signalling	Beekes et al. (1999); Xiang et al. (2004); Cristóvão and Gomes (2019); Spratt et al. (2019).
2.87	TTR	transthyretin	LXR/RXR Activation	Yu et al. (2003); Riemer et al. (2004); Rubenstein (2012); Lim et al. (2016); Dasari et al. (2019).

The table depicts the change in protein expression from pooled uninfected to infected buffy coat samples. The fold change refers to the H/L ratio, proteins with a value <1 are down regulated in the infected sample. There is no change in expression for proteins with a value of 1, and upregulated proteins have a value 1>. Out of the chosen potential buffy coat biomarkers two show decreased expression in infected samples, while five are increased.

4.2.4 Biomarker validation

Antibodies for each of the selected candidate biomarker proteins were tested on uninfected buffy coat samples, however the only one that appeared to bind specifically to its target was the anti-moesin antibody. This is likely down to most commercial antibodies recognising human proteins, while the samples used here are from sheep. Although only antibodies for proteins with high sequence similarity (as verified by human and ovine alignment using UniProt) or predicted to work with ovine samples were ordered, all but one did not work. Moesin has a 99% protein identity when comparing the amino acid similarity between human and sheep proteins; this indicates that the target human and sheep sequences are highly similar. The molecular weight of moesin is predicted to be 70-78 kD, and the antibody used detects a protein of this weight. Initial experiments were performed using pooled uninfected buffy coat. For efficient quantification, where changes in expression may be monitored easily, a thin western blot band is ideal. It was found that 8 µg of protein gave rise to consistent results.

Table 4.8 lists the antibodies tested for the chosen buffy coat biomarkers. It is important to be consistent when conducting antibody trials, thus rigorous western blotting procedures were instated. Following protein transfer, nitrocellulose membranes were blocked in commercial blocking buffer (containing bovine serum albumin). Membranes were then fully immersed in primary antibody (by placing them on rollers in individual falcon tubes) and incubated overnight. All membranes were thoroughly washed in PBS-T before use of secondary antibody. All primary antibodies were rabbit polyclonal, thus the same secondary antibody (Donkey anti-Rabbit IgG ThermoFisher Scientific 31238) and western blotting chemiluminescence detection kit (Roche BM) could be utilised. All primary antibodies were initially applied at the manufacturer's recommended dilution, with a range of sample protein concentration (uninfected pooled buffy coat). To enhance detection of western blot bands, a range of antibody dilutions were then tried. The recommended dilution for the secondary antibody is 1:10 000 - 1:200 000. The different concentrations of secondary antibody, primary antibody and sample protein concentrations that were tested is summarised in Table 4.9.

Table 4.8: List of antibodies for buffy coat potential biomarkers. In order to validate the findings from mass spectrometry where the protein expression of uninfected and infected buffy coat samples were compared, 7 candidate proteins were chosen for further testing. Most antibodies are produced to react with human samples. To ensure that these antibodies have a high chance of working on the sheep blood samples, a comparison was made between the human and ovine target peptide sequence on UniProt (https://www.uniprot.org/). The result is an amino acid sequence similarity (protein identity %), which is the overlap in similarity for protein. If there is a high level of identity between human and sheep proteins, then the antibody is more likely to cross-react with both human and sheep samples. However, after testing all of these antibodies, only moesin presented a quantifiable band pattern.

Protein	Western blot compatible Antibody Name	Company	Reference	Human and sheep amino acid similarity (protein identity %)	Species Reactivity
Spermine Synthase	Spermine synthase Antibody	Novusbio	NBP2-20470	94%	Human, mouse, rat
Heterogeneous nuclear ribonucleoprotein K	hnRNP K Polyclonal Antibody	ThermoFisher Scientific	PA5-27522	74%	Human, mouse
Inter-alpha-trypsin inhibitor heavy chain H2	ITIH2 Polyclonal Antibody	Invitrogen	PA5-13670	78%	Human
Parkinson disease protein 7	Rabbit PARK7 Polyclonal Antibody	AMS Biotechnology (Europe) Ltd	AMS.ESAP10665	68%	Human
Moesin	Moesin Antibody	Novusbio	NBP1-90372	99%	Human, mouse, rat
S100A8 S100 calcium binding	Rabbit IgG polyclonal antibody for Protein S100-A8(S100A8) detection	AMS Biotechnology (Europe) Ltd	AMS.ABO12428	64%	Human, mouse, rat
Transthyretin	Transthyretin Rabbit Polyclonal Antibody	Invitrogen	13461367	72%	Human, mouse, rat

Table 4.9: Testing conditions for potential buffy coat biomarkers. In order to optimise the use of each antibody a series of experiments were performed. A working antibody with a positive result would yield a reliable (consistently quantifiable) western blot band signal. Listed here are the ranges of conditions trialed. The cross reactivity observed with other antibodies refers to nonspecific bands appearing.

Protein	**Manufacturers recommended dilution for primary Antibody**	**Primary Antibody dilutions tested**	**Secondary Antibody dilutions tested**	**Protein Load tested (µg)**	**Western blot result**
Spermine Synthase	1:500-1:3000	1:5000 1:3000 1:2500 1:2000 1:1000 1:500	1:10 000 1:50 000 1:100 000 1:200 000	2, 4, 6, 8, 10	No band signal.
Heterogeneous nuclear ribonucleoprotein K	1:500-1:3000	1:5000 1:3000 1:1000 1:500	1:10 000 1:50 000 1:100 000 1:200 000	2, 4, 6, 8, 10	Cross reactivity (multiple nonspecific bands).
Inter-alpha-trypsin inhibitor heavy chain H2	1:1000	1:2000 1:1000 1:750 1:500	1:10 000 1:50 000 1:100 000 1:200 000	2, 4, 6, 8, 10	Cross reactivity.

Parkinson disease protein 7	1:500 - 1:2000	1:3000 1:2000 1:1000 1:500	1:10 000 1:50 000 1:100 000 1:200 000	2, 4, 6, 8, 10	No band signal.
Moesin	1:1000-1:5000	1:5000 1:3000 1:2500 1:2000 1:1000	1:10 000 1:50 000 1:100 000 1:200 000	2, 4, 6, 8, 10, 12	Good band signal achieved with 8 µg of buffy coat sample, 1:2500 primary antibody dilution and 1:5000 secondary antibody dilution.
S100A8 S100 calcium binding	1:500 - 1:2000	1:3000 1:2000 1:1000 1:500	1:10 000 1:50 000 1:100 000 1:200 000	2, 4, 6, 8, 10	Cross reactivity.
Transthyretin	1:1000	1:2000 1:1000 1:750 1:500	1:10 000 1:50 000 1:100 000 1:200 000	2, 4, 6, 8, 10	Cross reactivity.

Buffy coat samples from nine sheep at an uninfected time point (prechallenge) were pooled, and buffy coat samples from the same nine sheep at an infected time point (12 months) were pooled. Portions of these were used for uninfected and infected samples used in mass spectrometry analysis, the remainder stored at -80 ^{o}C. Once the moesin antibody had been optimised (tested for consistent and quantifiable results) validation of the mass spectrometry predictions began. Pooled uninfected and infected buffy coat samples were removed from -80 ^{o}C storage, diluted in RIPA buffer (to prevent protein precipitation) and samples taken for microBCA assay. After calculating protein concentration, stock dilutions and aliquots in sample buffer were prepared. For the pooled buffy coat experiments four replicate pairs of uninfected and infected pooled samples were then resolved side by side on the same gel (thus moesin expression for each experiment is an average between 4 repeat comparisons). Two gels were generated at the same time in one tank. One gel was stained Coomassie InstantBlue™ for analysing whole protein content of the lanes. The second gel was taken through the western blot procedure and moesin bands for individual sheep captured by LI-COR scanning. Six experiments were performed and to plot the graph in Figure 4.5 a ratio of the normalized signal for infected samples to uninfected samples was calculated. The value for uninfected samples is set to 1 to reflect what the value for infected samples are in relation (values >1 for moesin indicate increased expression). Figure 4.6 show example gels for measuring moesin expression in pooled buffy coat samples from one of the experiment. Across the 6 repeat experiments the standard deviation calculated on comparison values is low (table in Figure 4.5). This indicates that the data is not widely spread but all values are close to the average, so can be considered reliable.

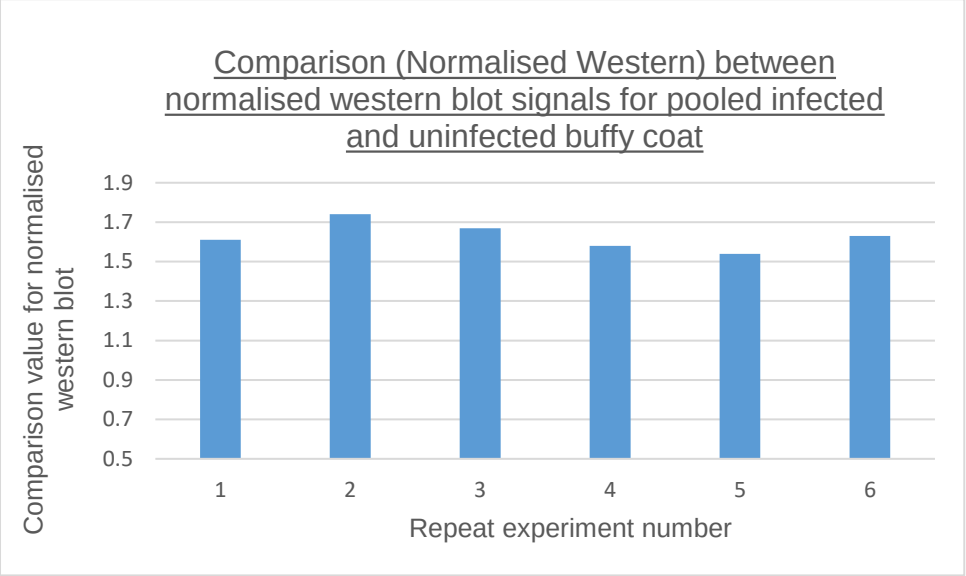

Experiment no.	Comparison (Normalised Western)
1	1.61
2	1.74
3	1.67
4	1.58
5	1.54
6	1.63
Mean	1.63
Std Dev	0.070
SEM	0.029

Figure 4.5 Results for moesin expression in pooled uninfected and infected buffy coat samples. Uninfected and infected buffy coat samples were resolved side-by-side 4 times on the same gel. The mass spectrometry data predicted an increase in moesin in the infected buffy coat sample. Across 6 repeat experiments (where 4 replicate comparisons of uninfected and infected buffy coat moesin expression was averaged per gel), the expression of moesin was shown to increase. The graph shows a ratio of the normalized signal for infected samples to uninfected samples (values >1 for moesin indicate increased expression). The table illustrates that the results between experiments are similar. Across the six repeat experiments the standard deviation (0.070) is very low. The SEM, an indicator for the precision of the estimated mean, is also low. It is thus likely that these findings accurately reflect differences in moesin expression between the uninfected and infected pooled buffy coat samples.

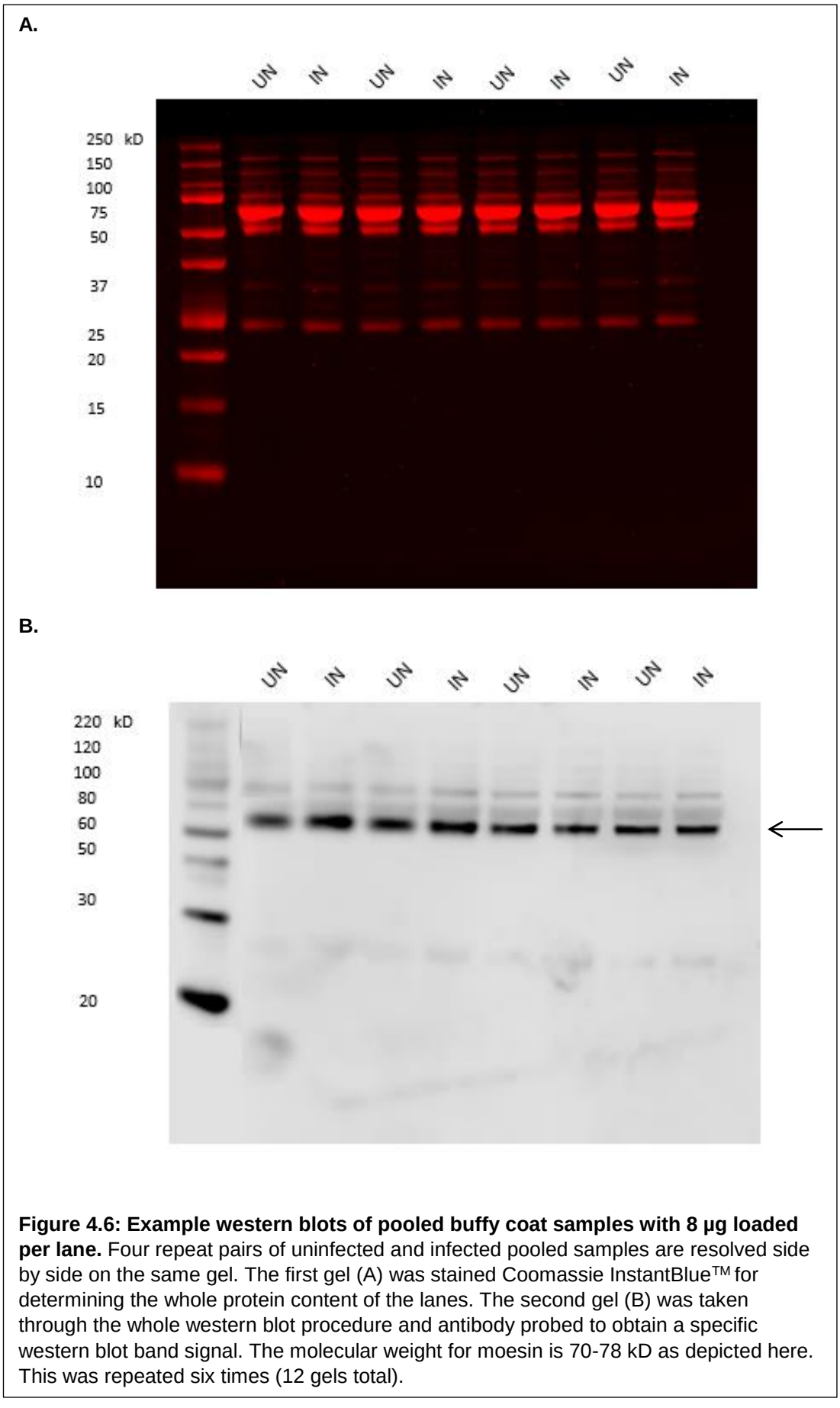

Figure 4.6: Example western blots of pooled buffy coat samples with 8 µg loaded per lane. Four repeat pairs of uninfected and infected pooled samples are resolved side by side on the same gel. The first gel (A) was stained Coomassie InstantBlue™ for determining the whole protein content of the lanes. The second gel (B) was taken through the whole western blot procedure and antibody probed to obtain a specific western blot band signal. The molecular weight for moesin is 70-78 kD as depicted here. This was repeated six times (12 gels total).

Upregulation of moesin in the infected pooled buffy coat was reported from the mass spectrometry analysis. This is successfully validated in western blotting of the pooled buffy coat samples. Validation using individual sheep samples was the next step. Buffy coat samples from the same nine sheep as those used in the pooled buffy coat experiments (at the same two time points) were taken from -80 ^{o}C storage and diluted in RIPA buffer. Following microBCA assay to calculate the protein concentration of each sample, stock solutions were prepared and samples made ready for gel electrophoresis. Samples from three control sheep (age-matched but not exposed to BSE) were resolved on all gels. Gels were processed with samples from the same sheep at two time points (prechallenge and 12 months) resolved side by side for better comparison. As before, two gels are resolved at the same time. One is stained over night in Coomassie Instant Blue™ to quantify the whole protein content per lane and the other gel is antibody probed to obtain a western blot band signal. To plot the graph in Figure 4.7 A a normalised western blot signal is calculated. A ratio value is obtained by dividing the whole protein signal (from the Coomassie Instant Blue™ stained gel) by the highest whole protein signal across the gel (as the same protein concentration for each of the nine sheep samples should have been loaded, thus taking into account loading discrepancies). The western blot signal (detected from LI-COR scanning the antibody probed, chemiluminescence stained nitrocellulose membrane) is then divided by the ratio and this 'normalised' value plotted. The results are an average of two repeat experiments (of all nine sheep at the two time points), the data values were under 4% difference from each other. Highlighted on Figure 4.7 A are comparisons with significant values. The paired T test result for control sheep at prechallenge and at 12 months gives a P value of 0.2687. This shows that there is not a significant difference in protein expression for control sheep. The paired T test for infected sheep at prechallenge and 12 months gives a P value of 0.0001. This is very significant. It highlights that there is definitely a difference in protein expression at the two time points for infected sheep. The unpaired T test P value of control and infected sheep at the prechallenge time point is 0.1165 (this is not significant and no difference in expression between the groups are expected at this stage). The unpaired T test P value for controls and test sheep at 12 months is 0.0021 (a significant result reflecting change in moesin expression before and after sheep are exposed to BSE). To plot Figure 4.7 B the normalised western blot band signal at the prechallenge time point is subtracted from the normalised western blot band signal at 12 months. This gives a comparison or difference in moesin expression for control and infected sheep at the two time points. It is a significant difference and the T test P value is 0.0255.Example gels for the individual sheep buffy coat samples are displayed in Figure 4.8.

A.

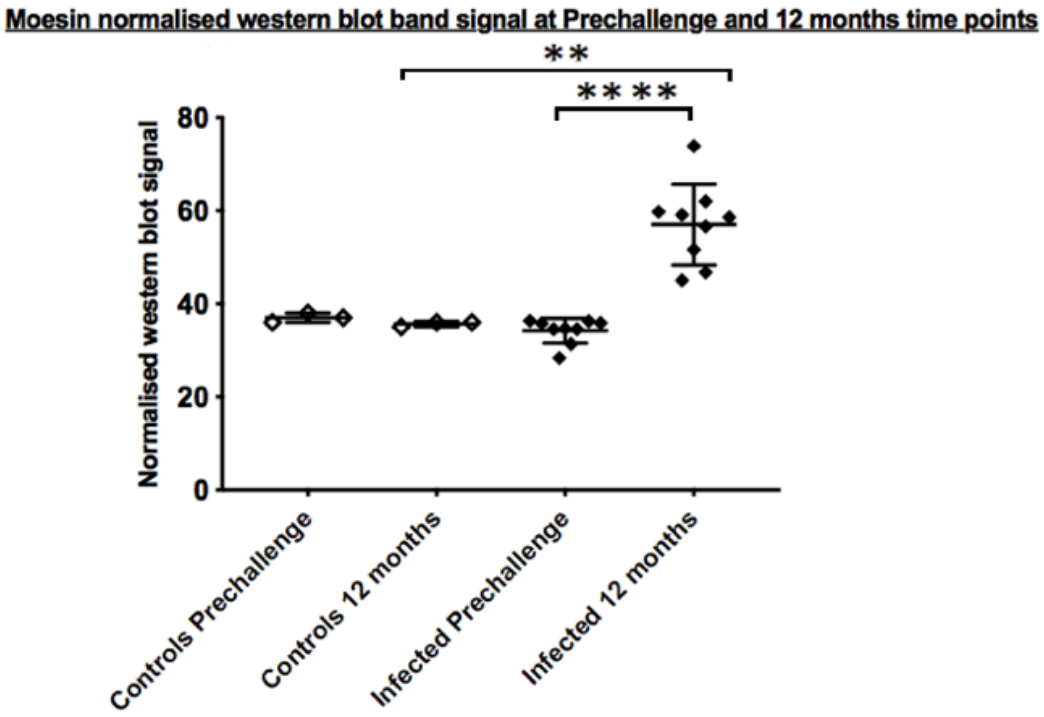

B.

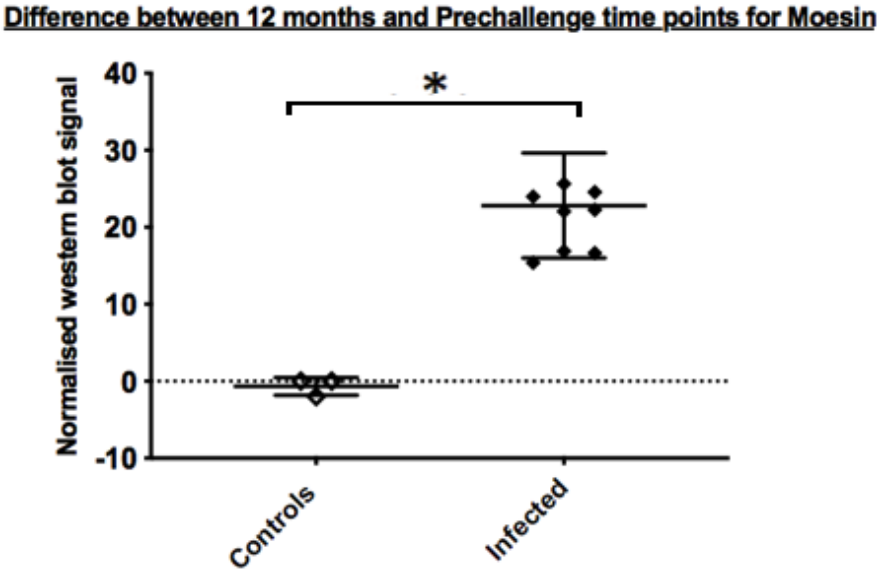

Figure 4.7: Moesin expression in individual sheep at Prechallenge compared to 12 months. This plotted data is an average of two repeat experiments (results varied by 4%). Graph (A) depicts an increase in moesin expression in infected sheep at the 12 months time point compared to at Prechallenge. A paired T test with a significant result (P=<0.0001) is seen between Prechallenge and 12 months for infected samples. Another comparison with a statistically significant T test result is that of moesin expression in control sheep at 12 months and infected sheep at 12 months (0.0021). Graph (B) is the difference between 12 months and Prechallenge (normalised western blot band signal subtracting the prechallenge values from the 12 month value) plotted for control sheep and infected sheep. A significant value was calculated in the T test perfomed (P = 0.0255).

A.

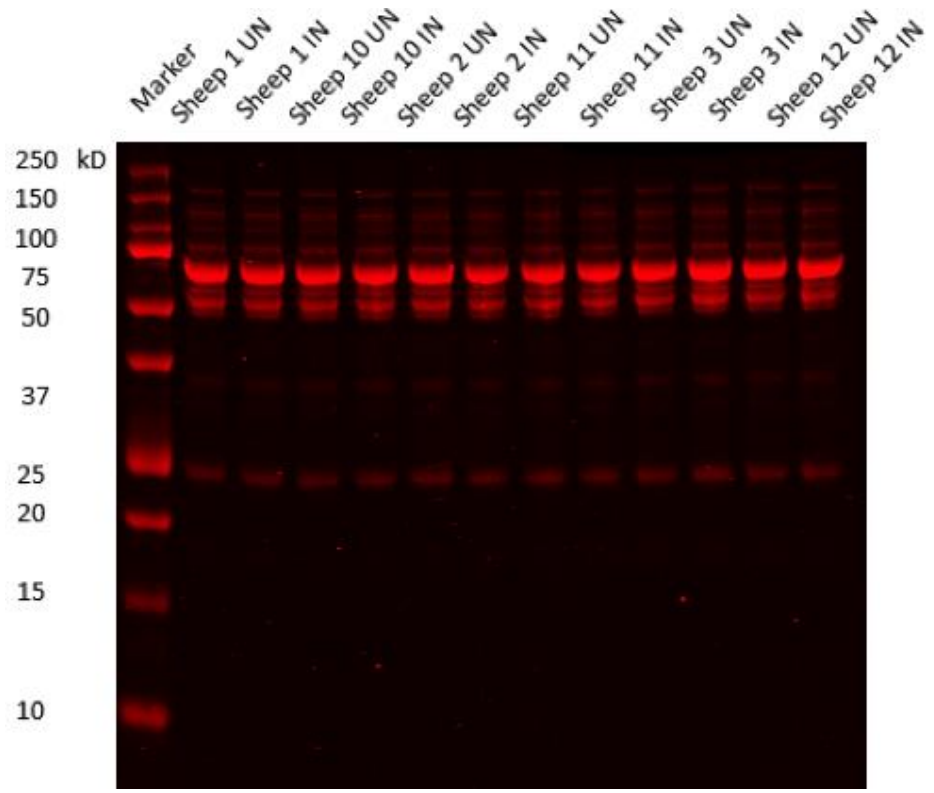

B.

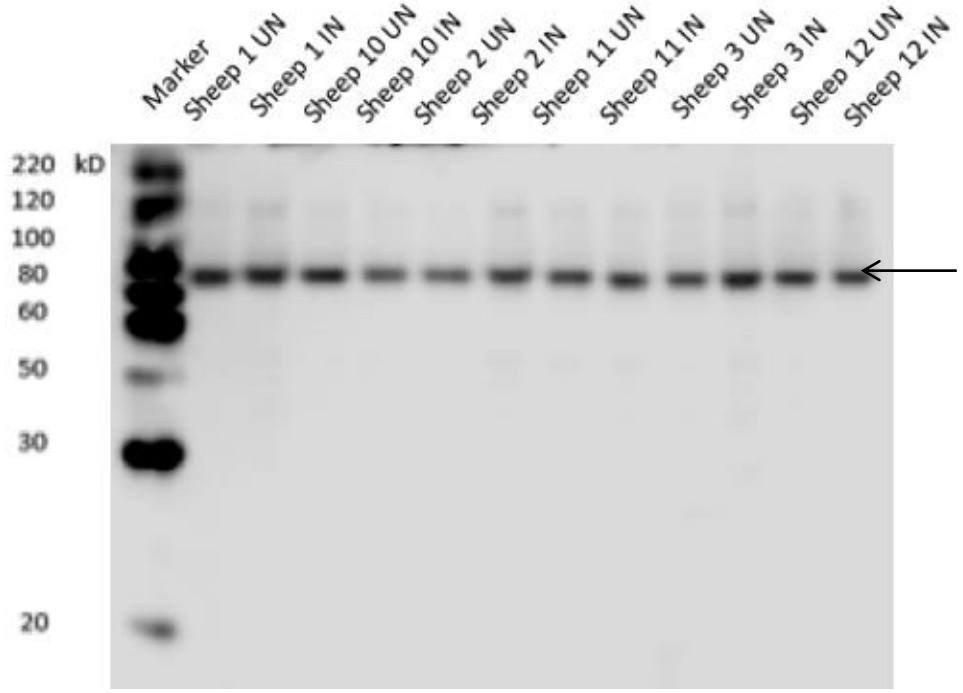

Figure 4.8: Example western blots of moesin expression for individual sheep buffy coat samples with 8 µg of protein loaded per lane. Two gels resolved at the same time, with UN or uninfected (Prechallenge) and IN or infected (12 month) placed side by side for easy comparison. The first (A) is Coomassie Blue stained to obtain the whole protein signal. Protein on the second gel is transferred to a membrane, which is then probed with moesin antibody, and LI-COR scanned (B). The arrow indicates the band of interest.

4.3 Discussion

Through identification of novel biomarkers proteomic analysis has clear potential in aiding the development of a highly sought after preclinical prion disease diagnostic test to complement detection of PrP^{Sc}. While the list of potential biomarkers is growing, validation studies are not being carried out at the same pace. This is due to some of the inherent problems of prion disease such as the small number of clinical cases, long incubation period and limited availability of preclinical human samples (Huzarewich et al. 2010). Additionally there are technical issues of readiness of compatible assays or working antibodies. Many proteomic studies of prion diseases focus on the analysis of brain or CNS tissues, here I present presymptomatic changes in protein expression from the buffy coat blood fraction of sheep exposed to BSE. By utilising IPA analysis and reported associations in published literature, the list of 124 mass spectrometry identified differentially regulated buffy coat proteins were shortlisted to seven biomarkers. These were spermine synthase, heterogeneous nuclear ribonucleoprotein K, inter-alpha-trypsin inhibitor heavy chain H2, Parkinson disease protein 7, moesin, s100A8 S100 calcium binding and transthyretin. After attempting validation by western blotting, only moesin was successfully validated using the original pooled sheep buffy coat samples. These findings were then found to be reflected in the individual sheep buffy coat samples from the same time points.

4.3.1 Biological interpretation

A number of problems were encountered during attempted validation of the seven biomarkers chosen from the buffy coat dataset, this is predominantly down to the antibodies not being compatible with sheep samples. However, there are examples of previously published proteomic/genomic studies on blood that present findings similar to my work. To detect gene expression changes with microarray analysis, Panelli et al. (2011) fractionated WBCs from the blood of cattle one year after oral BSE challenge. The majority of differentially regulated proteins were related to immune function, with significantly modified expression of genes linked to T and B cell development and activation, as well as inflammatory responses. Xerxa et al. (2016) performed whole blood gene expression profiling from preclinical and clinical cattle infected with atypical BSE. Gene enrichment analysis (performed using DAVID bioinformatics tool) revealed that the preclinical stage was characterised by enrichment in gene clusters related to chemokine signalling, extracellular

matrix, immune response, B cell proliferation and RNA metabolic process. These studies corroborate our findings and give a degree of confidence in what we are seeing.

At the 10 month time point post after exposure to BSE, where the mass spectrometry analysed infected samples were taken from, PrP^{Sc} accumulation is not detectable in the brain or lymphoid tissues of the sheep (Jeffrey, Martin, et al. 2001). However, prion misfolding and PrP^{Sc} replication is undoubtedly taking place as the blood is infectious at this stage (as shown by transmission of disease to blood recipient sheep). By reviewing the association to neurodegenerative diseases of the IPA suggested pathways, as well as the functions of the differentially regulated buffy coat proteins, a picture of what may be occurring at the preclinical stage of infection can be formed. Proteins of the immune system are highly featured. This may indicate that preclinical prion infection is associated with low level activation of the body's early defence mechanism or innate immunity. The responses taking place are unlikely to be that of adaptive immunity this is because PrP^{Sc} is tolerated by the host immune system due to the widespread expression of PrP^{C} throughout the body. Thus specific cell-mediated activity and antibody production, which normally respond to and remove foreign viruses or bacteria, is prevented (Furr, Young, and Richt 2012).

Immune cells are critical for prion disease propagation. PrP^{Sc} accumulate first upon follicular dendritic cells (FDCs) as they make their way from the site of infection to the CNS (Mabbott, Mackay, et al. 2000); (Montrasio et al. 2000); (McCulloch et al. 2011). Their importance has been established by the lack of PrP^{Sc} accumulation in the spleen and subsequent neuroinvasion in immunodeficient mice lacking FDC (Klein et al. 2001). B cells regulate FDC maturation but also are likely to be responsible for movement of PrP^{Sc} (Mackay and Browning 1998); (Cinamon et al. 2008); (Mok et al. 2012). Conventional dendritic cells are able to capture and retain intact pathogens and migrate into B cell follicles, hence PrP^{Sc} may exploit them for propagation (Huang et al. 2002); (Raymond, Aucouturier, and Mabbott 2007); (Sethi et al. 2007). Within a matter of weeks of their initial multiplication within the draining lymphoid tissue, PrP^{Sc} are subsequently propagated to most other secondary lymphoid tissues (SLO), including the spleen. This implies dissemination via the blood and lymph (Mohan, Bruce, and Mabbott 2005); (Glaysher and Mabbott 2007).

One of the key pathways highlighted by IPA analysis of the buffy coat dataset was the leukocyte extravasation signalling pathway. Also called diapedesis, it is the process whereby leukocytes move out of the circulatory system, cross blood vessels and head towards the site of tissue damage or infection. This may occur through tightly apposed endothelial

borders (paracellular transmigration) and in some cases, through the endothelial cells themselves (transcellular migration) (Muller 2013). Moesin is one of the proteins of this pathway. It orchestrates complex procedures involved in cell shape changes. The ERM protein family (erzin and radixin, moesin) regulates cortical morphogenesis and cell adhesion through connection of membrane adhesion receptors to the actin-based cytoskeleton. Both moesin and ezrin interact with the vascular cell adhesion molecule (VCAM)-1 during leukocyte adhesion and transendothelial migration. Moesin thus plays an essential role in the firm adhesion of leukocytes to the endothelium (Barreiro et al. 2002). Up regulation of moesin was observed in the pooled, infected buffy coat samples. Previous studies have also shown upregulation of moesin in prion disease states (Xiang et al. 2004; Chadwick et al. 2010; Jayasena et al. 2015). The increase in moesin may be facilitating movement of leukocytes through an enhanced ability to connect cells. This would enable their migration to lymphoid organs in the early stage of disease and mediate effective dissemination of PrP^{Sc}.

Due to the crucial role the immune system plays in peripheral pathogenesis of prion disease, it could be argued that it promotes rather than protects against the disease. This is supported by the finding that repetitive immunization enhances susceptibility of mice to intraperitoneal administration of scrapie (Bremer et al. 2009). Acute phase signalling is an essential part of innate immunity which include vascular permeability and leucocytosis (Lu et al. 2011). The presence of acute phase proteins in the buffy coat dataset and the identification of the acute phase response signalling pathway by IPA suggests an occurrence of inflammation or inflammation-like incidents at the preclinical time point. Host inflammation has been shown to significantly influence prion disease pathogenesis, through enhancing PrP^{Sc} uptake or expanding their tissue distribution (Heikenwalder et al. 2008); (Sigurdson et al. 2009). During inflammation, dilation and increased permeability of blood vessels leads to increased local blood flow and the leakage of fluid results in heat, redness and swelling. Cytokines and complement fragments have significant affects on the adhesive properties of the endothelial cells of the blood vessel wall, causing circulating leukocytes to stick to the endothelium and migrate between them to the site of infection to which they are attracted to by chemokines (Janeway CA Jr 2001). Stimulation of leukocytes and their change in shape and adhesiveness is a prerequisite to the entry of effector cells such as neutrophils, monocytes and effector T cells to sites of infection, injury and stress (Nourshargh and Alon 2014). Thus, these activities promote cell movement, which is important for the spread of PrP^{Sc}.

In omic based searches for non-PrP^{Sc} markers of prion diseases there are many genes and proteins that are linked to the acute phase response (Huzarewich et al. 2010). The

occurrence of an acute phase response has been detected in sheep with clinical scrapie (Meling, Bårdsen, and Ulvund 2012). Serum transthyretin has been found to discriminate healthy from scrapie infected sheep both at preclinical and clinical stages of disease (Batxelli-Molina et al. 2010). Serum amyloid P is increased with the onset and progression of clinical signs in an experimental scrapie murine model (Coe, Race, and Ross 2001). Protein C-reactive protein (CRP) was increased in the plasma samples of CJD patients compared to healthy controls (Volkel et al. 2001).

The three proteins from the buffy coat dataset chosen for further validation were S100A8 calcium binding protein, heterogeneous nuclear ribonucleoprotein K and inter-alpha-trypsin inhibitor heavy chain H2, all were identified by IPA as belonging to the acute phase response signalling pathway. S100A8 plays a prominent role in the regulation of inflammatory processes (Ryckman et al. 2003),this is achieved by stimulating leukocyte recruitment and inducing cytokine secretion (Wang et al. 2018). Heterogeneous nuclear ribonucleoprotein K is one of the major RNA-binding proteins and is involved in many processes that compose nucleic acid metabolism and gene expression, including mRNA processing and translation (Geuens, Bouhy, and Timmerman 2016). Not much is known about inter-alpha-trypsin H2 but it is down regulated during an inflammatory response (Daveau et al. 1993). Although there is a mix of up/down regulation of these proteins in the buffy coat dataset, their involvement further suggests immune effects, such as movement of WBCs, occurring at the preclinical stage of prion infection. Perhaps activities occurring at the preclinical phase are characterised by a systemic acute phase response.

The stimulation of immune cells and their movement or circulation around the body requires a vast amount of energy, hence a number of proteins involved in energy pathways and metabolic processes are upregulated in the dataset. Bioinformatic analysis of the mass spectrometry data suggests an involvement of cellular energy pathways, such as glycolysis/gluconeogenesis. While, FDCs are major cell populations in lymphoid nodules (Manuelidis et al. 2000), macrophages are also present throughout the lymphoid nodule and ingest apoptotic B cells. Cells of myeloid lineages depend almost exclusively on glycolysis to derive their energy. In comparison lymphocytes utilize predominantly oxidative phosphorylation (Fox, Hammerman, and Thompson 2005). T and B cells exploit amino acids, glucose and lipids as energy sources during oxidative phosphorylation. Stimulated proliferation can result in nearly twenty-fold increase in glucose (Kominsky, Campbell, and Colgan 2010). Perhaps metabolic reprograming (and regulation of cellular energy pathways) of these nodular cell populations, is a part of the early disease response. Thus facilitating

uptake, transport and elimination of PrP^{Sc}, culminating in accumulation of PrP^{Sc} within the lymph nodules and ultimately aiding neuroinvasion later during disease.

Another key pathway identified by IPA analysis of the buffy coat data is the LXR/RXR activation pathway. It has also been described as a top canonical pathway from gene expression profiling of BSE infected macaques (Barbison et al. 2014) as well as of potential importance in AD (Bogdanovic et al. 2001); (Patel and Forman 2004). The liver X receptors (LXRs) and the retinoid X receptors (RXRs) are central to lipid metabolism. LXRs regulate the expression of several genes involved in reverse cholesterol transport in peripheral cells such as macrophages (Castrillo and Tontonoz 2004). This is done not only by inducing cholesterol transporter proteins (ABCA1 and ABCG1) but also through increased production of cholesterol acceptors (apoE and apoCs) and lipoprotein remodelling proteins (PLTP and LPL) (Beaven and Tontonoz 2006). The RXRs also act as negative regulators of the immune responses (inflammatory response and macrophage activation). RXR is able to control macrophage gene transcription through its hetrodimerisation with other nuclear receptors (Roszer et al. 2013). In addition to the role as cholesterol sensors, LXRs have also been shown to be implicated in modulating the innate and adaptive immune response suggesting a crosstalk between inflammatory and metabolic pathways. It has been shown that LXRs dependent gene expression is important for macrophage survival, there is an LXR-dependent repression of inflammatory gene expression in activated macrophages. LXRs inhibit inflammatory genes after LPS, TNF-α or IL-1β stimulation (Joseph et al. 2003). IPA analysis has suggested a downregulation in LXR/RXR activation during preclinical prion disease. It is possible that there is a suppression of negative regulation of the immune system during preclinical infection, thus leading to heightened macrophage activity. The increased macrophage activity may relate to enhanced accumulation of the infectious prion agent, transport and delivery to neuronal cells (Carp and Callahan 1981); (Jeffrey et al. 2000); (Mabbott and MacPherson 2006).

Bioinformatic analysis of the buffy coat data also revealed spermine biosynthesis as an important biological pathway. The candidate biomarker chosen for further investigation was spermine synthase which converts spermidine into spermine. Both are present in millimolar concentrations in almost all cells as they are inherently involved in cellular metabolism (Coffino 2000). Spermine has been shown to be able to inhibit nucleic acid induced polymerisation of prion protein, acting as a protective agent. Through induction of autophagy and other stress response pathways, spontaneous prion formation is prevented (Bera and Nandi 2007). The mass spectrometry data suggests a decrease in spermine synthase (and thus less spermine) in the infected buffy coat samples. This may suggest a loss of these

protective agents during disease progression promoting PrP^{Sc} production at the early, preclinical stage of disease.

The final IPA pathway further looked at in this chapter was mitochondrial dysfunction. Mitochondria are able to stimulate the innate immune signalling cascade to intensify inflammation, through distinct stress signals or damage associated molecular patterns (DAMPs) such as reactive oxygen species (ROS) (Chen, Zhou, and Min 2018). Keller et al. (2019) found that in genetic prion disease (using mice modelling E200K CJD) oxidative damage, associated with mitochondrial dysfunction, is initiated well before clinical manifestations. Furthermore, gene expression changes associated with mitochondrial dysfunction have been detected in the blood of patients with early AD using microarray technology (Lunnon et al. 2012). Hence, altered changes are not just restricted to the brain in such neurodegenerative disease and they may prove to be sufficient to specifically classify disease before diagnosis. IPA of the buffy coat dataset identified Parkinson disease protein 7 as part of the mitochondrial dysfunction pathway. Defects in the gene cause autosomal recessive, early onset Parkinson's disease. Parkinson disease protein 7 plays an important part in regulation of the ROS production through interaction with the $p47^{phox}$, a subunit of NADPH oxidase (Liu et al. 2015; Cheng et al. 2018). ROS are key mediators in initiating toll-like receptor (TLR) signalling pathways to activate macrophages (Gallego et al. 2011); (West et al. 2011). In the buffy coat data there is an increase in Parkinson disease protein 7 in the infected samples, perhaps indicating activation and activity of leukocytes.

Even though further studies are required to investigate the specific involvement of all the identified protein biomarkers, the mass spectrometry identified proteins in the buffy coat samples show an important role for immune system regulation in prion pathogenesis of BSE-infected sheep. This is perhaps reflected in other prion and neurodegenerative diseases in general. In fact, immune markers such as increased TREM2 in CSF, have been predominantly and reproducibly associated with the early presymptomatic stages of AD (Villegas-Llerena et al. 2016); (Brosseron et al. 2019); (Falcon et al. 2019); (Nordengen et al. 2019); (Suarez-Calvet et al. 2019). It suggests that the innate immune system may undergo sequential changes towards inflammatory activation and that inflammation is associated with neurodegeneration.

4.3.2 Limitations

A limitation of this work is perhaps the strong focus on the IPA interpretation of the mass

spectrometry buffy coat dataset and its suggested ingenuity pathways. The proteins chosen for validation came from pathways with significant scoring P values as calculated by IPA using a Right-Tailed Fisher's Exact Test. It is unlikely that the proteins appear in these pathways due to random chance. Although there are similarities to other published studies on prion disease, focusing on the proteins previously identified as of interest may show some bias and result in missing potential proteins of interest. Due to the lack of preclinical samples many studies are not focused on this stage of disease so may not pick up on specific preclinical proteins. A lot of prion disease biomarker studies also only look at brain-derived material so may not be as relevant. Furthermore, as infectivity has not been found in the blood of cattle with BSE and atypical BSE, studies focused on these samples may be different from the BSE infected sheep investigated here.

4.3.3 Conclusion

The aim of this work is to look for proteins besides PrP that may be utilised for following prion infection in blood of sheep orally infected with BSE. While it likely that at the time when infected blood was taken during the transfusion study (12 months) there would not have been an accumulation of abnormal prion protein in the brain, there is likely to be other events occurring in the body in response to infection. It may be possible to identify changes in protein expression for use as diagnostic markers and to indicate disease status. However, the identification of non-prion protein biomarkers from blood remains challenging due to the inherent complexity and vast dynamic range of proteins present. In addition, a key issue with using blood for biomarker discovery is that its cellular components may change dramatically during infection or inflammation. Mass spectrometry based proteomics technology has been utilized to aid biomarker discovery and propel advancements in diagnostics. Here, alterations in protein expression of infected buffy coat samples were established by mass spectrometry. IPA analysis was able to predict a number of disease pathways of interest and the potential involvement of an active immune response has been highlighted. Seven proteins were suggested for a biomarker and validation of moesin by western blotting was achieved with both pooled and individual buffy coat samples.

4.3.4 Future work

The strong data generated from mass spectrometry of comparing uninfected and infected buffy coat samples requires further exploration. This work presents an array of relevant proteins, provides theories for their particular involvement in disease progression and gives an indication for their possible use in early detection. Following the success of moesin

validation, it essential that other proteins of the pathways highlighted as important by IPA are also tested. Validation of a full biomarker panel is the first step in a premortem test and would prevent the inadvertent transfusion of infected blood, enable accurate prediction of TSE epidemics as well as allow for greater understanding of disease pathogenesis (Wei et al. 2011a). However, it would be necessary to overcome the issues faced here in finding antibodies compatible with sheep blood. Repeat experiments would better confirm the mass spectrometry predicted trends and including a greater number of control sheep would also strengthen the statistical comparison between the two groups. Performing mass spectrometry on individual sheep buffy coat samples or from more time points across the transfusion study would indicate which proteins have the greatest differential expression and when this occurs along the time the course of disease progression. For further work, validation on clinical samples to confirm application to human blood is crucial.

Additionally, investigation of the biochemical properties of moesin may provide a greater insight into the mechanism of prion diseases by further defining the physiological process through cellular interaction and protein function. Overall, this will help in progressing the field of neurodegenerative diseases as a more comprehensive understanding of the molecular basis of neuronal damage is essential in development of effective therapy.

Chapter 5: Development of an in vitro assay for blood borne prion infectivity

5.1 Introduction

In Chapter 4 I explored how WBCs were important for prion disease pathogenesis and proposed a biomarker panel based on the buffy coat proteome of BSE-infected sheep for diagnostic purposes. The objective of the work in this chapter was to develop a system to study the processes by which live WBCs transfer infection to other cells, and then to investigate if they are more efficient than infection by brain homogenate. Blood derived PrP^{Sc} and brain derived PrP^{Sc} are likely to have different properties in regards to aggregate size, solubility and even resistance to PK digestion. The brain is a solid organ that permits aggregate accumulation on infected nerve cells. It has been suggested that the large amyloid fibrils seen in the brains of patients with prion disease are actually protective agents, sequestering the more hazardous smaller fibrils into innocuous deposits (Caughey and Lansbury 2003); (Piccardo et al. 2007). Smaller, non-fibrillar PrP^{Sc} containing aggregates are more efficient initiators of prion disease (Silveira et al. 2005); (Chiovitti et al. 2007), as they provide an increased number of multiplication seeds. With blood being a fluid, moving medium and having a high cell turn over, it does not allow for the build up of the large aggregate deposits seen in the brain. Thus, as blood borne PrP^{Sc} is predominantly found in smaller aggregates (Chang et al. 2007); (Bannach et al. 2012) it may actually be more infectious.

5.1.1 Current cell lines

Cell lines were initially used to explore PrP^{Sc} propagation, in recent years they have been used as models for screening therapeutic compounds. However, cell lines pose a difficulty in that many are not permissive to prion infection or replication. Even those that can be infected are not necessarily permissive to infection by all prion agents and strains. Table 5.1 gives examples of some cell lines and the prion strains which they can replicate. The mouse neuroblastoma N2a cell line is the most extensively used cell line to date (Race, Fadness, and Chesebro 1987). Klöhn et al. (2003) isolated N2a cells (fast growing mouse neuroblastoma) highly susceptible to RML scrapie prions thus allowing the study of scrapie infectivity.

The RK13 cell line are rabbit kidney epithelial cells which do not express endogenous rabbit PrP^{C}. To achieve a high level of ovine PrP expression, the Rov9 cell line was created by transfection of RK13 with plasmid vectors containing the tetracycline-inducible (tet-on) system cloned PRNP gene sequence from sheep (VRQ allele) (Vilette et al. 2001). It is the

first cell model that can be infected by natural scrapie isolates which have not been previously passaged and adapted to rodents. In the presence of the antibiotic tetracycline (or one of its derivatives such as doxycycline), the cell line synthesises highly glycosylated PrP at levels similar to that seen in sheep brain (Neale et al. 2010). The susceptibility of sheep to scrapie is mediated by PRNP, the allele VRQ confers high susceptibility combined with a short incubation time for sheep exposed to the scrapie agent. In contrast ARR is associated with clinical resistance to the disease (Hunter 1997). Rov9 cells were used in the experiments for this chapter.

Table 5.1: Cell lines permissive to prion infection. Below is a list with examples of current cell lines used to study prions *in vitro* (van der Merwe et al. 2015).

Cell Designation	Species	Origin	Prion Strain
Neuronal			
N2a	Mouse	Neuroblastoma	Chandler, RML, 139A, 22L, C506, Fukuoka-1, FU CJD
GT1	Mouse	Hypothalamic	Chandler, RML, 139A, 22L, FU CJD, M1000
SMB	Mouse	Scrapie-infected mesodermal cells	Chandler, 139A, 22F, 79A
SN56	Mouse	Cholinergic septal cells	Chandler, ME7, 22L
CAD	Mouse	Catecholaminerguc	RML, 22L, ME7, 301C
PC12	Rat	Pheochromocytoma	139A, ME7
Non-Neuronal Cell Lines			
C2C12	Mouse	Myotubes	RML, ME7, 22L
NTH/3T3	Mouse	Fibroblast	22L
moRK12	Rabbit	Epithelial cell line expressing mouse PrP^C	22L, Chandler, M1000, mo sCJD, Fukuoka-1
voRK13	Rabbit	Epithelial cell line expressing vole PrP^C	Vole-adapted BSE
OvRK13/Rov9	Rabbit	Epithelial cell line expressing ovine PrP^C	PG127, LA404, SSBP/1, scrapie field isolates
SSCA Cell Lines			
PK1	Mouse	N2a	RML, 22L
R33	Mouse	N2a	RML, 22L
CAD5	Mouse	CAD	RML, 22L, me7, 301C
LD9	Mouse	L929	RML, 22L, ME7
L929	Mouse	Fibroblast	RML, 22L, ME7
Elk21	Rabbit	RK12: epithelial cell line expressing elk PrP^C	CWD

5.1.2 Factors that affect cell line susceptibility and propagation of prions in culture

It is apparent that one cell line can be infected by several prion strains. Conversely, it is clear that one strain can infect several different cell lines. There are likely to be several factors that promote and assist this occurrence. For instance, the confirmation or glycosylation pattern of

PrP molecules expressed affects the cell line susceptibility to carry infection. Additionally, the general trafficking of PrP (such as the endogenous cleavage and degradation pathways of PrP) may be involved (Solassol, Crozet, and Lehmann 2003). Additionally, C1 cleavage is associated with resistance of cell lines to prion infection, while susceptible cell lines have a greater proportion of full length PrP^{C} (Lewis et al. 2009). Another potentially important factor is the varying expression of co-factors necessary for replication of the agent (Telling et al. 1994). Two types of cofactors, lipids and polyanions, have been identified as influencing prion propagation and infectivity, however the precise mechanism remains unclear (Ma 2012); (Supattapone 2014).

The formation of PrP^{Sc} in cell culture is initiated following the translocation of PrP^{C} to the cell surface (Caughey and Raymond 1991). However PrP^{Sc} uptake is independent of PrP^{C} expression and does not indicate a productive infection as it is also observed in nonpermissive cell lines (Paquet, Daude, et al. 2007). The continuous presence of PrP^{Sc} over multiple cell passages is indicative of a productive infection of the cell culture. This may be detected by western blot analysis of cell lysates treated with PK (50 µg/mL, 37°C, 1 hr) or by indirect immunofluorescence in fixed cells following antigen retrieval by denaturants such as guanidinium hydrochloride (Taraboulos, Serban, and Prusiner 1990); (Veith et al. 2009).

The vertical spread from mother to daughter cells where cell division occurs affects the aggregate load of the cell, diluting the number of infectious particles by half. The continuous prion propagation in cell culture implies that there are fragmentation mechanisms in place for seed multiplication. The mechanical force of endocytosis possibly segregates large PrP^{Sc} aggregates, alternatively unidentified cofactors catalyse the fragmentation of larger aggregates (Krauss and Vorberg 2013). Prions are not only transmitted to progeny cells but are also spread to adjacent cells. Horizontal transmission by contact of neighbouring cells induces a prion phenotype in the recipient cells that again spreads vertically and horizontally. It has been shown that direct proximity between donor and recipient cells greatly increases infection (Kanu 2002).

5.1.3 PK digestion and glycosylation pattern of prion protein

There are a number of different ways to identify the presence of abnormal prion protein, the method used in this chapter is a well-characterised western blot. The key to a western blot assay for PrP^{Sc} is the use of proteinase K (PK). Normal PrP^{C} is sensitive to PK digestion while PrP^{Sc} is resistant to PK digestion. Based on these differences, it is possible to unambiguously distinguish between the cellular form and abnormal form of prion protein in a sample by western blot. PrP^{C} resolves as a triplet on SDS-PAGE gels, showing three distinct migration bands that are associated with the un-, mono- and di-glycosyl groups. There is an

absence of these bands in PK treated samples containing PrP^{C} as the procedure results in small peptides. Conversely, in PK treated samples containing PrP^{Sc} the bands remain although shifted to a lower molecular weight (Riesner 2003b). These are the N-terminally truncated forms of PrP^{Sc}, Figure 5.1 shows how PrP is cleaved resulting in this fully infectious amino acid sequence (of approximately 142 amino acids) referred to as PrP 27-30.

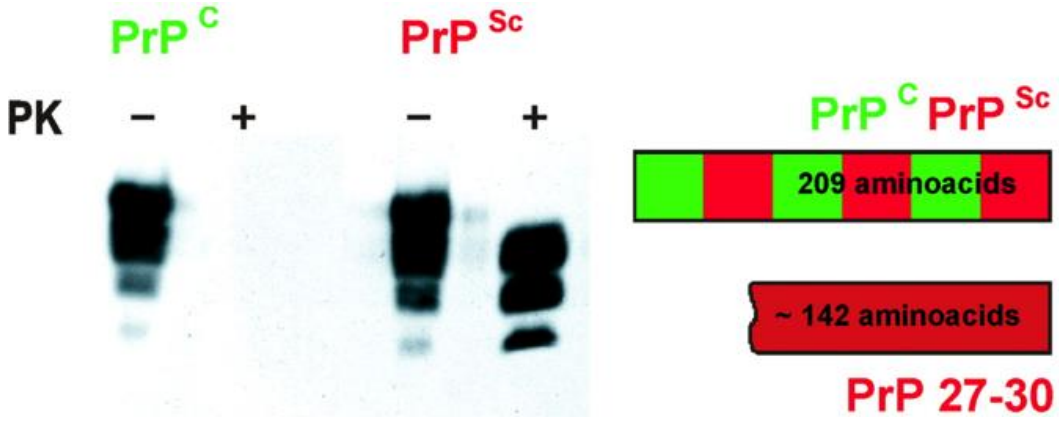

Figure 5.1: Example of PK treated PrP. Western blot of PrP^{C} and PrP^{Sc} following PK digestion with diagram of PK cleavage product, N-terminal truncated PrP 27-30 (Riesner 2003b).

Although the diagnosis of prion disease by detection of PrP^{Sc} using PK is a well-established method, studies have shown that PK sensitive pathological isoforms of PrP also play an important role in disease pathogenesis (Tzaban et al. 2002); (Tremblay et al. 2004); (Pastrana et al. 2006).

5.1.4 Peripheral Blood Mononuclear Cells (PBMCs)

Further to investigating the infectious nature of blood, this chapter looks at the particular ability of certain blood components to infect the Rov9 cell line. PBMCs refer to all blood cells with a round nucleus. These include monocytes, T cells, B cells, natural killer cells and a small number of dendritic cells. Hence, the PBMC portion of the blood contain cell types vital for immune monitoring events (Koncarevic et al. 2014). As mentioned in previous chapters, these cells have a critical role in the early pathogenesis of peripherally acquired prion disease particularly due to their function within the lymphoreticular system and sequential dissemination of prions throughout the body (Andreoletti et al. 2000). Previous studies indicate that PrP^{C} surface expression and thus potential infectivity is associated with peripheral blood mononuclear cells (PBMC) (Herrmann et al. (2001); (Andreoletti et al. 2012; Halliday, Houston, and Hunter 2005). The presence of prion infectivity in different PBMC populations, such as lymphocytes and monocytes has been reported in scrapie-infected sheep (Lacroux, Vilette, et al. 2012). The ability to transmit disease by blood transfusion correlated with the presence of infectivity in WBCs and PBMCs as detected by bioassay in tg338 mice and with PrP^{Sc} identification using PMCA (Lacroux et al. 2012).

It is known that as little as 0.1 mL of whole blood from an asymptomatic scrapie infected sheep can transmit the disease and that 10^5 were the minimal number of WBCs required to transfer infection (Douet et al. 2016). Douet et al. (2016) also assessed the capacity of different PBMC subpopulations to transmit scrapie. They found that the intravenous administration of 10^6 CD45/B220$^+$ (predominantly B lymphocyte) cells resulted in transmission in all recipient sheep, however the same number of CD14$^+$ cells (monocyte lineage) failed to infect any recpients. Only some recipients of 10^6 CD4$^+$/8$^+$ (T lymphocytes) were positive, while none of the sheep that received 10^5 cells (CD45/B220$^+$, CD14$^+$ or CD4$^+$/8$^+$) developed clinical scrapie or accumulated PrP^{Sc} in their tissues. This suggests PBMC populations display different abilities to transmit scrapie and that CD45/B220$^+$ and CD4$^+$/8$^+$ are not responsible for the entire capacity of WBCs to transmit blood-borne prion disease but instead that the other cell populations participate in this process.

Further to these findings, live WBCs seem to be important for efficient transmission of scrapie by intravenous transfusion. When blood components from preclinical VRQ/VRQ sheep infected with the PG127 scrapie strain were administered intravenously to VRQ/VRQ TSE free recipients, WBCs displayed the same ability as whole blood to infect recipients. Fixation of WBCs with paraformaldehyde impaired disease transmission by transfusion in sheep. Whereas all recipient who received fresh WBCs succumbed to clinical disease, only two out four recipient sheep given PFA fixed WBCs became infected and had longer incubation periods than those transfused with live WBCs. This suggests that PFA fixation reduces the WBC associated infectivity. However, Andreoletti et al. (2012) also found that PFA fixation did not affect infectivity titre as measured by intracerebral inoculation in tg338 mice (transgenic for the VRQ allele of ovine PrP). From this it can be determined that although the transmission of prion disease by blood transfusion is highly efficient, it is dependent on the viability of transfused cells rather than their infectious titre. Treatment with formaldehyde crosslinks cell membrane surface proteins (chemically bonding adjacent molecules). This impairs cellular interactions as it prevents the cell from making changes to its membrane. As demonstrated in cell culture studies conversion of PrP^C to PrP^{Sc} during transmission of infection, is critically dependent on cell to cell contact (Kanu 2002). Perhaps the ability of blood to efficiently transmit disease via the blood transfusion route depends on the ability of blood cells to interact with the host.

5.1.5 Aims of work

It is previously been shown that the Rov9 cell line is capable of supporting infection from scrapie source material. SSBP1 brain homogenate (an experimental scrapie strain) and natural scrapie brain homogenate from the Roslin Cheviot Scrapie Flock have also been

shown to infect Rov9 cells (Salamat, MFK; unpublished data). Halliez et al. (2014) demonstrated that the Rov9 cell line can be infected with WBC homogenates from sheep inoculated with PG127 scrapie strain. The question raised here is whether the differential treatment of PBMCs from scrapie infected sheep affects their infectivity ability.

The aim of this work is to develop an in vitro system in which to understand the processes by which live scrapie-infected WBCs transfer infection to other cells. The initial objective was to establish whether WBCs from scrapie infected sheep of the Roslin Scrapie Flock can infect the Rov9 cell line. This would reinforce the findings of Halliez et al. (2014) (who used the experimental scrapie source PG127), but with a natural scrapie isolate.

The second aim of the work was to investigate whether live PBMC are more efficient at infecting Rov9 cells than either lysed PBMC or fixed PBMC. This may shed light on how intact (non-fixed) cells initiate infection and whether cellular interactions based on cell membrane surface proteins are detrimental to passing disease. The hypothesis for the experiments performed in this chapter is that PBMCs from infected (VRQ/VRQ) sheep will be able to cause infection in the Rov9 cell line but that their treatment with PFA will reduce the efficiency of infection by impairing cellular interactions.

5.2 Methods

5.2.1 Experiment 1

Rov9 cells were thawed and cultured until they reached confluency in a 6 well plate, as described in Methods chapter (section 2.2.1). The inoculum was prepared by isolating PBMCs from 50 mL blood from a sheep in the Roslin Scrapie Flock, which had the PRNP genotype VRQ/VRQ and was showing clinical signs of scrapie, by density gradient centrifugation (as described in Methods 2.2.2).

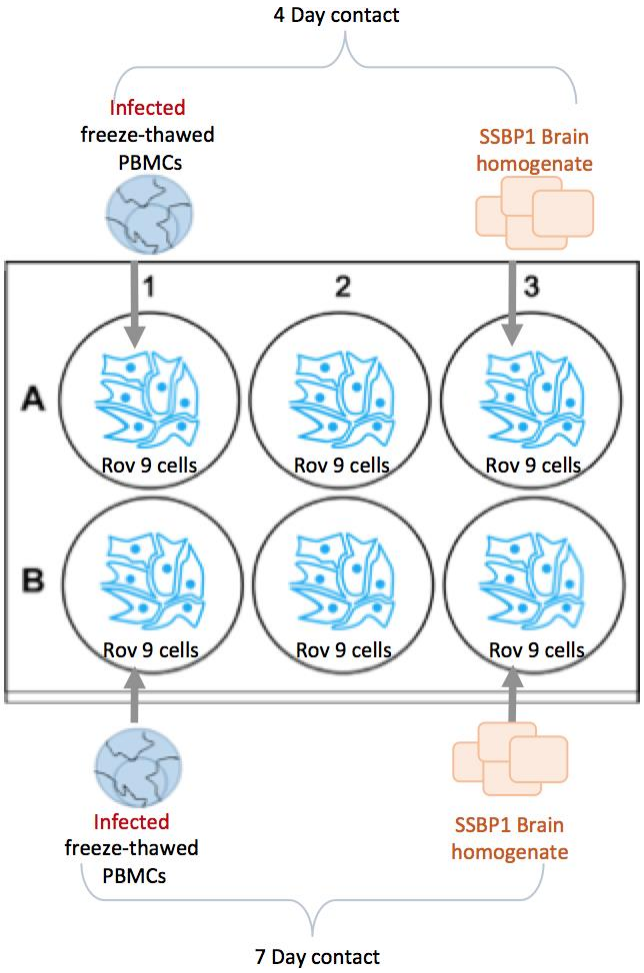

Figure 5.2: Plate outline for preliminary experiment. Rov9 cells were inoculated with freeze-thawed 1x10^7 PBMC pellets or SSBP1 brain homogenate. Two methods were compares, the first set of cells were passaged after 4 days of incubation with the inoculum. For comparison, the second were passaged after 7 days in contact with inoculum.

Pellets of 1 x 10^7 PBMCs were freeze thawed (10 mins on ice, 10 mins at room temperature) three times in succession to lyse cells before being taken up in 1 mL of Opti-Mem media warmed to 37 ^oC. Two wells of the 6 well plate coated in Rov9 cells were inoculated with 1

mL of PBMC lysate. The negative control refers to plate wells of Rov9 cells where no PBMCs were added. The positive controls are Rov9 cells infected with SSBP1 brain homogenate (1% final concentration in the same medium as used for the cells). This is illustrated in Figure 5.2. At Day 2, all wells were provided with fresh Opti-Mem medium supplemented with doxycycline.

Two methods of passaging cells were then tested. In the first method cells were infected at day 0 and left in contact with the inoculum for 4 days before passaging. In the second method cells were in contact with the inoculum for 7 days before passaging weekly as described in Materials and Methods 2.2.1. Samples were collected, PK treated and Western blotted (Materials and Methods 2.2.4),

5.2.2. Experiment 2

In this experiment, PBMC were prepared in three different ways before being used as inoculum for the Rov9 cell line: lysed (freeze thawed, as in Experiment 1), fresh (live), or PFA fixed. Rov9 cells were thawed and grown to confluency in two 12 well plates, as previously described (Methods 2.2.3). PBMC isolated from two sheep were used in this experiment, one with the resistant genotype ARR/ARR (as an uninfected negative control) and one with the scrapie susceptible genotype VRQ/VRQ, which was showing clinical signs of scrapie. PBMC were isolated by density gradient centrifugation as previously described. Following counting, fresh PBMC were suspended in Opti-Mem medium warmed to 37 ^{o}C and diluted to final concentrations of 1 x 10^7 cells/mL, 1x 10^6 and 1x 10^5 cell/mL, and 1 mL of each cell concentration added to individual wells of the 12 well plate. For preparation of fixed PBMC, aliquots of PBMC (uninfected and infected) were suspended at 1 x 10^7, 1 x 10^6, and 1 x 10^5 cells/mL in 2 % PFA diluted in Opti-Mem medium and placed on ice for 10 mins. They were washed three times in PBS before being added to wells of the 12 well plate. Lysed PBMC were prepared from suspensions of 1 x 10^7, 1 x 10^6, and 1 x 10^5 cells/mL by freeze thawing, as described for Experiment 1, and 1ml of each cell lysate added to individual wells of the 12 well plate. Figure 5.3 is a flowchart of events and Figure 5.4 depicts the plate layout. For a positive control Rov9 cells were inoculated with SSBP1 brain homogenate (1 % final concentration). Rov 9 cells were also inoculated with natural scrapie (NS) brain homogenate (1% final concentration). As a negative control Rov9 cells inoculated with uninfected PBMC and Rov9 cells with no PBMCs (or any additional cells) were used. Cells were passaged up to passage 9 (Materials and Methods 2.2.1). Cell lysates were collected, PK treated and Western blotted (Materials and Methods 2.2.4),

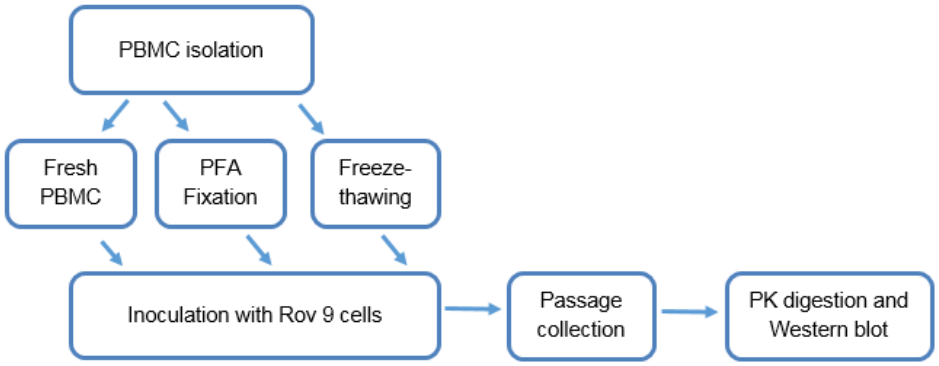

Figure 5.3: Flowchart of events. The series of preparation steps involved in upscale of the experiment. Different sized pellets of fresh, whole PBMCs were used to inoculate the Rov9 cell line. For comparison and to test levels of infectivity, pellets of different sized PBMCs were differentially treated (either fixed in 2% PFA on ice or freeze thawed three times on ice and at room temperature) and also added to the Rov9 cell line. Following passages and collection of cell lysate, PK digestion and western blotting was used to determine infectivity of the PBMCs.

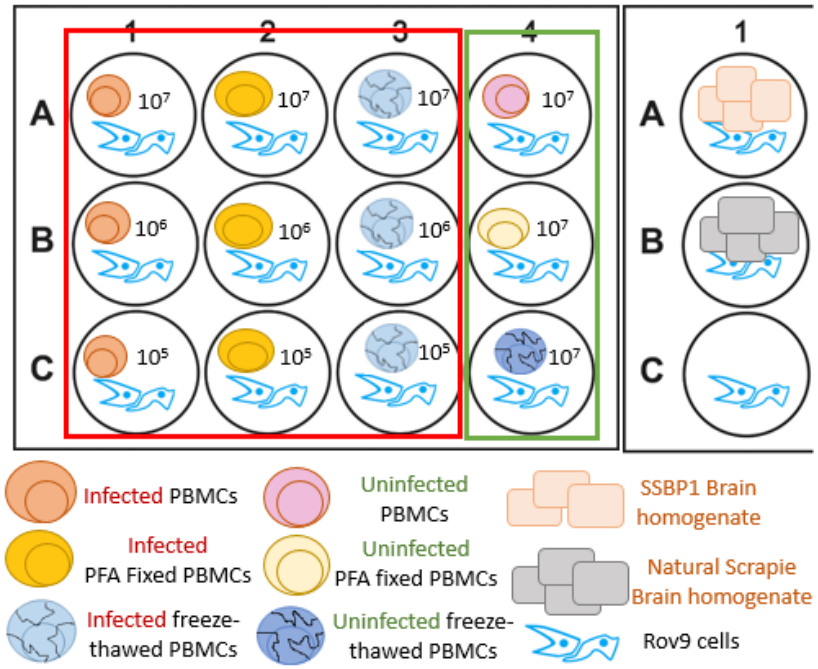

Figure 5.4: Plate outline for Experiment 2. PBMCs that were treated in three different ways (fresh, freeze thawed and PFA fixed) were used to inoculate the Rov9 cell line to assess how infectivity is passed between cells. Rov9 cells were initially grown up in 12 well plates. PBMC pellets of three sizes were used (10^7, 10^6 and 10^5 cells). The positive control was Rov9 cells inoculated with 1% SSBP1 brain homogenate, Rov9 cells were also inoculated with 1% natural scrapie brain homogenate and the negative control were Rov9 cells with no PBMCs (or any additional cells) added.

5.2.3 Experiment 3

This was essentially a repeat of Experiment 2, except that Rov9 cells were inoculated only with 1 x 10^7 fresh, PFA fixed, or lysed PBMC isolated from scrapie-resistant (ARR/ARR) or susceptible (VRQ/VRQ) sheep. For this experiment, the VRQ/VRQ sheep used was not showing clinical signs of scrapie (as for the previous 2 experiments) but was predicted to be in the late preclinical phase of infection. The plate plan for how the Rov9 cells were inoculated is shown in Figure 5.5. Following transfer of cells lines into T25 flasks and a week of growth (as previously described), cell lines were passaged into T75 flasks. 400 µL of 1x trypsin was added to T25 flasks and flasks were incubated for 5 mins at 37 ^oC. Cells were then disrupted with a stripette, 3.6 mL of fresh Opti-Mem media added and this cell suspension added to T75 flasks containing 15 mL of fresh Opt-Mem media with Doxycycline (1 µg/mL). Cells were passaged after a week, 1.5 mL of 1x trypsin was added to each T75 flask and flasks incubated at 37 ^oC for 5 mins. Cells were then disrupted with a stripette and 7.5 mL of fresh Opti-Mem media added. 1 mL of this cell suspension was frozen and stored at -80 ^oC, 4 mL was treated with TL1 buffer to collect samples for western blotting and the remaining 4 mL of cell suspension was carried forward for passaging (placed into fresh flasks containing 15 mL Opti-Mem with Doxycycline (1 µg/mL). This was repeated weekly until passage 7 (Materials and Methods 2.2.1). Cell lysates were immunoblotted after PK-digestion for the presence of PK-resistant form (Materials and Methods 2.2.4).

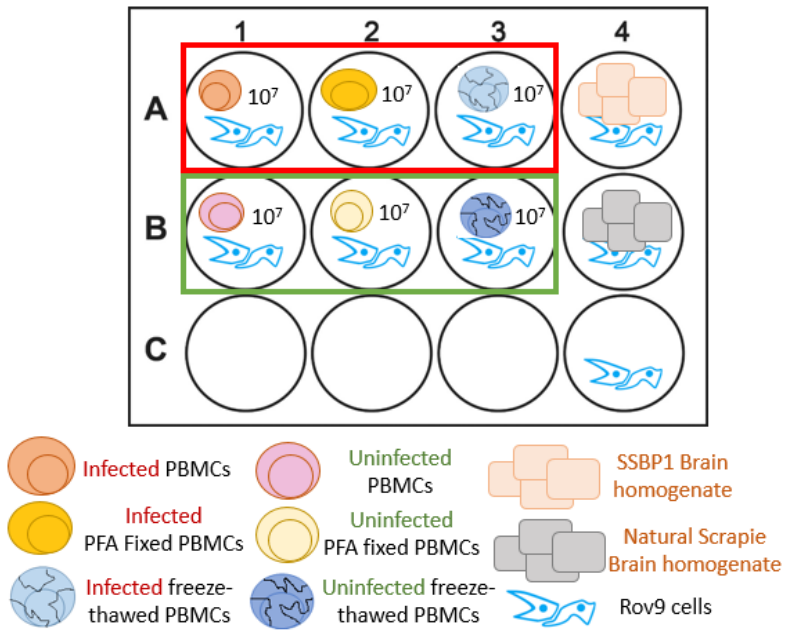

Figure 5.5: Plate outline for Experiment 3. Pellets of 1x10^7 PBMCs (fresh, freeze thawed and PFA fixed) were used to inoculate the Rov9 cells. SSBP1 brain homogenate was used as a positive control.

5.3 Results

5.3.1 Optimisation steps

5.3.1.1 Rov9 cell line

Before inoculation of Rov9 cells with PBMC, initial experiments were performed to test the procedure for passaging, PK digestion and western blotting. Two methods of Rov9 cell collection were compared using uninfected Rov9 cell frozen stock. Cells were thawed, grown to confluency and after the addition of doxycycline to induce PrP expression, two different methods of cell collection were implemented and samples processed for comparison by western blotting. One method of harvesting cells was by using RIPA buffer and a scraper. The second method was with incubation with TL1 buffer (Figure 5.6). Little difference was seen between the two cell collection methods but the TL1 buffer method was continued with. From this work it was found that cell lysate collected from a 25 cm^2 flask in 1.5 mL TL1 buffer is equivalent to 1 mg/mL protein content. It was decided that loading 12 µg in 2X sample buffer gave precise and clear bands so was used for all future work (taking into account the maximum loading of 24 µL in 20 well gels). The concentration of PK required for PrP^C digestion was also tested (Figure 5.7), 4 µg/mL was found to be optimal at all exposure times.

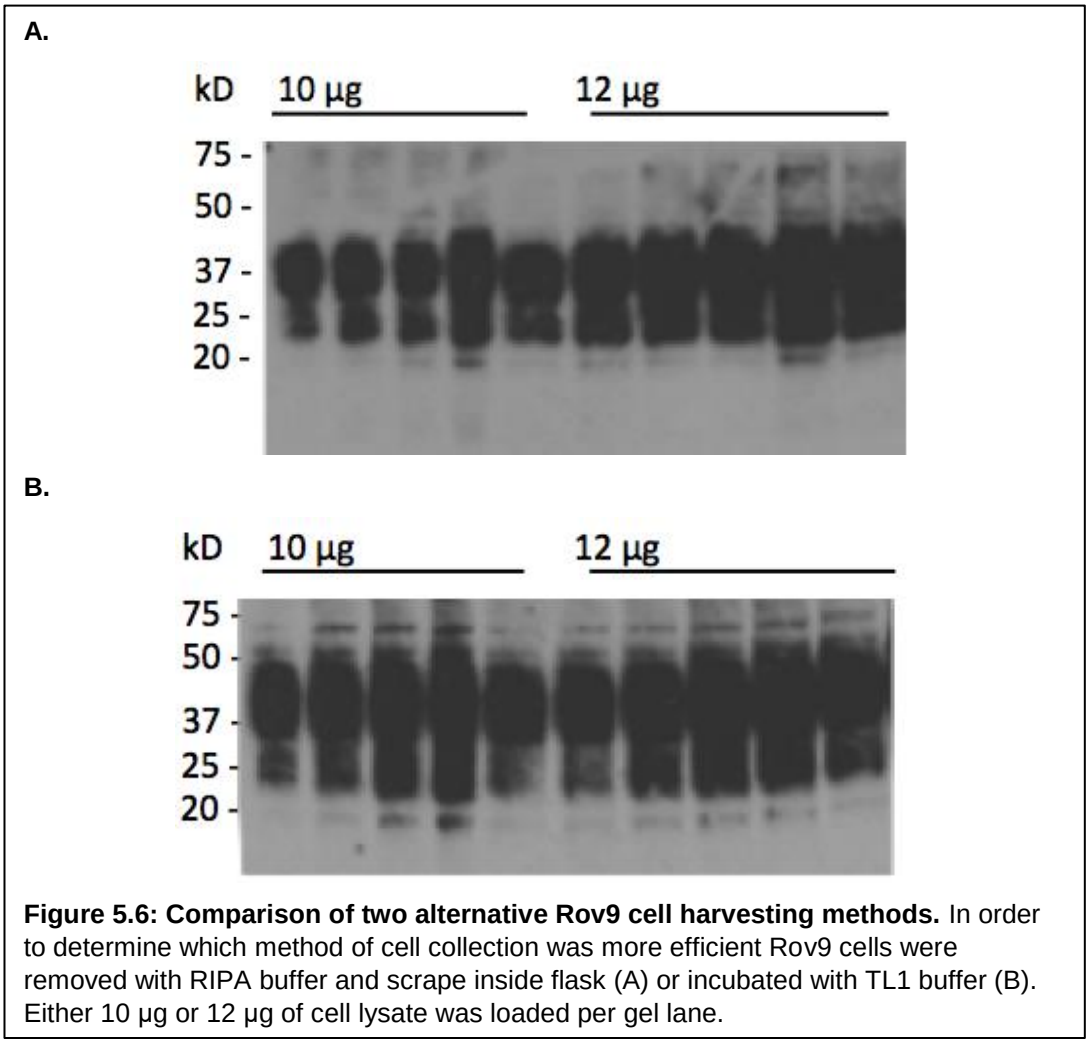

Figure 5.6: Comparison of two alternative Rov9 cell harvesting methods. In order to determine which method of cell collection was more efficient Rov9 cells were removed with RIPA buffer and scrape inside flask (A) or incubated with TL1 buffer (B). Either 10 µg or 12 µg of cell lysate was loaded per gel lane.

The effect of increasing PK concentrations on PrP^{Sc} was tested using infected cell lysate (Figure 5.8). It was found that 4 µg/mL of PK did not digest PrP^{Sc}.

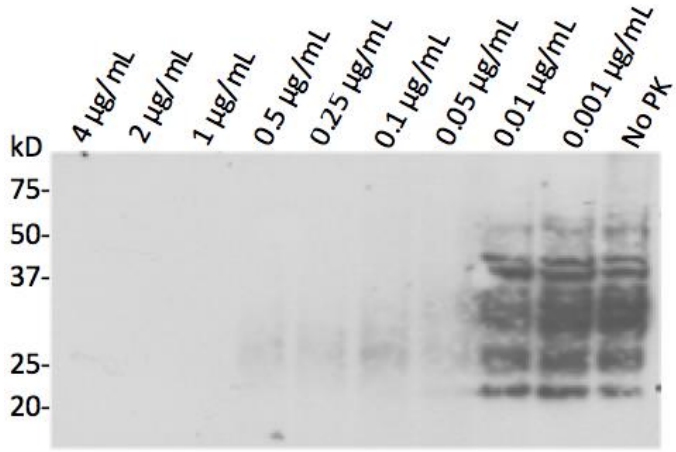

Figure 5.7: Testing a range of PK concentrations for PrP^{C} digestion. In order to determine the correct PK concentration to use on uninfected Rov9 cell lysate a range of PK concentrations were tested.

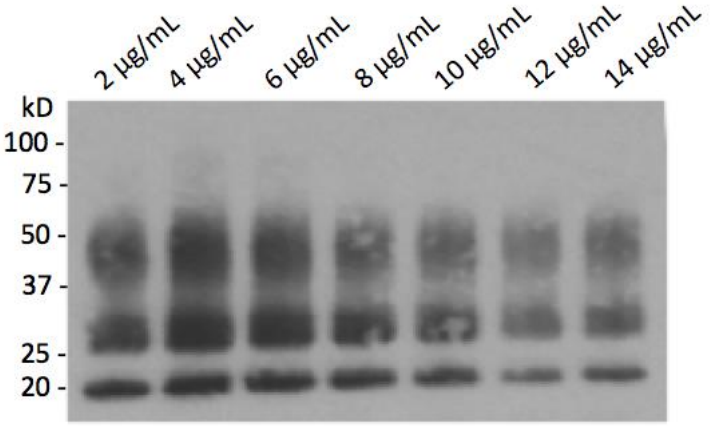

Figure 5.8: Testing the effect of increasing PK concentrations on PrP^{Sc}. To investigate the effect of PK digestion on PrP^{Sc}, increasing concentrations of PK were used to treat infected cell lysate and resolved by western blot.

5.3.1.2 Positive control

RecPrP, scrapie-infected brain homogenate and Rov9 cells infected with brain homogenate were all tested for use as positive controls. The process of protein purification to obtain recPrP from bacterial glycerol stocks and NanoDrop to determine protein concentration, as well as the procedure used to prepare brain homogenate is detailed in the Methods chapter (Methods 2.2.6 and 2.2.5 respectively). The loading concentrations of each material, along

with western blot procedure (time and type of washing, blocking and transfer buffer) and PK digestion were refined alongside the type and concentration of antibody and xograph film exposure time (Figures 5.9, 5.10 and 5.11 show some example western blots). The final conditions decided upon are detailed in the Methods chapter (section 2.2.4).

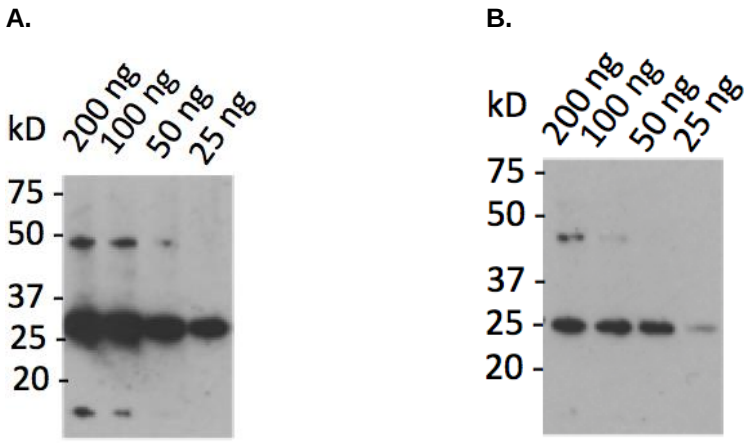

Figure 5.9: Western blots for the comparison of different antibodies for recPrP. Duplicate gels resolved with recPrP dilutions (concentration determined by NanoDrop) were processed simultaneously, however one was probed with BC6 antibody (A) and one with FH11 antibody (B).

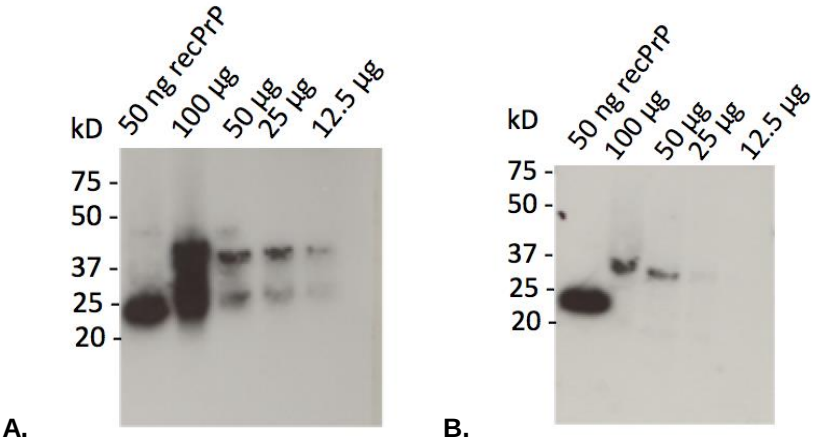

Figure 5.10: Western blots for trialling different antibodies on uninfected brain homogenate. Following preparation of brain homogenate and microBCA for protein concentration, BC6 (A) and FH11 (B) were tested on dilutions of brain homogenate (with 50 ng of recPrP resolved for comparison).

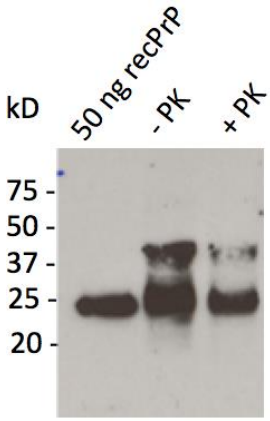

Figure 5.11: PK digestion of Rov9 cells infected with brain homogenate. Initial experiments were performed where Rov9 cells were inoculated with SSBP1 brain homogenate for 4 days, passaged weekly and processed for western blotting.

5.3.2 Experiment 1

The initial aim of this work was to repeat Halliez et al. (2014) work of infecting the Rov9 cell line with scrapie infected WBCs. Rather than use sheep infected with the PG127 isolate, here the WBCs were from a flock with natural scrapie. In the Experiment 1, Rov9 cells were inoculated with freeze thawed PBMCs isolated on the same day from blood of a VRQ/VRQ sheep with clinical signs of scrapie then incubated for either 4 or 7 days before washing and passaging at weekly intervals. This was to test whether increasing the contact time of Rov9 cells with the inoculum would improve efficiency of infection and conversion of PrP^{C} to PK resistant PrP^{Sc}. The results for Rov9 cells infected with freeze thawed PBMCs in the preliminary experiment were positive after passage 4. Figure 5.12 shows the western blot of PK treated cell lysates. The banding pattern is similar to that of the positive control (PK treated SSBP1 brain homogenate). This confirms that lysed, disrupted PBMC from a scrapie-infected sheep are capable of initiating infection not only in those cells infected with usual method of infection of 4 days (Salamat et al. 2011) but also in a longer incubation with inoculum (7 days). No bands were observed for the negative control (cell lysate collected from Rov9 cells with no inoculum) up to passage 5.

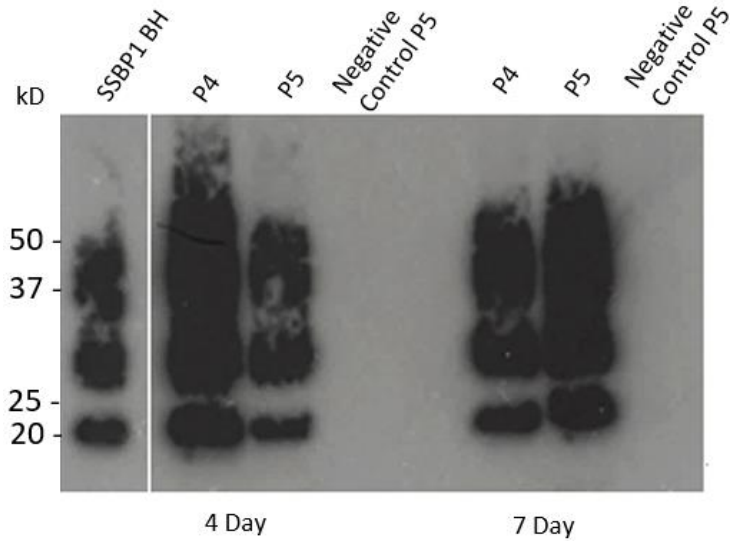

Figure 5.12: Preliminary experiment results. Rov9 cell line was infected with lysed, freeze thawed PBMC ($1x10^{7}$). Positive signal was achieved after passage 4. The image shows band pattern for PrP^{Sc} in PK treated cell lysates collected at passage 4 (P4) and passage 5 (P5) as well as the positive control (cells infected with SSBP1 brain homogenate). No signal is seen for uninfected cell lysate, where no PrP^{C} or PrP^{Sc} is present following PK digestion. The western blot shows comparison of cells passaged after 4 days and after 7 days of incubation with inoculum.

5.3.3 Experiment 2

In order to replicate the findings of Experiment 1 and to determine whether live PBMCs were more efficient at infecting the cell line than lysed or PFA fixed PBMCs, a larger-scale experiment was performed. Here, PBMCs prepared by three different methods (fresh/live, PFA fixed, and lysed) were used to inoculate Rov9 cells at three different concentrations: 1 x 10^7, 1 x 10^6 and 1 x 10^5 PBMC/well. For the negative control, cells inoculated with PBMC from an ARR/ARR scrapie resistant sheep were used. As an additional negative control, no PBMCs were added to the Rov9 cells (referred to as 'uninfected Rov9'). For the positive controls Rov9 cells were inoculated with 1 % SSBP1 brain homogenate or 1 % natural scrapie brain homogenate and passaged weekly alongside other cell lines.

Each cell line was passaged 9 times, and cell lysates from each passage were analysed for the presence of proteinase K (PK) resistant PrP^{Sc} by western blotting. Figure 5.13 shows the results of PK treated samples at passage 5. The only bands present are those for recPrP and 1% SSBP1 brain homogenate (Control 1) and Rov9 cells inoculated with 1% SSBP1 brain homogenate cells. Figure 5.14 shows results obtained at passages 6 and passage 9. From passage 6 to passage 9 a positive signal was achieved for Rov9 cells infected with 1% SSBP1 brain homogenate and Rov9 cells inoculated with 1% natural scrapie brain homogenate. None of the Rov9 cell cultures inoculated with PBMC preparations from either scrapie susceptible (VRQ/VRQ) or scrapie resistant (ARR/ARR) sheep showed a positive signal for PrP^{Sc} in any passage up to passage 9.

The results of Experiment 2 were unexpected since it was partly a repeat of Experiment 1. Both Experiment 1 and Experiment 2 used 10^7 lysed PBMC as inoculum (which did infect the Rov9 cells in Experiment 1). However, the major differences between the two experiments were the sheep (it is possible that their blood titre was significantly different) and also the size of flasks and method of passaging the cells. Experiment 2 was repeated but stopped before reaching passage 9 due to contamination and death of cell lines. PK digestion of cells at passage 4 of the Experiment 2 repeat showed no positive results (none of the PBMC inoculated cell lines became infected).

Passage 5

Figure 5.13: PK treated samples at passage 5. RecPrP is not PK treated. Control 1 is 1% SSBP1 brain homogenate on its own which has been PK treated. The western blot shows the first appearance of a positive signal in the Rov9 treated cell lines is at passage 5. The bands are for Rov9 cells inoculated with 1% SSBP1 brain homogenate. No bands appear for Rov9 cells inoculated with differentially treat PBMC (fresh, freeze-thawed or PFA fixed). IN=infected (VRQ/VRQ), UN=uninfected (ARR/ARR).

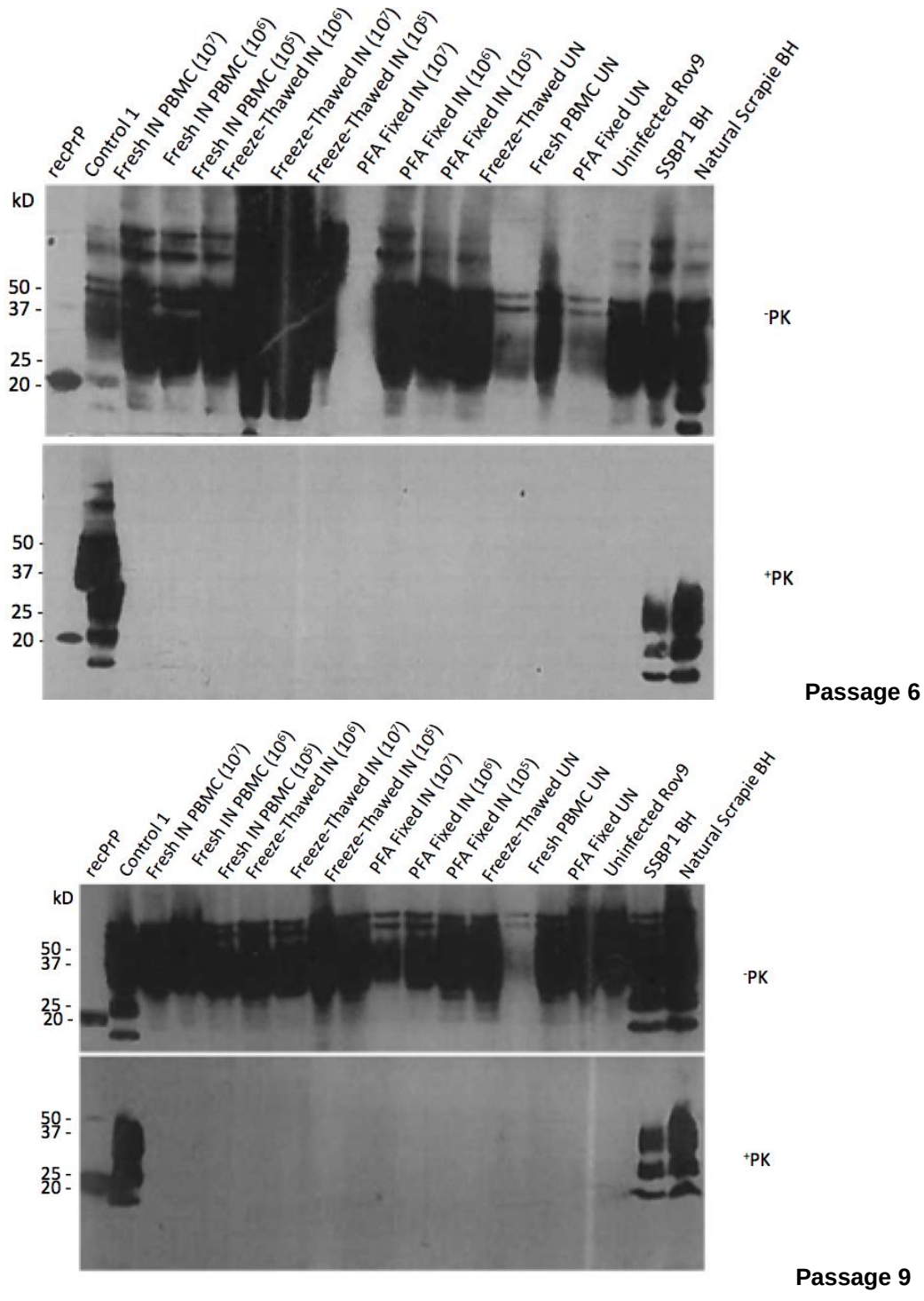

Figure 5.14: Non-PK and PK treated samples at passage 6 and passage 9, 5 min exposure. RecPrP is not PK treated. Control 1 is 1% SSBP1 brain homogenate on its own which has been PK treated. Passages 6 to 9 show positive signals for Rov9 cells inoculated with 1% SSBP1 brain homogenate and Rov9 cells inoculated with 1% Natural Scrapie brain homogenate. No bands show for PK treated Rov9 cells inoculated with differentially treat PBMC (fresh, freeze-thawed or PFA fixed). IN=infected (VRQ/VRQ), UN=uninfected (ARR/ARR).

5.3.4 Experiment 3

In Experiment 3, three types of PBMCs were used to evaluate the efficiency of live WBCs in initiating infection: fresh, freeze-thawed and PFA-fixed. 1x 10^7 uninfected cells and 1x 10^7 infected cells (for each of the three PBMC types) were used to inoculate Rov9 cells. Only after passage 5 was a positive signal following PK digestion seen for Rov9 cells inoculated with 1% SSBP1 brain homogenate. At passage 6, PrP^{Sc} was detected in cell cultures inoculated with fresh, fixed and lysed PBMC from an infected sheep indicating that they had became infected, but also (unexpectedly) the lines inoculated with fixed and lysed PBMC from the uninfected scrapie resistant, negative control sheep also became infected (Figure 5.15). For all samples equal volumes were loaded, the lack of bands for samples not PK treated may be due to poor technique in sample preparation, uneven cell collection or improper solubilisation of cell pellets. However, due to the results being similar in both passages it may be attributed to a much lower number of cells present in these samples, or that these particular samples stopped expressing PrP^{C}.

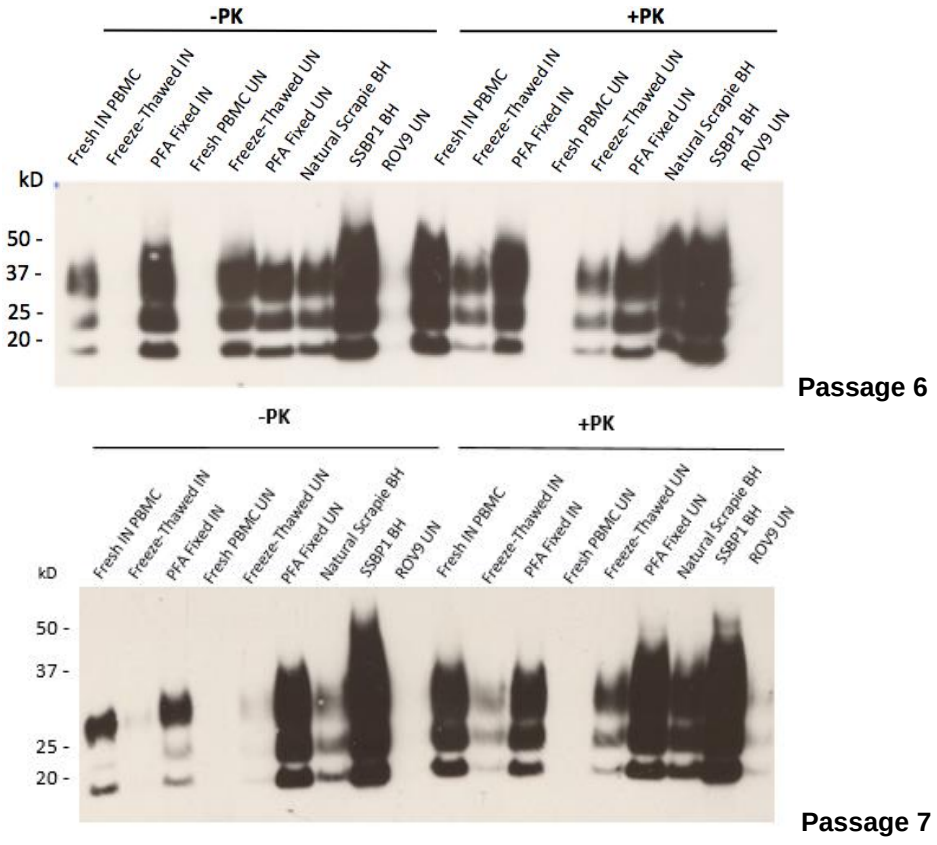

Figure 5.15: Non-PK and PK treated samples for passage 6 and 7, 5 minute exposure. Rov9 cells inoculated with differentially treated PBMCs (fresh, freeze-thawed or PFA fixed). Infected (IN) PBMC are from a scrapie-positive VRQ/VRQ sheep and uninfected (UN) from a scrapie-resistant ARR/ARR sheep. Both non-PK and PK treated samples are resolved on the same gel. For positive controls Rov9 cells inoculated with either natural scrapie brain homogenate (natural scrapie BH) or SSBP1 brain homogenate (SSBP1 BH) were passaged weekly alongside experimental cell lines. As a negative control Rov9 cells with no inoculum were used (ROV9 UN) (P7 western blot shows some spill over from neighbouring lane).

5.4 Discussion

Measuring prion infectivity is a necessary requirement for various procedures, such as determining the efficacy of a treatment or infectivity of a prion purification procedure. Cell line assays allow for quantitative *in vitro* analysis of prion strains, titres and biological properties. Here the Rov9 cell line is used to investigate the infectivity of PBMCs that have been differentially treated. I confirmed that lysed PBMC from a scrapie-infected sheep of the Roslin Cheviot Scrapie Flock were able to infect Rov9 cells. These results confirm that of Halliez et al. (2014) where disrupted PBMCs from sheep with PG127 classical scrapie were capable of passing infection to the Rov9 cell line.

In Experiment 2, PBMC pellets of different sizes were differentially treated and added to plates of Rov9 cells. Collection and analysis of PK treated samples up to passage 9 achieved no positive results. This is unexpected following the successful infection of the Rov9 cell line in the preliminary experiment. A key difference between Experiment 1 and Experiment 2 was the sheep that was used. It is possible that they had different titres of scrapie infectivity in their blood. Additionally, the method of passaging was different (T25 flasks used in Experiment 1 compared to T75 flasks in Experiment 2). The advantage of using T75 flasks for continuing the passage of cells is that it prevents changes to the cell line being missed by using flasks that are passaged but not analysed by western blot.

For Experiment 3, it was decided to run a simpler version of the second experiment. Only one size of PBMC pellet was utilized and focus was given to inoculum preparation. To avoid clumping (and any suppression of infectivity) each inoculum was added to the plate as soon as it was prepared. Rov9 cells inoculated with scrapie infected fresh, lysed and fixed PBMC became infected. The Rov9 cells inoculated with uninfected lysed or fixed (but not fresh) PBMC from the scrapie resistant sheep became infected. No evidence of infection in the cell lines inoculated with PBMC is seen until passage 6. SSBP1 brain homogenate inoculated Rov9 cells were positive at passage 5. This possibly indicates that the T25 passage method may result in more efficient infection of the cell line (as in Experiment 1 infection with the SSBP1 control can be detected at passage 4). This may be due to the two ways that infection can spread within a cell culture, either passed from an infected cell to an uninfected cell or when an infected cell replicates. Using a larger flask would allow for a greater portion of the cell suspension to be passaged rather than discarded, thus a greater number of the few infected cells may be retained and are able to pass on infection. Although, perhaps uninfected cells replicate at a faster rate than infected cells and compete for presence within the T75 flasks, leading to loss of infected cells over time (rather than seeing an increased portion).

This is an unexpected result as uninfected blood should not be able to pass infection. There may have been cross contamination, perhaps cells inoculated with the SSBP1 brain homogenate positive control got mixed with those of differentially treated PBMCs before or after passaging. To determine if this is the case, the experiment would need to be repeated to see if the same results would be achieved, rule out cross contamination and see and if this was a genuine finding. Although ARR/ARR sheep appear to be resistant to infection, as they do not develop scrapie following exposure to infection, if their WBCs are shown to transmit infection it may indicate that they can actually be carriers of infection. Previous studies have indicated the possibility of ARR/ARR sheep carrying infection. Classical scrapie of ARR/ARR sheep has been reported in three sheep of Germany and France (Groschup et al. 2007) as well as one in Japan (Ikeda et al. 1995). PrP^{Sc} was present in buccal swabs from ARR/ARR sheep, although at lower levels than sheep of other genotypes. Their presence indicate that orally available prions may be a common feature in these sheep but will never progress to clinical scrapie (Gough et al. 2012). However, due to the low number of positive results in ARR/ARR sheep, positive results could possibly be attributed to environmental contamination of the infected farm. Thus conclusions made from such results should be looked at with caution. Though, Jeffrey et al. (2014) have also shown incidence of infection in ARR/ARR sheep after experimental inoculation or natural exposure to classical scrapie and Nor98 scrapie cases have been reported in ARR/ARR sheep (Le Dur et al. 2005). Le Dur et al. (2005) demonstrated that 3 ARR/ARR sheep efficiently transmitted Nor98 scrapie to transgenic mice expressing ovine PrP. It is important to note however, that these incidents in ARR/ARR sheep are very rare and that the evidence for their occurrence is not as strong as that compared to ARR/ARR sheep being resistant (Goldmann 2008).

Understanding how prions move from cell to cell and progressively spread within infected tissue is critical for developing an intervention or delay in disease progression. Cell to cell transmission of infectious prions (and the conversion of PrP^{C} to PrP^{Sc}) may occur via a number of different pathways, such as cell-cell contacts (Kanu 2002); (Paquet, Daude, et al. 2007), cytoplasmic bridges or tunnelling nanotubes (Gousset et al. 2009) and also contact independent mechanisms via secretion of extracellular vesicles (Vilette et al. 2018; Fevrier and Raposo 2004). From work with Rov9 and MovS (another non-neuronal cell line derived from peripheral neuroglial cells, Schwann cell type) cell lines, it has been suggested that the cell to cell spread of prions, and progression of infection, results mainly through infection of neighbouring cells despite the presence of extracellular, cell-free infectivity. Analysing the spatial distribution of newly infected cells revealed cells proximal to the infected donor cells consistently accumulated more PrP^{Sc} (Paquet, Langevin, et al. 2007). An additional study that highlights the need for cell contact in order for a scrapie prion infected cell to convert a neighbouring infected cell is that by Kanu (2002). Here scrapie infected mouse SMB cells

were able to convert target cells by coculture. Even when SMB cells were killed by fixation in aldehyde they were found to retain conversion activity. This aligns with the ability of scrapie infectivity to be resistant in conditions of aldehyde fixation, which is capable of killing cells (Pattison 1965).

Although the underlying mechanisms involved in dissemination of infection among living cells is not clear, some active biological processes may be required to also occur during contact between closely apposed PrP^{C} and PrP^{Sc}. For instance, in trogocytosis there is transfer of plasma membrane fragments which may also allow PrP^{Sc} to be incorporated in the membrane of apposed acceptor cells. This process occurs at the immune synapse during the interaction between antigen presenting cells and T cells but it has also been suggested that circulating dendritic cells (DCs) exploit the same pathway to transmit PrP^{Sc} (Klohn, Castro-Seoane, and Collinge 2013). In some cell culture models, prions are secreted into the cell culture supernatant (Baron et al. 2006); (Maas et al. 2007). A few studies have demonstrated that prions are often associated with exosomes released by donor cells and these exosomes containing PrP^{Sc} have been shown to efficiently intiate prion propagation in recpient cells (Kanu 2002). How exosomes make contact and how incorporated prions then induce infection is not currently know. It is unclear if the observed differences in spreading mechanisms are due to different cell culture models or strain-specific dissemination strategies (Krauss and Vorberg 2013).

There are several activities of live cells that could initiate infection after close apposition, such as the release of PrP^{Sc} and its GPI-anchor with the subsequent insertion into the target cell membrane, a process referred to as ‘painting’ (Kooyman, Byrne, and Logan 1998). Studies of prion liposome complexes may provide an explanation for the activity of PrP^{Sc} in intact cells. There is evidence that when prion rods are solubilised and incorporated into lipid vesicles, there is an increase of infectivity of about 100-fold (Gabizon et al. 1988). The presentation of smaller, monomeric or oligomeric PrP^{Sc} embedded or anchored in a lipid membrane is more effective at converting cells than presentation of aggregates in suspension. Within the cell culture a template mechanism for conversion of PrP^{C} may be taking place. The PrP^{Sc} of an infected cells may be able to act on PrP^{C} of the target uninfected cell, either directly or through cleavage and transfer to the target cell. This in itself would catalyse the process, promoting further interaction between PrP^{Sc} and other PrP^{C} along the target membrane.

In conclusion, I was able to show that the Rov9 cell line could be infected using PBMC isolated from the Roslin natural scrapie flock. However, the results presented here are preliminary findings and more work is required to optimise the cell culture system. Repeat experiments looking at differently treated scrapie infected PBMCs would need to be

undertaken to confirm the results seen here. It may shed light on the requirement of 'live' (fresh not fixed) cells to pass infection and help to investigate the mechanisms of PrP^{Sc} propagation within cell culture. A possible way of exploring the mixed results seen in Experiment 3 would be to use PBMC from sheep susceptible but not exposed to scrapie, such as the New Zealand flock of sheep. Following this, it may be possible to compare the efficiency of blood and brain material to pass infection through inoculation of Rov9 cells.
In order to explore blood-borne infectivity it would be potentially interesting to further separate the PBMCs into distinct cell populations (T cells, B cells NK cells and monocytes) and see which of the individual cells are the carriers or transmitters of prion infection in cell culture. Additionally, as we know plasma and platelets can pass infection (Mathiason et al. 2010); (Andreoletti et al. 2012) it may be of interest to look at the susceptibility of Rov9 cells to different blood component fractions. As highlighted previously, BSE-infected sheep show signs of infection in their blood that may be used as an important model in the study of human blood product safety. The experiments may be repeated using blood from animals with various prion diseases (scrapie, BSE, CWD) to assess differences in their ability to transmit infection. Alternative model systems may also be implemented to investigate activity of blood derived PrP^{Sc} and if PBMCs are able to initiate infection more efficiently than brain homogenate. Examples of such models include be cath–a-differentiated or CAD cells (a neuronal cell line established from mice) or cultured brain slices.

Chapter 6: Discussion

6.1 Background

The UK population was exposed to a significant level of BSE infectivity when it entered the food chain in the 1980s and early 1990s. Until 2015 where there was an incident of vCJD in a heterozygous individual (MV), all cases had been MM at codon 129 (Mok et al. 2017). It raises the possibility of a further outbreak so although the vCJD epidemic is clearly in decline, it may be premature to be complacent about concerns for public health. Furthermore, the secondary transmission of vCJD through transfusion of non-leucodepleted blood has resulted in three clinical cases of vCJD (donations were from recipients who later went on to develop vCJD themselves) (Urwin et al. 2016). The incidence of vCJD in the general UK population has been studied via immunohistochemistry of appendectomy samples. This has lead to an estimation of the prevalence being 1 in 2000 of the relevant age group (Gill et al. 2013b). It is a matter of concern since the incubation period of vCJD may be over a decade, resulting in an asymptomatic state (which cannot yet be identified), representing the unintentional risk of horizontal transmission of vCJD infection by blood transfusion, blood products or contaminated surgical instruments (Ironside et al. 2006).

The development of a blood test to ensure the safety of blood transfusions is top priority for public health and the prevention of further infections. As yet there is no operational test and this is due to the numerous difficulties that need to be overcome. While blood from vCJD patients has been proven to be infectious, the concentration of infectious material is much lower than that of central nervous system tissue. Several studies have determined that the bulk of infectivity is associated with white blood cells, however plasma is also clearly infectious (Halliez et al. 2014; Andreoletti et al. 2012). Very little is known about the biochemical properties of the PrP^{Sc} in the different blood fractions, for instance the size of the formed aggregates and whether they are resistant to proteinase K digestion (a treatment on which most current rapid tests are based) (Sajnani and Requena 2012).

In terms of diagnostics, there are a few methods available. Currently there is a reliance on tests typically performed post-mortem with the use of immunohistochemistry or enzyme-linked immunosorbent assay (ELISA) to detect abnormal prion protein from diseased brains or lymphoid tissues. However, an ante-mortem method of diagnosis that could be performed using body fluid is highly desirable. PrP^{Sc} was detectable by PMCA in plasma from patients with clinical vCJD and additionally, in preclinical blood samples from two vCJD patients who donated blood prior to onset of their symptoms (Moda et al. 2014; Concha-Marambio et al. 2016b; Bougard, Brandel, Belondrade, et al. 2016). However, the large-scale screening of

blood is not feasible by PMCA and routine use is limited by the procedure being technically challenging and involving long incubation periods.

An alternative to identifying PrP^{Sc} is to look for other disease associated markers. It is imperative to find non-PrP changes relating to preclinical prion infection that can be detected and easily exploited for diagnostic use or for monitoring responses to treatment. Elevated levels of 14-3-3, S100b and tau in cerebrospinal fluid (CSF) are the current clinical biomarkers in use for patients with CJD (Green et al. 2001). Protein biomarkers may be established by proteomic profiling and mass spectrometry is a popular tool for biomarker discovery due to its properties of high sensitivity, speed, chemical specificity and capability for processing complex mixtures. However, there are a number of issues to consider when analysing proteomic mass spectrometric data for classification such as analyte suppression from highly abundant species that may obscure detection of low abundant analytes of interest in a highly complex mixture (Herbst et al. 2009). Mass spectrometry has previously been used to determine non-prion biomarkers for the diagnosis of prion disease, for example apolipoprotein E (ApoE) was identified as upregulated in plasma samples from C57/B16 mice intraperitoneally inoculated with brain homogenate from mice clinically affected with RML prion strain (compared to those inoculated with brain homogenate from control unaffected mice) (Wei et al. 2011a). ApoE functions as a component of lipoproteins, transporting lipids through the bloodstream among various cells and tissues of the body (Herz and Bock 2002); (Huang and Mahley 2014).

In order to tackle these issues regarding diagnostics, archived samples from the transfusion study on BSE infected sheep have been used. Investigating the differential expression of proteins occurring at a preclinical stage compared to an infectious time point may shed light on changes occurring in biological systems and highlight alternative markers of infection with potential diagnostic use.

6.2 Proteomic markers that distinguish prion infected and uninfected blood

Following mass spectrometry analysis of plasma and buffy coat samples at preclinical and infectious time points, three potential protein biomarkers were validated in plasma and one potential biomarker validated in buffy coat by western blotting and LI-COR imaging. The four proteins that have been successfully validated here demonstrate that this approach to biomarker identification works and that the infection specific changes in protein concentration identified through mass spectrometry can be verified through western blotting. However, further proteins of interest have been highlighted in the mass spectrometry datasets and had working antibodies been available they may also have been verified. Bioinformatic analysis

of the buffy coat dataset suggested involvement of multiple preclinical, biological pathways as supported by published literature on prion and neurodegenerative diseases.

The three biomarkers validated in plasma were fibulin 1, vitamin D binding protein and hemopexin. Moesin was validated in buffy coat samples. Fibulin 1 is an extracellular matrix protein involved in matrix organization. Fibulin 1 associated with fibronectin modulates cell interactions, orientation, adhesion, spreading and motility (Twal et al. 2001). It is likely to contribute to prion infection susceptibility of cells through its role in the molecular organisation of the extracellular matrix (ECM). Cells with poorly developed ECM have more PrP^{C} deposition in their matrix that may be converted to PrP^{Sc} and thus facilitate further infection (Imberdis and Harris 2014). The key role of vitamin D binding protein is in the transport of vitamin D metabolites (Chun 2012), high concentrations of vitamin D binding protein in serum affects T cell differentiation and responses (Kongsbak et al. 2014). It has previously been established as a serum biomarker for Alzheimer's disease (AD), where levels were elevated in CSF (Bishnoi, Palmer, and Royall 2015). Hemopexin has previously been shown to be upregulated in CSF of patients with AD (Castano et al. 2006). It is the major vehicle for transportation of heme in plasma (preventing oxidative stress), is mainly expressed in the liver and is one of the acute phase reactants of which synthesis is induced after inflammation (Tolosano and Altruda 2002). The function of moesin is in maintaining epithelial integrity by regulating cell signalling events that affect actin organisation and polarity (Speck et al. 2003). Previous studies have also shown upregulation of moesin in prion disease states (Xiang et al. 2004; Chadwick et al. 2010; Jayasena et al. 2015). It is likely to be facilitating the movement of leukocytes and the dispersion of infection within the body during the early stages of disease.

One of the key functions highlighted through Ingenuity Pathway Analysis (IPA) of the buffy coat data was the involvement of an immune response. A number of studies have also identified a significant number of genes associated with the immune response, including genes involved in the complement activation and inflammatory response pathways. Xiang et al. (2004) showed increased expression of genes in these pathways when analysing scrapie infected mouse brains. It has been suggested that the enhancement of complement proteins and inflammatory factors and the subsequent glial activation in the diseased brain are important pathogenic events in prion disease (Giese and Kretzschmar 2001). A number of complement proteins (C1QB, C5, C3, C1S) were also shown to have expression changes in the plasma dataset. C3 has previously been identified in the serum and plasma of AD and Parkinson's (Zhang et al. 2004; Goldknopf et al. 2006). Riemer et al. (2004) also show a role for immune and inflammatory response in the scrapie infected brain. Among the genes differentially expressed in their study were components of the complement system (C1qa,

C1qb, C3, C4) and markers for microglial activation and differentiation. This is confirmation of the results from mass spectrometry relating to other prion diseases and provides further evidence for the involvement of inflammatory processes, such as complement activation, in neurodegenerative disorders. However, Riemer et al. (2004) suggest the proinflammatory response is a result of peptide fragments that contribute to neuronal damage shown to be implicated in the pathogenesis of stroke and AD (Huang et al. 1999; McGeer and McGeer 2002). It is unlikely that this is occurring at the 12 months post inoculation, when blood was taken for the infected samples of BSE infected sheep in this study, as this is early during disease progression.

Another critical pathway identified by IPA was leukocyte extravasation signalling. A key feature of the inflammatory processes (and also normal immune surveillance) is the migration of leukocytes from circulation, across the endothelium and basement membrane into affected tissue. The mechanism of extravasation is induced by proinflammatory chemokines. For this to take place, leukocytes must first adhere to the luminal surface of the endothelium via integrins and their ligands, including immunoglobulin like intracellular adhesion molecules (Middleton et al. 2002). Leukocyte transendothelial migration, complement and coagulation cascades as well as chemokine signalling pathways were identified by analysis of differentially expressed genes from different mouse strain-prion combination models as biologically important pathways by Newaz, Sriram, and Bera (2015). They concluded that the transcriptomic data showed neuronal dysfunction in prion disease is strongly related to the immunological pathways. IPA of proteins associated with the amyloid and nonamyloid disease phenotypes depicted an association with pathways related to transport, cell morphology, maintenance and assembly (Moore et al. 2014). Localisation and metabolic processes were found to be important in bioinformatics analysis of plasma from mice intraperitoneally inoculated with brain homogenate from mice clinically affected with the RML prion strain (Wei et al. 2011b). Furthermore, leukocyte extravasation has previously been reported by Hwang et al. (2009). Prion infected mouse brain genes involved in this process include selectin ligands, adhesion molecules, chemokines and their receptors, transendothelial migration genes and intracellular signalling molecules. Activation of endothelial cells from microglia and astrocytes would enhance migration of leukocytes from blood and their differentiation into microglia. Genes related to cell adhesion and cell movement were also identified by Almeida et al. (2011) from the gene expression study of BSE infected medulla tissue. Hence, this is not a unique finding but instead shows that it may be a common feature amongst prion diseases.

A number of proteins in the plasma and buffy coat datasets were acute phase proteins and/or implemented in the acute phase response signalling pathway. The acute phase response leads to alterations in blood plasma composition which is thought to prevent

microbial growth and help to restore homeostasis. Some acute phase proteins opsonize microorganisms and activate complement and others scavenge cellular remnants or neutralize proteolytic enzymes (Gruys et al. 2005a). Riemer et al. (2004) also identified acute phase proteins that were strongly induced in their dataset. Most strongly induced was serine proteinase inhibitor 2 (SPI-2). Barbisin et al. (2014) showed that acute phase signalling was an important function conveyed by the genes with differential expression from transcriptionally profiling brains of BSE infected macaques. They showed an upregulation in TTR which has been shown to have a neuroprotective role in AD brains (Buxbaum et al. 2008), suggesting it may be marker of neurodegenerative disease.

Analysis of the buffy coat dataset showed downregulation of the LXR/RXR activation pathway. It has been shown that LXR dependent gene expression is important for macrophage survival and the innate immune response (Joseph et al. 2003). The inhibition of inflammatory gene expression has been reported to occur when LXR ligands inhibit LPS- or cytokine- induced expression of inflammatory genes such as iNOS and IL-6 by interfering with NF-kB signalling (Joseph et al. 2004). A downregulation of this inhibition may lead to reduced inflammation. LXRs also play an important role in cholesterol uptake. The top canonical pathway from differentially expressed genes of BSE infected macaques in a study performed by Barbisin et al. (2014) was also LXR/RXR activation. They concluded that lipid transport is deregulated in prion infected macaques. Brown et al. (2005) show an activation of cholesterol biosynthesis pathways or upregulation of their genes. This suggests that alterations in cholesterol metabolism may be a common consequence of amyloidgenic process in AD and prion diseases.

Some of the proteins identified in the buffy coat proteins have a link to metabolism and energy conversion pathways, such as PSMB10, ATP5H and IDH2. This link between metabolism and prion diseases has previously been suggested. From their list of differentially expressed proteins in the blood of BSE infected cattle, Xerxa et al. (2016) propose that there is a switch from glucose catabolism to fatty acid utilization, with increased production of ketone bodies during prion disease. It has been shown that these molecules are able to cross the blood brain barrier, thus Xerxa et al. (2016) suggest that during prion disease the concentration of ketone bodies would rise and act in the brain as neuroprotective molecules to prevent the neurodegeneration induced by prions. In accordance to the finding in this study of a number of proteins to do with energy pathways in the datasets from BSE infected sheep, Skretting et al. (2004) revealed genes involved in ATP production in their study of cDNA from the Peyer's patches of lambs with scrapie. Chen et al. (2014) showed that the most affected pathways of genes differentially expressed in the CSF of patients with sCJD were to do with glycolysis and gluconeogenesis.

IPA also highlighted mitochondrial dysfunction to be a major pathway associated with the proteins in the buffy coat dataset. Mitochondria are double membrane bound organelles involved in ATP generation, programmed cell death and signal transduction (Friedman and Nunnari 2014; Shadel and Horvath 2015). Mitochondrial dysfunction has previously been shown to be a trigger of innate immune responses and inflammation. Due to the pleiotropic roles for mitochondria in cellular physiology, their dysfunction can drastically alter cell and tissue homeostasis and has thus been implemented in a number of diseases including neurodegeneration, cancer and inflammatory disorders (Dromparis and Michelakis 2013; Nunnari and Suomalainen 2012; Wallace 2005). Brown et al. (2005) analysed gene expression from mice with scrapie infected brains, the results showed activated ER and mitochondrial apoptosis pathways. Neuronal loss in prion disease has been documented to be, at least in part, associated with apoptosis (Hetz et al. 2003; Lucassen et al. 1995; Puig and Ferrer 2001; Williams et al. 1997). The caspase-dependent apoptotic cascade can be initiated by cell surface receptors, mitochondrial stress or by ER stress (Szegezdi et al. 2006; Senft and Ronai 2015). Perhaps dysfunction of mitochondrial activity is an early event in the disease process. A study performed by Skinner et al. (2006a) also showed major alterations in genes to with the mitochondria, they highlighted that energy production is critical for neuronal survival.

These are important findings in dissecting the molecular mechanisms that underline early prion disease pathogenesis and the eventual neurotoxicity. Visualization of gene or protein expression changes in critical biological modules indicate what is occurring in cellular and subcellular compartments over the course of disease. They offer a dynamic scheme for the processes that characterise an early disease response. Further validation of the roles of specific proteins and of identified disease pathways in the definable stages of disease progression may yield greater insights into the importance of these processes for transmission of infection. For instance, epigenomic analysis will inform gene regulation, while proteomic and metabolomics will confirm and reveal new downstream effector pathways and potential molecular targets for therapeutics and preventative interventions (Omenn 2009).

In regards to an ante-mortem prion disease test, it is likely that a panel of different proteins, rather than use of just one protein, would be the most efficient route. Combined signatures of multiple biomarkers can take into account patient heterogeneity and thus, provide a more accurate indication of patient health. Perhaps at least one protein from each pathway identified by IPA analysis and shown by other prion studies, would be beneficial. Blood from different disease stages during the transfusion study are available in the archive, they could be further compared by performing mass spectrometry and analysing the resulting datasets. Validation of results from these transfusion experiments performed with BSE infected sheep may be achieved by looking at blood from patients with vCJD. Additionally, the biomarkers

may be confirmed by looking at blood from other prion disease models which could be used to find distinctions between strains.

To strengthen the preclinical test and improve the pre-mortem assay, the panel of biomarker proteins may be paired with microRNAs (miRNAs). These are a small class of non-coding RNAs that regulate protein levels post-transcriptionally (Etheridge et al. 2011). They are ideal biomarkers for studying normal cellular processes, pathological conditions and response to therapeutic intervention (Rifai, Gillette, and Carr 2006). They have a presence in plasma thus can be accessed through non-invasive methods and are highly stable in circulation. Their tissue specific expression patterns have been shown to fluctuate in response to inflammation, acute and chronic tissue injury and even cancer. While the low abundance of some proteins significantly hinder their detection, most circulating miRNAs can be detected by PCR. Hence, miRNAs possess many desirable properties that can only strengthen diagnostics when combined with protein biomarkers (Moldovan et al. 2014) Most recently, Norsworthy et al. (2020) identified blood miRNA signatures that were able to discriminate patients with sCJD from AD patients.

There may be challenges of translating these experimental findings into a routine diagnostic test to be used in hospitals and transfusion service laboratories. The test would need to be robustly sensitive and specific when implemented on a large scale with a high throughput of samples (Rifai, Gillette, and Carr 2006). New biomarkers are only likely to be introduced into clinical biochemistry departments if there is strong evidence the results will improve patient management and outcome (Sturgeon et al. 2010). A test such as this would meet the criteria. A robust assay would identify silent carriers of infection and prevent transmission of disease by blood transfusion. In the case of blood based biomarkers for other neurodegenerative diseases, much progress is still required for the identification of asymptomatic individuals (Lashley et al. 2018). For comparison, in AD amyloid β can be measured in plasma but their correlation with cerebral β-amyloidosis is weak when assessed immunochemically (Olsson et al. 2016). However, clinically significant correlations between amyloid β and cerebral β-amyloidosis has been measured by mass spectrometry (Kaneko et al. 2014; Nakamura et al. 2018; Ovod et al. 2017).

6.3 Development of an in vitro assay for blood borne prion infectivity

It is striking that although prion infection by blood transfusion is efficient, the titres of infectivity in blood is much lower than that of the brain. This may be due to how cells transfer infection. Live white blood cells (WBCs) seem to be important for efficient transmission of disease via the transfusion route as illustrated by Andreoletti et al. (2012) with the use of preclinical blood from preclinical VRQ/VRQ sheep. Fixation of WBCs in 2%

paraformaldehyde (PFA) seemed to impair disease transmission, with fewer recipient VRQ/VRQ, prion disease free sheep succumbing to scrapie. Andreoletti et al. (2012) however also found that PFA fixation did not affect infectivity titre as measured by intracerebral inoculation in tg338 mice. From this, it can be hypothesised that transmission of prion disease is dependent on the viability of transfused cells. Treatment with PFA impairs cell to cell interactions by crosslinking cell surface proteins (Kim et al. 2017). Interaction of blood cells with the host is potentially vital for efficient transmission via the transfusion route. A viable cell culture system may help to explore these issues by comparing the efficiency of infection transmission of different cell types or treated cells.

This work has established that the Rov9 cell line (rabbit kidney cells modified to overexpress VRQ sheep PrP) can be infected with lysed PBMC from blood of the Roslin Natural Scrapie Flock sheep. If more time was available the cell culture system could be further used to investigate whether involvement of cellular membrane protein interactions is necessary for efficient infection. The experiments would need to be repeated to clearly establish the effects of differential treatment (fresh, lysed, PFA fixed) on PBMCs ability to pass infection. Potential future work with this cell line in exploring of blood borne prion infectivity is to look at different PBMC populations (B cells, T cells, NK cells, monocytes), different blood components (plasma, platelets) or even blood from animals with different prion diseases (BSE, CWD).

6.4 Summary

The outbreak of BSE and the following vCJD epidemic in the UK have prompted the need for a rapid, reliable and inexpensive screening method of blood. Current diagnostic tests for prion diseases have focused on detection of the causal agent, or neurological proteins that correlate with the neurological disease. The tests are inadequate because they are post-mortem, low throughput and/or not sensitive enough to detect infection early on, in the preclinical stage of the disease. There have been a wide range in approaches used to identify viable prion disease markers that permit testing of blood samples. By comparing uninfected and infected sheep blood samples from a previous transfusion study, mass spectrometry has been able to identify a panel of potential biomarkers. Early physiological changes associated with prion infection (before the accumulation of PrP^{Sc} in the blood and the brain) have been hypothesised. This is one of the few studies to focus on changes detectable in blood rather than the brain, and to also to use blood of known infectivity. Thus, it is crucial for further work to be conducted in order for the development of a rapid and sensitive ante-mortem, preclinical test (Parveen et al. 2005).

In experimental scrapie infection of an animal, the initial inoculum of PrP^{Sc} is rapidly cleared. The subsequent propagation of the infection depends on the ability of infected cells to

convert uninfected target cells to produce PrP^{Sc} (Kanu 2002). However, the mechanism of this cell based infection is not understood. Investigating the dissemination of infection amongst cells may shed light on disease processes and help in the development of interventions or treatments to stop disease progression. This may be done through experiments using infectious blood components and cell assays, such as PBMC from the Roslin Scrapie Flock and Rov9 cells as used here.

References

Afagh, A., B. J. Cummings, D. H. Cribbs, C. W. Cotman, and A. J. Tenner. 1996. 'Localization and cell association of C1q in Alzheimer's disease brain', *Exp Neurol*, 138: 22-32.

Aguzzi, A., F. L. Heppner, M. Heikenwalder, M. Prinz, K. Mertz, H. Seeger, and M. Glatzel. 2003. 'Immune system and peripheral nerves in propagation of prions to CNS', *Br Med Bull*, 66: 141-59.

Aguzzi, A., M. Nuvolone, and C. Zhu. 2013. 'The immunobiology of prion diseases', *Nat Rev Immunol*, 13: 888-902.

Aguzzi, Adriano, and Markus Glatzel. 2006. 'Prion infections, blood and transfusions', *Nature Clinical Practice Neurology*, 2: 321.

Ahn, Hyung Jin, Daria Zamolodchikov, Marta Cortes-Canteli, Erin H. Norris, J. Fraser Glickman, and Sidney Strickland. 2010. 'Alzheimer's disease peptide β-amyloid interacts with fibrinogen and induces its oligomerization', *Proceedings of the National Academy of Sciences*, 107: 21812-17.

Al-Ahmad, A. J., R. Patel, S. P. Palecek, and E. V. Shusta. 2019. 'Hyaluronan impairs the barrier integrity of brain microvascular endothelial cells through a CD44-dependent pathway', *J Cereb Blood Flow Metab*, 39: 1759-75.

Almeida, L. M., U. Basu, B. Khaniya, M. Taniguchi, J. L. Williams, S. S. Moore, and L. L. Guan. 2011. 'Gene expression in the medulla following oral infection of cattle with bovine spongiform encephalopathy', *J Toxicol Environ Health A*, 74: 110-26.

Andersen, H. H., K. B. Johnsen, and T. Moos. 2014. 'Iron deposits in the chronically inflamed central nervous system and contributes to neurodegeneration', *Cell Mol Life Sci*, 71: 1607-22.

Andreoletti, O., P. Berthon, D. Marc, P. Sarradin, J. Grosclaude, L. van Keulen, F. Schelcher, J. M. Elsen, and F. Lantier. 2000. 'Early accumulation of PrP(Sc) in gut-associated lymphoid and nervous tissues of susceptible sheep from a Romanov flock with natural scrapie', *J Gen Virol*, 81: 3115-26.

Andreoletti, O., C. Lacroux, A. Chabert, L. Monnereau, G. Tabouret, F. Lantier, P. Berthon, F. Eychenne, S. Lafond-Benestad, J. M. Elsen, and F. Schelcher. 2002. 'PrP(Sc) accumulation in placentas of ewes exposed to natural scrapie: influence of foetal PrP genotype and effect on ewe-to-lamb transmission', *J Gen Virol*, 83: 2607-16.

Andreoletti, O., C. Litaise, H. Simmons, F. Corbiere, S. Lugan, P. Costes, F. Schelcher, D. Vilette, J. Grassi, and C. Lacroux. 2012. 'Highly efficient prion transmission by blood transfusion', *PLoS Pathog*, 8: e1002782.

Andreoletti, O., L. Orge, S. L. Benestad, V. Beringue, C. Litaise, S. Simon, A. Le Dur, H. Laude, H. Simmons, S. Lugan, F. Corbiere, P. Costes, N. Morel, F. Schelcher, and C. Lacroux. 2011. 'Atypical/Nor98 scrapie infectivity in sheep peripheral tissues', *PLoS Pathog*, 7: e1001285.

Antony, T., W. Hoyer, D. Cherny, G. Heim, T. M. Jovin, and V. Subramaniam. 2003. 'Cellular polyamines promote the aggregation of alpha-synuclein', *J Biol Chem*, 278: 3235-40.

Appocher, Chiara, Fatemeh Mohagheghi, Sara Cappelli, Cristiana Stuani, Maurizio Romano, Fabian Feiguin, and Emanuele Buratti. 2017. 'Major hnRNP proteins act as general TDP-43 functional modifiers both in Drosophila and human neuronal cells', *Nucleic Acids Research*, 45: 8026-45.

Apweiler, R., C. Aslanidis, T. Deufel, A. Gerstner, J. Hansen, D. Hochstrasser, R. Kellner, M. Kubicek, F. Lottspeich, E. Maser, H. W. Mewes, H. E. Meyer, S. Müllner, W. Mutter, M. Neumaier, P. Nollau, H. G. Nothwang, F. Ponten, A. Radbruch, K. Reinert, G. Rothe, H. Stockinger, A. Tárnok, M. J. Taussig, A. Thiel, J. Thiery, M. Ueffing, G. Valet,

J. Vandekerckhove, C. Wagener, O. Wagner, and G. Schmitz. 2009. 'Approaching clinical proteomics: current state and future fields of application in cellular proteomics', *Cytometry A*, 75: 816-32.

Arellano-Anaya, Z. E., J. Savistchenko, J. Mathey, A. Huor, C. Lacroux, O. Andreoletti, and D. Vilette. 2011. 'A simple, versatile and sensitive cell-based assay for prions from various species', *PLoS One*, 6: e20563.

Ashton, N. J., S. J. Kiddle, J. Graf, M. Ward, A. L. Baird, A. Hye, S. Westwood, K. V. Wong, R. J. Dobson, G. D. Rabinovici, B. L. Miller, H. J. Rosen, A. Torres, Z. Zhang, L. Thurfjell, A. Covin, C. T. Hehir, D. Baker, C. Bazenet, and S. Lovestone. 2015. 'Blood protein predictors of brain amyloid for enrichment in clinical trials?', *Alzheimers Dement (Amst)*, 1: 48-60.

Asuni, Ayodeji A., Bryony Gray, Joanne Bailey, Paul Skipp, V. Hugh Perry, and Vincent O'Connor. 2014. 'Analysis of the Hippocampal Proteome in ME7 Prion Disease Reveals a Predominant Astrocytic Signature and Highlights the Brain-restricted Production of Clusterin in Chronic Neurodegeneration', *Journal of Biological Chemistry*, 289: 4532-45.

Atarashi, R., K. Satoh, K. Sano, T. Fuse, N. Yamaguchi, D. Ishibashi, T. Matsubara, T. Nakagaki, H. Yamanaka, S. Shirabe, M. Yamada, H. Mizusawa, T. Kitamoto, G. Klug, A. McGlade, S. J. Collins, and N. Nishida. 2011. 'Ultrasensitive human prion detection in cerebrospinal fluid by real-time quaking-induced conversion', *Nat Med*, 17: 175-8.

Bagyinszky, Eva, Vo Van Giau, Young Chul Youn, Seong Soo A. An, and SangYun Kim. 2018. 'Characterization of mutations in PRNP (prion) gene and their possible roles in neurodegenerative diseases', *Neuropsychiatric disease and treatment*, 14: 2067-85.

Baker, C., O. Belbin, N. Kalsheker, and K. Morgan. 2007. 'SERPINA3 (aka alpha-1-antichymotrypsin)', *Front Biosci*, 12: 2821-35.

Baker, Christopher A., Zhi Yun Lu, and Laura Manuelidis. 2004. 'Early induction of interferon-responsive mRNAs in Creutzfeldt-Jakob disease', *Journal of neurovirology*, 10: 29-40.

Balaban, R. S. 1990. 'Regulation of oxidative phosphorylation in the mammalian cell', *Am J Physiol*, 258: C377-89.

Banks, W. A. 1999. 'Physiology and pathology of the blood-brain barrier: implications for microbial pathogenesis, drug delivery and neurodegenerative disorders', *J Neurovirol*, 5: 538-55.

Bannach, O., E. Birkmann, E. Reinartz, K. E. Jaeger, J. P. Langeveld, R. G. Rohwer, L. Gregori, L. A. Terry, D. Willbold, and D. Riesner. 2012. 'Detection of prion protein particles in blood plasma of scrapie infected sheep', *PLoS One*, 7: e36620.

Barbisin, M., S. Vanni, A. C. Schmadicke, J. Montag, D. Motzkus, L. Opitz, G. Salinas-Riester, and G. Legname. 2014. 'Gene expression profiling of brains from bovine spongiform encephalopathy (BSE)-infected cynomolgus macaques', *BMC Genomics*, 15: 434.

Baron, G. S., A. C. Magalhaes, M. A. Prado, and B. Caughey. 2006. 'Mouse-adapted scrapie infection of SN56 cells: greater efficiency with microsome-associated versus purified PrP-res', *J Virol*, 80: 2106-17.

Barreiro, O., M. Yanez-Mo, J. M. Serrador, M. C. Montoya, M. Vicente-Manzanares, R. Tejedor, H. Furthmayr, and F. Sanchez-Madrid. 2002. 'Dynamic interaction of VCAM-1 and ICAM-1 with moesin and ezrin in a novel endothelial docking structure for adherent leukocytes', *J Cell Biol*, 157: 1233-45.

Barron, R. M., D. King, M. Jeffrey, G. McGovern, S. Agarwal, A. C. Gill, and P. Piccardo. 2016. 'PrP aggregation can be seeded by pre-formed recombinant PrP amyloid fibrils without the replication of infectious prions', *Acta Neuropathol*, 132: 611-24.

Bartz, Jason C., Crista DeJoia, Tammy Tucker, Anthony E. Kincaid, and Richard A. Bessen. 2005. 'Extraneural Prion Neuroinvasion without Lymphoreticular System Infection', *Journal of Virology*, 79: 11858-63.

Batxelli-Molina, I., N. Salvetat, O. Andreoletti, L. Guerrier, G. Vicat, F. Molina, and C. Mourton-Gilles. 2010. 'Ovine serum biomarkers of early and late phase scrapie', *BMC Vet Res*, 6: 49.

Beaven, S. W., and P. Tontonoz. 2006. "Nuclear receptors in lipid metabolism: Targeting the heart of dyslipidemia." In *Annual Review of Medicine*, 313-29.

Beekes, M., and P. A. McBride. 2007. 'The spread of prions through the body in naturally acquired transmissible spongiform encephalopathies', *Febs j*, 274: 588-605.

Beekes, M., M. Otto, J. Wiltfang, E. Bahn, S. Poser, and M. Baier. 1999. 'Late increase of serum S100 beta protein levels in hamsters after oral or intraperitoneal infection with scrapie', *J Infect Dis*, 180: 518-20.

Bell, R. D., and B. V. Zlokovic. 2009. 'Neurovascular mechanisms and blood-brain barrier disorder in Alzheimer's disease', *Acta Neuropathol*, 118: 103-13.

Bellworthy, S. J., S. A. C. Hawkins, R. B. Green, I. Blamire, G. Dexter, I. Dexter, R. Lockey, S. Ryder, C. Berthelin-Baker, M. M. Simmons, and M. Jeffrey. 2005. 'Tissue distribution of bovine spongiform encephalopathy infectivity in Romney sheep up to the onset of clinical disease after oral challenge', *Veterinary Record*, 156: 197-202.

Bera, A., and P. K. Nandi. 2007. 'Biological polyamines inhibit nucleic-acid-induced polymerisation of prion protein', *Arch Virol*, 152: 655-68.

Berson, A., S. Barbash, G. Shaltiel, Y. Goll, G. Hanin, D. S. Greenberg, M. Ketzef, A. J. Becker, A. Friedman, and H. Soreq. 2012. 'Cholinergic-associated loss of hnRNP-A/B in Alzheimer's disease impairs cortical splicing and cognitive function in mice', *EMBO Mol Med*, 4: 730-42.

Biacabe, A. G., J. L. Laplanche, S. Ryder, and T. Baron. 2004. 'Distinct molecular phenotypes in bovine prion diseases', *EMBO Rep*, 5: 110-5.

Bishnoi, R. J., R. F. Palmer, and D. R. Royall. 2015. 'Vitamin D binding protein as a serum biomarker of Alzheimer's disease', *J Alzheimers Dis*, 43: 37-45.

Bishop, M. T., D. L. Ritchie, R. G. Will, J. W. Ironside, M. W. Head, V. Thomson, M. Bruce, and J. C. Manson. 2008. 'No major change in vCJD agent strain after secondary transmission via blood transfusion', *PLoS One*, 3: e2878.

Blanchong, J. Scribner, K. Eppperson, B. Winterstein, S. 2010. 'Changes in Artificial Feeding Regulations Impact White-Tailed Deer Fine-Scale Spatial Genetic Structure', *The Journal of Wildlife Management. The Wildlife Society.* , 70: 17-22.

Boersema, P. J., R. Raijmakers, S. Lemeer, S. Mohammed, and A. J. R. Heck. 2009. 'Multiplex peptide stable isotope dimethyl labeling for quantitative proteomics', *Nature Protocols*, 4: 484-94.

Bogdanovic, N., L. Bretillon, E. G. Lund, U. Diczfalusy, L. Lannfelt, B. Winblad, D. W. Russell, and I. Bjorkhem. 2001. 'On the turnover of brain cholesterol in patients with Alzheimer's disease. Abnormal induction of the cholesterol-catabolic enzyme CYP46 in glial cells', *Neurosci Lett*, 314: 45-8.

Bongianni, M., C. Orru, B. R. Groveman, L. Sacchetto, M. Fiorini, G. Tonoli, G. Triva, S. Capaldi, S. Testi, S. Ferrari, A. Cagnin, A. Ladogana, A. Poleggi, E. Colaizzo, D. Tiple, L. Vaianella, S. Castriciano, D. Marchioni, A. G. Hughson, D. Imperiale, T. Cattaruzza, G. M. Fabrizi, M. Pocchiari, S. Monaco, B. Caughey, and G. Zanusso. 2017. 'Diagnosis of Human Prion Disease Using Real-Time Quaking-Induced Conversion Testing of Olfactory Mucosa and Cerebrospinal Fluid Samples', *JAMA Neurol*, 74: 155-62.

Botto, M., C. Dell'Agnola, A. E. Bygrave, E. M. Thompson, H. T. Cook, F. Petry, M. Loos, P. P. Pandolfi, and M. J. Walport. 1998. 'Homozygous C1q deficiency causes glomerulonephritis associated with multiple apoptotic bodies', *Nat Genet*, 19: 56-9.

Bougard, D., J. P. Brandel, M. Belondrade, V. Beringue, C. Segarra, H. Fleury, J. L. Laplanche, C. Mayran, S. Nicot, A. Green, A. Welaratne, D. Narbey, C. Fournier-Wirth, R. Knight, R. Will, P. Tiberghien, S. Haik, and J. Coste. 2016. 'Detection of prions in the plasma of presymptomatic and symptomatic patients with variant Creutzfeldt-Jakob disease', *Sci Transl Med*, 8: 370ra182.

Bougard, Daisy, Jean-Philippe Brandel, Maxime Bélondrade, Vincent Béringue, Christiane Segarra, Hervé Fleury, Jean-Louis Laplanche, Charly Mayran, Simon Nicot, Alison Green, Arlette Welaratne, David Narbey, Chantal Fournier-Wirth, Richard Knight, Robert Will, Pierre Tiberghien, Stéphane Haïk, and Joliette Coste. 2016. 'Detection of prions in the plasma of presymptomatic and symptomatic patients with variant Creutzfeldt-Jakob disease', *Science Translational Medicine*, 8: 370ra182-370ra182.

Bourgognon, J. M., and J. R. Steinert. 2019. 'The metabolome identity: basis for discovery of biomarkers in neurodegeneration', *Neural Regen Res*, 14: 387-90.

Bracken, M. B. 2009. 'Why animal studies are often poor predictors of human reactions to exposure', *J R Soc Med*, 102: 120-2.

Bradford, Barry M., and Neil A. Mabbott. 2012. 'Prion disease and the innate immune system', *Viruses*, 4: 3389-419.

Bradley, R. 1999. 'BSE transmission studies with particular reference to blood', *Dev Biol Stand*, 99: 35-40.

Brechlin, P., O. Jahn, P. Steinacker, L. Cepek, H. Kratzin, S. Lehnert, S. Jesse, B. Mollenhauer, H. A. Kretzschmar, J. Wiltfang, and M. Otto. 2008. 'Cerebrospinal fluid-optimized two-dimensional difference gel electrophoresis (2-D DIGE) facilitates the differential diagnosis of Creutzfeldt-Jakob disease', *Proteomics*, 8: 4357-66.

Bremer, J., M. Heikenwalder, J. Haybaeck, C. Tiberi, N. J. Krautler, M. O. Kurrer, and A. Aguzzi. 2009. 'Repetitive immunization enhances the susceptibility of mice to peripherally administered prions', *PLoS One*, 4: e7160.

Bribian, A., X. Fontana, F. Llorens, R. Gavin, M. Reina, J. M. Garcia-Verdugo, J. M. Torres, F. de Castro, and J. A. del Rio. 2012. 'Role of the cellular prion protein in oligodendrocyte precursor cell proliferation and differentiation in the developing and adult mouse CNS', *PLoS One*, 7: e33872.

Brosseron, Frederic, Carl-Christian Kolbe, Francesco Santarelli, Stephanie Carvalho, Anna Antonell, Sergio Castro-Gomez, Pawel Tacik, Aishwarya Alex Namasivayam, Graziella Mangone, Reinhard Schneider, Eicke Latz, Ullrich Wüllner, Per Svenningsson, Raquel Sánchez-Valle, José Luis Molinuevo, Jean-Christophe Corvol, Michael T. Heneka, Phil Scordis, Martin Hofmann-Apitius, Johan Van der Lei, Michael Heneka, Jean-Christophe Corvol, Raquel Sánchez-Valle, Nikolaus Forgo, Tamas Letoha, Reinhard Schneider, Jean Georges, Per Svenningsson, Ana Graf, Luc Canard, Nathan Lawless, Viktor Jirsa, José Luis Molinuevo, Phil Scordis, Martin Hofmann-Apitius, Reinhard Schneider, Nathan Lawless, Luc Canard, Nikolaus Forgo, Ana Graf, Jean-Christophe Corvol, Jacqueline Marovac, Stephan Springstubbe, Jean-Christophe Corvol, Ullrich Wüllner, Per Svenningsson, Eloi Magnin, Olivier Rascol, Wassilios Meissner, Michael Heneka, Bruno Dubois, Stephane Epelbaum, Albert Lladó, Graziella Mangone, Ioanna Markaki, Lorena Rami, Mircea alasam, Pawel Tacik, Panagiota Tsitsi, Raffaele Cacciaglia, Oriol Grau, Holger Froehlich, Sarah Bujac, Boris Labrador, Samir Bekadar, Anna Antonell, Sofia Bergström, Frederic rosseron, Peter Nilsson, Ina Schmitt, Matthew Page, Gregory Operto, Beatriz Bosch, Cecile Gaudebout, Stephanie Carvalho, Aishwarya Alex Namasivayam, Noemí Carranza,

Dianne Gove, Ana Diaz, and Marc Stauch. 2019. 'Multicenter Alzheimer's and Parkinson's disease immune biomarker verification study', *Alzheimer's & Dementia*.

Brown, A. R., A. R. Blanco, G. Miele, S. A. Hawkins, J. Hopkins, J. K. Fazakerley, J. Manson, and M. Clinton. 2007. 'Differential expression of erythroid genes in prion disease', *Biochem Biophys Res Commun*, 364: 366-71.

Brown, A. R., S. Rebus, C. S. McKimmie, K. Robertson, A. Williams, and J. K. Fazakerley. 2005. 'Gene expression profiling of the preclinical scrapie-infected hippocampus', *Biochem Biophys Res Commun*, 334: 86-95.

Brown, D. R., K. Qin, J. W. Herms, A. Madlung, J. Manson, R. Strome, P. E. Fraser, T. Kruck, A. Von Bohlen, W. Schulz-Schaeffer, A. Giese, D. Westaway, and H. Kretzschmar. 1997. 'The cellular prion protein binds copperin vivo', *Nature*, 390: 684-87.

Brown, K. L., K. Stewart, D. L. Ritchie, N. A. Mabbott, A. Williams, H. Fraser, W. I. Morrison, and M. E. Bruce. 1999. 'Scrapie replication in lymphoid tissues depends on prion protein-expressing follicular dendritic cells', *Nat Med*, 5: 1308-12.

Brown, K., and J. A. Mastrianni. 2010. 'The prion diseases', *J Geriatr Psychiatry Neurol*, 23: 277-98.

Brown, P., R. G. Rohwer, B. C. Dunstan, C. MacAuley, D. C. Gajdusek, and W. N. Drohan. 1998. 'The distribution of infectivity in blood components and plasma derivatives in experimental models of transmissible spongiform encephalopathy', *Transfusion*, 38: 810-6.

Brown, P.; Cervenáková, L.; McShane, L. M.; Barber, P.; Rubenstein, R.; Drohan, W. N.; . 1999. 'Further studies of blood infectivity in an experimental model of transmissible spongiform encephalopathy, with an explanation of why blood components do not transmit Creutzfeldt-Jakob disease in humans', *Transfusion*, 39: 1169-78.

Bruce, M., A. Chree, I. McConnell, J. Foster, G. Pearson, and H. Fraser. 1994. 'Transmission of bovine spongiform encephalopathy and scrapie to mice: strain variation and the species barrier', *Philos Trans R Soc Lond B Biol Sci*, 343: 405-11.

Bruce, M. E., A. Boyle, S. Cousens, I. McConnell, J. Foster, W. Goldmann, and H. Fraser. 2002. 'Strain characterization of natural sheep scrapie and comparison with BSE', *J Gen Virol*, 83: 695-704.

Bruce, M. E., R. G. Will, J. W. Ironside, I. McConnell, D. Drummond, A. Suttie, L. McCardle, A. Chree, J. Hope, C. Birkett, S. Cousens, H. Fraser, and C. J. Bostock. 1997. 'Transmissions to mice indicate that 'new variant' CJD is caused by the BSE agent', *Nature*, 389: 498-501.

Burkhard, P. R., J. C. Sanchez, T. Landis, and D. F. Hochstrasser. 2001. 'CSF detection of the 14-3-3 protein in unselected patients with dementia', *Neurology*, 56: 1528-33.

Burthem, J., B. Urban, A. Pain, and D. J. Roberts. 2001. 'The normal cellular prion protein is strongly expressed by myeloid dendritic cells', *Blood*, 98: 3733-8.

Busche, M. A., M. Kekus, H. Adelsberger, T. Noda, H. Forstl, I. Nelken, and A. Konnerth. 2015. 'Rescue of long-range circuit dysfunction in Alzheimer's disease models', *Nat Neurosci*, 18: 1623-30.

Buschmann, Anne, and Martin H. Groschup. 2005. 'Highly Bovine Spongiform Encephalopathy–Sensitive Transgenic Mice Confirm the Essential Restriction of Infectivity to the Nervous System in Clinically Diseased Cattle', *The Journal of Infectious Diseases*, 192: 934-42.

Buxbaum, J. N., Z. Ye, N. Reixach, L. Friske, C. Levy, P. Das, T. Golde, E. Masliah, A. R. Roberts, and T. Bartfai. 2008. 'Transthyretin protects Alzheimer's mice from the behavioral and biochemical effects of Abeta toxicity', *Proc Natl Acad Sci U S A*, 105: 2681-6.

Calizzani, Gabriele, Stefania Vaglio, Vito Vetrugno, Marisa Delbò, Luca Pani, and Giuliano Grazzini. 2014. 'Management of notifications of donors with Creutzfeldt-Jakob disease (post-donation information)', *Blood transfusion = Trasfusione del sangue*, 12: 22-27.

Carney, Ellen F. 2018. 'A link between mitochondrial dysfunction and innate immune activation in FSGS', *Nature Reviews Nephrology*, 14: 721-21.

Carp, R. I., and S. M. Callahan. 1981. 'In vitro interaction of scrapie agent and mouse peritoneal macrophages', *Intervirology*, 16: 8-13.

Casalone, Cristina, Gianluigi Zanusso, Pierluigi Acutis, Sergio Ferrari, Lorenzo Capucci, Fabrizio Tagliavini, Salvatore Monaco, and Maria Caramelli. 2004. 'Identification of a second bovine amyloidotic spongiform encephalopathy: Molecular similarities with sporadic Creutzfeldt-Jakob disease', *Proceedings of the National Academy of Sciences of the United States of America*, 101: 3065-70.

Castano, E. M., A. E. Roher, C. L. Esh, T. A. Kokjohn, and T. Beach. 2006. 'Comparative proteomics of cerebrospinal fluid in neuropathologically-confirmed Alzheimer's disease and non-demented elderly subjects', *Neurol Res*, 28: 155-63.

Castellani, R. J., G. Perry, and M. A. Smith. 2004. 'Prion disease and Alzheimer's disease: pathogenic overlap', *Acta Neurobiol Exp (Wars)*, 64: 11-7.

Castilla, J., C. Hetz, and C. Soto. 2004. 'Molecular mechanisms of neurotoxicity of pathological prion protein', *Curr Mol Med*, 4: 397-403.

Castilla, J., P. Saa, and C. Soto. 2005. 'Detection of prions in blood', *Nat Med*, 11: 982-5.

Castrillo, A., and P. Tontonoz. 2004. 'Nuclear receptors in macrophage biology: at the crossroads of lipid metabolism and inflammation', *Annu Rev Cell Dev Biol*, 20: 455-80.

Caudle, W. M., S. Pan, M. Shi, T. Quinn, J. Hoekstra, R. P. Beyer, T. J. Montine, and J. Zhang. 2008. 'Proteomic identification of proteins in the human brain: Towards a more comprehensive understanding of neurodegenerative disease', *Proteomics Clin Appl*, 2: 1484-97.

Caughey, B., and P. T. Lansbury. 2003. 'Protofibrils, pores, fibrils, and neurodegeneration: separating the responsible protein aggregates from the innocent bystanders', *Annu Rev Neurosci*, 26: 267-98.

Caughey, B., and G. J. Raymond. 1991. 'The scrapie-associated form of PrP is made from a cell surface precursor that is both protease- and phospholipase-sensitive', *J Biol Chem*, 266: 18217-23.

CDC, Centre for Disease Control and Prevention. 2018. 'Chronic Wsting Disease (CWD)'.

Cerovic, V., S. A. Houston, J. Westlund, L. Utriainen, E. S. Davison, C. L. Scott, C. C. Bain, T. Joeris, W. W. Agace, R. A. Kroczek, A. M. Mowat, U. Yrlid, and S. Wf Milling. 2014. 'Lymph-borne CD8α+ dendritic cells are uniquely able to cross-prime CD8+ T cells with antigen acquired from intestinal epithelial cells', *Mucosal Immunology*, 8: 38.

Cervenakova, L., O. Yakovleva, C. McKenzie, S. Kolchinsky, L. McShane, W. N. Drohan, and P. Brown. 2003. 'Similar levels of infectivity in the blood of mice infected with human-derived vCJD and GSS strains of transmissible spongiform encephalopathy', *Transfusion*, 43: 1687-94.

Chadwick, W., R. Brenneman, B. Martin, and S. Maudsley. 2010. 'Complex and multidimensional lipid raft alterations in a murine model of Alzheimer's disease', *Int J Alzheimers Dis*, 2010: 604792.

Chang, Binggong, Xin Cheng, Shaoman Yin, Tao Pan, Hongtao Zhang, Poki Wong, Shin-Chung Kang, Fan Xiao, Huimin Yan, Chaoyang Li, Lisa L. Wolfe, Michael W. Miller, Thomas Wisniewski, Mark I. Greene, and Man-Sun Sy. 2007. 'Test for Detection of Disease-

Associated Prion Aggregate in the Blood of Infected but Asymptomatic Animals', *Clinical and Vaccine Immunology*, 14: 36-43.

Chen, C., D. Xiao, W. Zhou, Q. Shi, H. F. Zhang, J. Zhang, C. Tian, J. Z. Zhang, and X. P. Dong. 2014. 'Global protein differential expression profiling of cerebrospinal fluid samples pooled from Chinese sporadic CJD and non-CJD patients', *Mol Neurobiol*, 49: 290-302.

Chen, Y., Z. Zhou, and W. Min. 2018. 'Mitochondria, Oxidative Stress and Innate Immunity', *Front Physiol*, 9: 1487.

Chhabra, E. S., and H. N. Higgs. 2007. 'The many faces of actin: matching assembly factors with cellular structures', *Nat Cell Biol*, 9: 1110-21.

Chiovitti, K., A. Corsaro, S. Thellung, V. Villa, D. Paludi, C. D'Arrigo, C. Russo, A. Perico, A. Ianieri, D. Di Cola, A. Vergara, A. Aceto, and T. Florio. 2007. 'Intracellular accumulation of a mild-denatured monomer of the human PrP fragment 90-231, as possible mechanism of its neurotoxic effects', *J Neurochem*, 103: 2597-609.

Cho, W. C. 2007. 'Proteomics technologies and challenges', *Genomics Proteomics Bioinformatics*, 5: 77-85.

Choi, B., Lee Y. S., Ju Y. R., Kim C., and Kim S. Y. 2016. 'Proteomics-based Development of Biomarkers for Prion Diseases', *Journal of Proteomics and Bioinformatics*, 9:3.

Chun, R. F. 2012. 'New perspectives on the vitamin D binding protein', *Cell Biochem Funct*, 30: 445-56.

Cinamon, G., M. A. Zachariah, O. M. Lam, F. W. Foss, Jr., and J. G. Cyster. 2008. 'Follicular shuttling of marginal zone B cells facilitates antigen transport', *Nat Immunol*, 9: 54-62.

Coe, J. E., R. E. Race, and M. J. Ross. 2001. 'Serological evidence for an inflammatory response in murine scrapie', *J Infect Dis*, 183: 185-91.

Coffino, P. 2000. 'Polyamines in spermiogenesis: not now, darling', *Proc Natl Acad Sci U S A*, 97: 4421-3.

Collinge, J., and A. R. Clarke. 2007. 'A general model of prion strains and their pathogenicity', *Science (New York, N.Y.)*, 318: 930-6.

Collinge, J., M. A. Whittington, K. C. Sidle, C. J. Smith, M. S. Palmer, A. R. Clarke, and J. G. Jefferys. 1994. 'Prion protein is necessary for normal synaptic function', *Nature*, 370: 295-7.

Comoy, Emmanuel E., Jacqueline Mikol, Nina Jaffré, Vincent Lebon, Etienne Levavasseur, Nathalie Streichenberger, Chryslain Sumian, Armand Perret-Liaudet, Marc Eloit, Olivier Andreoletti, Stéphane Haïk, Philippe Hantraye, and Jean-Philippe Deslys. 2017. 'Experimental transfusion of variant CJD-infected blood reveals previously uncharacterised prion disorder in mice and macaque', *Nature communications*, 8: 1268-68.

Concha-Marambio, L., M. A. Chacon, and C. Soto. 2020. 'Preclinical Detection of Prions in Blood of Nonhuman Primates Infected with Variant Creutzfeldt-Jakob Disease', *Emerg Infect Dis*, 26: 34-43.

Concha-Marambio, L., S. Pritzkow, F. Moda, F. Tagliavini, J. W. Ironside, P. E. Schulz, and C. Soto. 2016a. 'Detection of prions in blood from patients with variant Creutzfeldt-Jakob disease', *Sci Transl Med*, 8: 370ra183.

Concha-Marambio, Luis, Sandra Pritzkow, Fabio Moda, Fabrizio Tagliavini, James W. Ironside, Paul E. Schulz, and Claudio Soto. 2016b. 'Detection of prions in blood from patients with variant Creutzfeldt-Jakob disease', *Science Translational Medicine*, 8: 370ra183-370ra183.

Conner, M. M., M. R. Ebinger, J. A. Blanchong, and P. C. Cross. 2008. 'Infectious disease in cervids of North America: data, models, and management challenges', *Ann N Y Acad Sci*, 1134: 146-72.
Cook, R. W., J. Bingham, A. S. Besier, C. L. Bayley, M. Hawes, P. L. Shearer, M. Yamada, J. Bergfeld, D. T. Williams, and D. J. Middleton. 2016. 'Atypical scrapie in Australia', *Aust Vet J*, 94: 452-55.
Cooper, J. D., and S. M. Bird. 2003. 'Predicting incidence of variant Creutzfeldt-Jakob disease from UK dietary exposure to bovine spongiform encephalopathy for the 1940 to 1969 and post-1969 birth cohorts', *International Journal of Epidemiology*, 32: 784-91.
Criado, J. R., M. Sanchez-Alavez, B. Conti, J. L. Giacchino, D. N. Wills, S. J. Henriksen, R. Race, J. C. Manson, B. Chesebro, and M. B. Oldstone. 2005. 'Mice devoid of prion protein have cognitive deficits that are rescued by reconstitution of PrP in neurons', *Neurobiol Dis*, 19: 255-65.
Cristóvão, Joana S., and Cláudio M. Gomes. 2019. 'S100 Proteins in Alzheimer's Disease', *Frontiers in Neuroscience*, 13.
Cunningham, Andrew A., James K. Kirkwood, Michael Dawson, Yvonne I. Spencer, Robert B. Green, and Gerald A. H. Wells. 2004. 'Bovine spongiform encephalopathy infectivity in greater kudu (Tragelaphus strepsiceros)', *Emerging infectious diseases*, 10: 1044-49.
Cunningham, C., D. C. Wilcockson, D. Boche, and V. H. Perry. 2005. 'Comparison of Inflammatory and Acute-Phase Responses in the Brain and Peripheral Organs of the ME7 Model of Prion Disease', *J Virol*, 79: 5174-84.
Dagleish, M. P., S. M. Rodger, M. M. Simmons, J. Finlayson, D. Buxton, and F. Chianini. 2008. 'Atypical scrapie in a sheep in Scotland', *Vet Rec*, 162: 518-9.
Dandoy-Dron, F., F. Guillo, L. Benboudjema, J. P. Deslys, C. Lasmezas, D. Dormont, M. G. Tovey, and M. Dron. 1998. 'Gene expression in scrapie. Cloning of a new scrapie-responsive gene and the identification of increased levels of seven other mRNA transcripts', *J Biol Chem*, 273: 7691-7.
Dasari, A. K. R., I. Hung, Z. Gan, and K. H. Lim. 2019. 'Two distinct aggregation pathways in transthyretin misfolding and amyloid formation', *Biochim Biophys Acta Proteins Proteom*, 1867: 344-49.
Dassanayake, R. P., S. A. Madsen-Bouterse, T. C. Truscott, D. Zhuang, M. R. Mousel, W. C. Davis, and D. A. Schneider. 2016. 'Classical scrapie prions are associated with peripheral blood monocytes and T-lymphocytes from naturally infected sheep', *BMC Vet Res*, 12: 27.
Dassati, S., A. Waldner, and R. Schweigreiter. 2014. 'Apolipoprotein D takes center stage in the stress response of the aging and degenerative brain', *Neurobiol Aging*, 35: 1632-42.
Daveau, M., P. Rouet, M. Scotte, L. Faye, M. Hiron, J. P. Lebreton, and J. P. Salier. 1993. 'Human inter-alpha-inhibitor family in inflammation: simultaneous synthesis of positive and negative acute-phase proteins', *Biochem J*, 292 (Pt 2): 485-92.
DAVID. 2007. 'Functional Annotation Tool', Accessed 01/01/2020. https://david.ncifcrf.gov/helps/functional_annotation.html

.
Dawson, M., R. C. Moore, and S. C. Bishop. 2008. 'Progress and limits of PrP gene selection policy', *Vet Res*, 39: 25.
de la Torre, J. C. 2004. 'Is Alzheimer's disease a neurodegenerative or a vascular disorder? Data, dogma, and dialectics', *Lancet Neurol*, 3: 184-90.

de Marco, M. F., J. Linehan, O. N. Gill, J. P. Clewley, and S. Brandner. 2010. 'Large-scale immunohistochemical examination for lymphoreticular prion protein in tonsil specimens collected in Britain', *J Pathol*, 222: 380-7.

Demaerel, P., L. Heiner, W. Robberecht, R. Sciot, and G. Wilms. 1999. 'Diffusion-weighted MRI in sporadic Creutzfeldt-Jakob disease', *Neurology*, 52: 205-05.

Dieks, J. K., J. Gawinecka, A. R. Asif, D. Varges, K. Gmitterova, J. H. Streich, H. Dihazi, U. Heinemann, and I. Zerr. 2013. 'Low-abundant cerebrospinal fluid proteome alterations in dementia with Lewy bodies', *J Alzheimers Dis*, 34: 387-97.

Dominguez, R., and K. C. Holmes. 2011. 'Actin structure and function', *Annu Rev Biophys*, 40: 169-86.

Donaldson, D. S., and N. A. Mabbott. 2016. 'The influence of the commensal and pathogenic gut microbiota on prion disease pathogenesis', *J Gen Virol*, 97: 1725-38.

Donaldson, D. S., A. Sehgal, D. Rios, I. R. Williams, and N. A. Mabbott. 2016. 'Increased Abundance of M Cells in the Gut Epithelium Dramatically Enhances Oral Prion Disease Susceptibility', *PLoS Pathog*, 12: e1006075.

Donaldson, David S., Kathryn J. Else, and Neil A. Mabbott. 2015. 'The Gut-Associated Lymphoid Tissues in the Small Intestine, Not the Large Intestine, Play a Major Role in Oral Prion Disease Pathogenesis', *Journal of Virology*, 89: 9532-47.

Douet, J. Y., C. Lacroux, N. Aron, M. W. Head, S. Lugan, C. Tillier, A. Huor, H. Cassard, M. Arnold, V. Beringue, J. W. Ironside, and O. Andreoletti. 2017. 'Distribution and Quantitative Estimates of Variant Creutzfeldt-Jakob Disease Prions in Tissues of Clinical and Asymptomatic Patients', *Emerg Infect Dis*, 23: 946-56.

Douet, J. Y., C. Lacroux, C. Litaise, S. Lugan, F. Corbiere, M. Arnold, H. Simmons, N. Aron, P. Costes, C. Tillier, H. Cassard, and O. Andreoletti. 2016. 'Mononucleated Blood Cell Populations Display Different Abilities To Transmit Prion Disease by the Transfusion Route', *J Virol*, 90: 3439-45.

Douet, Jean Yves, Saima Zafar, Armand Perret-Liaudet, Caroline Lacroux, Séverine Lugan, Naima Aron, Herve Cassard, Claudia Ponto, Fabien Corbière, Juan Maria Torres, Inga Zerr, and Olivier Andreoletti. 2014. 'Detection of infectivity in blood of persons with variant and sporadic Creutzfeldt-Jakob disease', *Emerging infectious diseases*, 20: 114-17.

Dromparis, P., and E. D. Michelakis. 2013. "Mitochondria in vascular health and disease." In *Annual Review of Physiology*, 95-126.

Duffy, P., J. Wolf, G. Collins, A. G. DeVoe, B. Streeten, and D. Cowen. 1974. 'Letter: Possible person-to-person transmission of Creutzfeldt-Jakob disease', *N Engl J Med*, 290: 692-3.

Eaton, S. L., S. L. Roche, M. Llavero Hurtado, K. J. Oldknow, C. Farquharson, T. H. Gillingwater, and T. M. Wishart. 2013. 'Total protein analysis as a reliable loading control for quantitative fluorescent Western blotting', *PLoS One*, 8: e72457.

Edgeworth, J. A., M. Farmer, A. Sicilia, P. Tavares, J. Beck, T. Campbell, J. Lowe, S. Mead, P. Rudge, J. Collinge, and G. S. Jackson. 2011. 'Detection of prion infection in variant Creutzfeldt-Jakob disease: a blood-based assay', *Lancet*, 377: 487-93.

EFSA, Panel on Biological Hazards, Kostas Koutsoumanis, Ana Allende, Avelino Alvarez-Ordoňez, Declan Bolton, Sara Bover-Cid, Marianne Chemaly, Robert Davies, Alessandra De Cesare, Lieve Herman, Friederike Hilbert, Roland Lindqvist, Maarten Nauta, Luisa Peixe, Giuseppe Ru, Panagiotis Skandamis, Elisabetta Suffredini, Olivier Andreoletti, Sylvie L Benestad, Emmanuel Comoy, Romolo Nonno, Teresa da Silva Felicio, Angel Ortiz-Pelaez, and Marion M Simmons. 2019. 'Update on chronic wasting disease (CWD) III', *EFSA Journal*, 17: e05863.

Erlich, P., C. Dumestre-Pérard, W. L. Ling, C. Lemaire-Vieille, G. Schoehn, G. J. Arlaud, N. M. Thielens, J. Gagnon, and J. Y. Cesbron. 2010. 'Complement protein C1q forms a complex with cytotoxic prion protein oligomers', *J Biol Chem*, 285: 19267-76.

Espenes, A., C. M. Press, T. Landsverk, M. A. Tranulis, M. Aleksandersen, G. Gunnes, S. L. Benestad, R. Fuglestveit, and M. J. Ulvund. 2006. 'Detection of PrP(Sc) in rectal biopsy and necropsy samples from sheep with experimental scrapie', *J Comp Pathol*, 134: 115-25.

Espinosa, Juan Carlos, Mónica Morales, Joaquín Castilla, Mark Rogers, and Juan María Torres. 2007. 'Progression of prion infectivity in asymptomatic cattle after oral bovine spongiform encephalopathy challenge', *Journal of General Virology*, 88: 1379-83.

Etheridge, A., I. Lee, L. Hood, D. Galas, and K. Wang. 2011. 'Extracellular microRNA: a new source of biomarkers', *Mutat Res*, 717: 85-90.

Falcon, Carles, Gemma C. Monté-Rubio, Oriol Grau-Rivera, Marc Suárez-Calvet, Raquel Sánchez-Valle, Lorena Rami, Beatriz Bosch, Christian Haass, Juan Domingo Gispert, and José Luis Molinuevo. 2019. 'CSF glial biomarkers YKL40 and sTREM2 are associated with longitudinal volume and diffusivity changes in cognitively unimpaired individuals', *NeuroImage: Clinical*, 23: 101801.

Fediaevsky, Alexandre, Patrick Gasqui, Didier Calavas, and Christian Ducrot. 2010. 'Discrepant epidemiological patterns between classical and atypical scrapie in sheep flocks under French TSE control measures', *The Veterinary Journal*, 185: 338-40.

Fevrier, B., and G. Raposo. 2004. 'Exosomes: endosomal-derived vesicles shipping extracellular messages', *Curr Opin Cell Biol*, 16: 415-21.

Filali, Hicham, Inmaculada Martín-Burriel, Frank Harders, Luis Varona, Carlos Hedman, Diego R. Mediano, Marta Monzón, Alex Bossers, Juan J. Badiola, and Rosa Bolea. 2014. 'Gene expression profiling of mesenteric lymph nodes from sheep with natural scrapie', *BMC genomics*, 15: 59-59.

Flores-Langarica, A., Y. Sebti, D. A. Mitchell, R. B. Sim, and G. G. MacPherson. 2009. 'Scrapie pathogenesis: the role of complement C1q in scrapie agent uptake by conventional dendritic cells', *J Immunol*, 182: 1305-13.

Forgac, M. 2007. 'Vacuolar ATPases: rotary proton pumps in physiology and pathophysiology', *Nat Rev Mol Cell Biol*, 8: 917-29.

Foster, J. D., M. Bruce, I. McConnell, A. Chree, and H. Fraser. 1996. 'Detection of BSE infectivity in brain and spleen of experimentally infected sheep', *Veterinary Record*, 138: 546-48.

Foster, J. D., D. W. Parnham, N. Hunter, and M. Bruce. 2001. 'Distribution of the prion protein in sheep terminally affected with BSE following experimental oral transmission', *J Gen Virol*, 82: 2319-26.

Fox, C. J., P. S. Hammerman, and C. B. Thompson. 2005. 'Fuel feeds function: energy metabolism and the T-cell response', *Nat Rev Immunol*, 5: 844-52.

Fraser, H., M. E. Bruce, A. Chree, I. McConnell, and G. A. Wells. 1992. 'Transmission of bovine spongiform encephalopathy and scrapie to mice', *J Gen Virol*, 73 (Pt 8): 1891-7.

Fraser, H., and A. G. Dickinson. 1970. 'Pathogenesis of Scrapie in the Mouse: the Role of the Spleen', *Nature*, 226: 462.

Fratini, F., S. Principe, M. Puopolo, A. Ladogana, A. Poleggi, P. Piscopo, G. Bruno, S. Castrechini, R. Pascone, A. Confaloni, L. Minghetti, F. Cardone, M. Pocchiari, and M. Crescenzi. 2012. 'Increased levels of acute-phase inflammatory proteins in plasma of patients with sporadic CJD', *Neurology*, 79: 1012-8.

Friedman, J. R., and J. Nunnari. 2014. 'Mitochondrial form and function', *Nature*, 505: 335-43.
Frigg, R., M. A. Klein, I. Hegyi, R. M. Zinkernagel, and A. Aguzzi. 1999. 'Scrapie pathogenesis in subclinically infected B-cell-deficient mice', *J Virol*, 73: 9584-8.
FSA, Food Standards Agency. 2017. 'Meat Industry Guide: Transmissible Spongiform Encephalopathy (TSE) Testing '. https://www.foodstandards.gov.scot/downloads/MIG_-_Chapter_20.pdf.
Fung, T. C., C. A. Olson, and E. Y. Hsiao. 2017. 'Interactions between the microbiota, immune and nervous systems in health and disease', *Nat Neurosci*, 20: 145-55.
Furr, A., A. J. Young, and J. Richt. 2012. 'The Immune System in the Pathogenesis and Prevention of Prion Diseases', *Journal of Bioterrorism & Biodefense*, S1:012.
Gabizon, R., M. P. McKinley, D. F. Groth, L. Kenaga, and S. B. Prusiner. 1988. 'Properties of scrapie prion protein liposomes', *Journal of Biological Chemistry*, 263: 4950-55.
Gale, Roberts H. 2018. 'Situation Assessment: Update on Chronic Wasting Disease in Europe ', Department for Environment, Food and Rural Affairs, Animal & Plant Health Agency.
Galeno, R., M. A. Di Bari, R. Nonno, F. Cardone, M. Sbriccoli, S. Graziano, L. Ingrosso, M. Fiorini, A. Valanzano, G. Pasini, A. Poleggi, R. Vinci, A. Ladogana, M. Puopolo, S. Monaco, U. Agrimi, G. Zanusso, and M. Pocchiari. 2017. 'Prion Strain Characterization of a Novel Subtype of Creutzfeldt-Jakob Disease', *J Virol*, 91.
Gallego, C., D. Golenbock, M. A. Gomez, and N. G. Saravia. 2011. 'Toll-like receptors participate in macrophage activation and intracellular control of Leishmania (Viannia) panamensis', *Infect Immun*, 79: 2871-9.
Gambetti, P., Q. Kong, W. Zou, P. Parchi, and S. G. Chen. 2003. 'Sporadic and familial CJD: classification and characterisation', *Br Med Bull*, 66: 213-39.
Gehlenborg, N., D. Hwang, I. Y. Lee, H. Yoo, D. Baxter, B. Petritis, R. Pitstick, B. Marzolf, S. J. Dearmond, G. A. Carlson, and L. Hood. 2009. 'The Prion Disease Database: a comprehensive transcriptome resource for systems biology research in prion diseases', *Database (Oxford)*, 2009: bap011.
Geuens, T., D. Bouhy, and V. Timmerman. 2016. 'The hnRNP family: insights into their role in health and disease', *Hum Genet*, 135: 851-67.
Geyer, P. E. 2017. 'Revisiting biomarker discovery by plasma proteomics', 13.
Geyer, P. E., N. A. Kulak, G. Pichler, L. M. Holdt, D. Teupser, and M. Mann. 2016. 'Plasma Proteome Profiling to Assess Human Health and Disease', *Cell Syst*, 2: 185-95.
Giese, A., and H. A. Kretzschmar. 2001. 'Prion-induced neuronal damage--the mechanisms of neuronal destruction in the subacute spongiform encephalopathies', *Curr Top Microbiol Immunol*, 253: 203-17.
Gilch, S., N. Chitoor, Y. Taguchi, M. Stuart, J. E. Jewell, and H. M. Schatzl. 2011. 'Chronic wasting disease', *Top Curr Chem*, 305: 51-77.
Gill, Andrew C., and Andrew R. Castle. 2018. 'Chapter 2 - The cellular and pathologic prion protein.' in Maurizio Pocchiari and Jean Manson (eds.), *Handbook of Clinical Neurology* (Elsevier).
Gill, O Noel, Yvonne Spencer, Angela Richard-Loendt, Carole Kelly, Reza Dabaghian, Lynnette Boyes, Jacqueline Linehan, Marion Simmons, Paul Webb, Peter Bellerby, Nick Andrews, David A Hilton, James W Ironside, Jon Beck, Mark Poulter, Simon Mead, and Sebastian Brandner. 2013a. 'Prevalent abnormal prion protein in human appendixes after bovine spongiform encephalopathy epizootic: large scale survey', *BMJ : British Medical Journal*, 347.
Gill, O. N., Y. Spencer, A. Richard-Loendt, C. Kelly, R. Dabaghian, L. Boyes, J. Linehan, M. Simmons, P. Webb, P. Bellerby, N. Andrews, D. A. Hilton, J. W. Ironside, J. Beck, M.

Poulter, S. Mead, and S. Brandner. 2013b. 'Prevalent abnormal prion protein in human appendixes after bovine spongiform encephalopathy epizootic: large scale survey', *Bmj*, 347: f5675.

Gill, O. Noel, Yvonne Spencer, Angela Richard-Loendt, Carole Kelly, David Brown, Katy Sinka, Nick Andrews, Reza Dabaghian, Marion Simmons, Philip Edwards, Peter Bellerby, David J. Everest, Mark McCall, Linda M. McCardle, Jacqueline Linehan, Simon Mead, David A. Hilton, James W. Ironside, and Sebastian Brandner. 2020. 'Prevalence in Britain of abnormal prion protein in human appendices before and after exposure to the cattle BSE epizootic', *Acta Neuropathologica*.

Glatzel, M., and A. Aguzzi. 2000. 'Peripheral pathogenesis of prion diseases', *Microbes Infect*, 2: 613-9.

Glaysher, B. R., and N. A. Mabbott. 2007. 'Role of the GALT in scrapie agent neuroinvasion from the intestine', *J Immunol*, 178: 3757-66.

Goldknopf, I. L., E. A. Sheta, J. Bryson, B. Folsom, C. Wilson, J. Duty, A. A. Yen, and S. H. Appel. 2006. 'Complement C3c and related protein biomarkers in amyotrophic lateral sclerosis and Parkinson's disease', *Biochem Biophys Res Commun*, 342: 1034-9.

Goldmann, W. 2008. 'PrP genetics in ruminant transmissible spongiform encephalopathies', *Vet Res*, 39: 30.

Gonzalez, L., M. P. Dagleish, S. Martin, G. Dexter, P. Steele, J. Finlayson, and M. Jeffrey. 2008. 'Diagnosis of preclinical scrapie in live sheep by the immunohistochemical examination of rectal biopsies', *Vet Rec*, 162: 397-403.

Gonzalez, L., S. Martin, I. Begara-McGorum, N. Hunter, F. Houston, M. Simmons, and M. Jeffrey. 2002. 'Effects of agent strain and host genotype on PrP accumulation in the brain of sheep naturally and experimentally affected with scrapie', *J Comp Pathol*, 126: 17-29.

Gonzalez, L., S. Martin, F. E. Houston, N. Hunter, H. W. Reid, S. J. Bellworthy, and M. Jeffrey. 2005. 'Phenotype of disease-associated PrP accumulation in the brain of bovine spongiform encephalopathy experimentally infected sheep', *J Gen Virol*, 86: 827-38.

González, L., J. L. Pitarch, S. Martin, L. Thurston, H. Simmons, C. Acín, and M. Jeffrey. 2014. 'Influence of Polymorphisms in the Prion Protein Gene on the Pathogenesis and Neuropathological Phenotype of Sheep Scrapie after Oral Infection', *Journal of Comparative Pathology*, 150: 57-70.

Gough, K. C., and B. C. Maddison. 2010. 'Prion transmission: prion excretion and occurrence in the environment', *Prion*, 4: 275-82.

Gough, Kevin C., Claire A. Baker, Helen C. Rees, Linda A. Terry, John Spiropoulos, Leigh Thorne, and Ben C. Maddison. 2012. 'The oral secretion of infectious scrapie prions occurs in preclinical sheep with a range of PRNP genotypes', *Journal of Virology*, 86: 566-71.

Gousset, K., E. Schiff, C. Langevin, Z. Marijanovic, A. Caputo, D. T. Browman, N. Chenouard, F. de Chaumont, A. Martino, J. Enninga, J. C. Olivo-Marin, D. Mannel, and C. Zurzolo. 2009. 'Prions hijack tunnelling nanotubes for intercellular spread', *Nat Cell Biol*, 11: 328-36.

Green, A. J., E. J. Thompson, G. E. Stewart, M. Zeidler, J. M. McKenzie, M. A. MacLeod, J. W. Ironside, R. G. Will, and R. S. Knight. 2001. 'Use of 14-3-3 and other brain-specific proteins in CSF in the diagnosis of variant Creutzfeldt-Jakob disease', *Journal of neurology, neurosurgery, and psychiatry*, 70: 744-48.

Green, R., C. Horrocks, A. Wilkinson, S. A. Hawkins, and S. J. Ryder. 2005. 'Primary isolation of the bovine spongiform encephalopathy agent in mice: agent definition based on a review of 150 transmissions', *J Comp Pathol*, 132: 117-31.

Greenlee, J. J. 2018. 'Review: Update on Classical and Atypical Scrapie in Sheep and Goats', *Vet Pathol*: 300985818794247.
Greenough, M. A., J. Camakaris, and A. I. Bush. 2013. 'Metal dyshomeostasis and oxidative stress in Alzheimer's disease', *Neurochem Int*, 62: 540-55.
Gregori, Luisa, Patrick V. Gurgel, Julia T. Lathrop, Peter Edwardson, Brian C. Lambert, Ruben G. Carbonell, Steven J. Burton, David J. Hammond, and Robert G. Rohwer. 2006. 'Reduction in infectivity of endogenous transmissible spongiform encephalopathies present in blood by adsorption to selective affinity resins', *The Lancet*, 368: 2226-30.
Groschup, M. H., C. Lacroux, A. Buschmann, G. Luhken, J. Mathey, M. Eiden, S. Lugan, C. Hoffmann, J. C. Espinosa, T. Baron, J. M. Torres, G. Erhardt, and O. Andreoletti. 2007. 'Classic scrapie in sheep with the ARR/ARR prion genotype in Germany and France', *Emerg Infect Dis*, 13: 1201-7.
Grosset, A., K. Moskowitz, C. Nelsen, T. Pan, E. Davidson, and C. S. Orser. 2005. 'Rapid presymptomatic detection of PrPSc via conformationally responsive palindromic PrP peptides', *Peptides*, 26: 2193-200.
Groveman, B. R., C. D. Orrú, A. G. Hughson, M. Bongianni, M. Fiorini, D. Imperiale, A. Ladogana, M. Pocchiari, G. Zanusso, and B. Caughey. 2017. 'Extended and direct evaluation of RT-QuIC assays for Creutzfeldt-Jakob disease diagnosis', *Ann Clin Transl Neurol*, 4: 139-44.
Groveman, Bradley R., Gregory J. Raymond, Katrina J. Campbell, Brent Race, Lynne D. Raymond, Andrew G. Hughson, Christina D. Orrú, Allison Kraus, Katie Phillips, and Byron Caughey. 2017. 'Role of the central lysine cluster and scrapie templating in the transmissibility of synthetic prion protein aggregates', *PLoS pathogens*, 13: e1006623-e23.
Growdon, M. E. 2011. 'Ethical issues in the early diagnosis of Alzheimer disease', *Virtual Mentor*, 13: 868-72.
Gruys, E., M. J. M. Toussaint, T. A. Niewold, and S. J. Koopmans. 2005a. 'Acute phase reaction and acute phase proteins', *Journal of Zhejiang University. Science. B*, 6: 1045-56.
Gruys, E., M. J. Toussaint, T. A. Niewold, and S. J. Koopmans. 2005b. 'Acute phase reaction and acute phase proteins', *J Zhejiang Univ Sci B*, 6: 1045-56.
GSSO, Norwegian Government Security and Service Organisation. 2018. 'Chronic Wasting Disease: All known animals in Nordfjella dispatched'. https://www.regjeringen.no/en/aktuelt/skrantesjuke-alle-kjente-dyr-felt-i-nordfjella/id2591233/.
Gygi, S. P., Y. Rochon, B. R. Franza, and R. Aebersold. 1999. 'Correlation between protein and mRNA abundance in yeast', *Mol Cell Biol*, 19: 1720-30.
Halliday, S., F. Houston, and N. Hunter. 2005. 'Expression of PrPC on cellular components of sheep blood', *J Gen Virol*, 86: 1571-9.
Halliez, S., E. Jaumain, A. Huor, J. Y. Douet, S. Lugan, H. Cassard, C. Lacroux, V. Beringue, O. Andreoletti, and D. Vilette. 2014. 'White blood cell-based detection of asymptomatic scrapie infection by ex vivo assays', *PLoS One*, 9: e104287.
Hase, Koji, Kazuya Kawano, Tomonori Nochi, Gemilson Soares Pontes, Shinji Fukuda, Masashi Ebisawa, Kazunori Kadokura, Toru Tobe, Yumiko Fujimura, Sayaka Kawano, Atsuko Yabashi, Satoshi Waguri, Gaku Nakato, Shunsuke Kimura, Takaya Murakami, Mitsutoshi Iimura, Kimiyo Hamura, Shin-Ichi Fukuoka, Anson W. Lowe, Kikuji Itoh, Hiroshi Kiyono, and Hiroshi Ohno. 2009. 'Uptake through glycoprotein 2 of FimH+ bacteria by M cells initiates mucosal immune response', *Nature*, 462: 226.
Heikenwalder, M., M. O. Kurrer, I. Margalith, J. Kranich, N. Zeller, J. Haybaeck, M. Polymenidou, M. Matter, J. Bremer, W. S. Jackson, S. Lindquist, C. J. Sigurdson, and

A. Aguzzi. 2008. 'Lymphotoxin-dependent prion replication in inflammatory stromal cells of granulomas', *Immunity*, 29: 998-1008.
Hennig, Sven, Geraldine Kong, Taro Mannen, Agata Sadowska, Simon Kobelke, Amanda Blythe, Gavin J. Knott, K. Swaminathan Iyer, Diwei Ho, Estella A. Newcombe, Kana Hosoki, Naoki Goshima, Tetsuya Kawaguchi, Danny Hatters, Laura Trinkle-Mulcahy, Tetsuro Hirose, Charles S. Bond, and Archa H. Fox. 2015. 'Prion-like domains in RNA binding proteins are essential for building subnuclear paraspeckles', *Journal of Cell Biology*, 210: 529-39.
Herbst, Allen, Sean McIlwain, Joshua J. Schmidt, Judd M. Aiken, C. David Page, and Lingjun Li. 2009. 'Prion disease diagnosis by proteomic profiling', *Journal of proteome research*, 8: 1030-36.
Herrmann, L. M., W. C. Davis, D. P. Knowles, K. J. Wardrop, M. S. Sy, P. Gambetti, and O' Rourke KI. 2001. 'Cellular prion protein is expressed on peripheral blood mononuclear cells but not platelets of normal and scrapie-infected sheep', *Haematologica*, 86: 146-53.
Herz, J., and H. H. Bock. 2002. 'Lipoprotein receptors in the nervous system', *Annu Rev Biochem*, 71: 405-34.
Hetz, C., M. Russelakis-Carneiro, K. Maundrell, J. Castilla, and C. Soto. 2003. 'Caspase-12 and endoplasmic reticulum stress mediate neurotoxicity of pathological prion protein', *EMBO Journal*, 22: 5435-45.
Hewitt, P. E., C. A. Llewelyn, J. Mackenzie, and R. G. Will. 2006. 'Creutzfeldt-Jakob disease and blood transfusion: results of the UK Transfusion Medicine Epidemiological Review study', *Vox Sang*, 91: 221-30.
Hijazi, N., Y. Shaked, H. Rosenmann, T. Ben-Hur, and R. Gabizon. 2003. 'Copper binding to PrPC may inhibit prion disease propagation', *Brain Res*, 993: 192-200.
Hill, A. F., R. J. Butterworth, S. Joiner, G. Jackson, M. N. Rossor, D. J. Thomas, A. Frosh, N. Tolley, J. E. Bell, M. Spencer, A. King, S. Al-Sarraj, J. W. Ironside, P. L. Lantos, and J. Collinge. 1999. 'Investigation of variant Creutzfeldt-Jakob disease and other human prion diseases with tonsil biopsy samples', *Lancet*, 353: 183-9.
Hill, A. F., and J. Collinge. 2003. 'Subclinical prion infection', *Trends Microbiol*, 11: 578-84.
Hill, Andrew F., Martin Zeidler, James Ironside, and John Collinge. 1997. 'Diagnosis of new variant Creutzfeldt-Jakob disease by tonsil biopsy', *The Lancet*, 349: 99-100.
Hilton, D. A., E. Fathers, P. Edwards, J. W. Ironside, and J. Zajicek. 1998. 'Prion immunoreactivity in appendix before clinical onset of variant Creutzfeldt-Jakob disease', *Lancet*, 352: 703-4.
Hilton, D. A., A. C. Ghani, L. Conyers, P. Edwards, L. McCardle, D. Ritchie, M. Penney, D. Hegazy, and J. W. Ironside. 2004. 'Prevalence of lymphoreticular prion protein accumulation in UK tissue samples', *J Pathol*, 203: 733-9.
Hilton, David A., Azra C. Ghani, Lisa Conyers, Philip Edwards, Linda McCardle, Mark Penney, Diane Ritchie, and James W. Ironside. 2002. 'Accumulation of prion protein in tonsil and appendix: review of tissue samples', *BMJ (Clinical research ed.)*, 325: 633-34.
Hoffmann, Christine, Martin Eiden, Martin Kaatz, Markus Keller, Ute Ziegler, Ron Rogers, Bob Hills, Anne Balkema-Buschmann, Lucien van Keulen, Jorg G. Jacobs, and Martin H. Groschup. 2011. 'BSE infectivity in jejunum, ileum and ileocaecal junction of incubating cattle', *Veterinary Research*, 42: 21.
Holada, K., and J. G. Vostal. 2000. 'Different levels of prion protein (PrPc) expression on hamster, mouse and human blood cells', *Br J Haematol*, 110: 472-80.
Hortin, G. L., D. Sviridov, and N. L. Anderson. 2008. 'High-abundance polypeptides of the human plasma proteome comprising the top 4 logs of polypeptide abundance', *Clin Chem*, 54: 1608-16.

Hosszu, K. K., F. Santiago-Schwarz, E. I. Peerschke, and B. Ghebrehiwet. 2010. 'Evidence that a C1q/C1qR system regulates monocyte-derived dendritic cell differentiation at the interface of innate and acquired immunity', *Innate Immun*, 16: 115-27.
Houston, F., J. D. Foster, A. Chong, N. Hunter, and C. J. Bostock. 2000. 'Transmission of BSE by blood transfusion in sheep', *Lancet*, 356: 999-1000.
Houston, F., S. McCutcheon, W. Goldmann, A. Chong, J. Foster, S. Siso, L. Gonzalez, M. Jeffrey, and N. Hunter. 2008. 'Prion diseases are efficiently transmitted by blood transfusion in sheep', *Blood*, 112: 4739-45.
Hu, Ping Ping, and Cheng Zhi Huang. 2013. 'Prion protein: structural features and related toxicity', *Acta Biochimica et Biophysica Sinica*, 45: 435-41.
Huang, Fang-Ping, Christine F. Farquhar, Neil A. Mabbott, Moira E. Bruce, and G. Gordon MacPherson. 2002. 'Migrating intestinal dendritic cells transport PrPSc from the gut', *Journal of General Virology*, 83: 267-71.
Huang, J., L. J. Kim, R. Mealey, H. C. Marsh Jr, Y. Zhang, A. J. Tenner, E. S. Connolly Jr, and D. J. Pinsky. 1999. 'Neuronal protection in stroke by an sLe(x)-glycosylated complement inhibitory protein', *Science (New York, N.Y.)*, 285: 595-99.
Huang, N., S. K. Marie, J. A. Livramento, R. Chammas, and R. Nitrini. 2003. '14-3-3 protein in the CSF of patients with rapidly progressive dementia', *Neurology*, 61: 354-57.
Huang, Y., and R. W. Mahley. 2014. 'Apolipoprotein E: structure and function in lipid metabolism, neurobiology, and Alzheimer's diseases', *Neurobiol Dis*, 72 Pt A: 3-12.
Hunter, N. 1997. 'PrP genetics in sheep and the applications for scrapie and BSE', *Trends Microbiol*, 5: 331-4.
Hunter, N., J. D. Foster, W. Goldmann, M. J. Stear, J. Hope, and C. Bostock. 1996. 'Natural scrapie in a closed flock of Cheviot sheep occurs only in specific PrP genotypes', *Arch Virol*, 141: 809-24.
Hunter, N.; Foster, J.; Chong, A.; McCutcheon, S.; Parnham D.; Eaton, S.; MacKenzie, C.; Houston, F. 2002. 'Transmission of prion diseases by blood transfusion', *Journal of General Virology*, 83: 2897-905.
Huzarewich, R. L., S. Medina, C. Robertson, D. Parchaliuk, and S. A. Booth. 2011. 'Transcriptional modulation in a leukocyte-depleted splenic cell population during prion disease', *Journal of toxicology and environmental health. Part A*, 74: 1504-20.
Huzarewich, R. L., C. G. Siemens, and S. A. Booth. 2010. 'Application of "omics" to prion biomarker discovery', *J Biomed Biotechnol*, 2010: 613504.
Hwang, D., I. Y. Lee, H. Yoo, N. Gehlenborg, J. H. Cho, B. Petritis, D. Baxter, R. Pitstick, R. Young, D. Spicer, N. D. Price, J. G. Hohmann, S. J. Dearmond, G. A. Carlson, and L. E. Hood. 2009. 'A systems approach to prion disease', *Mol Syst Biol*, 5: 252.
Ikeda, T., M. Horiuchi, N. Ishiguro, Y. Muramatsu, G. D. Kai-Uwe, and M. Shinagawa. 1995. 'Amino acid polymorphisms of PrP with reference to onset of scrapie in Suffolk and Corriedale sheep in Japan', *J Gen Virol*, 76 (Pt 10): 2577-81.
Imberdis, T., and D. A. Harris. 2014. 'Prion permissive pathways: extracellular matrix genes control susceptibility to prion infection', *Embo j*, 33: 1506-8.
Imran, M., and S. Mahmood. 2011. 'An overview of human prion diseases', *Virol J*, 8: 559.
Ingrosso, L., V. Vetrugno, F. Cardone, and M. Pocchiari. 2002. 'Molecular diagnostics of transmissible spongiform encephalopathies', *Trends Mol Med*, 8: 273-80.
Ironside, J. W., and M. W. Head. 2004. 'Neuropathology and molecular biology of variant Creutzfeldt-Jakob disease', *Curr Top Microbiol Immunol*, 284: 133-59.
Ironside, J. W., L. McCardle, A. Horsburgh, Z. Lim, and M. W. Head. 2002. 'Pathological diagnosis of variant Creutzfeldt-Jakob disease', *Apmis*, 110: 79-87.
Ironside, James W., Matthew T. Bishop, Kelly Connolly, Doha Hegazy, Suzanne Lowrie, Margaret Le Grice, Diane L. Ritchie, Linda M. McCardle, and David A. Hilton. 2006.

'Variant Creutzfeldt-Jakob disease: prion protein genotype analysis of positive appendix tissue samples from a retrospective prevalence study', *BMJ (Clinical research ed.)*, 332: 1186-88.

Jackson, G. S., J. Burk-Rafel, J. A. Edgeworth, A. Sicilia, S. Abdilahi, J. Korteweg, J. Mackey, C. Thomas, G. Wang, J. M. Schott, C. Mummery, P. F. Chinnery, S. Mead, and J. Collinge. 2014. 'Population screening for variant Creutzfeldt-Jakob disease using a novel blood test: diagnostic accuracy and feasibility study', *JAMA Neurol*, 71: 421-8.

Janeway CA Jr, Travers P, Walport M. 2001. *Immunobiology: The Immune System in Health and Disease. Principles of innate and adaptive immunity* (Garland Sciene: New York).

Jayasena, T., A. Poljak, N. Braidy, G. Smythe, M. Raftery, M. Hill, H. Brodaty, J. Trollor, N. Kochan, and P. Sachdev. 2015. 'Upregulation of glycolytic enzymes, mitochondrial dysfunction and increased cytotoxicity in glial cells treated with Alzheimer's disease plasma', *PLoS One*, 10: e0116092.

Jeffrey, M., and L. Gonzalez. 2007. 'Classical sheep transmissible spongiform encephalopathies: pathogenesis, pathological phenotypes and clinical disease', *Neuropathol Appl Neurobiol*, 33: 373-94.

Jeffrey, M., W. G. Halliday, J. Bell, A. R. Johnston, N. K. MacLeod, C. Ingham, A. R. Sayers, D. A. Brown, and J. R. Fraser. 2000. 'Synapse loss associated with abnormal PrP precedes neuronal degeneration in the scrapie-infected murine hippocampus', *Neuropathol Appl Neurobiol*, 26: 41-54.

Jeffrey, M., S. Martin, J. R. Thomson, W. S. Dingwall, I. Begara-McGorum, and L. Gonzalez. 2001. 'Onset and distribution of tissue prp accumulation in scrapie-affected suffolk sheep as demonstrated by sequential necropsies and tonsillar biopsies', *J Comp Pathol*, 125: 48-57.

Jeffrey, M., S. Ryder, S. Martin, S. A. Hawkins, L. Terry, C. Berthelin-Baker, and S. J. Bellworthy. 2001. 'Oral inoculation of sheep with the agent of bovine spongiform encephalopathy (BSE). 1. Onset and distribution of disease-specific PrP accumulation in brain and viscera', *J Comp Pathol*, 124: 280-9.

Jeffrey, M., and G. A. Wells. 1988. 'Spongiform encephalopathy in a nyala (Tragelaphus angasi)', *Vet Pathol*, 25: 398-9.

Jeffrey, Martin, Stuart Martin, Francesca Chianini, Samantha Eaton, Mark P. Dagleish, and Lorenzo González. 2014. 'Incidence of infection in Prnp ARR/ARR sheep following experimental inoculation with or natural exposure to classical scrapie', *PLoS One*, 9: e91026-e26.

Jonckheere, A. I., J. A. Smeitink, and R. J. Rodenburg. 2012. 'Mitochondrial ATP synthase: architecture, function and pathology', *J Inherit Metab Dis*, 35: 211-25.

Joseph, S. B., A. Castrillo, B. A. Laffitte, D. J. Mangelsdorf, and P. Tontonoz. 2003. 'Reciprocal regulation of inflammation and lipid metabolism by liver X receptors', *Nature Medicine*, 9: 213-19.

Joseph, Sean B., Michelle N. Bradley, Antonio Castrillo, Kevin W. Bruhn, Puiying A. Mak, Liming Pei, John Hogenesch, Ryan M. O'Connell, Genhong Cheng, Enrique Saez, Jeffery F. Miller, and Peter Tontonoz. 2004. 'LXR-Dependent Gene Expression Is Important for Macrophage Survival and the Innate Immune Response', *Cell*, 119: 299-309.

Kaatz, M., C. Fast, U. Ziegler, A. Balkema-Buschmann, B. Hammerschmidt, M. Keller, A. Oelschlegel, L. McIntyre, and M. H. Groschup. 2012. 'Spread of classic BSE prions from the gut via the peripheral nervous system to the brain', *Am J Pathol*, 181: 515-24.

Kaneko, N., A. Nakamura, Y. Washimi, T. Kato, T. Sakurai, Y. Arahata, M. Bundo, A. Takeda, S. Niida, K. Ito, K. Toba, K. Tanaka, and K. Yanagisawa. 2014. 'Novel plasma biomarker

surrogating cerebral amyloid deposition', *Proc Jpn Acad Ser B Phys Biol Sci*, 90: 353-64.

Kanu, N.; Imokawa, Y.; Drechsel D. N.; Williamson, A.; Birkett, C. R.; Bostock, C. J.; Brockes, J. P. 2002. 'Transfer of Scrapie Prion Infectivity by Cell Contact in Culture', *Current Biology*, 12: 523-30.

Keane, D., D. Barr, R. Osborn, J. Langenberg, K. O'Rourke, D. Schneider, and P. Bochsler. 2009. 'Validation of use of rectoanal mucosa-associated lymphoid tissue for immunohistochemical diagnosis of chronic wasting disease in white-tailed deer (Odocoileus virginianus)', *J Clin Microbiol*, 47: 1412-7.

Kell, D. B., and S. G. Oliver. 2004. 'Here is the evidence, now what is the hypothesis? The complementary roles of inductive and hypothesis-driven science in the post-genomic era', *Bioessays*, 26: 99-105.

Keller, G., O. Binyamin, K. Frid, A. Saada, and R. Gabizon. 2019. 'Mitochondrial dysfunction in preclinical genetic prion disease: A target for preventive treatment?', *Neurobiol Dis*, 124: 57-66.

Keppler, S. J., M. Burbage, F. Gasparrini, L. Hartjes, S. Aggarwal, M. J. Massaad, R. S. Geha, A. Bruckbauer, and F. D. Batista. 2018. 'The Lack of WIP Binding to Actin Results in Impaired B Cell Migration and Altered Humoral Immune Responses', *Cell Rep*, 24: 619-29.

Kiachopoulos, S., J. Heske, J. Tatzelt, and K. F. Winklhofer. 2004. 'Misfolding of the prion protein at the plasma membrane induces endocytosis, intracellular retention and degradation', *Traffic*, 5: 426-36.

Kim, Hyeon O., Greg P. Snyder, Tyler M. Blazey, Richard E. Race, Bruce Chesebro, and Pamela J. Skinner. 2008. 'Prion disease induced alterations in gene expression in spleen and brain prior to clinical symptoms', *Advances and applications in bioinformatics and chemistry : AABC*, 1: 29-50.

Kim, Seong-Oh, Joonhui Kim, Takaharu Okajima, and Nam-Joon Cho. 2017. 'Mechanical properties of paraformaldehyde-treated individual cells investigated by atomic force microscopy and scanning ion conductance microscopy', *Nano convergence*, 4: 5-5.

Kimberlin, R. H., and C. A. Walker. 1979. 'Pathogenesis of mouse scrapie: dynamics of agent replication in spleen, spinal cord and brain after infection by different routes', *J Comp Pathol*, 89: 551-62.

Kirkwood, and Cunningham. 2007. *Portrait of prion diseases in zoo animals. Prions in humans and animals.* (Berlin).

Kirkwood, J. K., and A. A. Cunningham. 1994. 'Epidemiological observations on spongiform encephalopathies in captive wild animals in the British Isles', *Vet Rec*, 135: 296-303.

Klein, M. A., P. S. Kaeser, P. Schwarz, H. Weyd, I. Xenarios, R. M. Zinkernagel, M. C. Carroll, J. S. Verbeek, M. Botto, M. J. Walport, H. Molina, U. Kalinke, H. Acha-Orbea, and A. Aguzzi. 2001. 'Complement facilitates early prion pathogenesis', *Nat Med*, 7: 488-92.

Klein, Michael A., Rico Frigg, Eckhard Flechsig, Alex J. Raeber, Ulrich Kalinke, Horst Bluethmann, Frank Bootz, Marc Suter, Rolf M. Zinkernagel, and Adriano Aguzzi. 1997. 'A crucial role for B cells in neuroinvasive scrapie', *Nature*, 390: 687.

Klohn, P. C., R. Castro-Seoane, and J. Collinge. 2013. 'Exosome release from infected dendritic cells: a clue for a fast spread of prions in the periphery?', *J Infect*, 67: 359-68.

Klöhn, P.-C., L. Stoltze, E. Flechsig, M. Enari, and C. Weissmann. 2003. 'A quantitative, highly sensitive cell-based infectivity assay for mouse scrapie prions', *Proceedings of the National Academy of Sciences*, 100: 11666-71.

Kocisko, D. A., J. H. Come, S. A. Priola, B. Chesebro, G. J. Raymond, P. T. Lansbury, and B. Caughey. 1994. 'Cell-free formation of protease-resistant prion protein', *Nature*, 370: 471-74.

Kominsky, Douglas J., Eric L. Campbell, and Sean P. Colgan. 2010. 'Metabolic shifts in immunity and inflammation', *Journal of immunology (Baltimore, Md. : 1950)*, 184: 4062-68.

Koncarevic, S., C. Lossner, K. Kuhn, T. Prinz, I. Pike, and H. D. Zucht. 2014. 'In-depth profiling of the peripheral blood mononuclear cells proteome for clinical blood proteomics', *Int J Proteomics*, 2014: 129259.

Kongsbak, Martin, Marina Rode von Essen, Trine Bøegh Levring, Peter Schjerling, Anders Woetmann, Niels Ødum, Charlotte Menné Bonefeld, and Carsten Geisler. 2014. 'Vitamin D-binding protein controls T cell responses to vitamin D', *BMC immunology*, 15: 35-35.

Konold, T., S. J. Moore, S. J. Bellworthy, and H. A. Simmons. 2008. 'Evidence of scrapie transmission via milk', *BMC Vet Res*, 4: 14.

Konold, Timm, S. Jo Moore, Susan J. Bellworthy, Linda A. Terry, Leigh Thorne, Andrew Ramsay, F. Javier Salguero, Marion M. Simmons, and Hugh A. Simmons. 2013. 'Evidence of effective scrapie transmission via colostrum and milk in sheep', *BMC Veterinary Research*, 9: 99-99.

Kooyman, D. L., G. W. Byrne, and J. S. Logan. 1998. 'Glycosyl phosphatidylinositol anchor', *Experimental Nephrology*, 6: 148-51.

Korth, C., P. Streit, and B. Oesch. 1999. "Monoclonal antibodies specific for the native, disease-associated isoform of the prion protein." In *Methods in Enzymology*, 106-22.

Krauss, S., and I. Vorberg. 2013. 'Prions Ex Vivo: What Cell Culture Models Tell Us about Infectious Proteins', *Int J Cell Biol*, 2013: 704546.

Krishnan, K., and P. D. J. Moens. 2009. 'Structure and functions of profilins', *Biophys Rev*, 1: 71-81.

Lacroux, C., E. Comoy, M. Moudjou, A. Perret-Liaudet, S. Lugan, C. Litaise, H. Simmons, C. Jas-Duval, I. Lantier, V. Beringue, M. Groschup, G. Fichet, P. Costes, N. Streichenberger, F. Lantier, J. P. Deslys, D. Vilette, and O. Andreoletti. 2014. 'Preclinical detection of variant CJD and BSE prions in blood', *PLoS Pathog*, 10: e1004202.

Lacroux, C., S. Simon, S. L. Benestad, S. Maillet, J. Mathey, S. Lugan, F. Corbiere, H. Cassard, P. Costes, D. Bergonier, J. L. Weisbecker, T. Moldal, H. Simmons, F. Lantier, C. Feraudet-Tarisse, N. Morel, F. Schelcher, J. Grassi, and O. Andreoletti. 2008. 'Prions in milk from ewes incubating natural scrapie', *PLoS Pathog*, 4: e1000238.

Lacroux, C., D. Vilette, N. Fernandez-Borges, C. Litaise, S. Lugan, N. Morel, F. Corbiere, S. Simon, H. Simmons, P. Costes, J. L. Weisbecker, I. Lantier, F. Lantier, F. Schelcher, J. Grassi, J. Castilla, and O. Andreoletti. 2012. 'Prionemia and leukocyte-platelet-associated infectivity in sheep transmissible spongiform encephalopathy models', *J Virol*, 86: 2056-66.

Lacroux, Caroline, Daisy Bougard, Claire Litaise, Hugh Simmons, Fabien Corbiere, Dominique Dernis, René Tardivel, Nathalie Morel, Stephanie Simon, Séverine Lugan, Pierrette Costes, Jean Louis Weisbecker, François Schelcher, Jacques Grassi, Joliette Coste, and Olivier Andréoletti. 2012. 'Impact of leucocyte depletion and prion reduction filters on TSE blood borne transmission', *PLoS One*, 7: e42019-e19.

Laegreid, W. W., M. L. Clawson, M. P. Heaton, B. T. Green, K. I. O'Rourke, and D. P. Knowles. 2008. 'Scrapie Resistance in ARQ Sheep', *Journal of Virology*, 82: 10318-20.

Langeveld, Jan P. M., Jo H. F. Erkens, Ines Rammel, Jorg G. Jacobs, Aart Davidse, Fred G. van Zijderveld, Alex Bossers, and Hermann Schildorfer. 2011. 'Four independent

molecular prion protein parameters for discriminating new cases of C, L, and h bovine spongiform encephalopathy in cattle', *Journal of clinical microbiology*, 49: 3026-28.

Lashley, Tammaryn, Jonathan M. Schott, Philip Weston, Christina E. Murray, Henny Wellington, Ashvini Keshavan, Sandrine C. Foti, Martha Foiani, Jamie Toombs, Jonathan D. Rohrer, Amanda Heslegrave, and Henrik Zetterberg. 2018. 'Molecular biomarkers of Alzheimer's disease: progress and prospects', *Disease models & mechanisms*, 11: dmm031781.

Lasmezas, C. I., J. P. Deslys, R. Demaimay, K. T. Adjou, F. Lamoury, D. Dormont, O. Robain, J. Ironside, and J. J. Hauw. 1996. 'BSE transmission to macaques', *Nature*, 381: 743-4.

Law, R. H. P., Q. Zhang, S. McGowan, A. M. Buckle, G. A. Silverman, W. Wong, C. J. Rosado, C. G. Langendorf, R. N. Pike, P. I. Bird, and J. C. Whisstock. 2006. 'An overview of the serpin superfamily', *Genome Biol*, 7: 216.

Le Dur, Annick, Vincent Béringue, Olivier Andréoletti, Fabienne Reine, Thanh Lan Laï, Thierry Baron, Bjørn Bratberg, Jean-Luc Vilotte, Pierre Sarradin, Sylvie L. Benestad, and Hubert Laude. 2005. 'A newly identified type of scrapie agent can naturally infect sheep with resistant PrP genotypes', *Proceedings of the National Academy of Sciences of the United States of America*, 102: 16031-36.

Lewis, V., A. F. Hill, C. L. Haigh, G. M. Klug, C. L. Masters, V. A. Lawson, and S. J. Collins. 2009. 'Increased proportions of C1 truncated prion protein protect against cellular M1000 prion infection', *J Neuropathol Exp Neurol*, 68: 1125-35.

Lezmi, S., A. Bencsik, E. Monks, T. Petit, and T. Baron. 2003. 'First case of feline spongiform encephalopathy in a captive cheetah born in France: PrP(sc) analysis in various tissues revealed unexpected targeting of kidney and adrenal gland', *Histochem Cell Biol*, 119: 415-22.

Li, J., W. Yin, Y. Jing, D. Kang, L. Yang, J. Cheng, Z. Yu, Z. Peng, X. Li, Y. Wen, X. Sun, B. Ren, and C. Liu. 2018. 'The Coordination Between B Cell Receptor Signaling and the Actin Cytoskeleton During B Cell Activation', *Front Immunol*, 9: 3096.

Liberski, P. P., and J. W. Ironside. 2004. 'An outline of the neuropathology of transmissible spongiform encephalopathies (prion diseases)', *Folia Neuropathol*, 42 Suppl B: 39-58.

Ligios, C., C. J. Sigurdson, C. Santucciu, G. Carcassola, G. Manco, M. Basagni, C. Maestrale, M. G. Cancedda, L. Madau, and A. Aguzzi. 2005. 'PrPSc in mammary glands of sheep affected by scrapie and mastitis', *Nat Med*, 11: 1137-8.

Lim, Kwang Hun, Anvesh K. R. Dasari, Ivan Hung, Zhehong Gan, Jeffery W. Kelly, and David E. Wemmer. 2016. 'Structural Changes Associated with Transthyretin Misfolding and Amyloid Formation Revealed by Solution and Solid-State NMR', *Biochemistry*, 55: 1941-44.

Linden, R., V. R. Martins, M. A. Prado, M. Cammarota, I. Izquierdo, and R. R. Brentani. 2008. 'Physiology of the prion protein', *Physiol Rev*, 88: 673-728.

Liu, Xinyu. 2019. 'New advances in analytical methods for mass spectrometry-based large-scale metabolomics study', *Trends in analytical chemistry*, v. 121: 2019 v.121.

Llewelyn, C. A., P. E. Hewitt, R. S. G. Knight, K. Amar, S. Cousens, J. Mackenzie, and R. G. Will. 2004. 'Possible transmission of variant Creutzfeldt-Jakob disease by blood transfusion', *The Lancet*, 363: 417-21.

Lowe, R., N. Shirley, M. Bleackley, S. Dolan, and T. Shafee. 2017. 'Transcriptomics technologies', *PLoS Comput Biol*, 13: e1005457.

Lu, Jinghua, Kristopher Marjon, Lorraine Marnell, Carolyn Mold, Terry Du Clos, and Peter Sun. 2011. 'The Structure and Function of Acute Phase Proteins: C-Reactive Protein

and Serum Amyloid A in Innate Immunity (110.21)', *The Journal of Immunology*, 186: 110.21-10.21.
Lucassen, P. J., A. Williams, W. C. J. Chung, and H. Fraser. 1995. 'Detection of apoptosis in murine scrapie', *Neuroscience Letters*, 198: 185-88.
Lunnon, K., Z. Ibrahim, P. Proitsi, A. Lourdusamy, S. Newhouse, M. Sattlecker, S. Furney, M. Saleem, H. Soininen, I. Kloszewska, P. Mecocci, M. Tsolaki, B. Vellas, G. Coppola, D. Geschwind, A. Simmons, S. Lovestone, R. Dobson, and A. Hodges. 2012. 'Mitochondrial dysfunction and immune activation are detectable in early Alzheimer's disease blood', *J Alzheimers Dis*, 30: 685-710.
Ma, J. 2012. 'The role of cofactors in prion propagation and infectivity', *PLoS Pathog*, 8: e1002589.
Maas, E., M. Geissen, M. H. Groschup, R. Rost, T. Onodera, H. Schatzl, and I. M. Vorberg. 2007. 'Scrapie infection of prion protein-deficient cell line upon ectopic expression of mutant prion proteins', *J Biol Chem*, 282: 18702-10.
Mabbott, N. A. 2017. 'How do PrP(Sc) Prions Spread between Host Species, and within Hosts?', *Pathogens*, 6.
Mabbott, N. A., M. E. Bruce, M. Botto, M. J. Walport, and M. B. Pepys. 2001. 'Temporary depletion of complement component C3 or genetic deficiency of C1q significantly delays onset of scrapie', *Nat Med*, 7: 485-7.
Mabbott, N. A., and G. G. MacPherson. 2006. 'Prions and their lethal journey to the brain', *Nat Rev Microbiol*, 4: 201-11.
Mabbott, Neil A., J. Kenneth Baillie, Atsushi Kobayashi, David S. Donaldson, Hitoshi Ohmori, Sun-Ok Yoon, Arnold S. Freedman, Tom C. Freeman, and Kim M. Summers. 2011. 'Expression of mesenchyme-specific gene signatures by follicular dendritic cells: insights from the meta-analysis of microarray data from multiple mouse cell populations', *Immunology*, 133: 482-98.
Mabbott, Neil A., Fabienne Mackay, Fiona Minns, and Moira E. Bruce. 2000. 'Temporary inactivation of follicular dendritic cells delays neuroinvasion of scrapie', *Nature Medicine*, 6: 719.
Mabbott, Neil A., Alun Williams, Christine F. Farquhar, Manolis Pasparakis, Giorgos Kollias, and Moira E. Bruce. 2000. 'Tumor Necrosis Factor Alpha-Deficient, but Not Interleukin-6-Deficient, Mice Resist Peripheral Infection with Scrapie', *Journal of Virology*, 74: 3338-44.
MacGregor, I., J. Hope, G. Barnard, L. Kirby, O. Drummond, D. Pepper, V. Hornsey, R. Barclay, H. Bessos, M. Turner, and C. Prowse. 1999. 'Application of a time-resolved fluoroimmunoassay for the analysis of normal prion protein in human blood and its components', *Vox Sang*, 77: 88-96.
Mackay, Fabienne, and Jeffrey L. Browning. 1998. 'Turning off follicular dendritic cells', *Nature*, 395: 26.
Macron, C., L. Lane, A. Núñez Galindo, and L. Dayon. 2018. 'Deep Dive on the Proteome of Human Cerebrospinal Fluid: A Valuable Data Resource for Biomarker Discovery and Missing Protein Identification', *J Proteome Res*, 17: 4113-26.
Maddison, B. C., J. P. Owen, K. Bishop, G. Shaw, H. C. Rees, and K. C. Gough. 2010. 'The interaction of ruminant PrP(Sc) with soils is influenced by prion source and soil type', *Environ Sci Technol*, 44: 8503-8.
Makarava, N., and I. V. Baskakov. 2008. 'Expression and purification of full-length recombinant PrP of high purity', *Methods Mol Biol*, 459: 131-43.
Manson, J., J. D. West, V. Thomson, P. McBride, M. H. Kaufman, and J. Hope. 1992. 'The prion protein gene: a role in mouse embryogenesis?', *Development*, 115: 117-22.

Manuelidis, L., T. Chakrabarty, K. Miyazawa, N. A. Nduom, and K. Emmerling. 2009. 'The kuru infectious agent is a unique geographic isolate distinct from Creutzfeldt-Jakob disease and scrapie agents', *Proc Natl Acad Sci U S A*, 106: 13529-34.

Manuelidis, L., I. Zaitsev, P. Koni, Z. Y. Lu, R. A. Flavell, and W. Fritch. 2000. 'Follicular dendritic cells and dissemination of Creutzfeldt-Jakob disease', *Journal of Virology*, 74: 8614-22.

Manzoni, Claudia, Demis A Kia, Jana Vandrovcova, John Hardy, Nicholas W Wood, Patrick A Lewis, and Raffaele Ferrari. 2016. 'Genome, transcriptome and proteome: the rise of omics data and their integration in biomedical sciences', *Briefings in Bioinformatics*, 19: 286-302.

Mathews, D., and D. H. Unwin. 2001. 'Quantitative cerebral blood flow imaging in a patient with the Heidenhain variant of Creutzfeldt-Jakob disease', *Clin Nucl Med*, 26: 770-3.

Mathiason, C. K., J. Hayes-Klug, S. A. Hays, J. Powers, D. A. Osborn, S. J. Dahmes, K. V. Miller, R. J. Warren, G. L. Mason, G. C. Telling, A. J. Young, and E. A. Hoover. 2010. 'B cells and platelets harbor prion infectivity in the blood of deer infected with chronic wasting disease', *J Virol*, 84: 5097-107.

Mathiason, C. K., S. A. Hays, J. Powers, J. Hayes-Klug, J. Langenberg, S. J. Dahmes, D. A. Osborn, K. V. Miller, R. J. Warren, G. L. Mason, and E. A. Hoover. 2009. 'Infectious prions in pre-clinical deer and transmission of chronic wasting disease solely by environmental exposure', *PLoS One*, 4: e5916.

Matsuda, M., K. Tabata, T. Hattori, J. Miki, and S. Ikeda. 2001. 'Brain SPECT with 123I-IMP for the early diagnosis of Creutzfeldt-Jakob disease', *J Neurol Sci*, 183: 5-12.

McCulloch, L., K. L. Brown, B. M. Bradford, J. Hopkins, M. Bailey, K. Rajewsky, J. C. Manson, and N. A. Mabbott. 2011. 'Follicular dendritic cell-specific prion protein (PrP) expression alone is sufficient to sustain prion infection in the spleen', *PLoS Pathog*, 7: e1002402.

McCutcheon, S., J. P. Langeveld, B. C. Tan, A. C. Gill, C. de Wolf, S. Martin, L. Gonzalez, J. Alibhai, A. R. Blanco, L. Campbell, N. Hunter, and E. F. Houston. 2014. 'Prion protein-specific antibodies that detect multiple TSE agents with high sensitivity', *PLoS One*, 9: e91143.

McCutcheon, Sandra, Anthony Richard Alejo Blanco, E. Fiona Houston, Christopher de Wolf, Boon Chin Tan, Antony Smith, Martin H. Groschup, Nora Hunter, Valerie S. Hornsey, Ian R. MacGregor, Christopher V. Prowse, Marc Turner, and Jean C. Manson. 2011. 'All Clinically-Relevant Blood Components Transmit Prion Disease following a Single Blood Transfusion: A Sheep Model of vCJD', *PLoS One*, 6: e23169.

McFarlin, D. E., M. C. Raff, E. Simpson, and S. H. Nehlsen. 1971. 'Scrapie in Immunologically Deficient Mice', *Nature*, 233: 336.

McGeer, P. L., and E. G. McGeer. 2002. 'The possible role of complement activation in Alzheimer disease', *Trends in Molecular Medicine*, 8: 519-23.

McGuire, L. I., A. H. Peden, C. D. Orrú, J. M. Wilham, N. E. Appleford, G. Mallinson, M. Andrews, M. W. Head, B. Caughey, R. G. Will, R. S. Knight, and A. J. Green. 2012. 'Real time quaking-induced conversion analysis of cerebrospinal fluid in sporadic Creutzfeldt-Jakob disease', *Ann Neurol*, 72: 278-85.

Meier, Shelby, Michelle Bell, Danielle N. Lyons, Alexandria Ingram, Jing Chen, John C. Gensel, Haining Zhu, Peter T. Nelson, and Jose F. Abisambra. 2015. 'Identification of Novel Tau Interactions with Endoplasmic Reticulum Proteins in Alzheimer's Disease Brain', *Journal of Alzheimer's disease : JAD*, 48: 687-702.

Meling, Siv, Kjetil Bårdsen, and Martha J. Ulvund. 2012. 'Presence of an acute phase response in sheep with clinical classical scrapie', *BMC Veterinary Research*, 8: 113.

Middleton, Jim, Angela M. Patterson, Lucy Gardner, Caroline Schmutz, and Brian A. Ashton. 2002. 'Leukocyte extravasation: chemokine transport and presentation by the endothelium', *Blood*, 100: 3853-60.

Minter, M. R., C. Zhang, V. Leone, D. L. Ringus, X. Zhang, P. Oyler-Castrillo, M. W. Musch, F. Liao, J. F. Ward, D. M. Holtzman, E. B. Chang, R. E. Tanzi, and S. S. Sisodia. 2016. 'Antibiotic-induced perturbations in gut microbial diversity influences neuro-inflammation and amyloidosis in a murine model of Alzheimer's disease', *Sci Rep*, 6: 30028.

Mitchell, G. B., K. I. O'Rourke, N. P. Harrington, A. Soutyrine, M. M. Simmons, S. Dudas, D. Zhuang, H. Laude, and A. Balachandran. 2010. 'Identification of atypical scrapie in Canadian sheep', *J Vet Diagn Invest*, 22: 408-11.

Miyazawa, K., T. Kanaya, S. Tanaka, I. Takakura, K. Watanabe, S. Ohwada, H. Kitazawa, M. T. Rose, S. Sakaguchi, S. Katamine, T. Yamaguchi, and H. Aso. 2007. 'Immunohistochemical characterization of cell types expressing the cellular prion protein in the small intestine of cattle and mice', *Histochem Cell Biol*, 127: 291-301.

Moda, F., P. Gambetti, S. Notari, L. Concha-Marambio, M. Catania, K. W. Park, E. Maderna, S. Suardi, S. Haik, J. P. Brandel, J. Ironside, R. Knight, F. Tagliavini, and C. Soto. 2014. 'Prions in the urine of patients with variant Creutzfeldt-Jakob disease', *N Engl J Med*, 371: 530-9.

Mohan, J., M. E. Bruce, and N. A. Mabbott. 2005. 'Follicular dendritic cell dedifferentiation reduces scrapie susceptibility following inoculation via the skin', *Immunology*, 114: 225-34.

Mok, Simon W. F., Richard L. Proia, Volker Brinkmann, and Neil A. Mabbott. 2012. 'B cell-specific S1PR1 deficiency blocks prion dissemination between secondary lymphoid organs', *Journal of immunology (Baltimore, Md. : 1950)*, 188: 5032-40.

Mok, T. H., and S. Mead. 2020. 'Preclinical biomarkers of prion infection and neurodegeneration', *Curr Opin Neurobiol*, 61: 82-88.

Mok, T., Z. Jaunmuktane, S. Joiner, T. Campbell, C. Morgan, B. Wakerley, F. Golestani, P. Rudge, S. Mead, H. R. Jager, J. D. Wadsworth, S. Brandner, and J. Collinge. 2017. 'Variant Creutzfeldt-Jakob Disease in a Patient with Heterozygosity at PRNP Codon 129', *N Engl J Med*, 376: 292-94.

Moldovan, L., K. E. Batte, J. Trgovcich, J. Wisler, C. B. Marsh, and M. Piper. 2014. 'Methodological challenges in utilizing miRNAs as circulating biomarkers', *J Cell Mol Med*, 18: 371-90.

Montrasio, F., R. Frigg, M. Glatzel, M. A. Klein, F. Mackay, A. Aguzzi, and C. Weissmann. 2000. 'Impaired prion replication in spleens of mice lacking functional follicular dendritic cells', *Science (New York, N.Y.)*, 288: 1257-59.

Montrasio, Fabio, Antonio Cozzio, Eckhard Flechsig, Daniela Rossi, Michael A. Klein, Thomas Rülicke, Alex J. Raeber, Christian A. J. Vosshenrich, Juliane Proft, Adriano Aguzzi, and Charles Weissmann. 2001. 'B lymphocyte-restricted expression of prion protein does not enable prion replication in prion protein knockout mice', *Proceedings of the National Academy of Sciences*, 98: 4034-37.

Moore, R. A., D. E. Sturdevant, B. Chesebro, and S. A. Priola. 2014. 'Proteomics analysis of amyloid and nonamyloid prion disease phenotypes reveals both common and divergent mechanisms of neuropathogenesis', *J Proteome Res*, 13: 4620-34.

Morris, R. J., C. J. Parkyn, and A. Jen. 2006. 'Traffic of prion protein between different compartments on the neuronal surface, and the propagation of prion disease', *FEBS Lett*, 580: 5565-71.

Moxon, J. V., M. P. Padula, B. R. Herbert, and J. Golledge. 2009. 'Challenges, Current Status and Future Perspectives of Proteomics in Improving Understanding, Diagnosis and

Treatment of Vascular Disease', *European Journal of Vascular and Endovascular Surgery*, 38: 346-55.
Muenchhoff, J., A. Poljak, A. Thalamuthu, V. B. Gupta, P. Chatterjee, M. Raftery, C. L. Masters, J. C. Morris, R. J. Bateman, A. M. Fagan, R. N. Martins, and P. S. Sachdev. 2016. 'Changes in the plasma proteome at asymptomatic and symptomatic stages of autosomal dominant Alzheimer's disease', *Sci Rep*, 6: 29078.
Muffat, J., and D. W. Walker. 2010. 'Apolipoprotein D: an overview of its role in aging and age-related diseases', *Cell Cycle*, 9: 269-73.
Muller, W. A. 2013. 'Getting leukocytes to the site of inflammation', *Veterinary pathology*, 50: 7-22.
Nägga, K., O. Hansson, D. van Westen, L. Minthon, and M. Wennström. 2014. 'Increased levels of hyaluronic acid in cerebrospinal fluid in patients with vascular dementia', *J Alzheimers Dis*, 42: 1435-41.
Nakamura, A., N. Kaneko, V. L. Villemagne, T. Kato, J. Doecke, V. Dore, C. Fowler, Q. X. Li, R. Martins, C. Rowe, T. Tomita, K. Matsuzaki, K. Ishii, K. Ishii, Y. Arahata, S. Iwamoto, K. Ito, K. Tanaka, C. L. Masters, and K. Yanagisawa. 2018. 'High performance plasma amyloid-beta biomarkers for Alzheimer's disease', *Nature*, 554: 249-54.
Naslavsky, N., R. Stein, A. Yanai, G. Friedlander, and A. Taraboulos. 1997. 'Characterization of detergent-insoluble complexes containing the cellular prion protein and its scrapie isoform', *J Biol Chem*, 272: 6324-31.
NCJDRSU, The National CJD Research and Surveillance Unit. 2013. 'Creutzfeldt-Jakob Disease Surveillance in the UK'. https://www.cjd.ed.ac.uk/sites/default/files/report22.pdf.
———. 2017. 'Referral System, Data and Reports, Diagnosis and Testing'.
Neale, M. H., S. J. Mountjoy, J. C. Edwards, D. Vilette, H. Laude, O. Windl, and G. C. Saunders. 2010. 'Infection of cell lines with experimental and natural ovine scrapie agents', *J Virol*, 84: 2444-52.
Newaz, Khalique, K. Sriram, and Debajyoti Bera. 2015. 'Identification of Major Signaling Pathways in Prion Disease Progression Using Network Analysis', *PLoS One*, 10: e0144389-e89.
Nguyen, T. P., L. Caberlotto, M. J. Morine, and C. Priami. 2014. 'Network analysis of neurodegenerative disease highlights a role of Toll-like receptor signaling', *Biomed Res Int*, 2014: 686505.
NHS, National Health Service, Blood and Transport. 2018. 'Transfusion FAQs '. https://www.nhsbt.nhs.uk/what-we-do/blood-services/blood-transfusion/transfusion-faqs/.
NICE, The National Institute for Health and Care Excellence. 2015. 'Blood transfusion'. https://www.nice.org.uk/guidance/ng24/chapter/context.
Nordengen, K., B. E. Kirsebom, K. Henjum, P. Selnes, B. Gisladottir, M. Wettergreen, S. B. Torsetnes, G. R. Grontvedt, K. K. Waterloo, D. Aarsland, L. N. G. Nilsson, and T. Fladby. 2019. 'Glial activation and inflammation along the Alzheimer's disease continuum', *J Neuroinflammation*, 16: 46.
Norsworthy, Penny, Andrew Thompson, Tze Mok, Ross Paterson, Jonathan Schott, John Collinge, Simon Mead, and Emmanuelle Viré. 2020. *A blood miRNA signature associates with sporadic Creutzfeldt-Jakob disease diagnosis and rate of progression*.
Nourshargh, Sussan, and Ronen Alon. 2014. 'Leukocyte Migration into Inflamed Tissues', *Immunity*, 41: 694-707.
Nozaki, I., T. Hamaguchi, N. Sanjo, M. Noguchi-Shinohara, K. Sakai, Y. Nakamura, T. Sato, T. Kitamoto, H. Mizusawa, F. Moriwaka, Y. Shiga, Y. Kuroiwa, M. Nishizawa, S. Kuzuhara, T. Inuzuka, M. Takeda, S. Kuroda, K. Abe, H. Murai, S. Murayama, J.

Tateishi, I. Takumi, S. Shirabe, M. Harada, A. Sadakane, and M. Yamada. 2010. 'Prospective 10-year surveillance of human prion diseases in Japan', *Brain*, 133: 3043-57.

Nunnari, J., and A. Suomalainen. 2012. 'Mitochondria: In sickness and in health', *Cell*, 148: 1145-59.

O'Rourke, K. I., J. V. Duncan, J. R. Logan, A. K. Anderson, D. K. Norden, E. S. Williams, B. A. Combs, R. H. Stobart, G. E. Moss, and D. L. Sutton. 2002. 'Active surveillance for scrapie by third eyelid biopsy and genetic susceptibility testing of flocks of sheep in Wyoming', *Clin Diagn Lab Immunol*, 9: 966-71.

Ogbonnaya, E. S., G. Clarke, F. Shanahan, T. G. Dinan, J. F. Cryan, and O. F. O'Leary. 2015. 'Adult Hippocampal Neurogenesis Is Regulated by the Microbiome', *Biol Psychiatry*, 78: e7-9.

Okroj, M., E. Holmquist, J. Sjolander, L. Corrales, T. Saxne, H. G. Wisniewski, and A. M. Blom. 2012. 'Heavy chains of inter alpha inhibitor (IalphaI) inhibit the human complement system at early stages of the cascade', *J Biol Chem*, 287: 20100-10.

Olsson, B., R. Lautner, U. Andreasson, A. Ohrfelt, E. Portelius, M. Bjerke, M. Holtta, C. Rosen, C. Olsson, G. Strobel, E. Wu, K. Dakin, M. Petzold, K. Blennow, and H. Zetterberg. 2016. 'CSF and blood biomarkers for the diagnosis of Alzheimer's disease: a systematic review and meta-analysis', *Lancet Neurol*, 15: 673-84.

Omenn, Gilbert S. 2009. 'A landmark systems analysis of prion disease of the brain', *Molecular systems biology*, 5: 254-54.

Orrú, Christina D., Jason M. Wilham, Lynne D. Raymond, Franziska Kuhn, Björn Schroeder, Alex J. Raeber, and Byron Caughey. 2011. 'Prion Disease Blood Test Using Immunoprecipitation and Improved Quaking-Induced Conversion', *mBio*, 2.

Otto, M., J. Wiltfang, L. Cepek, M. Neumann, B. Mollenhauer, P. Steinacker, B. Ciesielczyk, W. Schulz-Schaeffer, H. A. Kretzschmar, and S. Poser. 2002. 'Tau protein and 14-3-3 protein in the differential diagnosis of Creutzfeldt-Jakob disease', *Neurology*, 58: 192-7.

Ovod, V., K. N. Ramsey, K. G. Mawuenyega, J. G. Bollinger, T. Hicks, T. Schneider, M. Sullivan, K. Paumier, D. M. Holtzman, J. C. Morris, T. Benzinger, A. M. Fagan, B. W. Patterson, and R. J. Bateman. 2017. 'Amyloid beta concentrations and stable isotope labeling kinetics of human plasma specific to central nervous system amyloidosis', *Alzheimers Dement*, 13: 841-49.

Palmer, M. S., A. J. Dryden, J. T. Hughes, and J. Collinge. 1991. 'Homozygous prion protein genotype predisposes to sporadic Creutzfeldt-Jakob disease', *Nature*, 352: 340-2.

Paquet, S., N. Daude, M. P. Courageot, J. Chapuis, H. Laude, and D. Vilette. 2007. 'PrPc does not mediate internalization of PrPSc but is required at an early stage for de novo prion infection of Rov cells', *J Virol*, 81: 10786-91.

Paquet, S., C. Langevin, J. Chapuis, G. S. Jackson, H. Laude, and D. Vilette. 2007. 'Efficient dissemination of prions through preferential transmission to nearby cells', *J Gen Virol*, 88: 706-13.

Parikh, Rajul, Annie Mathai, Shefali Parikh, G. Chandra Sekhar, and Ravi Thomas. 2008. 'Understanding and using sensitivity, specificity and predictive values', *Indian journal of ophthalmology*, 56: 45-50.

Park, J. H., Y. G. Choi, Y. J. Lee, S. J. Park, H. S. Choi, K. C. Choi, E. K. Choi, and Y. S. Kim. 2016. 'Real-Time Quaking-Induced Conversion Analysis for the Diagnosis of Sporadic Creutzfeldt-Jakob Disease in Korea', *J Clin Neurol*, 12: 101-6.

Parveen, I., J. Moorby, G. Allison, and R. Jackman. 2005. 'The use of non-prion biomarkers for the diagnosis of Transmissible Spongiform Encephalopathies in the live animal', *Vet Res*, 36: 665-83.

Pastrana, M. A., G. Sajnani, B. Onisko, J. Castilla, R. Morales, C. Soto, and J. R. Requena. 2006. 'Isolation and characterization of a proteinase K-sensitive PrPSc fraction', *Biochemistry*, 45: 15710-7.

Patel, N. V., and B. M. Forman. 2004. 'Linking lipids, Alzheimer's and LXRs?', *Nucl Recept Signal*, 2: e001.

Pattison, I. H. 1965. 'Resistance of the scrapie agent to formalin', *Journal of Comparative Pathology*, 75: 159-64.

Peden, A. H., M. W. Head, D. L. Ritchie, P. J. E. Bell, and P. J. W. Ironside. 2004. 'Preclinical vCJD after blood transfusion in a PRNP codon 129 heterozygous patient', *Lancet*, 364: 527-29.

Perrin, R. J., R. Craig-Schapiro, J. P. Malone, A. R. Shah, P. Gilmore, A. E. Davis, C. M. Roe, E. R. Peskind, G. Li, D. R. Galasko, C. M. Clark, J. F. Quinn, J. A. Kaye, J. C. Morris, D. M. Holtzman, R. R. Townsend, and A. M. Fagan. 2011. 'Identification and validation of novel cerebrospinal fluid biomarkers for staging early Alzheimer's disease', *PLoS One*, 6: e16032.

Phadwal, K., D. Kurian, M. K. F. Salamat, V. E. MacRae, A. B. Diack, and J. C. Manson. 2018. 'Spermine increases acetylation of tubulins and facilitates autophagic degradation of prion aggregates', *Sci Rep*, 8: 10004.

PHE, Public Health England. 2016 'Summary results of the third national survey of abnormal prion prevalence in archived appendix specimens '.

Piccardo, Pedro, Jean C. Manson, Declan King, Bernardino Ghetti, and Rona M. Barron. 2007. 'Accumulation of prion protein in the brain that is not associated with transmissible disease', *Proceedings of the National Academy of Sciences*, 104: 4712-17.

Pitt, James J. 2009. 'Principles and applications of liquid chromatography-mass spectrometry in clinical biochemistry', *The Clinical biochemist. Reviews*, 30: 19-34.

Piubelli, C., M. Fiorini, G. Zanusso, A. Milli, E. Fasoli, S. Monaco, and P. G. Righetti. 2006. 'Searching for markers of Creutzfeldt-Jakob disease in cerebrospinal fluid by two-dimensional mapping', *Proteomics*, 6 Suppl 1: S256-61.

Priemer, Grit, Anne Balkema-Buschmann, Bob Hills, and Martin H. Groschup. 2013. 'Biochemical Characteristics and PrP(Sc) Distribution Pattern in the Brains of Cattle Experimentally Challenged with H-type and L-type Atypical BSE', *PLoS One*, 8: e67599-e99.

Pritzkow, S., R. Morales, F. Moda, U. Khan, G. C. Telling, E. Hoover, and C. Soto. 2015. 'Grass plants bind, retain, uptake, and transport infectious prions', *Cell Rep*, 11: 1168-75.

Prusiner, S. B. 1998. 'Prions', *Proc Natl Acad Sci U S A*, 95: 13363-83.

Prusiner, Stanley B., Amanda L. Woerman, Daniel A. Mordes, Joel C. Watts, Ryan Rampersaud, David B. Berry, Smita Patel, Abby Oehler, Jennifer K. Lowe, Stephanie N. Kravitz, Daniel H. Geschwind, David V. Glidden, Glenda M. Halliday, Lefkos T. Middleton, Steve M. Gentleman, Lea T. Grinberg, and Kurt Giles. 2015. 'Evidence for α-synuclein prions causing multiple system atrophy in humans with parkinsonism', *Proceedings of the National Academy of Sciences*, 112: E5308-E17.

Puig, B., and I. Ferrer. 2001. 'Cell death signaling in the cerebellum in Creutzfeldt-Jakob disease', *Acta Neuropathologica*, 102: 207-15.

Qiagen. 2012. 'IPA Training: Maximizing the Biological Interpretation of Gene, Transcript & Protein Expression Data with IPA', Accessed 01/01/2020. https://bioinformatics.rockefeller.edu/wp-content/uploads/IPA-Training-Dev.pdf.

Race, R. E., L. H. Fadness, and B. Chesebro. 1987. 'Characterization of scrapie infection in mouse neuroblastoma cells', *J Gen Virol*, 68 (Pt 5): 1391-9.

Raeber, A. J.; Klein M. A.; Frigg, R.; Flechsig, E.; Aguzzi, A.; Weissmann, C. 1999. 'PrP-dependent association of prions with splenic but not circulating lymphocytes of scrapie-infected mice', *The EMBO Journal*, 18: 2702-06.

Ramadori, G., and B. Christ. 1999. 'Cytokines and the hepatic acute-phase response', *Semin Liver Dis*, 19: 141-55.

Rappsilber, J., M. Mann, and Y. Ishihama. 2007. 'Protocol for micro-purification, enrichment, pre-fractionation and storage of peptides for proteomics using StageTips', *Nature Protocols*, 2: 1896-906.

Raymond, C. R., P. Aucouturier, and N. A. Mabbott. 2007. 'In vivo depletion of CD11c+ cells impairs scrapie agent neuroinvasion from the intestine', *J Immunol*, 179: 7758-66.

Riek, R., S. Hornemann, G. Wider, R. Glockshuber, and K. Wuthrich. 1997. 'NMR characterization of the full-length recombinant murine prion protein, mPrP(23-231)', *FEBS Lett*, 413: 282-8.

Riemer, C., S. Neidhold, M. Burwinkel, A. Schwarz, J. Schultz, J. Kratzschmar, U. Monning, and M. Baier. 2004. 'Gene expression profiling of scrapie-infected brain tissue', *Biochem Biophys Res Commun*, 323: 556-64.

Riesner, D. 2003a. 'Biochemistry and structure of PrP(C) and PrP(Sc)', *Br Med Bull*, 66: 21-33.

———. 2003b. 'Biochemistry and structure of PrP^{C} and PrP^{Sc}', *British Medical Bulletin*, 66: 21-33.

Rifai, N., M. A. Gillette, and S. A. Carr. 2006. 'Protein biomarker discovery and validation: the long and uncertain path to clinical utility', *Nat Biotechnol*, 24: 971-83.

Roszer, T., M. P. Menendez-Gutierrez, M. Cedenilla, and M. Ricote. 2013. 'Retinoid X receptors in macrophage biology', *Trends Endocrinol Metab*, 24: 460-8.

Rubenstein, R. 2012. 'Proteomic analysis of prion diseases: creating clarity or causing confusion?', *Electrophoresis*, 33: 3631-43.

Rudd, P. M., T. Endo, C. Colominas, D. Groth, S. F. Wheeler, D. J. Harvey, M. R. Wormald, H. Serban, S. B. Prusiner, A. Kobata, and R. A. Dwek. 1999. 'Glycosylation differences between the normal and pathogenic prion protein isoforms', *Proc Natl Acad Sci U S A*, 96: 13044-9.

Ryckman, C., K. Vandal, P. Rouleau, M. Talbot, and P. A. Tessier. 2003. 'Proinflammatory activities of S100: proteins S100A8, S100A9, and S100A8/A9 induce neutrophil chemotaxis and adhesion', *J Immunol*, 170: 3233-42.

Saa, P., J. Castilla, and C. Soto. 2006. 'Presymptomatic detection of prions in blood', *Science (New York, N.Y.)*, 313: 92-4.

Saá, Paula, Joaquín Castilla, and Claudio Soto. 2006. 'Presymptomatic Detection of Prions in Blood', *Science (New York, N.Y.)*, 313: 92-94.

Saba, R., and S. A. Booth. 2013. 'The Genetics of Susceptibility to Variant Creutzfeldt-Jakob Disease', *Public Health Genomics*, 16: 17-24.

SaBTO, Advisory Committee on the Safety of Blood, Tissues and Organs. 2015. 'Measures currently in place in the UK to reduce the potential risk of tranmitting variant Creutzfeldt-Jakob disease via blood'. https://assets.publishing.service.gov.uk/government/uploads/system/uploads/attachment_data/file/407681/measures-vcjd.pdf.

Sajnani, Gustavo, and Jesús R. Requena. 2012. 'Prions, proteinase K and infectivity', *Prion*, 6: 430-32.

Salamat, Muhammad K., Michel Dron, Jérôme Chapuis, Christelle Langevin, and Hubert Laude. 2011. 'Prion propagation in cells expressing PrP glycosylation mutants', *Journal of Virology*, 85: 3077-85.

Sales, N., K. Rodolfo, R. Hassig, B. Faucheux, L. Di Giamberardino, and K. L. Moya. 1998. 'Cellular prion protein localization in rodent and primate brain', *Eur J Neurosci*, 10: 2464-71.

Sampson, T. R., J. W. Debelius, T. Thron, S. Janssen, G. G. Shastri, Z. E. Ilhan, C. Challis, C. E. Schretter, S. Rocha, V. Gradinaru, M. F. Chesselet, A. Keshavarzian, K. M. Shannon, R. Krajmalnik-Brown, P. Wittung-Stafshede, R. Knight, and S. K. Mazmanian. 2016. 'Gut Microbiota Regulate Motor Deficits and Neuroinflammation in a Model of Parkinson's Disease', *Cell*, 167: 1469-80.e12.

Sanchez-Alavez, M., B. Conti, G. Moroncini, and J. R. Criado. 2007. 'Contributions of neuronal prion protein on sleep recovery and stress response following sleep deprivation', *Brain Res*, 1158: 71-80.

Sasaki, T., K. Mann, G. Murphy, M. L. Chu, and R. Timpl. 1996. 'Different susceptibilities of fibulin-1 and fibulin-2 to cleavage by matrix metalloproteinases and other tissue proteases', *Eur J Biochem*, 240: 427-34.

Satoh, J., K. Kurohara, M. Yukitake, and Y. Kuroda. 1999. 'The 14-3-3 protein detectable in the cerebrospinal fluid of patients with prion-unrelated neurological diseases is expressed constitutively in neurons and glial cells in culture', *Eur Neurol*, 41: 216-25.

Sawiris, G. P., K. G. Becker, E. J. Elliott, R. Moulden, and R. G. Rohwer. 2007. 'Molecular analysis of bovine spongiform encephalopathy infection by cDNA arrays', *J Gen Virol*, 88: 1356-62.

Sawyer, E. B., J. A. Edgeworth, C. Thomas, J. Collinge, and G. S. Jackson. 2015. 'Preclinical detection of infectivity and disease-specific PrP in blood throughout the incubation period of prion disease', *Sci Rep*, 5: 17742.

Schaller, O., R. Fatzer, M. Stack, J. Clark, W. Cooley, K. Biffiger, S. Egli, M. Doherr, M. Vandevelde, D. Heim, B. Oesch, and M. Moser. 1999. 'Validation of a Western immunoblotting procedure for bovine PrPSc detection and its use as a rapid surveillance method for the diagnosis of bovine spongiform encephalopathy (BSE)', *Acta Neuropathologica*, 98: 437-43.

Schmidt, Timothy H., Oliver Bannard, Elizabeth E. Gray, and Jason G. Cyster. 2013. 'CXCR4 promotes B cell egress from Peyer's patches', *The Journal of Experimental Medicine*, 210: 1099-107.

Schneider, D. A., S. A. Madsen-Bouterse, D. Zhuang, T. C. Truscott, R. P. Dassanayake, and K. I. O'Rourke. 2015. 'The placenta shed from goats with classical scrapie is infectious to goat kids and lambs', *J Gen Virol*, 96: 2464-9.

Schuler, K. L., J. A. Jenks, C. S. DePerno, M. A. Wild, and C. C. Swanson. 2005. 'Tonsillar biopsy test for chronic wasting disease: Two sampling approaches in mule deer and white-tailed deer', *J Wildl Dis*, 41: 820-4.

Schulman, I. G. 2017. 'Liver X receptors link lipid metabolism and inflammation', *FEBS Lett*, 591: 2978-91.

Seed, C. R., P. E. Hewitt, R. Y. Dodd, F. Houston, and L. Cervenakova. 2018. 'Creutzfeldt-Jakob disease and blood transfusion safety', *Vox Sang*, 113: 220-31.

Senft, D., and Z. A. Ronai. 2015. 'UPR, autophagy, and mitochondria crosstalk underlies the ER stress response', *Trends Biochem Sci*, 40: 141-8.

Sethi, S., K. M. Kerksiek, T. Brocker, and H. Kretzschmar. 2007. 'Role of the CD8+ dendritic cell subset in transmission of prions', *J Virol*, 81: 4877-80.

Shadel, G. S., and T. L. Horvath. 2015. 'Mitochondrial ROS Signaling in Organismal Homeostasis', *Cell*, 163: 560-69.

Shi, Q., K. Xiao, B. Y. Zhang, X. M. Zhang, L. N. Chen, C. Chen, C. Gao, and X. P. Dong. 2015. 'Successive passaging of the scrapie strains, ME7-ha and 139A-ha, generated by the interspecies transmission of mouse-adapted strains into hamsters markedly

shortens the incubation times, but maintains their molecular and pathological properties', *Int J Mol Med*, 35: 1138-46.
Shi, Qi, Li-Na Chen, Bao-Yun Zhang, Kang Xiao, Wei Zhou, Cao Chen, Xiao-Mei Zhang, Chan Tian, Chen Gao, Jing Wang, Jun Han, and Xiao-Ping Dong. 2015. 'Proteomics Analyses for the Global Proteins in the Brain Tissues of Different Human Prion Diseases', *Molecular & Cellular Proteomics*, 14: 854-69.
Sigurdson, C. J., E. S. Williams, M. W. Miller, T. R. Spraker, K. I. O'Rourke, and E. A. Hoover. 1999. 'Oral transmission and early lymphoid tropism of chronic wasting disease PrPres in mule deer fawns (Odocoileus hemionus)', *J Gen Virol*, 80 (Pt 10): 2757-64.
Sigurdson, Christina J., Mathias Heikenwalder, Giuseppe Manco, Manja Barthel, Petra Schwarz, Bärbel Stecher, Nike J. Krautler, Wolf-Dietrich Hardt, Burkhardt Seifert, Andrew J. S. MacPherson, Irène Corthesy, and Adriano Aguzzi. 2009. 'Bacterial Colitis Increases Susceptibility to Oral Prion Disease', *The Journal of Infectious Diseases*, 199: 243-52.
Sikorska, B., and P. P. Liberski. 2012. 'Human prion diseases: from Kuru to variant Creutzfeldt-Jakob disease', *Subcell Biochem*, 65: 457-96.
Silveira, Jay R., Gregory J. Raymond, Andrew G. Hughson, Richard E. Race, Valerie L. Sim, Stanley F. Hayes, and Byron Caughey. 2005. 'The most infectious prion protein particles', *Nature*, 437: 257-61.
Simmons, M. M., P. Harris, M. Jeffrey, S. C. Meek, I. W. Blamire, and G. A. Wells. 1996. 'BSE in Great Britain: consistency of the neurohistopathological findings in two random annual samples of clinically suspect cases', *Vet Rec*, 138: 175-7.
Simon, Sharon L. R., Lise Lamoureux, Margot Plews, Michael Stobart, Jillian LeMaistre, Ute Ziegler, Catherine Graham, Stefanie Czub, Martin Groschup, and J. David Knox. 2008. 'The identification of disease-induced biomarkers in the urine of BSE infected cattle', *Proteome Science*, 6: 23.
Singh, A., A. O. Isaac, X. Luo, M. L. Mohan, M. L. Cohen, F. Chen, Q. Kong, J. Bartz, and N. Singh. 2009. 'Abnormal brain iron homeostasis in human and animal prion disorders', *PLoS Pathog*, 5: e1000336.
Siso, S., L. Gonzalez, F. Houston, N. Hunter, S. Martin, and M. Jeffrey. 2006. 'The neuropathologic phenotype of experimental ovine BSE is maintained after blood transfusion', *Blood*, 108: 745-8.
Siso, S., L. Gonzalez, and M. Jeffrey. 2010. 'Neuroinvasion in prion diseases: the roles of ascending neural infection and blood dissemination', *Interdiscip Perspect Infect Dis*, 2010: 747892.
Siso, S., M. Jeffrey, and L. Gonzalez. 2009. 'Neuroinvasion in sheep transmissible spongiform encephalopathies: the role of the haematogenous route', *Neuropathol Appl Neurobiol*, 35: 232-46.
Siso, S., M. Jeffrey, P. Steele, G. McGovern, S. Martin, J. Finlayson, F. Chianini, and L. Gonzalez. 2008. 'Occurrence and cellular localization of PrPd in kidneys of scrapie-affected sheep in the absence of inflammation', *J Pathol*, 215: 126-34.
Skinner, P. J., H. Abbassi, B. Chesebro, R. E. Race, C. Reilly, and A. T. Haase. 2006a. 'Gene expression alterations in brains of mice infected with three strains of scrapie', *BMC Genomics*, 7: 114.
Skinner, Pamela J., Hayet Abbassi, Bruce Chesebro, Richard E. Race, Cavan Reilly, and Ashley T. Haase. 2006b. 'Gene expression alterations in brains of mice infected with three strains of scrapie', *BMC Genomics*, 7: 114.
Skretting, G., A. Espenes, M. J. Ulvund, and I. Olsaker. 2004. 'cDNA representational difference analysis of ileal Peyer's patches in lambs after oral inoculation with scrapie', *Biochem Biophys Res Commun*, 316: 272-9.

Solassol, Jérôme, Carole Crozet, and Sylvain Lehmann. 2003. 'Prion propagation in cultured cells', *British Medical Bulletin*, 66: 87-97.

Song, F., A. Poljak, N. A. Kochan, M. Raftery, H. Brodaty, G. A. Smythe, and P. S. Sachdev. 2014. 'Plasma protein profiling of Mild Cognitive Impairment and Alzheimer's disease using iTRAQ quantitative proteomics', *Proteome Sci*, 12: 5.

Soto, C., L. Anderes, S. Suardi, F. Cardone, J. Castilla, M. J. Frossard, S. Peano, P. Saa, L. Limido, M. Carbonatto, J. Ironside, J. M. Torres, M. Pocchiari, and F. Tagliavini. 2005. 'Pre-symptomatic detection of prions by cyclic amplification of protein misfolding', *FEBS Lett*, 579: 638-42.

Speck, Olga, Sarah C. Hughes, Nicole K. Noren, Rima M. Kulikauskas, and Richard G. Fehon. 2003. 'Moesin functions antagonistically to the Rho pathway to maintain epithelial integrity', *Nature*, 421: 83.

Speldewinde, S. H., and C. M. Grant. 2015. 'Spermidine cures yeast of prions', *Microb Cell*, 3: 46-48.

Spratt, Donald E., Kathryn R. Barber, Nicole M. Marlatt, Vy Ngo, Jillian A. Macklin, Yiming Xiao, Lars Konermann, Martin L. Duennwald, and Gary S. Shaw. 2019. 'A subset of calcium-binding S100 proteins show preferential heterodimerization', *The FEBS Journal*, 286: 1859-76.

Stack, M. J., M. J. Chaplin, and J. Clark. 2002. 'Differentiation of prion protein glycoforms from naturally occurring sheep scrapie, sheep-passaged scrapie strains (CH1641 and SSBP1), bovine spongiform encephalopathy (BSE) cases and Romney and Cheviot breed sheep experimentally inoculated with BSE using two monoclonal antibodies', *Acta Neuropathol*, 104: 279-86.

Staffen, W., E. Trinka, B. Iglseder, P. Pilz, N. Homann, and G. Ladurner. 1997. 'Clinical and diagnostic findings in a patient with Creutzfeldt-Jakob disease (type Heidenhain)', *J Neuroimaging*, 7: 50-4.

Stimson, E., J. Hope, A. Chong, and A. L. Burlingame. 1999. 'Site-specific characterization of the N-linked glycans of murine prion protein by high-performance liquid chromatography/electrospray mass spectrometry and exoglycosidase digestions', *Biochemistry*, 38: 4885-95.

Sturgeon, Catharine, Robert Hill, Glen L. Hortin, and Douglas Thompson. 2010. 'Taking a new biomarker into routine use--a perspective from the routine clinical biochemistry laboratory', *Proteomics. Clinical applications*, 4: 892-903.

Suarez-Calvet, M., E. Morenas-Rodriguez, G. Kleinberger, K. Schlepckow, M. A. Araque Caballero, N. Franzmeier, A. Capell, K. Fellerer, B. Nuscher, E. Eren, J. Levin, Y. Deming, L. Piccio, C. M. Karch, C. Cruchaga, L. M. Shaw, J. Q. Trojanowski, M. Weiner, M. Ewers, and C. Haass. 2019. 'Early increase of CSF sTREM2 in Alzheimer's disease is associated with tau related-neurodegeneration but not with amyloid-beta pathology', *Mol Neurodegener*, 14: 1.

Sui, X., X. Ren, P. Huang, S. Li, Q. Ma, M. Ying, J. Ni, J. Liu, and X. Yang. 2014. 'Proteomic analysis of serum proteins in triple transgenic Alzheimer's disease mice: implications for identifying biomarkers for use to screen potential candidate therapeutic drugs for early Alzheimer's disease', *J Alzheimers Dis*, 40: 575-86.

Supattapone, Surachai. 2014. 'Elucidating the role of cofactors in mammalian prion propagation', *Prion*, 8: 100-05.

Suzuki, Kazuhiro, Irina Grigorova, Tri Giang Phan, Lisa M. Kelly, and Jason G. Cyster. 2009. 'Visualizing B cell capture of cognate antigen from follicular dendritic cells', *The Journal of Experimental Medicine*, 206: 1485-93.

Szegezdi, Eva, Susan E. Logue, Adrienne M. Gorman, and Afshin Samali. 2006. 'Mediators of endoplasmic reticulum stress-induced apoptosis', *EMBO reports*, 7: 880-85.

Taber, K. H., P. Cortelli, W. Staffen, and R. A. Hurley. 2002. 'The expanding role of imaging in prion disease', *J Neuropsychiatry Clin Neurosci*, 14: 371-6.
Tabrizi, S. J., C. L. Elliott, and C. Weissmann. 2003. 'Ethical issues in human prion diseases', *Br Med Bull*, 66: 305-16.
Takakura, I., K. Miyazawa, T. Kanaya, W. Itani, K. Watanabe, S. Ohwada, H. Watanabe, T. Hondo, M. T. Rose, T. Mori, S. Sakaguchi, N. Nishida, S. Katamine, T. Yamaguchi, and H. Aso. 2011. 'Orally administered prion protein is incorporated by m cells and spreads into lymphoid tissues with macrophages in prion protein knockout mice', *Am J Pathol*, 179: 1301-9.
Taraboulos, A., D. Serban, and S. B. Prusiner. 1990. 'Scrapie prion proteins accumulate in the cytoplasm of persistently infected cultured cells', *J Cell Biol*, 110: 2117-32.
Tarantino, Giovanni, Antonella Scalera, and Carmine Finelli. 2013. 'Liver-spleen axis: intersection between immunity, infections and metabolism', *World journal of gastroenterology*, 19: 3534-42.
Telling, G. C., M. Scott, K. K. Hsiao, D. Foster, S. L. Yang, M. Torchia, K. C. Sidle, J. Collinge, S. J. DeArmond, and S. B. Prusiner. 1994. 'Transmission of Creutzfeldt-Jakob disease from humans to transgenic mice expressing chimeric human-mouse prion protein', *Proc Natl Acad Sci U S A*, 91: 9936-40.
Terry, L. A., L. Howells, K. Bishop, C. A. Baker, S. Everest, L. Thorne, B. C. Maddison, and K. C. Gough. 2011. 'Detection of prions in the faeces of sheep naturally infected with classical scrapie', *Vet Res*, 42: 65.
Thompson, A. G. B., C. Luk, A. J. Heslegrave, H. Zetterberg, S. H. Mead, J. Collinge, and G. S. Jackson. 2018. 'Neurofilament light chain and tau concentrations are markedly increased in the serum of patients with sporadic Creutzfeldt-Jakob disease, and tau correlates with rate of disease progression', *J Neurol Neurosurg Psychiatry*, 89: 955-61.
Tolosano, E., and F. Altruda. 2002. 'Hemopexin: structure, function, and regulation', *DNA Cell Biol*, 21: 297-306.
Tran, H., A. Tanaka, S. V. Litvinovich, L. V. Medved, C. C. Haudenschild, and W. S. Argraves. 1995. 'The interaction of fibulin-1 with fibrinogen. A potential role in hemostasis and thrombosis', *J Biol Chem*, 270: 19458-64.
Tremblay, P., H. L. Ball, K. Kaneko, D. Groth, R. S. Hegde, F. E. Cohen, S. J. DeArmond, S. B. Prusiner, and J. G. Safar. 2004. 'Mutant PrPSc conformers induced by a synthetic peptide and several prion strains', *J Virol*, 78: 2088-99.
Treusch, Sebastian, Douglas M. Cyr, and Susan Lindquist. 2009. 'Amyloid deposits: protection against toxic protein species?', *Cell cycle (Georgetown, Tex.)*, 8: 1668-74.
Twal, W. O., A. Czirok, B. Hegedus, C. Knaak, M. R. Chintalapudi, H. Okagawa, Y. Sugi, and W. S. Argraves. 2001. 'Fibulin-1 suppression of fibronectin-regulated cell adhesion and motility', *J Cell Sci*, 114: 4587-98.
Tzaban, S., G. Friedlander, O. Schonberger, L. Horonchik, Y. Yedidia, G. Shaked, R. Gabizon, and A. Taraboulos. 2002. 'Protease-sensitive scrapie prion protein in aggregates of heterogeneous sizes', *Biochemistry*, 41: 12868-75.
Urwin, P. J., J. M. Mackenzie, C. A. Llewelyn, R. G. Will, and P. E. Hewitt. 2016. 'Creutzfeldt-Jakob disease and blood transfusion: updated results of the UK Transfusion Medicine Epidemiology Review Study', *Vox Sang*, 110: 310-6.
van der Merwe, J., J. Aiken, D. Westaway, and D. McKenzie. 2015. 'The standard scrapie cell assay: development, utility and prospects', *Viruses*, 7: 180-98.
Van Everbroeck, B., J. Boons, and P. Cras. 2005. 'Cerebrospinal fluid biomarkers in Creutzfeldt-Jakob disease', *Clin Neurol Neurosurg*, 107: 355-60.

van Horssen, R., E. Janssen, W. Peters, L. van de Pasch, M. M. Lindert, M. M. van Dommelen, P. C. Linssen, T. L. Hagen, J. A. Fransen, and B. Wieringa. 2009. 'Modulation of cell motility by spatial repositioning of enzymatic ATP/ADP exchange capacity', *J Biol Chem*, 284: 1620-7.

van Keulen, L. J., B. E. Schreuder, M. E. Vromans, J. P. Langeveld, and M. A. Smits. 2000. 'Pathogenesis of natural scrapie in sheep', *Arch Virol Suppl*: 57-71.

Vanni, S., F. Moda, M. Zattoni, E. Bistaffa, E. De Cecco, M. Rossi, G. Giaccone, F. Tagliavini, S. Haik, J. P. Deslys, G. Zanusso, J. W. Ironside, I. Ferrer, G. G. Kovacs, and G. Legname. 2017. 'Differential overexpression of SERPINA3 in human prion diseases', *Sci Rep*, 7: 15637.

Vascellari, M., R. Nonno, F. Mutinelli, M. Bigolaro, M. A. Di Bari, E. Melchiotti, S. Marcon, C. D'Agostino, G. Vaccari, M. Conte, L. De Grossi, F. Rosone, F. Giordani, and U. Agrimi. 2007. 'PrPSc in salivary glands of scrapie-affected sheep', *J Virol*, 81: 4872-6.

Veith, N. M., H. Plattner, C. A. Stuermer, W. J. Schulz-Schaeffer, and A. Burkle. 2009. 'Immunolocalisation of PrPSc in scrapie-infected N2a mouse neuroblastoma cells by light and electron microscopy', *Eur J Cell Biol*, 88: 45-63.

Vilette, D., O. Andreoletti, F. Archer, M. F. Madelaine, J. L. Vilotte, S. Lehmann, and H. Laude. 2001. 'Ex vivo propagation of infectious sheep scrapie agent in heterologous epithelial cells expressing ovine prion protein', *Proc Natl Acad Sci U S A*, 98: 4055-9.

Vilette, D., J. Courte, J. M. Peyrin, L. Coudert, L. Schaeffer, O. Andreoletti, and P. Leblanc. 2018. 'Cellular mechanisms responsible for cell-to-cell spreading of prions', *Cell Mol Life Sci*.

Villa, C., C. Fenoglio, M. De Riz, F. Clerici, A. Marcone, L. Benussi, R. Ghidoni, S. Gallone, F. Cortini, M. Serpente, C. Cantoni, G. Fumagalli, F. Martinelli Boneschi, S. Cappa, G. Binetti, M. Franceschi, I. Rainero, M. T. Giordana, C. Mariani, N. Bresolin, E. Scarpini, and D. Galimberti. 2011. 'Role of hnRNP-A1 and miR-590-3p in neuronal death: genetics and expression analysis in patients with Alzheimer disease and frontotemporal lobar degeneration', *Rejuvenation Res*, 14: 275-81.

Villegas-Llerena, C., A. Phillips, P. Garcia-Reitboeck, J. Hardy, and J. M. Pocock. 2016. 'Microglial genes regulating neuroinflammation in the progression of Alzheimer's disease', *Curr Opin Neurobiol*, 36: 74-81.

Volkel, D., K. Zimmermann, I. Zerr, T. Lindner, M. Bodemer, S. Poser, and H. P. Schwarz. 2001. 'C-reactive protein and IL-6: new marker proteins for the diagnosis of CJD in plasma?', *Transfusion*, 41: 1509-14.

Wallace, D. C. 2005. "A mitochondrial paradigm of metabolic and degenerative diseases, aging, and cancer: A dawn for evolutionary medicine." In *Annual Review of Genetics*, 359-407.

Wang, Siwen, Rui Song, Ziyi Wang, Zhaocheng Jing, Shaoxiong Wang, and Jian Ma. 2018. 'S100A8/A9 in Inflammation', *Frontiers in Immunology*, 9.

Watanabe, Y., Y. Hirao, K. Kasuga, T. Tokutake, Y. Semizu, K. Kitamura, T. Ikeuchi, K. Nakamura, and T. Yamamoto. 2019. 'Molecular Network Analysis of the Urinary Proteome of Alzheimer's Disease Patients', *Dement Geriatr Cogn Dis Extra*, 9: 53-65.

Wei, X., A. Herbst, D. Ma, J. Aiken, and L. Li. 2011a. 'A quantitative proteomic approach to prion disease biomarker research: delving into the glycoproteome', *J Proteome Res*, 10: 2687-702.

Wei, Xin, Allen Herbst, Di Ma, Judd Aiken, and Lingjun Li. 2011b. 'A quantitative proteomic approach to prion disease biomarker research: delving into the glycoproteome', *Journal of proteome research*, 10: 2687-702.

Weissmann, C., M. Enari, P. C. Klöhn, D. Rossi, and E. Flechsig. 2002. 'Transmission of prions', *Proceedings of the National Academy of Sciences of the United States of America*, 99 Suppl 4: 16378-83.

Wells, G. A., S. A. Hawkins, R. B. Green, A. R. Austin, I. Dexter, Y. I. Spencer, M. J. Chaplin, M. J. Stack, and M. Dawson. 1998. 'Preliminary observations on the pathogenesis of experimental bovine spongiform encephalopathy (BSE): an update', *Vet Rec*, 142: 103-6.

Wells, G. A., T. Konold, M. E. Arnold, A. R. Austin, S. A. Hawkins, M. Stack, M. M. Simmons, Y. H. Lee, D. Gavier-Widen, M. Dawson, and J. W. Wilesmith. 2007. 'Bovine spongiform encephalopathy: the effect of oral exposure dose on attack rate and incubation period in cattle', *J Gen Virol*, 88: 1363-73.

Wells, G. A., A. C. Scott, C. T. Johnson, R. F. Gunning, R. D. Hancock, M. Jeffrey, M. Dawson, and R. Bradley. 1987. 'A novel progressive spongiform encephalopathy in cattle', *Vet Rec*, 121: 419-20.

West, A. P., I. E. Brodsky, C. Rahner, D. K. Woo, H. Erdjument-Bromage, P. Tempst, M. C. Walsh, Y. Choi, G. S. Shadel, and S. Ghosh. 2011. 'TLR signalling augments macrophage bactericidal activity through mitochondrial ROS', *Nature*, 472: 476-80.

Whittington, M. A., K. C. Sidle, I. Gowland, J. Meads, A. F. Hill, M. S. Palmer, J. G. Jefferys, and J. Collinge. 1995. 'Rescue of neurophysiological phenotype seen in PrP null mice by transgene encoding human prion protein', *Nat Genet*, 9: 197-201.

Wilesmith, J. W., L. J. Hoinville, J. B. Ryan, and A. R. Sayers. 1992. 'Bovine spongiform encephalopathy: aspects of the clinical picture and analyses of possible changes 1986-1990', *Vet Rec*, 130: 197-201.

Wilesmith, J. W., J. B. Ryan, and M. J. Atkinson. 1991. 'Bovine spongiform encephalopathy: epidemiological studies on the origin', *Vet Rec*, 128: 199-203.

Wilham, J. M., C. D. Orru, R. A. Bessen, R. Atarashi, K. Sano, B. Race, K. D. Meade-White, L. M. Taubner, A. Timmes, and B. Caughey. 2010. 'Rapid end-point quantitation of prion seeding activity with sensitivity comparable to bioassays', *PLoS Pathog*, 6: e1001217.

Will, R. G., J. W. Ironside, M. Zeidler, S. N. Cousens, K. Estibeiro, A. Alperovitch, S. Poser, M. Pocchiari, A. Hofman, and P. G. Smith. 1996. 'A new variant of Creutzfeldt-Jakob disease in the UK', *Lancet*, 347: 921-5.

Will, R. G., M. Zeidler, G. E. Stewart, M. A. Macleod, J. W. Ironside, S. N. Cousens, J. Mackenzie, K. Estibeiro, A. J. Green, and R. S. Knight. 2000. 'Diagnosis of new variant Creutzfeldt-Jakob disease', *Ann Neurol*, 47: 575-82.

Williams, A., P. J. Lucassen, D. Ritchie, and M. Bruce. 1997. 'PrP deposition, microglial activation, and neuronal apoptosis in murine scrapie', *Experimental Neurology*, 144: 433-38.

Williams, E. S., and S. Young. 1980. 'Chronic wasting disease of captive mule deer: a spongiform encephalopathy', *J Wildl Dis*, 16: 89-98.

Wilson's, Wilson and. 2008. *Fundamentals of Advanced Omics Technologies: From Genes to Metabolites.* (Elsevier).

Windl, O., and M. Dawson. 2012. 'Animal prion diseases', *Subcell Biochem*, 65: 497-516.

Wroe, S. J., S. Pal, D. Siddique, H. Hyare, R. Macfarlane, S. Joiner, J. M. Linehan, S. Brandner, J. D. Wadsworth, P. Hewitt, and J. Collinge. 2006. 'Clinical presentation and pre-mortem diagnosis of variant Creutzfeldt-Jakob disease associated with blood transfusion: a case report', *Lancet*, 368: 2061-7.

Xerxa, E., M. Barbisin, M. N. Chieppa, H. Krmac, E. Vallino Costassa, P. Vatta, M. Simmons, M. Caramelli, C. Casalone, C. Corona, and G. Legname. 2016. 'Whole Blood Gene

Expression Profiling in Preclinical and Clinical Cattle Infected with Atypical Bovine Spongiform Encephalopathy', *PLoS One*, 11: e0153425.
Xiang, W., M. Hummel, G. Mitteregger, C. Pace, O. Windl, U. Mansmann, and H. A. Kretzschmar. 2007. 'Transcriptome analysis reveals altered cholesterol metabolism during the neurodegeneration in mouse scrapie model', *J Neurochem*, 102: 834-47.
Xiang, W., O. Windl, I. M. Westner, M. Neumann, I. Zerr, R. M. Lederer, and H. A. Kretzschmar. 2005. 'Cerebral gene expression profiles in sporadic Creutzfeldt-Jakob disease', *Ann Neurol*, 58: 242-57.
Xiang, W., O. Windl, G. Wunsch, M. Dugas, A. Kohlmann, N. Dierkes, I. M. Westner, and H. A. Kretzschmar. 2004. 'Identification of differentially expressed genes in scrapie-infected mouse brains by using global gene expression technology', *J Virol*, 78: 11051-60.
Xu, K., and X. P. Zhu. 2012. 'Endoplasmic reticulum stress and prion diseases', *Reviews in the Neurosciences*, 23: 79-84.
Yu, H. L., H. M. Chertkow, H. Bergman, and H. M. Schipper. 2003. 'Aberrant profiles of native and oxidized glycoproteins in Alzheimer plasma', *Proteomics*, 3: 2240-8.
Yusa, S., J. B. Oliveira-Martins, Y. Sugita-Konishi, and Y. Kikuchi. 2012. 'Cellular prion protein: from physiology to pathology', *Viruses*, 4: 3109-31.
Yusnita, Y., M. D. Norsiah, and A. J. Rahman. 2010. 'Mutations in mitochondrial NADH dehydrogenase subunit 1 (mtND1) gene in colorectal carcinoma', *Malays J Pathol*, 32: 103-10.
Zeidler, M., R. Knight, G. Stewart, J. W. Ironside, R. G. Will, A. J. Green, and M. Pocchiari. 1999. 'Diagnosis of Creutzfeldt-Jakob disease. Routine tonsil biopsy for diagnosis of new variant Creutzfeldt-Jakob disease is not justified', *BMJ (Clinical research ed.)*, 318: 538-38.
Zhang, M., L. V. Borovikova, H. Wang, C. Metz, and K. J. Tracey. 1999. 'Spermine inhibition of monocyte activation and inflammation', *Molecular medicine (Cambridge, Mass.)*, 5: 595-605.
Zhang, R., L. Barker, D. Pinchev, J. Marshall, M. Rasamoelisolo, C. Smith, P. Kupchak, I. Kireeva, L. Ingratta, and G. Jackowski. 2004. 'Mining biomarkers in human sera using proteomic tools', *Proteomics*, 4: 244-56.
Zlotnik, I., and J. C. Rennie. 1963. 'Further observations on the experimental transmission of scrapie from sheep and goats to laboratory mice', *J Comp Pathol*, 73: 150-62.

Appendix 1: Plasma mass spectrometry results

Accession	Median(H/L)	Gene Name
ENSOARP00000016410.1	0.21875	SERPINA3
ENSOARP00000019654.1	0.265625	HPX
ENSOARP00000009904.1	0.265625	IPSP
ENSOARP00000009080.1	0.28125	TF
ENSOARP00000004002.1	0.3125	HP
ENSOARP00000015963.1	0.359375	SERPINA1
ENSOARP00000013350.1	0.359375	IGL@
ENSOARP00000002222.1	0.359375	Q86SX2
ENSOARP00000010561.1	0.390625	SAA1
ENSOARP00000006793.1	0.390625	TTR
ENSOARP00000009964.1	0.390625	IPSP
ENSOARP00000014782.1	0.40625	ALB
ENSOARP00000001046.1	0.421875	A2M
ENSOARP00000019505.1	0.46875	IGL@
ENSOARP00000004100.1	0.53125	A1BG
ENSOARP00000000762.1	0.5625	C3
ENSOARP00000008560.1	0.5625	C1QB
ENSOARP00000020933.1	0.578125	ATP6V1A
ENSOARP00000013478.1	0.59375	IGL@
ENSOARP00000012213.1	0.59375	ATP5H
ENSOARP00000006008.1	0.59375	C5
ENSOARP00000000757.1	0.609375	ITIH4
ENSOARP00000013750.1	0.625	GC
ENSOARP00000000921.1	0.625	MT-ND1
ENSOARP00000001942.1	0.640625	CDH5
ENSOARP00000000771.1	0.65625	C3
ENSOARP00000001973.1	1.515625	C4A
ENSOARP00000005881.1	1.546875	GSN
ENSOARP00000015280.1	1.546875	SERPINF1
ENSOARP00000006714.1	1.578125	BPIA2
ENSOARP00000021893.1	1.609375	APOD
ENSOARP00000003016.1	1.640625	IGHM
ENSOARP00000016297.1	1.6875	SHBG
ENSOARP00000004994.1	1.78125	C1S
ENSOARP00000004316.1	1.796875	F2
ENSOARP00000010848.1	1.890625	CONG
ENSOARP00000013455.1	1.90625	HABP2
ENSOARP00000001607.1	1.953125	ITIH1
ENSOARP00000020846.1	2	FBLN1

ENSOARP00000014654.1	2.015625	ITIH2
ENSOARP00000007943.1	2.15625	C4BPA
ENSOARP00000007474.1	2.265625	CD5L
ENSOARP00000016248.1	2.375	SERPINA5
ENSOARP00000003094.1	2.734375	PON1

Appendix 2: Buffy coat mass spectrometry results

Accession	Median(H/L)	Gene Name
ENSOARP00000017452	0.33	SMS
ENSOARP00000007752	0.36	ISG15
ENSOARP00000016735	0.36	PRPF19
ENSOARP00000020212	0.39	LBP
ENSOARP00000000988	0.43	CFHR4
ENSOARP00000001942	0.43	CDH5
ENSOARP00000010561	0.44	SAA2
ENSOARP00000010686	0.48	SAA3
ENSOARP00000000559	0.49	PZP
ENSOARP00000001687	0.51	TIMM8A
ENSOARP00000014091	0.52	RNF114
ENSOARP00000006406	0.53	PAICS
ENSOARP00000013476	0.53	RUVBL2
ENSOARP00000015311	0.56	CCT5
ENSOARP00000015112	0.56	SERPINF2
ENSOARP00000010581	0.56	SAA1
ENSOARP00000003455	0.57	PSMB10
ENSOARP00000012339	0.57	ALDH9A1
ENSOARP00000003727	0.58	SPTBN1
ENSOARP00000010495	0.59	SPTAN1
ENSOARP00000002026	0.59	COPS3
ENSOARP00000016820	0.59	PDIA6
ENSOARP00000015018	0.59	LYPLA1
ENSOARP00000022524	0.6	TMOD3
ENSOARP00000009527	0.6	SH3GLB2
ENSOARP00000015560	0.61	CCT8
ENSOARP00000008923	0.61	SRSF1
ENSOARP00000022764	0.62	ACTN1
ENSOARP00000010798	0.63	MYL6
ENSOARP00000012882	0.63	IDH2
ENSOARP00000000794	0.63	GLUD1
ENSOARP00000005333	0.64	RUVBL1
ENSOARP00000004266	0.64	HNRNPF
ENSOARP00000010661	0.64	SMARCC2
ENSOARP00000022149	0.64	STRAP
ENSOARP00000014561	0.64	SRSF3
ENSOARP00000014259	0.64	RBBP7
ENSOARP00000009376	0.64	FH
ENSOARP00000007128	0.65	HNRNPK

ENSOARP00000006283	0.65	HNRNPL
ENSOARP00000013029	0.65	SUB1
ENSOARP00000022478	0.65	RBBP4
ENSOARP00000004520	0.65	CCDC6
ENSOARP00000006306	0.66	KHSRP
ENSOARP00000001874	0.66	PRDX3
ENSOARP00000012213	0.66	ATP5H
ENSOARP00000004875	0.66	TCP1
ENSOARP00000018724	0.66	PDLIM5
ENSOARP00000014672	0.66	LMNB2
ENSOARP00000010106	0.66	CS
ENSOARP00000011580	1.5	PRDX2
ENSOARP00000018140	1.5	TSC22D4
ENSOARP00000005022	1.5	CYB5 CYB5A
ENSOARP00000018174	1.5	BLVRA
ENSOARP00000011646	1.5	GSS
ENSOARP00000013845	1.51	SERPINC1
ENSOARP00000017187	1.52	UBE2L3
ENSOARP00000003070	1.53	PCMT1
ENSOARP00000000187	1.53	CIAPIN1
ENSOARP00000022054	1.53	FETUB
ENSOARP00000014553	1.53	PURA
ENSOARP00000003883	1.53	PSMD7
ENSOARP00000013259	1.53	ITGB2
ENSOARP00000009446	1.54	HSPA1A
ENSOARP00000010804	1.54	EFHD2
ENSOARP00000014654	1.56	ITIH2
ENSOARP00000002904	1.56	GBP1
ENSOARP00000012635	1.56	PRDX6
ENSOARP00000007392	1.57	COPS7A
ENSOARP00000010837	1.58	PARK7
ENSOARP00000012677	1.58	CCT7
ENSOARP00000005414	1.59	MSN
ENSOARP00000002274	1.59	CAMP
ENSOARP00000001333	1.62	MAP
ENSOARP00000013895	1.62	PITPNA
ENSOARP00000012513	1.62	BCCIP
ENSOARP00000011651	1.63	LCN2
ENSOARP00000021664	1.65	CAP1
ENSOARP00000010475	1.66	RAD23A
ENSOARP00000011240	1.66	PGLYRP1
ENSOARP00000017958	1.68	TKT
ENSOARP00000005586	1.69	ACP1

ENSOARP00000018006	1.71	FRZB
ENSOARP00000020200	1.74	PGK1
ENSOARP00000006715	1.74	ALAD
ENSOARP00000018863	1.74	APOL3
ENSOARP00000001607	1.74	ITIH1
ENSOARP00000016173	1.74	GBP1
ENSOARP00000014964	1.75	ARG1
ENSOARP00000018674	1.75	IGHG2
ENSOARP00000009256	1.76	LTF
ENSOARP00000022574	1.77	COPS2
ENSOARP00000008093	1.78	TSC22D1
ENSOARP00000004221	1.79	NUCB2
ENSOARP00000021574	1.8	UBE2N
ENSOARP00000022329	1.81	PLBD1
ENSOARP00000012500	1.82	AKR1C3
ENSOARP00000004816	1.82	NAMPT
ENSOARP00000007182	1.83	OLFM4
ENSOARP00000002425	1.84	RETN
ENSOARP00000006648	1.87	C1orf123
ENSOARP00000009374	1.88	PGK2
ENSOARP00000013912	1.88	HMBS
ENSOARP00000009640	1.88	FABP5
ENSOARP00000004428	1.9	ALDOA
ENSOARP00000008717	1.93	C8B
ENSOARP00000021247	1.94	AAK1
ENSOARP00000010386	1.94	PRTN3
ENSOARP00000009955	1.96	AKR1C1
ENSOARP00000017956	2.03	UQCRC1
ENSOARP00000009967	2.23	MPO
ENSOARP00000017556	2.24	PGLS
ENSOARP00000004100	2.26	A1BG
ENSOARP00000013929	2.6	ANG
ENSOARP00000019468	2.62	TIMM10B
ENSOARP00000019931	2.7	CAT
ENSOARP00000000416	2.77	S100A9
ENSOARP00000007106	2.79	BLVRB
ENSOARP00000000449	2.84	S100A8
ENSOARP00000006793	2.87	TTR
ENSOARP00000008379	2.89	INMT
ENSOARP00000019194	3.14	TXNRD2